Understanding the role of cAMP-binding proteins in mycobacterial physiology and assessment of antibiotics toxicity using mass-spectrometry approaches

SONIA REBOLLO RAMIREZ

Thesis submitted for the degree of
Doctor of Philosophy of Imperial
College London

Centre for Molecular Bacteriology and Infection, Department of Life Sciences, Imperial College London

Declaration of originality

I, Sonia Rebollo-Ramirez confirm that all work presented in this thesis is either my own or attributed to the respective authors.

Copyright declaration

'The copyright of this thesis rests with the author. Unless otherwise indicated, its contents are licensed under a Creative Commons Attribution-Non Commercial 4.0 International Licence (CC BY-NC). Under this licence, you may copy and redistribute the material in any medium or format. You may also create and distribute modified versions of the work. This is on the condition that: you credit the author and do not use it, or any derivative works, for a commercial purpose. When reusing or sharing this work, ensure you make the licence terms clear to others by naming the licence and linking to the licence text. Where a work has been adapted, you should indicate that the work has been changed and describe those changes. Please seek permission from the copyright holder for uses of this work that are not included in this licence or permitted under UK Copyright Law.'

Acknowledgements

I would like to thank my supervisor Dr Gerald Larrouy-Maumus, for the opportunity he gave me to pursue a PhD in his lab. Your energy, drive and support have been immensely helpful during my time in the lab and writing stage. I would also like to thank the Life Sciences Department of Imperial College London for funding my PhD as well as sponsoring me to attend the 10th International conference on the pathogenesis of mycobacterial infections.

I would like to acknowledge Nitya Krishan, Miles Priestman, Iria Uhia and Vani Subbarao from the Robertson group. I felt you were part of my group when it was only me during my first year. A special thank you for Nitya Krishnan, a friend and mentor who has always been there for me. I would also like to acknowledge the current members in my lab. Michael Thomson and Ashleigh Cheyne, since you joined on my second year everything changed! We did not just become PhD buddies but we became friends. How many experiences have we shared together! I would like to thank Charlie Millership and Jeanine Rismondo for the great conversations at lunchtime. Also the CMBI community, with specific mention to Julia Sanchez. Thanks for your help especially during the end of my PhD! Thank you Sina Krokowski for all microscopy work and helping me shape a story which became my first first-author paper.

This work would not have been possible without the support of Prof Sandhya S. Visweswariah from the Indian Institute of Science in Bangalore. Thank you for your support and advice from the very beginning!

Finally and most importantly I would like to thank my boyfriend Andy and my family. Your support has been invaluable in order to complete the journey that is a PhD project. Thank you so much for your moral support and positivity, they really made the difference! I cannot believe how lucky I am!

Abstract

Infection by *Mycobacterium tuberculosis* (Mtb) represents a significant healthcare burden, with approximately 10 million cases of human tuberculosis and 1.6 million deaths reported in 2017 by the WHO. As a result, there is an urgent need to develop new and more effective anti-tuberculosis drugs. However, the development of new antibiotics and the assessment of their toxicity represent an important challenge. Mtb is a successful intracellular pathogen that infects alveolar macrophages. Once inside, Mtb is able to resist hostile conditions such as acidic pH, osmotic stress, nitric oxide and reactive oxygen species, and it can adapt to these environmental cues. The second messenger 3',5'-cyclic adenosine monophosphate (cAMP) has been proposed to be involved in the adaptation of Mtb within the macrophage, which is rich in cholesterol and fatty acids. In this thesis, the link between osmotic stress and cAMP in mycobacteria is investigated. Thus, I provide the first evidence that in Mtb is the cAMP receptor protein (CRP_{Mt}) responsible for the production of high levels of cAMP after exposure to 250 mM NaCl. Then the role of Rv0998, a cAMP-dependent lysine acetyltransferase in Mtb physiology was investigated. Hence it was revealed that albumin is involved in the survival of an Mtb mutant lacking Rv0998 in acidic pH. Finally, I propose an alternative readout for addressing antibiotic toxicity by looking at changes in the lipidome on intact and unprocessed cells by matrix-assisted laser desorption ionisation mass spectrometry. Throughout this thesis, a combination of mass spectrometry approaches and tissue culture assays are used to understand Mtb adaptation and antibiotic toxicity. The data obtained in this thesis may help develop new strategies to combat the increasing threat that tuberculosis poses. Furthermore, it will help to rapidly assess the toxicity of aminoglycosides in HeLa and primary cells.

Contents

Declaration of originality ... 2
Copyright declaration ... 2
Abstract ... 4
Contents ... 5
List of figures ... 10
List of tables ... 14
Abbreviations ... 15
Chapter 1: Introduction ... 22
1.1 Tuberculosis ... 23
1.1.1 Disease epidemiology ... 23
1.1.1.2 HIV-coinfection ... 25
1.1.2 Mtb treatment ... 26
1.1.3 Prevention of Mtb ... 26
1.1.4 Current diagnostic tools ... 27
1.2 Mtb pathogenesis ... 28
1.2.1 Cell envelope lipids ... 28
1.2.2 Immune response against Mtb infection ... 30
1.2.2.1 Granuloma ... 32
1.3 Mtb metabolism within the host ... 36
1.3.1 Mtb central carbon catabolism ... 36
1.3.2.1 Fatty acid metabolism ... 38
1.3.2.2 Cholesterol metabolism ... 39
1.4 Bacterial adaptation ... 41
1.4.1 Bacterial adaptation mediated by second messengers ... 41
1.4.2 Cyclic nucleotides ... 42
1.4.3 Bacterial adaptation via cAMP ... 45
1.5 Mtb cAMP metabolism ... 46
1.5.1 Adenylate cyclases and their catalytic activity regulation in Mtb ... 46
1.5.2 cAMP production ... 50
1.5.3 Secretion of cAMP into host cells and role of secreted cAMP in macrophages ... 51
1.5.4 cAMP degradation ... 53
1.5.5 cAMP-binding proteins ... 53
1.6 Mass spectrometry ... 58

1.6.1 Ion sources ... 58
1.6.1.1 ESI ... 59
1.6.1.2 MALDI ... 60
1.6.2 The analyser ... 61
1.6.2.1 Quadrupole mass filter ... 61
1.6.2.2 TOF analyser ... 63
1.6.2.3 Tandem ... 64
1.6.3 Liquid Chromatography MS coupling (LC-MS) ... 64
Chapter 2: Materials and methods ... 66
2.1 Materials ... 67
2.2 Methods ... 67
2.2.1 Bacterial strains and growth conditions ... 67
2.2.1.1 7H9 liquid medium ... 67
2.2.1.2 7H10 solid medium ... 67
2.2.1.3 Medium supplement ... 67
2.2.2 Growth curves and Optical density (OD) monitoring ... 68
2.2.3 Measuring Mtb viability upon stress ... 69
2.2.4 Lipidomics analysis ... 69
2.2.4.1 Intact bacteria lipid profiling from solid and liquid culture ... 69
2.2.4.2 Lipid fingerprint analysis by MALDI-TOF MS ... 70
2.2.4.3 Intact cell lipid profiling ... 70
2.2.5 Metabolomics analysis ... 71
2.2.5.1 Sample preparation ... 71
2.2.5.2 Stable isotope tracing ^{13}C metabolomics ... 72
2.2.5.3 LC-MS analysis ... 72
2.2.5.4 Bicinchoninic acid assay (BCA) ... 73
2.2.6 Detecting acetylation using Mass Spectrometry ... 73
2.2.6.1 Sample preparation ... 73
2.2.6.2 LC-MS method used for proteomics ... 73
2.2.6.3 LC-MS/MS workflow for detection of acetylated proteins ... 74
2.2.7 Transcriptomics ... 74
2.2.8 Tissue culture assays ... 75
2.2.8.1 Culture of RAW 264.7 macrophages ... 75
2.2.8.2 Culture of HeLa cells ... 76
2.2.8.3 Isolation of mouse bone marrow-derived macrophages ... 76
2.2.8.4 Antibiotics treatments of mammalian cells ... 76

2.2.8.5 Seahorse XF Cell Mito Stress Test 76
2.2.8.6 Cell viability assay 77
2.2.8.7 Membrane potential measurement 77
2.2.8.8 Microscopy of HeLa cells 77
2.2.8.9 Infection with Mtb of resting and IFN-γ-activated macrophages 78
2.2.8.10 TNF-α production by activated and non-activated macrophages 78
2.2.9 Statistical analyses 78
Chapter 3: Intact cell lipidomics reveal changes to the ratio of cardiolipins to phosphatidylinositols in response to kanamycin 79
3.1 Introduction 80
3.1.1 Antibiotic toxicity 80
3.1.2 Mitochondria, an antibiotic target 80
3.1.2.1 Mitochondrial composition 80
3.1.2.3 Mitochondrial dysfunction 85
3.1.3 Available cell toxicity detection methods 85
3.1.4 Lipidomics to detect antibiotic toxicity 86
3.1.5 Seahorse: a tool to detect mitochondrial damage 87
3.1.6 Justification of the cell lines used 89
3.1.7 Justification of antibiotic treatment and dose 89
3.2 Results 90
3.2.1 Intact cell lipidomics identified different lipid classes in RAW 264.7 macrophages 90
3.2.2 Kanamycin treated HeLa cells suffer changes in the CL:PI ratio 91
3.2.3 Kanamycin alters the membrane potential and mitochondrial morphology in HeLa cells 96
3.2.4 Kanamycin but not levofloxacin nor ethambutol induces changes in the CL:PI ratio in a dose-dependent manner in HeLa cells and BMDM but not in RAW 264.7 99
3.2.6 Kanamycin, levofloxacin, and ethambutol decrease the maximal rate of mitochondrial respiration in HeLa cells and BMDMs 103
3.3 Discussion 105
Chapter 4: NaCl triggers the CRP-dependent increase of cAMP in Mtb 108
4.1 Introduction 109
4.1.1 Osmotic stress in bacteria 109
4.1.2 Mycobacterial adaptation to stress via cAMP 112
4.1.3 Osmotic stress in mycobacteria 112
4.1.4 The CRP_{Mt}, a potential candidate for Mtb osmoregulation 114
4.2 Results 118

4.2.1 A physiological concentration of NaCl leads to an increase in intracellular cAMP levels in Mtb 118

4.2.2 Mtb ACs are active upon exposure to 250 mM NaCl 123

4.2.3 Increase in intracellular cAMP levels is partially dependent on the PknD osmosensing signalling pathway in Mtb 125

4.2.4 The increase in the intracellular cAMP levels is dependent on the transcriptional regulator CRP_{Mt} in Mtb 129

4.3 Discussion 132

Chapter 5: Defining the role of the cAMP-dependent lysine acetyltransferase (Rv0998) in Mtb 138

5.1 Introduction 139

5.1.1 Post-translational modifications 139

5.1.2 Lysine acetylation 139

5.1.3 Lysine acetylation in mycobacteria 142

5.1.4 Rv0998, a cAMP-dependent lysine acetyltransferase in Mtb 143

5.1.4.1 cAMP-induced activation of Rv0998 144

5.1.4.2 Acetyl-CoA synthetase, an Rv0998 substrate 145

5.1.4.3 FadDs, an Rv0998 substrate 145

5.1.4.5 Transcription factor DosR, an Rv0998 substrate 147

5.1.5 Impact of Rv0998 in mycobacterial physiology 148

5.1.5.1 Cholesterol acquisition 148

5.1.5.2 Survival in acidic pH 148

5.2 Results 153

5.2.1 Albumin alters Mtb physiology 153

5.2.1.1 Presence or absence of BSA alters Mtb growth 153

5.2.1.2 Presence or absence of BSA alters intracellular levels of cAMP 154

5.2.1.3 BSA leads to a global metabolome remodelling 154

5.2.2 Effect of albumin in the physiology of a cAMP dependent lysine acetyltransferase mutant. 157

5.2.2.1 The presence of BSA in culture medium affects growth of Mtb *Δrv0998* 157

5.2.2.2 The presence of BSA in culture medium affects cAMP intracellular levels in Mtb 158

5.2.2.3 Impact of Rv0998 on Mtb viability under stress at low pH 159

5.2.2.4 Global metabolomics profiling of Mtb wild type, *Δrv0998* and complemented strains in the presence and absence of BSA 160

5.2.2.5 Turnover of TCA cycle metabolites of Mtb wild type, *Δrv0998* and complemented strain in the presence and absence of BSA 167

5.2.2.6 Investigation of Mtb cell envelope changes (PIMs) by MALDI-TOF 172

5.2.2.7 The presence of albumin in the culture medium causes changes in the Mtb acetylome 173

5.2.2.8 Role of Rv0998 in virulence and persistence. 182

5.3 Discussion 185

Chapter 6: Final discussion 194

Chapter 7: References 204

List of figures

Figure 1-1. World map of TB incidence rate in 2017. 24
Figure 1-2. Scheme displaying the Mtb cell envelope. 29
Figure 1-3. Schematic diagram showing how Mtb bacilli are detected by alveolar macrophages. 31
Figure 1-4. The Mtb granuloma. 33
Figure 1-5. Chemical structures of lipid virulence factors. 35
Figure 1-6. Diagram of Mtb central carbon metabolism. 37
Figure 1-7. Schematic diagram showing assimilation of host lipids. 40
Figure 1-8. Chemical structures of some of the main cyclic mono- and dinucleotides in bacteria. 43
Figure 1-9. Scheme showing how the environmental signals trigger downstream effects via cAMP production. 44
Figure 1-10. Schematic diagram of Mtb cAMP signalling pathways. 47
Figure 1-11. Schematic diagram with the downstream effects of cAMP upon macrophage phagocytosis. 52
Figure 1-12. Multiple sequence alignment of the cAMP-binding domains of Rv0998 and seven uncharacterised cAMP-binding proteins in Mtb. 57
Figure 1-13. Diagram of the three basic parts of a mass spectrometer. 58
Figure 1-14. Schematic representation of sample ionisation with Electrospray Ionisation (ESI). 59
Figure 1-15. Schematic representation of sample ionisation with MALDI. 61
Figure 1-16. Simplified scheme of the quadrupole mass analyser. 62
Figure 1-17. Scheme showing the general set up of TOF analysers. 63
Figure 2-1. Intact cell lipidomics. 70
Figure 2-2. Scheme showing preparation of samples for metabolomics. 72
Figure 2-3. Liquid chromatography tandem mass spectrometry workflow for proteomics. .. 74
Figure 3-1. Chemical structures of CL, PI, PC and PE. 81
Figure 3-2. Electron transport chain. 82
Figure 3-3. Scheme showing fatty acid synthesis in the mitochondria. 84
Figure 3-4. Mitochondrial respiration 88
Figure 3-5. Mass spectra of lipid fingerprint on intact macrophages by MALDI MS. 91
Figure 3-6. Lipid fingerprint of intact HeLa cells by MALDI-MS. 92
Figure 3-7. MS/MS mass spectra of peaks at *m/z* 835.4, *m/z* 861.4 and *m/z* 885.4. 93

Figure 3-8. MS/MS mass spectra of CL peaks at *m/z* 1399.8 and *m/z* 1427.8. 94
Figure 3-9. MS and MS/MS mass spectra of CL standards from mitochondria from bovine heart. 95
Figure 3-10. Kanamycin at 25 µg/mL for 24 hours induces changes in PLs in HeLa cells. 96
Figure 3-11. Kanamycin at 25 µg/mL for 24 hours induces a decrease in mitochondrial membrane potential. 97
Figure 3-12. Mitochondrial morphology in untreated and kanamycin-treated HeLa cells 98
Figure 3-13. Only Levofloxacin (5*Cmax) and Kanamycin (Cmax and 5*Cmax) have an impact on CL:PI ratio in HeLa and BMDMs. 100
Figure 3-14. Viability does not decrease after treating HeLa, RAW 264.7 and BMDM with Levofloxacin 5*Cmax and Kanamycin Cmax and 5*Cmax. 102
Figure 3-15. Kanamycin, levofloxacin, and ethambutol can induce mitochondrial dysfunction in HeLa cells and BMDMs. 104
Figure 4-1. Scheme showing a simplified model of the CRP osmoregulation. 111
Figure 4-2. NaCl concentrations Mtb encounters in culture media and humans. 113
Figure 4-3. Osmosensory regulation of Mtb mediated by PknD. 114
Figure 4-4. Amino acid sequence alignments of Mtb Rv3676 and CRP from E. coli. 115
Figure 4-5. Exposure to 250mM reduced growth of *M. smegmatis*, *M. marinum* and Mtb. 119
Figure 4-6. Only stress at 250 mM NaCl leads to an increase in intracellular cAMP levels in Mtb. 120
Figure 4-7. Confirmation of the assignment of the molecule of interest as 3',5'-cyclic adenosine monophosphate. 121
Figure 4-8. Confirmation of the assignment of the molecule as 3',5'-cyclic adenosine monophosphate by MS/MS mass spectrometry. 122
Figure 4-9. cAMP is synthesised de novo upon 250 mM NaCl stress. 124
Figure 4-10. There are no changes in expression of genes involved in cAMP synthesis in Mtb. 126
Figure 4-11. PknD is partly responsible for the cAMP increase at 250 mM NaCl in Mtb. 128
Figure 4-12. CRP_{Mt} orchestrates the cAMP increase of Mtb upon exposure to 250 mM NaCl. 130
Figure 4-13. Impairment in growth of Mtb *Δcrp* in a mouse intravenous infection. 136
Figure 4-14. CRP_{Mt} orchestrates the increase in intracellular levels of cAMP in response to exposure to 250 mM NaCl in Mtb. 137
Figure 5-1. General mechanism of lysine acetylation and deacetylation. 140

Figure 5-2. Sequence alignment of Rv0998 and its orthologue MSMEG_5458 in *M. smegmatis*. 144
Figure 5-3. Scheme showing the autoinhibition and cAMP-induced conformational changes of Rv0998. 145
Figure 5-4. Mycobactin (MBT) synthesis. 147
Figure 5-5. Mtb inside the macrophage. 149
Figure 5-6. Mtb *Δrv0998* grows better than the Mtb wild type strain at low pH in Sauton medium. 150
Figure 5-7. The presence of albumin alters the growth of the wild type strain of Mtb. 153
Figure 5-8. Intracellular levels of cAMP of Mtb wild type grown in culture medium with or without BSA. 154
Figure 5-9. Simplified scheme showing steps and MassHunter tools used in untargeted metabolomics data analysis. 155
Figure 5-10. Presence or absence of albumin determines the growth at pH 5.5 of *Δrv0998*. 158
Figure 5-11. Intracellular levels of cAMP of Mtb wild type, *Δrv0998* and complemented grown in culture medium with or without BSA. 159
Figure 5-12. Measurement of viable Mtb wild type (wt), mutant lacking *rv0998* (*Δrv0998*) and complemented (comp.) strains after exposing them for 48 hours to pH 6.8 or 5.5. 160
Figure 5-13. Untargeted metabolomics of Mtb wild type, *Δrv0998* and complemented strains in the presence or absence of BSA at pH 6.8 and 5.5 in positive and negative ion mode. 163
Figure 5-14. Untargeted metabolomics of Mtb wild type, *Δrv0998* and complemented strains in the presence or lack of BSA at pH 6.8 and 5.5 in positive and negative ion mode. 164
Figure 5-15. Untargeted metabolomics of Mtb *Δrv0998* in response to the presence or absence of BSA at pH 5.5. 166
Figure 5-16. Turnover of central carbon metabolism metabolites of Mtb wild type (wt), mutant lacking *rv0998* (*Δrv0998*) and complemented (comp.) strains after exposing them for 24 hours to pH 6.8 in the presence or absence of BSA. 168
Figure 5-17. Turnover of compounds of Mtb wild type (wt), mutant lacking *rv0998* (*Δrv0998*) and complemented (comp.) strains after exposure for 24 hours to pH 6.8 in the presence or absence of BSA. 169
Figure 5-18.Turnover of central carbon metabolism metabolites of Mtb wild type (wt), mutant lacking *rv0998* (*Δrv0998*) and complemented (comp.) strains after exposure for 24 hours to pH 5.5 in the presence or absence of BSA. 170

Figure 5-19. Turnover of compounds of Mtb wild type (wt), mutant lacking *rv0998* (*Δrv0998*) and complemented (comp.) strains after exposure for 24 hours to pH 5.5 in the presence or absence of BSA. 171
Figure 5-20. Relative abundance of Ac_3PIM_2, Ac_4PIM_2, Ac_3PIM_6 and Ac_4PIM_6 present in Mtb wild type (wt), mutant lacking *rv0998* (*Δrv0998*) and complemented (comp.) strains after exposing them for 0, 24 or 48 hours to pH 6.8 and pH 5.5. 173
Figure 5-21. Lysine acetylated proteins exclusive to the wild type strain of Mtb. 176
Figure 5-22. Growth of intracellular Mtb. 183
Figure 5-23. Quantification of TNF-α production by IFN-γ-activated or resting macrophages infected with wt, *Δrv0998* and the complemented strains of Mtb. 184

List of tables

Table 1-1. Domain compositions of the 16 class III adenylyl cyclases in Mtb H37Rv. 48

Table 1-2. ACs in Mtb H37Rv 50

Table 1-3. Ten Mtb cAMP-binding proteins and their domain compositions. 55

Table 1-4. Function of the 10 Mtb cAMP-binding proteins in different mycobacterial species. 56

Table 2-1. Strains used in this thesis. 68

Table 4-1. Functions and products of putative CRP_{Mt}-regulated genes. 117

Table 4-2. cDNA microarray of Mtb H37Rv upon exposure to 250 mM NaCl. 127

Table 4-3. cAMP levels in mycobacteria used in this study. 131

Table 5-1. List of eight lysine acetylated proteins involved in central carbon metabolism. . 143

Table 5-2. Components of both Middlebrook 7H9 culture medium and Sauton culture medium. 151

Table 5-3. Table showing changing features greater than 2-fold between Mtb wild type strain grown at different conditions. 156

Table 5-4. Gene names and potential functions of acetylated proteins in the Mtb wild type (wt) grown at pH 6.8 in the presence of BSA. 178

Table 5-5. Gene names and potential functions of acetylated proteins in the Mtb wild type (wt) grown at pH 6.8 in the absence of BSA. 179

Table 5-6. Gene names and potential functions of acetylated proteins in the Mtb wild type (wt) grown at pH 5.5 in the presence of BSA. 180

Table 5-7. Gene names and potential functions of acetylated proteins in the Mtb wild type (wt) grown at pH 5.5 in the absence of BSA. 181

Abbreviations

ABC	ATP-binding cassette
AC	adenylyl cyclase
Acetyl-CoA	acetyl-Coenzyme A
ACG	adenylate cyclase G
ACP	acyl carrier protein
ACS	acetyl-CoA synthetase
ADP	adenosine diphosphate
Ag	antigen
AG	arabinogalactan
AIDS	acquired immune deficiency syndrome
APCI	atmospheric pressure chemical ionisation
ASL	airway surface liquid
ASP	aspartate
ATP	adenosine triphosphate
BCA	bicinchoninic acid assay
BCG	Bacillus Calmette-Guérin
BMDM	bone marrow-derived macrophages
BSA	bovine serum albumin
cAMP	3',5' monophosphate cyclic adenosine monophosphate
CARD9	caspase recruitment domain family member 9
CBD	cAMP-binding domain
c-di-AMP	cyclic dimeric AMP
c-di-GMP	cyclic dimeric GMP
CEF	compound exchange format
CFU	colony forming unit
cGMP	3', 5' cyclic guanosine monophosphate
CIT	citrate
CL	cardiolipin
CLRs	c-type lectin receptors
Cmax	peak serum concentration
cMBT	carboxymycobactin

Cmr	cAMP and macrophage regulator
cNMP	cyclic nucleotide
CO	carbon monoxide
CREB	cAMP response element-binding
CRP	cAMP receptor protein
CSF	cerebrospinal fluid
DAPI	4’,6-diamidino-2-phenylindole
DAT	diacyltrehalose
dATP	deoxyadenosine triphosphate
DC	direct current
dCTP	deoxycytidine triphosphate
DE	delayed extraction
dGTP	deoxyguanosine triphosphate
2,5-DHB	2,5-dihydroxybenzoic acid
DMEM	Dulbecco's minimal essential medium
DMSO	dimethyl sulfoxide
dNTP	deoxyribonucleotide triphosphate
DosR	dormancy survival regulator
dTTP	thymidine triphosphate
ECAR	extracellular acidification rate
ECC	extracting compound chromatograms
EI	electron impact
EIC	extracted ion chromatogram
ELISA	enzyme-linked immunoabsorbent assay
ESAT-6	6 kDa early secretory antigenic target
ESI	electrospray ionisation
ESX1	early secretory system 1
ETC	electron transport chain
FAB	fast atom bombardment
FADH2	flavin adenine dinucleotide
FAS	fatty acid synthesis
FBP	fructose 1,6-bisphosphate
FBS	fetal bovine serum

FCCP	carbonycyanide p-(trifluoromethoxy) phenylhydrazone
FDA	US Food and Drug Administration
FM	foamy macrophages
FUM	fumarate
G3P	glyceraldehyde 3-phosphate
G-6-P	glucose-6-phosphate
GalNAc-Gal-Glc-ceramides	GalNAc, *N*-Acetyl-*D*-galactosamine; Gal, *D*-galactose; and Glc, *D*-glucose
GC	guanine-cytosine
GC-MS	gas chromatography-mass spectrometry
GlcB	malate synthase G
GLO	glyoxylate
GNAT	Gcn5-related *N*-acetyltransferase
H^+	proton
HABA	2-(4-Hydroxyphenylazo)benzoic acid
HAMP	histidine kinases, adenylyl cyclases, methyl-accepting proteins and phosphatases
HILIC	hydrophobic interaction liquid chromatography
HIV	human immunodeficiency virus
HspX	heat-shock protein X
HTH	helix-turn-helix
HTS	high-throughput screening
ICDH	isocitrate dehydrogenase
ICL	isocitrate lyase
IFN-γ	interferon-gamma
IGRA	interferon-gamma release assay
IL	interleukin
IMM	inner mitochondrial membrane
IMS	imaging mass spectrometry
ISOCIT	isocitrate lyase
KAT	lysine acetyltransferase
KDAC	lysine deacetylase
LB	lipid body

LC-MS	liquid chromatography-mass spectrometry
LDL	low-density lipoprotein
LldD1	L-lactate dehydrogenase 1
LldD2	L-lactate dehydrogenase 2
LM	lipomannan
LTBI	latent tuberculosis infection
m/z	mass to charge ratio
MAL	malate
MALDI	matrix-assisted laser desorption ionisation
Man-LAM	mannose-capped lipoarabinomannans
MAPK	mitogen-activated protein kinase
MB	methyl-branched
MBT	mycobactin
MbtA	salicyl-AMP ligase
MbtK	mycobactin synthetase protein K
MbtM	fatty acyl-AMP ligase
MCP	methylcitrate pathway
Mdh	malate dehydrogenase
MDR	multidrug resistant
MMP	methylmalonyl pathway
MOI	multiplicity of infection
MRSA	methicillin-resistant *Staphylococcus aureus*
MS/MS	tandem mass spectrometry
MscL	large-conductance mechanosensitive channel
Mtb	*Mycobacterium tuberculosis*
MTBC	*Mycobacterium tuberculosis* complex
NaCl	sodium chloride
NADH	nicotineamide-adeninedinucleotide
NF-kB	nuclear factor kappa beta
NK	natural killer
NLR	NOD-like receptor
NO	nitric oxide
OAA	oxaloacetate

OCR	oxygen consumption rate
OD	optical density
OMM	outer mitochondrial membrane
PAMPs	pathogen-associated molecular patterns
PAT	poly-acylated threaloses
Pat	protein acetyltransferase
PBC	phosphate binding cassette
PBS	phosphate-buffered saline
PCA	principal component analysis
PDE	phsphodiesterase
PDH	pyruvate dehydrogenase
PDIM	phthiocerol dimycocerosates
PE/PPE	N-terminal ProGlu and ProProGlu
PEP	phosphoenolpyruvate
PFA	paraformaldehyde
Pgk	phosphoglycerate kinase
PGL	phenolic glycolipids
p-HBA	*p*-hydroxybenzoic acid
PIMs	phosphatidyl-*myo*-inositol mannosides
PKA	protein kinase A
PknD	eukaryotic-like Serine/Threonine protein kinase
PLs	phospholipids
PPD	purified protein derivative
PPP	pentose phosphate pathways
(p)ppGpp	guanosine-tetra and pentaphosphate
PRRs	pattern recognition receptors
PTM	post-translational modification
PYR	pyruvate
Q	quadrupole
Q-TOF	quadrupole time-of-flight
RcsA	regulator of capsule synthesis A
RcsB	regulator of capsule synthesis B
Redox	reduction/oxidation

RF	radio frequency
RLRs	retinoic acid-inducible gene (RIG)-I-like receptor
RNI	reactive nitrogen intermediates
ROS	reactive oxygen species
RpfA	resuscitation promoting factor
SahH	S-adenosylhomocysteine hydrolase
SDS	sodium dodecyl sulfate
SGL	sulfoglycolipids
SigF	sigma factor
SIL	stable isotopically labelled
SILAC	stable isotope labelling with amino acids in cell culture
SL	sulfolipids
SR	scavenger receptor
SSC	sodium citrate
SUC	succinate
SUC-CoA	succinyl-CoA
Syk	spleen tyrosine kinase
T3SS	type III secretion system
TAG	triacylglycerol
TB	tuberculosis
TCA	tricarboxylic acid
TDM	trehalose-6,6´-dimycolate
Th	T helper
TLR	toll-like receptors
TMM	trehalose monomycolates
TNF-α	tumour necrosis factor-α
Tpi	triosephosphate isomerase
TSS	transcriptional start site
TST	Mantoux tuberculin skin test
Vfr	virulence factor regulator
WHO	world health organisation
XDR	extremely drug-resistant
αCHCA	alpha-cyano-4-hydroxycinnamin acid

α-KG	α-ketoglutarate
Δφm	mitochondrial transmembrane potential

Chapter 1: Introduction

1. Introduction

1.1 Tuberculosis

1.1.1 Disease epidemiology

Tuberculosis (TB) is an ancient infection caused by strains from the *Mycobacterium tuberculosis* complex (MTBC). Comas *et al.* established, after analysing 259 strains from the MTBC, that they emerged 70,000 years ago and have managed to adapt to the change in human populations.[1] TB used to kill one in five adults in Europe and North America between the seventeenth and nineteenth centuries.[2] Currently, TB is the leading cause of death by a single infectious agent. In 2017 it was estimated that 10 million people fell ill from TB and 1.6 million people died from this disease among human immunodeficiency virus (HIV)-negative people.[3] TB remains one of the major causes of morbidity as well as mortality, mainly in developing countries. According to the World Health Organisation (WHO), from the six regions of WHO Member States (Africa, the Americas, South-East Asia, Europe, the Eastern Mediterranean and Western Pacific), about 82% of TB deaths among HIV-negative people happened in the WHO African region and the WHO South East Asia region in 2017. India accounts for 32% of global TB deaths in HIV-negative people.[4] The eight countries with the highest TB incidence were India, Indonesia, China, the Philippines, Pakistan, Nigeria, Bangladesh and South Africa, accounting for 66% of the estimated cases (Figure 1-1). Globally, TB incidence and mortality are decreasing at a rate of about 2% and 3% annually respectively, which is not fast enough to reach the first milestone of the 'End TB Strategy' in 2020.[3] By that date the TB incidence rate should be falling at 4-5% per year, and the proportion of people with TB who die from it should fall to 10%.[4] Specific targets for 2030 are an 80% reduction in TB incidence and a 90% reduction in absolute number of TB deaths compared with 2015 levels.[4]

The phenomenon of drug resistance was first described in TB in 1948.[5] Demerec *et al*. showed evidence of how streptomycin and penicillin resistance originate spontaneously via genetic changes comparable to gene mutations.[5] The emergence of highly drug-resistant TB including MDR (multi-drug resistant TB) and XDR-TB (extremely drug-resistant TB) is a critical complication for effective TB control in many settings.[4] MDR-TB consists of resistance to at least rifampicin and isoniazid whereas XDR-TB is resistant to at least one fluoroquinolone (ciprofloxacin, ofloxacin, levofloxacin and moxifloxacin) and one injectable antitubercular antibiotic in addition to MDR. Drug-resistant TB happens to be particularly high in former Soviet Union countries, with 38% of all reported TB cases in Belarus being caused by MDR-TB, threatening to spread into low-burden countries.[4]

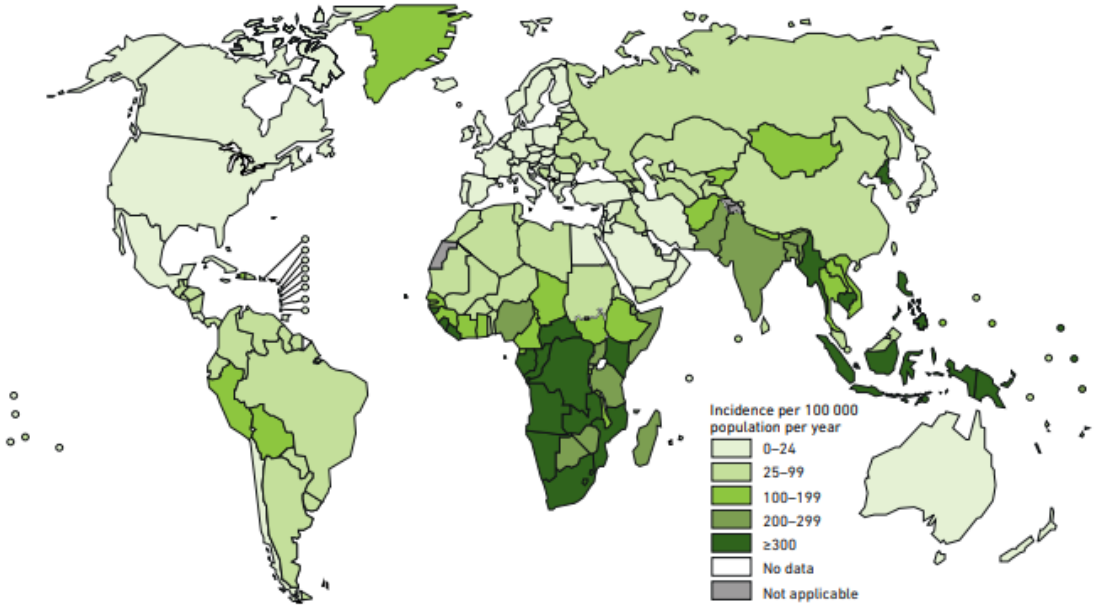


Figure 1-1. World map of TB incidence rate in 2017.
The annual number of incident TB cases relative to population size changed extensively among countries in 2017, from under 10 per 100,000 population in most high-income countries to 150–400 in most of the 30 high TB burden countries, and above 500 in a few countries including South Africa, Lesotho, the Democratic People's Republic of Korea, Mozambique and the Philippines. Figure reproduced from the WHO Global Tuberculosis Report 2018.[4]

Mycobacterium tuberculosis (Mtb) was isolated in 1882 by Robert Koch using methylene blue staining. He identified, isolated and cultivated the mycobacteria in animal serum and reproduced the disease by inoculating the pathogen into guinea pigs, rabbits and cats.[6,7] Mycobacteria are acid-fast organisms and can be stained with the Ziehl-Neelsen method. This method became known in the 1890s and consists of heat helping to drive the primary stain into the mycobacteria waxy cell walls.[8] Members of the same genus are pathogenic and include *M. leprae,* the causative agent of leprosy; *M. ulcerans*, the causative agent of Buruli ulcer*,* and *M. avium*, which in immunocompromised patients causes inflammation of the intestinal wall leading to chronic inflammatory bowel disease; it can also cause pulmonary disease.[9] The MTBC is composed of mycobacterial species able to cause TB. These are *M. microti*, *M. bovis*, *M. suricattae*, *M. africanum*, *M. canettii*, *M. caprae*, *M. pinnipedii*, *M. orygis*, *M. mungi* and Mtb.[10,11]

Mtb is transmitted via aerosols and it affects the lungs and extra-pulmonary tissues; TB meningitis accounts for about 5% of all extra-pulmonary TB cases.[12–14] Mtb infects alveolar macrophages and can be cleared by the innate immune response or by the adaptive immune response.[15,16] If the bacterium is not eliminated, TB leads to two clinically defined states: latent

TB infection (LTBI) or active TB infection. It is estimated that a third of the global population has a LTBI, which is asymptomatic and non-transmissible.[3,12] Regarding active TB, it is transmissible in the case of pulmonary TB and involves symptoms such as lack of appetite, weight loss, cough and haemoptysis.[12,15,16]

Mtb infection is transmitted from person to person via airborne droplets from the throat and lungs of active TB patients, produced while sneezing and coughing. The inhaled infectious droplets are deposited in the lower lungs,[17] where they are engulfed by alveolar macrophages. If alveolar macrophages fail to eliminate Mtb, the bacteria invade the lung interstitial tissue.[12] This can happen either as a result of the mentioned macrophages migrating to the lung parenchyma or if the bacilli infect the alveolar epithelium directly. Following this, inflammatory monocytes or dendritic cells transport Mtb to pulmonary lymph nodes for T cell priming, which leads to the recruitment of immune cells (T cells and B cells), to the lung parenchyma to form a granuloma. Mtb replicates within the growing granuloma and if the bacterial load becomes too high, the granuloma fails to contain the infection, leading to mycobacteria dissemination to other organs, including the brain. At this stage, Mtb can enter the bloodstream or re-enter the respiratory tract to be released and infect the next host.[12]

An individual can carry the latent form of the infection and never develop active TB (90% of cases).[18] However, under certain circumstances, such as HIV infection, undernutrition, type 2 diabetes mellitus, alcohol abuse or smoking, the macrophages in the granuloma can suffer necrosis supporting bacterial growth, hence active TB and transmission to the new host.[12,19]

1.1.1.2 HIV-coinfection

The WHO considers the risk of developing TB to be between 16-27 times higher in HIV-infected people compared to uninfected people. In 2017, 10 million people suffered from active TB globally, 900,000 of these were people living with HIV. Fifty-seven per cent of TB cases among people living with HIV were not diagnosed or treated, which led to 300,000 TB-related deaths among people living with HIV in 2017.[4] In high-burden TB areas such as sub-Saharan Africa, as many as three-quarters of TB patients are co-infected with HIV. In those countries, efforts to control the disease are overwhelmed by the increasing incidence of TB in parallel with the HIV/acquired immune deficiency syndrome (AIDS) epidemic.[4] TB is also the most common cause of AIDS-related death. Hence, HIV and Mtb act in synergy, accelerating the decline of immunological functions and resulting in subsequent death if untreated.[20]

1.1.2 Mtb treatment

Active TB, if not treated, can be fatal. Approximately 50% of patients who develop active TB disease will die from it if they do not receive treatment.[21] Treatments for patients with drug-sensitive TB last at least six months: the recommended treatment by the WHO is an initial two-month intensive phase (isoniazid, rifampicin, pyrazinamide, and ethambutol daily), continued by dual therapy isoniazid and rifampicin for the last four months. If the treatment is adhered to, treatment success is approximately 85%. Apart from the economic value and efficacy, the regimen is lengthy, hepatotoxic, and not well tolerated by a considerable proportion of patients to which the medication has been prescribed.[22]

Regarding MDR-TB, the most recent estimates suggest that there are approximately 480,000 new cases each year, of which only 20% are being treated.[4] Treatment of MDR-TB generally lasts 20 to 24 months and involves daily administration of different drugs on the basis of efficacy, cost and safety including one fluoroquinolone and one injectable drug which can be either capreomycin, kanamycin or amikacin.[23,24] Unfortunately, many of these drugs have serious side effects such as peripheral neuropathy and renal toxicity effects,[25] leading to an increased rate in early discontinuation of treatment, further increasing resistance. Adding to the TB burden are XDR-TB cases, which are resistant to the four first-line drugs and at least one second-line drug, making them very difficult to treat.[3]

1.1.3 Prevention of Mtb

The only licensed vaccine used to prevent active TB is the BCG vaccine.[4] BCG stands for 'Bacillus Calmette-Guérin', named after the two French scientists who developed the first TB vaccine, Albert Calmette and Camille Guérin, in 1919. The vaccine was made by passaging the animal pathogen *M. bovis* 230 times over a period of 11 years[26] to develop an attenuated strain, which was demonstrated to fail to produce progressive TB when used for the first time in an infant in 1921.[27] The BCG vaccine is mainly believed to mediate immunity via the development of antigen (Ag)-specific memory T cells that act fast after Mtb infection. This is the primary reason why BCG works against disseminated TB as well as TB meningitis.[28] Morbidity and mortality rates are high in children under the age of five suffering from TB. Studies in children in this age bracket have shown 50% to 80% efficacy of the BCG vaccine against severe, extra-pulmonary TB such as TB meningitis. Therefore, this vaccine is a priceless tool in preventing active TB disease in children.[29] However, the efficacy of this vaccine against pulmonary TB has been measured to be 0% to 80% and the reasons behind this high variability are not well understood.[30] Analyses of BCG vaccine efficacy have shown that the protection lasts in most cases no longer than 10 years, making it

unlikely to protect adolescents or adults, who happen to be the majority of transmissible, pulmonary active TB cases.[12] It still remains uncertain why BCG does not prevent primary infection, reactivation, and pulmonary TB. However, it is widely accepted that generating long-term protective immunity is necessary.[28]

1.1.4 Current diagnostic tools

To diagnose LTBI two main tests are available; the Mantoux tuberculin skin test (TST) and the Interferon-γ (IFN-γ) release assay (IGRA).[31] TST consists of injecting two or five tuberculin units of purified protein derivative (PPD) RT23 or Standard (S) respectively.[32] PPD-S was adopted as the international standard of tuberculin by the WHO in 1952[33] and in the year 2000s PPD-S2 was developed and is the current US standard for PPD tuberculin.[34] RT23 is produced by the Statens Serum Institute and is currently the most widely used PPD product globally.[33,35] The patient will develop a hypersensitivity reaction after 48 to 72 hours if it has cell-mediated immunity to the injected antigens.[32] This test is very useful in low-income countries. However, it is unable to differentiate between Mtb infection and BCG vaccination or exposure to non-tuberculous mycobacteria. Thus immune responses would be triggered by homologous antigens from BCG vaccination or environmental bacteria, hence giving false positive results.[33,36] Later on, in the 2000s, the IGRA was developed, aiming to replace TST since BCG vaccination does not alter the IGRA test results. The IGRA is an *in vitro* blood test, which measures the IFN- γ release by memory T-cells after being stimulated by RD-1 antigens.[37] These antigens are far more specific than PPD as they are not as widely spread in other mycobacteria such as *M. bovis* BCG or many non-tuberculous mycobacteria which avoids cross-reactivity.[31] Notably, neither test can differentiate between LTBI and active TB. Therefore, if they are positive, further tests are required.[12] When the risk of disease is higher, such as in patients unable to contain the infection due to immunosuppression, or those patients who are very old or very young or individuals with close contact to a person known to have an active TB infection; testing for LTBI is useful.[38] For the detection of active TB there are four main tools: imaging techniques, microscopy, bacterial cultures and molecular tests.[12] Although chest X-rays are used for screening, abnormal radiographies require microbiological diagnosis.[12] In low and middle-income countries, microscopy of sputum smear is the most widely used diagnostic tool. Nevertheless, a molecular assay-based technology named Xpert MTB/RIF is gaining popularity. The reason behind this is the higher accuracy compared to the microscopy test and the ability to detect rifampicin-resistant infections. The Xpert MTB/RIF assay is a real-time PCR, which may be used to detect Mtb DNA sequences in sputum samples.[39] Thus, this molecular test has become the WHO recommendation as the first-line diagnostic test for active TB suspected cases.[3] In addition to

Xpert MTB/RIF, the WHO recommends using loop-mediated isothermal amplification for pulmonary TB diagnosis and molecular line probe assays for fast drug sensitivity testing of first- and selected second-line drugs.[40–42]

1.2 Mtb pathogenesis

1.2.1 Cell envelope lipids

The cell envelope in mycobacteria plays a crucial role in bacteria survival within the host cell, which can be macrophages, neutrophils, monocytes or dendritic cells.[43] Mtb's cell envelope is unique in its composition and constitutes 60% of the dry cell mass.[44] It is composed of a plasma membrane, a cell wall core and the capsular layer (Figure 1-2).[44] Apart from the capsular layer the cell envelope is composed mainly of lipids such as triacylglycerol (TAG) and phospholipids (PLs), which are common in most bacteria such as *E. coli*, as well as others that are specific to *Actinomycetales*, including mycobacteria such as phosphatidyl-*myo*-inositol mannosides (PIMs), constituting 45% of the mycobacterial plasma membrane.[45–47] The cell wall core is made of the mycomembrane and peptidoglycan covalently linked to Arabinogalactan (AG).[48] The mycomembrane presents a bilayer arrangement; the inner leaflet is formed of α-alkyl, β-hydroxy long-chain mycolic acids, which are very long fatty acid chains (60 to 90 carbon atoms) linked to AG,[49] and the outer leaflet is made of free, lipids and glycolipids, which are non-covalently bound to the cell, like trehalose monomycolates (TMM), cardiolipin (CL), glycerol monomycolates, glycerophosphatidyl-ethanolamine (PE), glucose monomycolates, trehalose dimycolates (TDM), phthiocerol dimycocerosates (PDIM), poly-acylated threaloses (PAT), sulfolipids (SL), PIMs with up to six mannose residues, phenolic glycolipids (PGL) and mannose-capped lipoarabinomannans (Man-LAM).[50] Mycobacteria present low numbers of pore-forming proteins[51] in comparison to *E. coli,* which has a 45-fold higher number of porins.[52] This could explain both the limited permeability of mycobacterial cell envelopes and the generally rather low susceptibility of these bacteria to toxic agents.[49] The major components of the outermost capsular layer of Mtb are two polysaccharides (glucan and arabinomannan).[53,54]

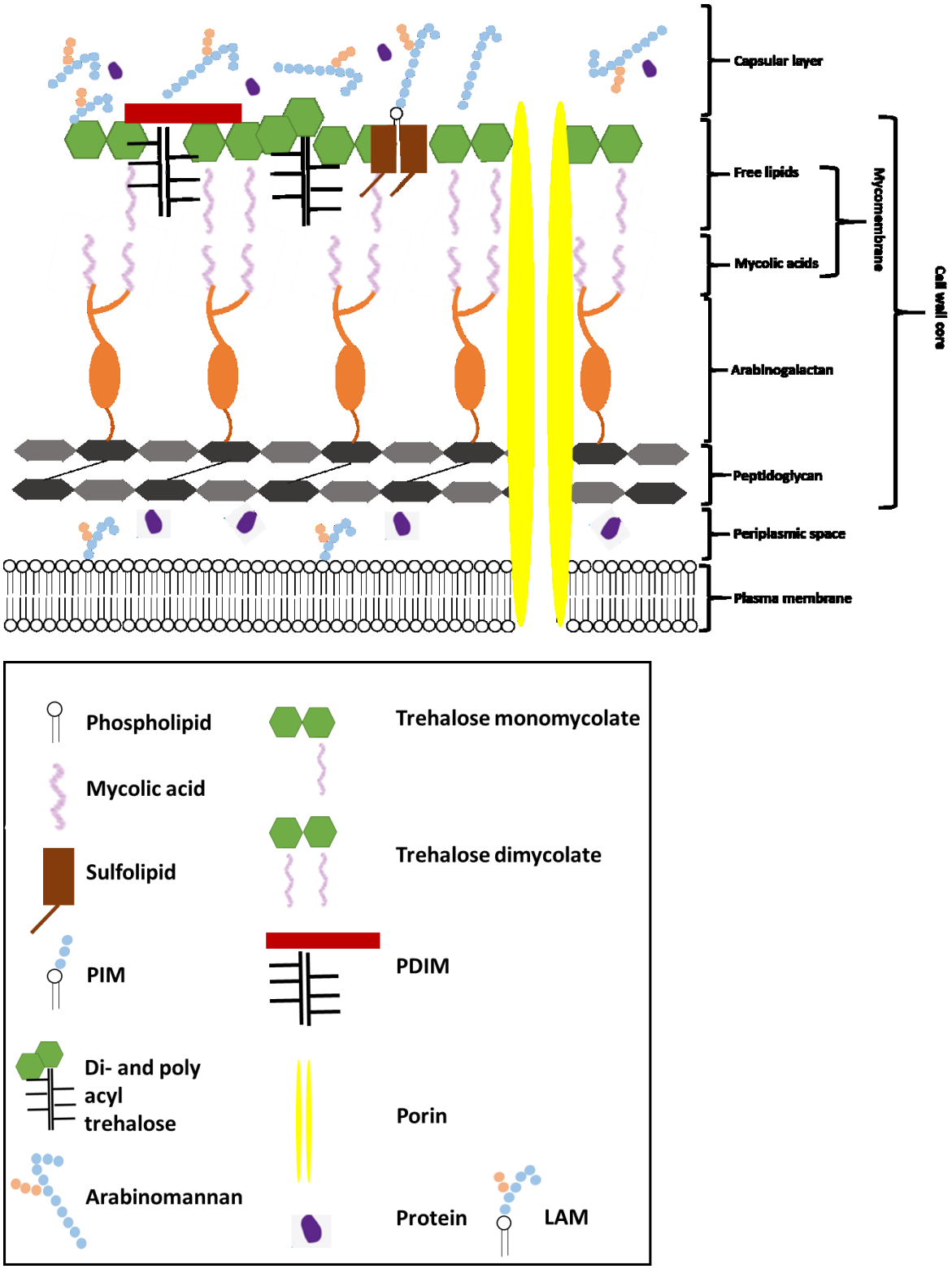


Figure 1-2. Scheme displaying the Mtb cell envelope.
The cell envelope is composed of the capsular layer, the cell wall core and the plasma membrane. The plasma membrane is made up of phospholipids. The cell wall core presents the mycomembrane and PG covalently linked to AG. The mycomembrane is organised as follows: an inner leaflet made up of long-chain mycolic acids linked to AG and an outer leaflet composed by free lipids. The figure legend shows different elements of the cell envelope. Figure adapted from Gago *et al.*[50]

Some lipids associated with the cell envelope, such as PDIM, play a role in Mtb virulence and have effects on the immune response from the host.[55]

1.2.2 Immune response against Mtb infection

Mtb is an intracellular pathogen and its elimination is achieved via a combination of different killing mechanisms, which include apoptosis of host macrophages.[56] This is led by T helper 1 (Th1) type pro-inflammatory cytokines, such as IFN-γ, crucial in the protective immune response to TB.[57] Upon infection of the lung, macrophages, neutrophils, monocytes or dendritic cells recognise pathogen-associated molecular patterns (PAMPs) on Mtb through their pattern recognition receptors (PRRs)[58] (Figure 1-3). PRRs are a family of receptor proteins from the host that sense the microbial infection by being able to recognize different PAMPs.[59] Both the innate and adaptive immune response against Mtb are dependent on recognition of Mtb by PRRs.[60] Different PRR families have been characterised, including transmembrane proteins such as the Toll-like receptors (TLRs), the c-type lectin receptors (CLRs), Scavenger receptors (SR) and cytoplasmic proteins like the NOD-like receptors (NLRs) and the Retinoic acid-inducible gene (RIG)-I-like receptors (RLRs).[58,61] Mtb is recognised by TLRs including TLR2, TLR4, TLR9 and TLR8.[58,62–66] Binding of Mtb ligands to TLRs initiates the release of pro-inflammatory cytokines, expression of adhesion molecules as well as the recruitment of macrophages, dendritic cells and polymorphonuclear leukocytes to the site of infection.[58,67] TLRs are a single membrane-spanning receptor family. Ten TLRs have been discovered in humans and 13 in mice.[62,68,69] They are of vital importance for innate immunity and the induction of adaptive immunity to infections.[58,70,71]

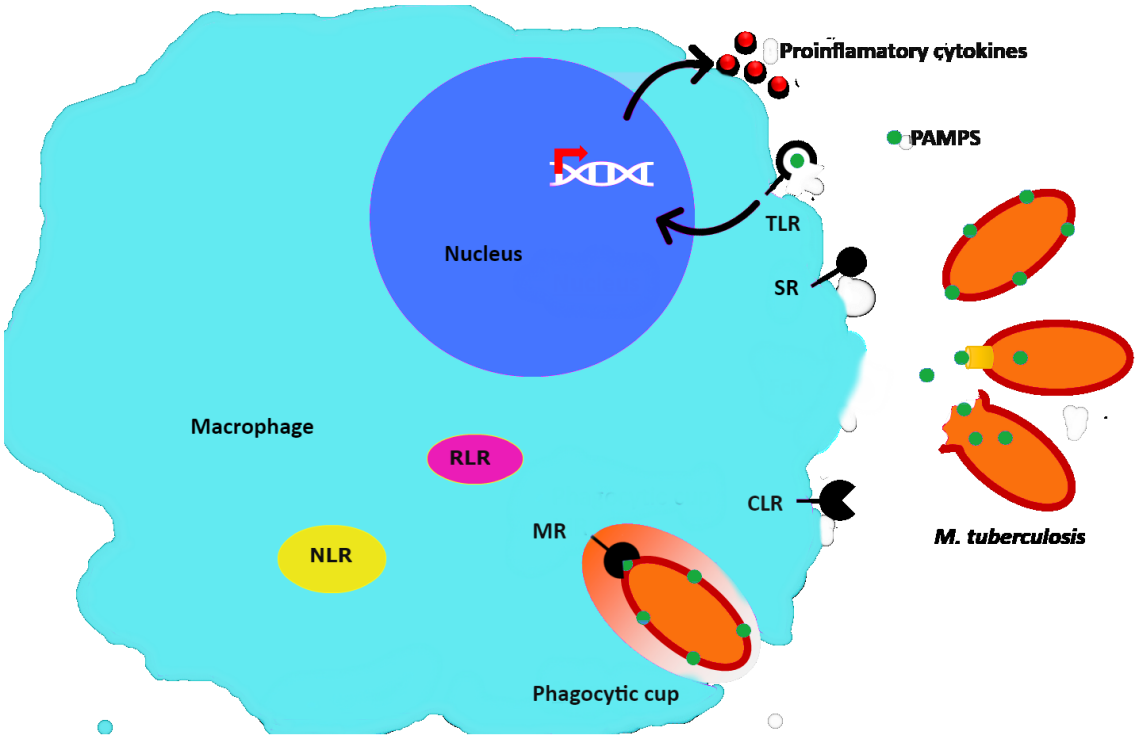


Figure 1-3. Schematic diagram showing how Mtb bacilli are detected by alveolar macrophages. Mtb presents pathogen-associated molecular patterns (PAMPs), which are recognised by pattern recognition receptors (PRRs) from the host cell. PAMPs are expressed at the bacterium cell envelope, released or secreted upon cell death. PRRs can be transmembrane or cytosolic. Transmembrane PRRs include Toll-like receptors (TLRs), Scavenger receptors (SRs) and c-type lectin receptors (CLRs). When lipoarabinomannan PAMPs bind to the mannose receptor (MR), which is a CLR, it triggers phagocytosis of Mtb. Nod-like receptors (NLRs) and Retinoic acid-inducible gene (RIG)-I-like receptors (RLRs) are cytosolic receptors. The binding of Mtb ligands to PRRs in the host cells promotes the release of pro-inflammatory cytokines such as interleukin (IL)-12 and IL-18 which results in the recruitment of macrophages and other immune cells to the site of infection. Figure adapted from Mortaz *et al.*[58]

TLRs recognise PAMPs or endogenous inflammation-associated molecules,[62,63] which are different molecular structures of microorganisms. Different microorganisms are detected by different TLRs[62–66] and their activation upregulates the transcription of pro-inflammatory cytokines by the activation of the nuclear factor kappa beta (NF-kB) and mitogen-activated protein kinase (MAPK) signalling pathways.[58,72] TLR2 has been reported to bind peptidoglycan lipoproteins as well as cell-wall glycolipids such as lipomannan (LM), LAM and PIM, which are released from viable mycobacteria and traffic out of the phagosome.[72–74] TLR4 has been shown to bind to tri- and tetra-acylated LMs *in vitro*[75] while unmethylated CpG motifs (cytosine triphosphate deoxynucleotide and guanosine triphosphate deoxynucleotide) from Mtb DNA have been seen to interact with TLR9, being a potent stimulus of TLR9-dependent pro-inflammatory cytokine production by macrophages and dendritic cells.[72] TLR2 is thought to be crucial in innate host defence initiation against Mtb.[76,77] Furthermore, TLR2 is required for the

production of interleukin (IL)-1β[78] and is also important for IL-12 release in macrophages.[79] Even though the innate immune response is critical to start the defence against Mtb, the adaptive immune response is needed in order to contain the infection in the chronic stage of TB.

In the adaptive immunity against Mtb, antigen specific CD4+ T cells secrete IFN-γ, which activates macrophages to kill intracellular bacteria.[80] Furthermore, CD8+ T-cells are also important for controlling Mtb during the chronic phase of infection.[81,82] It has also been shown that Th17 are involved in Mtb immune control.[58] They secrete IL-17, a proinflammatory cytokine, which provides IFN-γ-dependent or IFN-γ-independent protection against Mtb infection.[58,83] The secretion of cytokines like IL-12, tumour necrosis factor-α (TNF-α), IL-1α, IL-6, IL-1β, and nitric oxide (NO) with mycobactericidal activity,[84] plays an important role in the recruitment of immune cells to the site of infection and granuloma formation.[85,86] To maintain chemokine concentrations for cellular retention and recruitment, constant TNF-α signalling is required.[87–90] Furthermore this cytokine is considered a double-edged sword as it not only has a role in the apoptosis induction of infected cells and maturation of dendritic cells[86] but its dysregulation may impede an immune response against Mtb, via promoting mycobacterial growth in human monocytes and leading to extensive tissue damage.[86]

1.2.2.1 Granuloma

The early granuloma is made up of foamy macrophages (FM), activated macrophages named epitheloid cells and giant Langhans cells, which consist of fused macrophages; all surrounded by T-lymphocytes[91,92] (Figure 1-4). Macrophages become foamy cells via a dysregulation in the balance between the influx and efflux of low-density lipoprotein (LDL) particles from the serum.[93] LDL is internalised via LDL receptors or, in the oxidised form, through SR such as SRA and CD36. The LDL particles contain PLs, cholesterol, and TAG. Even though the majority of the PLs and TAGs are metabolised, the cholesterol is kept by the macrophage in an esterified form.[94] Once LDL has broken down, cholesterol is imported into the cell cytosol, where it is either esterified and sequestered into lipid bodies (LB) formed in the endoplasmic reticulum leaflet or pumped out of the cell by ATP-binding cassette (ABC) transporters.[90]

As the granuloma matures, the number of blood vessels penetrating into it starts to decrease and it develops a fibrous capsule. This capsule surrounds the macrophage core and prevents most of the lymphocytes from making contact with the granuloma core. Furthermore, as the granuloma matures, the number of FM in the fibrous capsule increases; this would be the reason why caseous debris accumulates in the centre of the granuloma.[94] This foresees the progression

to active TB. In the case of an immunocompetent individual, individual granulomas would have localised progression but the majority of granulomas in the tissue will be contained by the immune system. However, in immunodeficient patients, the caseus necrotic centre of the granuloma would liquefy and make cavitations, releasing thousands of Mtb bacilli into the airways.[90] Thus, Mtb can persist within the granuloma and it is able to reactivate leading to active TB.[92]

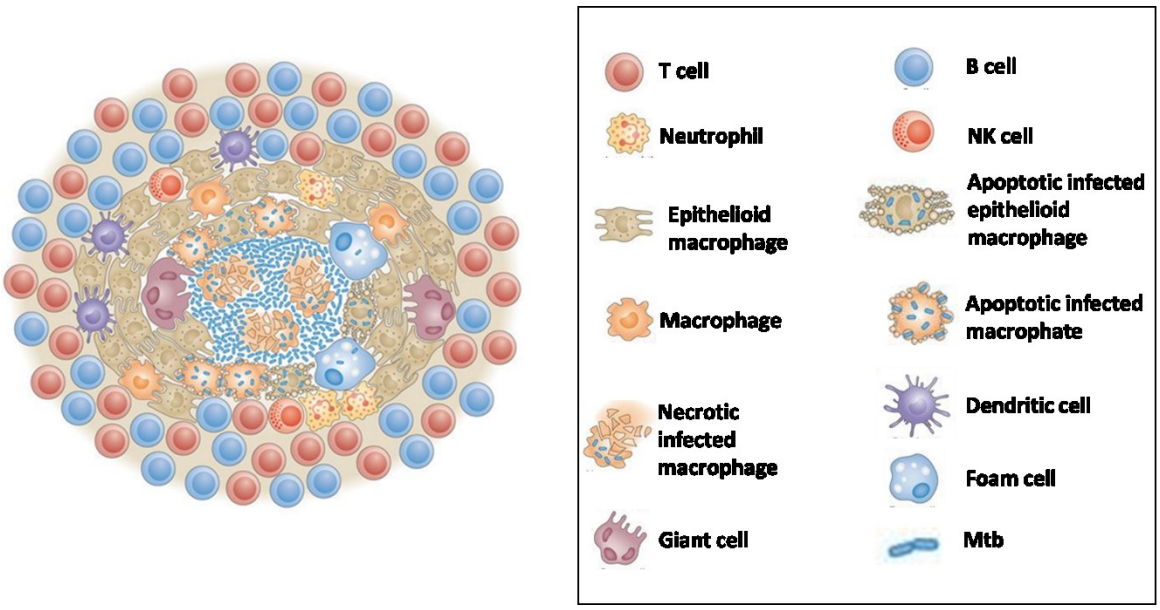


Figure 1-4. The Mtb granuloma.
The TB granuloma is an organised and compact aggregate of macrophages that have undergone a specialised transformation to have tightly interdigitated cell membranes that link adjacent cells. This type of macrophages are named epithelioid cells and may be highly phagocytic. Granuloma macrophages can fuse into multinucleated giant cells or differentiate into foam cells.. Foam cells and multinucleated giant cells contain only a few bacteria, if any. Mtb is most commonly found in the central necrotic areas in which dead and dying macrophages can be seen. Other cell types also populate the granuloma. These include dendritic cells, neutrophils, B and T cells, fibroblasts, natural killer cells, and cells that secrete extracellular matrix components. Figure reproduced from Ramakrishnan *et al.*[95]

1.2.3 Host immune evasion

Mtb is able to replicate inside macrophages and supress their microbicidal activity by inhibiting phagosome maturation, evading autophagy or inhibiting pro-inflammatory cytokine production. Lipids on the cell envelope facilitate some of these mechanisms;[19,96] for instance, ManLAM has been shown to impair the pro-inflammatory cytokine production and boost IL-10 production, an anti-inflammatory cytokine by dendritic cells.[96,97] Another example of undermining innate

immunity is the usage of sulfoglycolipids (SGL) as competitive antagonists of TLR2. This strategy inhibits NF-kB, the consequent expression of costimulatory molecules and the production of cytokines.[96] Furthermore, in murine bone marrow-derived macrophages (BMDM), when TDM binds to the PRR monocyte-inducible C-type lectin (Mincle), a member of the CLR family, pro- and anti-inflammatory cytokines are produced, some of which are TNF-α, NO and IL-10 via the spleen tyrosine kinase (Syk)/caspase recruitment domain family member 9 (CARD9) signalling axis.[98] It has also been shown how TDM delays the maturation of phagosomes and their fusion to lysosomes through the Fcγ receptor. Studies by Axelrod *et al.* showed that when TDM is coupled onto beads, it slows down phagosome maturation and the retention period in the early, non-acidified and hydrolytically restricted stage of the mycobacterial phagosome.[99,100]

Another mechanism used by Mtb to evade the immune system was revealed in recent work by Passemar *et al.*[101] By deleting multiple Mtb polyketide synthetases, which are enzymes involved in the biosynthesis of SL, diacyltrehalose (DAT)/PAT and PDIM; they disclosed how the functions of the lipids in the cell envelope overlap on host-pathogen interactions.[101] In fact, PDIM masked the function of other lipids appearing to be a dominant lipid virulence factor (Figure 1-5). PDIM are specific to pathogenic bacteria.[45,46,47] They mask the PAMPs present on the Mtb surface, which will not be recognised by TLR signalling. This way, PDIMs avoid the recruitment of microbicidal macrophages and so are required for virulence by mediating an immune evasion strategy.[102] This work also sheds light on how TLR-mediated immunity is non-essential in the protection against Mtb infection in both animal and human studies.[102,103] Mtb escapes the phagosome to reach the cytosol of the host cell. Once it has gained access to the cytosol, the bacterium induces necrosis so it can leave the infected cell and disseminate.[104–107] Quigley *et al*. suggest that PDIM could contribute to the exit of Mtb from the phagosome.[108] They also propose that the necrosis in the host cell could be a result of the high number of cytosolic bacteria. PDIM might have a direct role in necrosis induction in addition to its phagosomal escape function. This could happen through the potential interaction of PDIM with mitochondrial membranes, which would lead to an increase in reactive oxygen species (ROS) production thus initiating cell necrosis. It is known that the 6-kDa early secreted antigenic target (ESAT-6), also called EsxA, is required for Mtb to access the cytosol.[104,109,110] The work from Quigley *et al.* suggests that PDIM might function in synergy with EsxA to help Mtb escape the phagosome. Even though PDIM is not needed for EsxA pore formation, the insertion of this lipid into membranes of the phagosome can change the biophysical characteristics of the membrane to facilitate the insertion of EsxA.[108]

Another strategy used by mycobacteria to escape the immune response is to recruit growth permissive macrophages. This is mediated by the PGL (Figure 1-5) and CCR2 signalling previously seen to be involved in macrophage migration to Mtb. Cambier *et al.* demonstrated that PGL can increase infectivity through chemokine receptor 2 CCR2-mediated recruitment of permissive macrophages at the earliest stages of infection.[102]

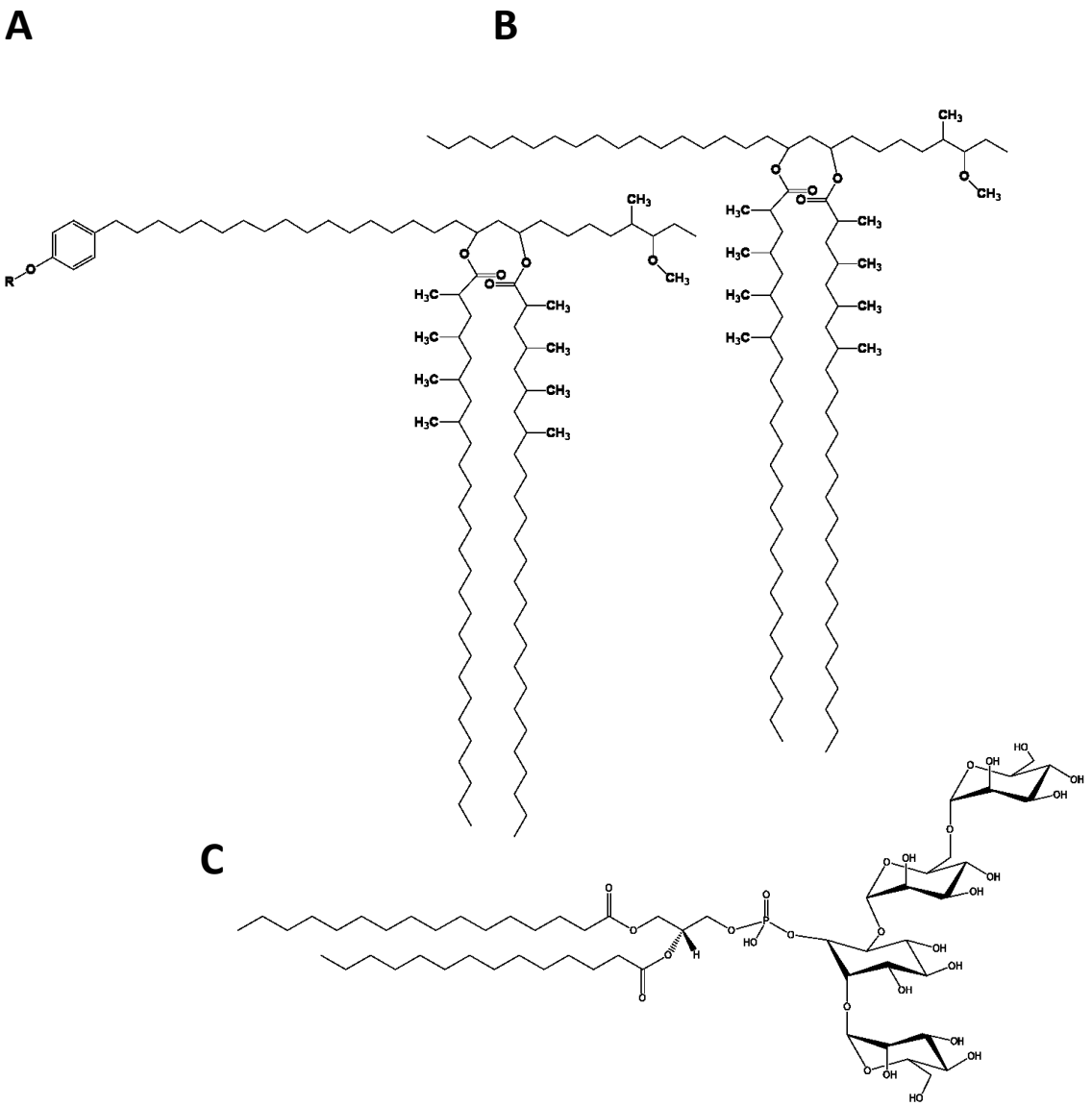


Figure 1-5. Chemical structures of lipid virulence factors.
PGL (A), PDIM (B) and PIM (C).

1.3 Mtb metabolism within the host

1.3.1 Mtb central carbon catabolism

Mtb is a unique microorganism in regard to carbon metabolism due to its unusual niche, which is the alveolar macrophage. Fatty acids and cholesterol are the main carbon sources used by Mtb during infection.[111] However, Mtb uses a diverse range of carbon sources including carbohydrates and amino acids throughout the different infection steps via numerous pathways, which include the tricarboxylic acid (TCA) cycle, glycolysis, the glyoxylate shunt and methylcitrate pathway (MCP) as well as pentose phosphate pathways (PPP).[50,111] De Carvalho *et al.* performed metabolomics studies using dextrose, acetate and glycerol as three model substrates in order to test the central carbon metabolism of Mtb (Figure 1-6).[112] Their data demonstrate that unlike other organisms such as *E. coli* and *Bacillus subtilis*, Mtb does not use carbon catabolite repression but is able to co-catabolise different carbon sources to increase its monophasic growth. This co-catabolism is achieved by the compartmentalisation of every single carbon source to a different metabolic fate meaning that different carbon sources including fatty acids and carbohydrates are used to feed different pathways. Nevertheless, Mtb can also direct simultaneous flux of each carbon source through the same metabolic pathways but in opposite directions; such is the case for glycolysis and gluconeogenesis.[112,113] The importance of glucose phosphorylation, as the first step of glycolysis, has been evaluated in work by Marrero *et al.* who have demonstrated how glucose is available for Mtb *in vivo* and how Mtb needs glucose phosphorylation in order to survive during chronic mouse infection.[114] Their work focused on two glucokinases named ppgK (Rv2702) and glkA (Rv0650).[114] Both are in charge of phosphorylating glucose to produce glucose-6-phosphate (G-6-P), this being the first step in glucose metabolism and thus activating glucose for oxidation through glycolysis (Figure 1-6). G-6-P is involved in the production of energy via glycolysis, reducing power reduction via the PPP and it is also a vital precursor of anabolic processes, which include nucleotide and cell wall biosynthesis. G-6-P could potentially be produced by gluconeogenesis but its production through glucokinase is less costly in terms of energy as it just consumes one molecule of ATP.[114] By generating an Mtb mutant strain lacking ppgK it was discovered that Mtb growth on glucose was attenuated compared to the wild type strain in glucose as a sole carbon source and the mutant incorporated glucose into the central carbon metabolism. The ability of glkA to produce G-6-P was not enough to support Mtb growth on glucose in the absence of ppgK. Mtb would then rely mainly on ppgK activity for growth on glucose as the sole carbon source *in vitro.*[114] Mtb lacking ppgK and glkA was not able to persist in mouse lungs; this provides a deeper insight into glucose metabolism and demonstrates a new

role for glucose phosphorylation in the pathogenesis of Mtb proving how these bacteria do not only rely on host lipid metabolism.[114]

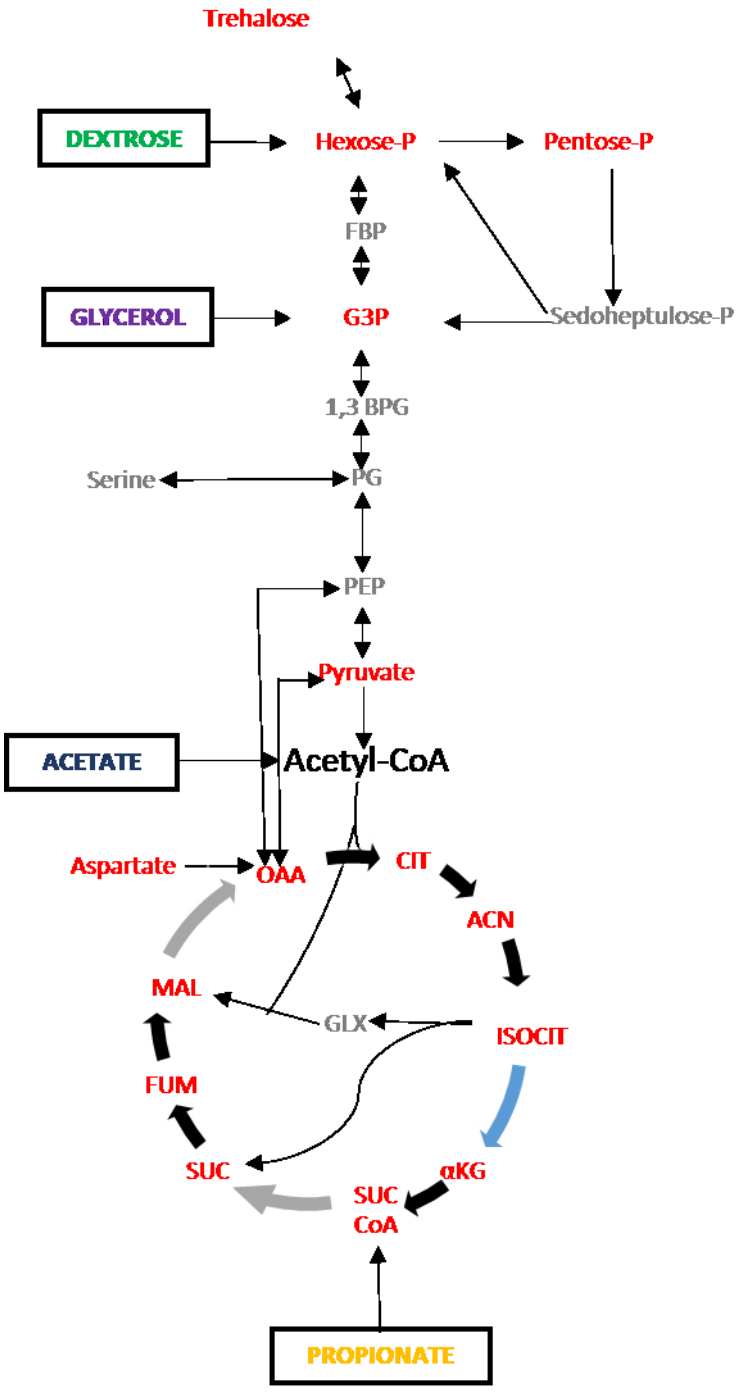


Figure 1-6. Diagram of Mtb central carbon metabolism.
The entry points of carbon sources dextrose, acetate, glycerol and propionate are shown in boxes. Glycolysis, the glyoxylate shunt and gluconeogenesis are shown. Abbreviations: α-KG, α-ketoglutarate; ASP, aspartate; CIT, citrate; FBP, fructose 1, 6-biphosphate; FUM, fumarate; G3P, glyceraldehyde 3-phosphate; GLO, glyoxylate; ISOCIT, isocitrate; MAL, malate; OAA,

oxaloacetate; PEP, phosphoenolpyruvate; PYR, pyruvate; SUC, succinate; and SUC-CoA, succinyl-CoA. Figure adapted from de Carvalho *et al.*[112]

1.3.2 Lipid metabolism

Host lipids are the primary source of carbon for Mtb *in vivo* or in cultured infected macrophages.[115] Mtb containing phagosomes inside the FM surround and gradually engulf the LB, where externally provided fatty acids are stored. These fatty acids, being TAGs, are acquired by hydrolysis of cellular lipids and they are used as nutrients by the mycobacteria.[116] As a consequence, Mtb undergoes changes in its physiology, which lead to a decrease in growth and metabolic activity, antibiotic resistance, and TAG being accumulated inside LB. All these changes are an indication of persistent and non-dividing Mtb.[50,111,117–120]

1.3.2.1 Fatty acid metabolism

There are two pathways needed for fatty acid utilisation. These are the β-oxidation cycle and the glyoxylate shunt (Figure 1-7). The first one degrades fatty acids to acetyl-coenzyme A (acetyl-CoA) (C2) in the case of even-chain fatty acids, and to acetyl-CoA and propionyl-CoA in the case of uneven-chain fatty acids.[118,121] The glyoxylate shunt is used during growth on fatty acids to replenish the TCA cycle if glycolytic substrates are lacking or scarce. These substrates are pyruvate and phosphoenolpyruvate (PEP), and the concentration of these needs to be sufficient to support anaplerosis via the conversion to oxaloacetate by pyruvate carboxylase or PEP carboxylase respectively.[118,121] The glyoxylate shunt (Figure 1-7) is also required when the production of biomass is dependent purely on fatty acids and thus the loss of carbon in the form of CO_2 needs to be avoided.[111,122,123] This loss can happen during the oxidation by α-ketoglutarate (α-KG) dehydrogenase and isocitrate dehydrogenase (ICDH) in the TCA cycle.[124] Isocitrate lyase (ICL) is the first enzyme in the glyoxylate shunt and cleaves isocitrate into succinate and glyoxylate. Then, the second enzyme in the pathway, malate synthetase, catalyses the conversion of acetyl-CoA and glyoxylate into malate and CoA, both allowing Mtb to assimilate biomass when cultured on even-chain fatty acids by bypassing the oxidative decarboxylation of two carbon units associated with the TCA cycle.[125] This has been shown to make malate synthetase crucial for Mtb survival during the acute and chronic stages of infection *in vivo* and conditionally essential for survival on fatty acid substrates *in vitro.*[125] Most Mtb strains express two isoforms of ICL encoded by *icl*1 and *icl*2. Muñoz-Elías *et al.* have shown in lungs from infected mice that Mtb lacking *icl*1 and *icl*2 are unable to grow using fatty acid substrates and are rapidly killed.[118]

Altogether it can be agreed that Mtb depends on the glyoxylate shunt for *in vivo* growth in fatty acids[111,122,123] by facilitating essential cell constituent biosynthesis from C2 units through the generation of C4 intermediates, which serve as biosynthetic precursors.[118,121] Furthermore, malate, as the end product of the glyoxylate shunt, can be oxidised to oxaloacetate which feeds into gluconeogenesis, a biosynthetic pathway, which is vital for the growth on fatty acids. Research performed by Marrero *et al.* has shown that gluconeogenesis is required for Mtb pathogenesis during both active and latent forms of TB since when fatty acids are the primary carbon source for Mtb during infections, mutations that inactivate gluconeogenesis abolish Mtb growth *in vivo.*[111]

1.3.2.2 Cholesterol metabolism

The Mtb cholesterol catabolism is not fully understood since genes have not been assigned to all steps as yet.[126] Cholesterol catabolism involves the oxygen-dependent cleavage of its HsaAB complex A and B steroid rings; the oxidative degradation of its C and D rings; as well as the degradation of its acyl side chain by rounds of β-oxidation[127–129] which yield two propionyl-CoA units and one acetyl-CoA unit per molecule of cholesterol (Figure 1-7). [126] At high concentrations, propionyl-CoA is toxic in Mtb by pyruvate dehydrogenase (PDH) inhibition. Therefore the bacterium can metabolise this precursor of potentially toxic metabolites via the MCP or methylmalonyl pathway (MMP) or synthesis of methyl-branched (MB) lipids.[130–132] The MCP leads to the production of succinate and pyruvate by ICL1 from propionyl-CoA, which feeds into the TCA cycle and generates CO_2.[117,132] An alternative pathway for propionyl-CoA detoxification is via the generation of methylmalonyl-CoA, which can enter the vitamin B12-dependent MMP. This leads to the production of succinyl-CoA.[131] Moreover, methylmalonyl-CoA can be used as building blocks for Mtb's cell wall lipids[133,134] including PDIM, SL, DAT, triacyltrehalose and PAT. These lipids are esterified with up to five multiple MB long-chain fatty acids such as mycolipenic, mycocerosic and mycolipanoic acids, which are synthesised by individual fatty acid synthase complexes from malonyl and methylmalonyl CoA that come from acetyl and propionyl-CoA respectively.[126,135]

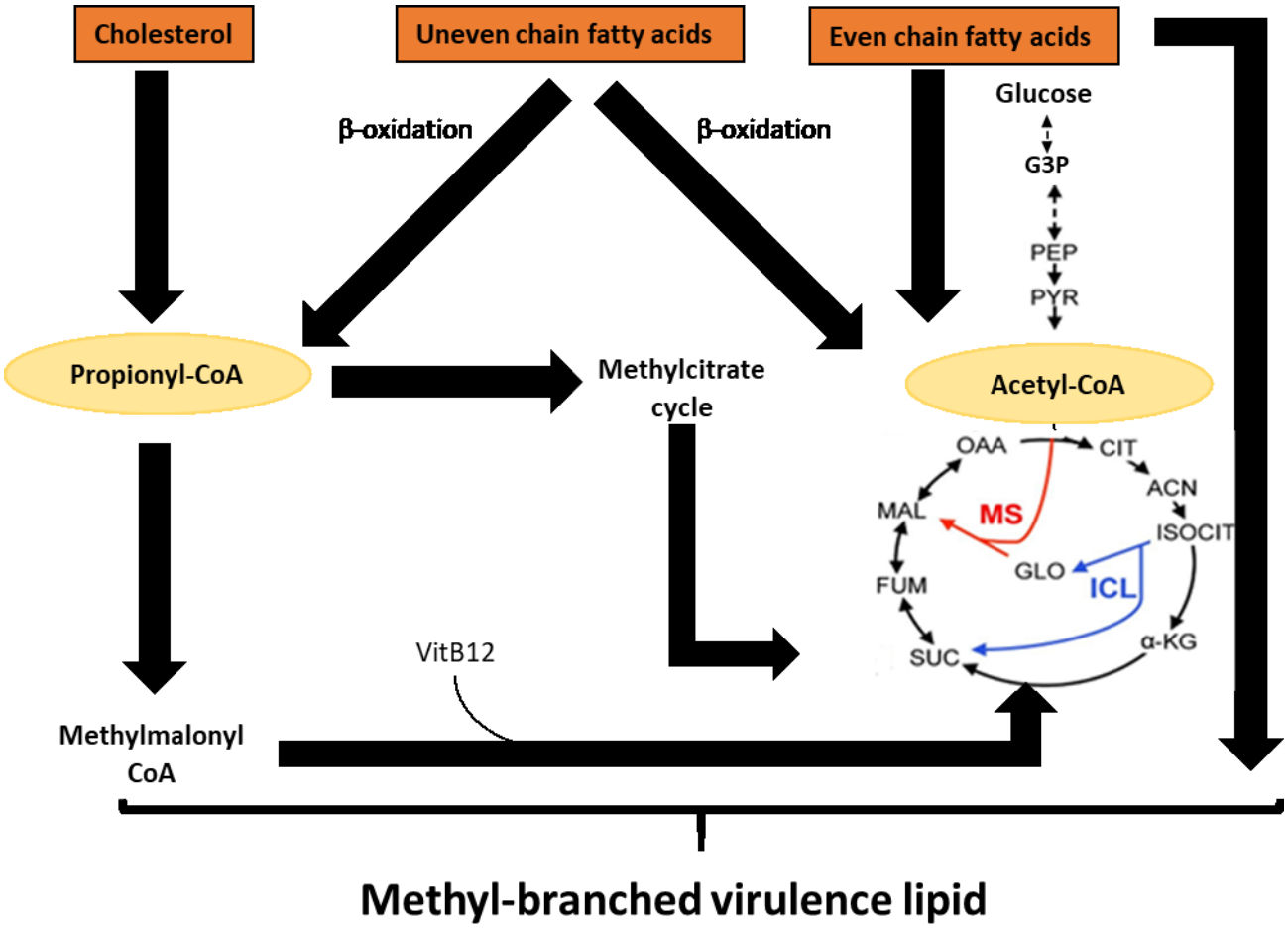


Figure 1-7. Schematic diagram showing assimilation of host lipids.
Mtb can get fatty acids and cholesterol from the macrophage. Degradation of even chain fatty acids by β-oxidation gets acetyl-CoA, which enters the TCA cycle, generating CO_2. However, the degradation of uneven chain fatty acids gets propionyl-CoA on top of acetyl-CoA. Cholesterol also expands the pool of propionyl-CoA. Its accumulation can be toxic for the cell since it can limit acetyl-CoA generation from pyruvate by PDH inhibition. Inhibition of PDH activity puts stronger pressure on the acetyl-CoA pool, which is used as malonyl-CoA for Mtb cell wall lipid assembly. Propionyl-CoA can also be converted to methylcitrate and enter the MCP obtaining succinate, which could enter the TCA cycle. Moreover, propionyl-CoA can enter the Vitamine B12 dependent MMP obtaining succinyl-coA, which would then enter the TCA cycle. Finally, methyl-branched cell wall lipids can be built using n-acyl primers by *de novo* synthesis or from preformed long chain fatty acids imported by Mtb. Figure adapted from Lee *et al.*[136]

ICL1 is crucial for relieving propionyl-CoA toxicity via the MCP.[118] Lee *et al.* used biochemical and genetic manipulation of the MMP and MCP to report the metabolic needs for propionyl-CoA incorporation into PDIM and other lipids of the bacterial cell wall associated with virulence. By using a strain lacking *icl1* (*Δicl1)* and the wild type Erdman Mtb strain Lee *et al*. demonstrate that both strains can access and use fatty acids from the host lipid stores in order to assemble MB precursors of the virulence lipids.[136] Furthermore, their work shows that the Mtb wild type

incorporates propionyl-CoA into TAG and PDIM when exogenous propionate is present. However, it can also be incorporated into the latter in the absence of propionate.[136] These data imply that propionate is routed into MB lipid as a first choice by Mtb and that MCP is activated as a response to added pressure from propionate since TAG generation from propionate is MCP dependent. Activation of MCP can produce more acetyl-CoA, which increases PDIM production.[136] Moreover it has been shown that when Mtb is inside the macrophage it has the MCP genes up-regulated.[137] Mtb has evolved to survive and persist inside human cells, and the interaction of MMP with MCP and the synthesis of MB lipids is are of high importance to this mycobacteria.[136]

Cholesterol is the main lipid needed for growth and persistence of Mtb in mice.[138] Nesbitt *et al.* showed that when *fadA5*, an acetyl-CoA thiolase involved in Mtb cholesterol catabolism, is deleted, Mtb grows in mice lungs with no difficulty in the early stages of infection. Nevertheless, the bacterial load in the lungs is reduced when the immune response is activated, demonstrating a phenotype in persistence. If cholesterol was the only carbon source available in the mouse lung, the *fadA5* mutant, unable to use cholesterol as its only carbon source, should not be able to grow.[139] Thus this evidence shows that this single component of host membranes is a crucial nutrient during chronic infection.[129] Moreover, this agrees with studies from Pandey *et al.* using the Mtb strains lacking the Mce4 transporter, which is the major Mtb cholesterol import system.[138] Their work showed that Mtb *Δmce4* has a decreased capacity to acquire and metabolise cholesterol *in vitro* and to grow on medium containing cholesterol as the main carbon source. This study gives evidence that although cholesterol is not required to establish infection, it is essential for persistence within the lungs of chronically infected mice and IFN-γ-activated macrophages.[138] IFN-γ-activated macrophages are crucial for controlling mycobacterial infections and have also been shown to restrict Mtb growth by restricting the availability of essential nutrients.[140,141,142] Thus, the ability to catabolise cholesterol present in the host membrane is vital to circumvent IFN-γ mediated defence.[138]

1.4 Bacterial adaptation

1.4.1 Bacterial adaptation mediated by second messengers

Adaptation is crucial for bacterial survival in their changing environment during infection.[143] Bacteria sense changes in the environment and translate these cues to behavioural, metabolic and physiological adaptations through signal transduction.[144] The phosphorylation or dephosphorylation of effector proteins by kinases and phosphatases, respectively, and the production of second messengers are the most common mechanisms of signal

transduction.[145] Second messengers send environmental signals which are detected by receptors on the cell surface to specific downstream effector molecules inside the cell. Upon changes in the extracellular environment, cyclases (adenylyl and guanylyl cyclases) and phosphodiesterases (PDEs) synthesise or degrade the second messengers. This way the intracellular levels of second messengers are controlled. The binding between second messengers and effector molecules causes the latter to have a conformational change thus inducing a physiological output.[143, 144,146]

1.4.2 Cyclic nucleotides

Cyclic nucleotides are second messengers and they include the firstly discovered in 1957 3',5' monophosphate cyclic adenosine monophosphate (cAMP), 3', 5' cyclic guanosine monophosphate (cGMP), guanosine-tetra and pentaphosphate ((p)ppGpp), and the cyclic dinucleotide forms cyclic dimeric GMP (c-di-GMP) and cyclic dimeric AMP (c-di-AMP)[143] (Figure 1-8). cAMP is widespread among eukaryotes, fungi, parasites, archaea and bacteria. It is synthesised from adenosine triphosphate (ATP) by adenylyl cyclases (ACs), which are triggered by environmental changes such as fluctuations in the levels of pH, nutrient starvation or osmotic stress.[147] cAMP can be hydrolytically degraded by PDEs to control the levels of this molecule inside the cell. Once cAMP is synthesised it can bind to cAMP-binding proteins, which include transcriptional regulators and protein kinases that will undergo conformational changes[148] (Figure 1-9). The result of this binding is the regulation of gene expression. In bacteria, transcription factors of the cAMP-receptor protein family (CRP family) are activated by direct binding of cAMP.[148]

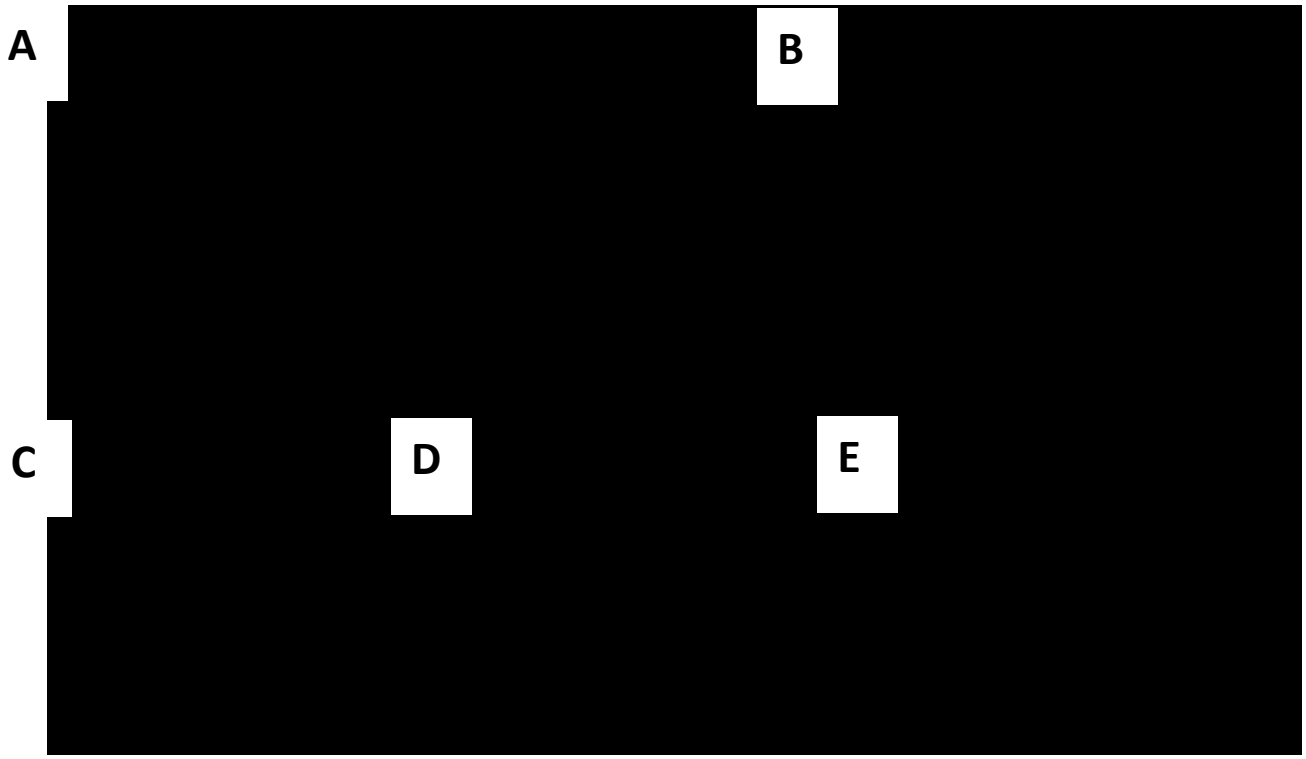


Figure 1-8. Chemical structures of some of the main cyclic mono- and dinucleotides in bacteria. Chemical structure of c-di-AMP (A); c-di-GMP (B); cGMP (C); cAMP (D); and ppGpp (E).

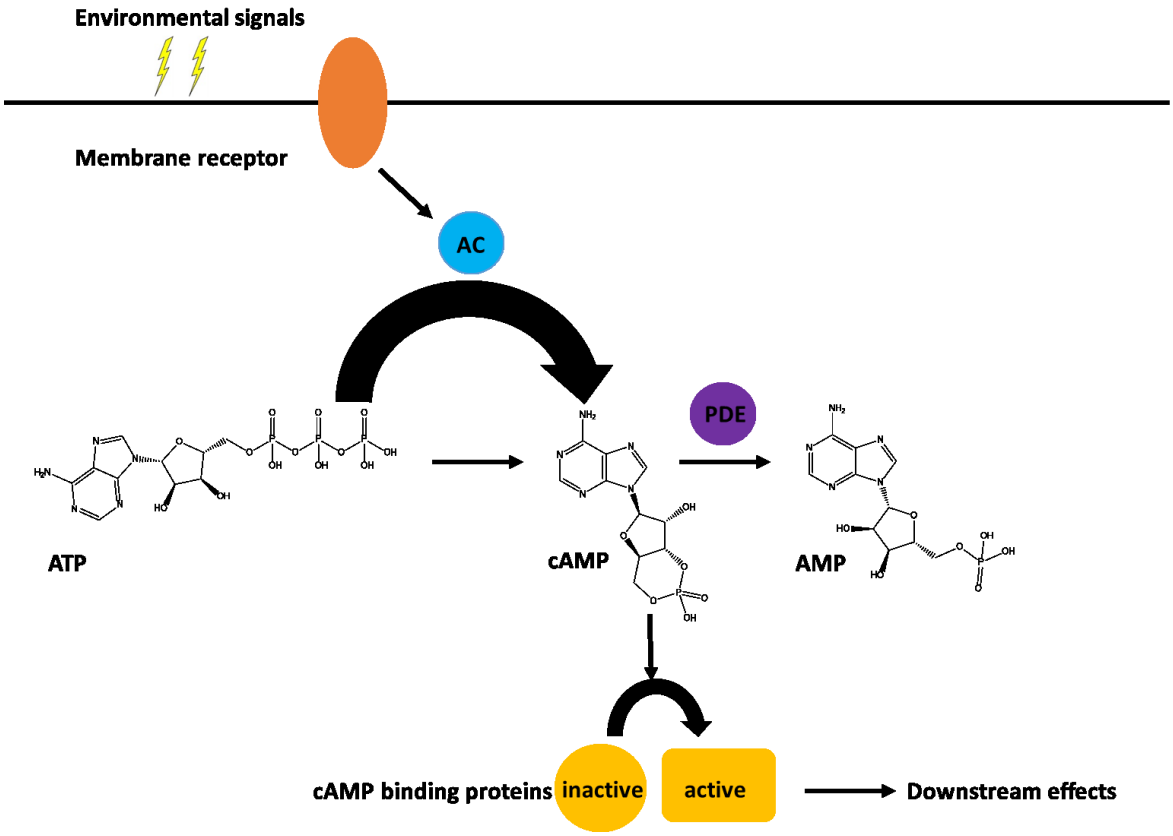


Figure 1-9. Scheme showing how the environmental signals trigger downstream effects via cAMP production.
ACs can be activated by environmental signals in a direct or indirect manner through membrane-bound receptors to convert ATP into cAMP. This second messenger allosterically activates cAMP-binding proteins, which can act directly as effector proteins, or transmit the signal to downstream effector proteins. cAMP is degraded by PDEs. Figure adapted from McDonough *et al.*[149]

cGMP was isolated from rat urine in 1963 but it was not until 1974 that it was demonstrated not only to be unique to eukaryotes but also to be involved in prokaryotic development.[143] cGMP works via a specific transcription factor, a CRP-like protein.[150,151] It has been shown that *Rhodospirillum centenum*, a purple photosynthetic bacterium, makes cGMP, which is crucial for cyst formation in this bacterium.[150,151] Regarding ppGpp and (p)ppGpp, they were first reported in 1970 in *E. coli*[152] but it was discovered in 2005 that they act in this bacterium as the ubiquitous second messenger in the 'stringent response'. RelA, a (p)ppGpp synthetase, is activated by amino acid starvation and heat shock. However, carbon, fatty acid, phosphate, nitrogen and iron starvation activate the (p)ppGpp synthetase activity of SpoT, a bifunctional synthetase/hydrolase enzyme. Once produced, (p)ppGpp modulates bacterial physiology by transcriptional reprogramming and the direct adjustment of target protein activities. Across diverse organisms and experimental models, mutants unable to produce (p)ppGpp often show

reduced levels of persister formation.[153,154] The cyclic dinucleotide form c-di-GMP was discovered in 1987 and is involved in a wide range of biological processes. One of its essential functions is mediating the transition between the motile single cell with planktonic lifestyle and the sessile, biofilm-forming state of Proteobacteria. This transition is regulated by the production of extracellular polysaccharides, pili, flagella and adhesive proteins among other mechanisms.[143] Another cyclic dinucleotide form is c-di-AMP, which was discovered in 2008 in *Bacillus subtilis* and has gained attention as another potentially global bacterial second messenger. It is involved in controlling DNA damage response, cell wall homeostasis, and membrane stress. Furthermore, it is known to be required for the viability of the Gram positive bacteria *Listeria monocytogenes*[155] and *Staphylococcus aureus.*[156]

1.4.3 Bacterial adaptation via cAMP

cAMP was first discovered in eukaryotes, where it is involved in hormone signal transduction.[157] Currently we know that the role of cAMP signalling in eukaryotes goes as far as metabolism to memory formation and innate immunity.[148] Furthermore, cAMP was also discovered in *E. coli,* where it is mainly involved in carbon catabolite repression mediated by the cAMP-CRP complex.[158,159] The CRP controls over 100 promoters and is activated by the allosteric binding of cAMP to its N-terminal region. This causes a conformational change in the tertiary structure of the protein.[160] This change induces binding of the C-terminal DNA-binding domain of CRP to sequence-specific DNA sites in or near the promoter sequences, enabling transcription via protein-protein interactions with RNA polymerase.[161,162] When there is a decrease in the levels of glucose, the *lac* operon is activated which leads to the usage of lactose as a secondary carbon source.[158] However, when glucose is present (catabolite repression), the production of cAMP is reduced and the expression of the *lac* operon is inhibited as a consequence.[158] Apart from mediating the 'glucose response' or catabolite repression, cAMP has also been recognised to have a role in microbial virulence.[149] For instance, in the opportunistic gram-negative bacterium *Pseudomonas aeruginosa,* three ACs are expressed: CyaA, CyaB, and ExoY.[149,163] The first two remain within the bacterium cytosol, where they are exposed to low Ca^{+2} concentrations. In living organisms, Ca^{+2} is thought to be the single most widely used signalling molecule for communicating internal and external states. In contrast to other messengers, it is neither created nor destroyed, but just moved around inside and outside the cell through transporters, pumps and channels to alter its concentration in specific cellular locations. These changes in free Ca^{+2} concentrations are then detected by a wide array of Ca^{+2}-binding effector proteins whose affinities are appropriately turned to respond to a particular type of Ca^{+2} concentration change.[164] Low calcium concentration induce CyaA and CyaB, which leads to an increase in the

levels of cAMP. The second messenger would then bind to virulence factor regulator (Vfr), a CRP-family transcription factor.[165] This binding regulates virulence gene expression, type III secretion system (T3SS), the *las* quorum sensing system, the formation of type IV pili and ultimately upregulates the expression of CpdA, the phosphodiesterase in charge of degrading cAMP. ExoY is a host-dependent AC toxin, which is exported into host eukaryotic cells via the T3SS. Once inside the host, it increases the levels of cAMP and causes changes in cell morphology.[165,149]

1.5 Mtb cAMP metabolism

Mtb H37Rv encodes for 16 distinct ACs, which form cAMP from ATP in a metal-dependent manner[145] (Figure 1-10). This is an exceptionally large number compared to other bacteria such as *E. coli*, where just one AC is present in its genome. The high number and variety of ACs compared to *E. coli* suggests that cAMP signalling has a complex and important role in mycobacteria.[166]

1.5.1 Adenylate cyclases and their catalytic activity regulation in Mtb

ACs are distributed in six classes according to their primary amino acid sequence. Class III includes all ACs in eukaryotes and some in prokaryotes including all 16 ACs in the Mtb strain H37Rv and 17 ACs in Mtb CDC1551.[145] Thus class III ACs are the most abundant and widely-distributed group of cAMP-producing enzymes.[167] Shenoy *et al.* found that *M. smegmatis*, *M. avium*, and *M. marinum* encode for 10, 12 and 31 class III ACs respectively.[168] From the 16 ACs encoded by the Mtb H37Rv genome, 10 have been shown to be biochemically active and they include Rv1625c, Rv1264, Rv1319, Rv0386, Rv1318, Rv1320, Rv1647, Rv3645, Rv2212 and Rv1900c (Table 1-1). A pseudogene (Rv1120c) has been identified in Mtb H37Rv, and a single base deletion causes its inactivation leading to early truncation of the protein.[168] Furthermore, Mtb CDC1551 presents an additional AC, MT1360.[169] ACs in Mtb can be soluble or membrane-associated proteins.[168] In order to become catalytically active, they have to dimerise in order to form the substrate-binding site at the dimer interface. The cyclases Rv2435c and Rv1625c can be grouped with the eukaryotic cyclases since they present mammalian-like catalytic sites.[168] In addition to the catalytic domain, the majority of Mtb ACs have associated domains, which can increase their effector functions as well as regulate the activity of the AC in response to a wide range of environmental conditions,[168] which include hypoxia and starvation providing the first level of control over cAMP production in Mtb.[170] The activation of these genes is in response to

host-associated signals like fatty acids, ATP, pH in the phagolysosome, CO_2 and bicarbonate levels (Figure 1-10).

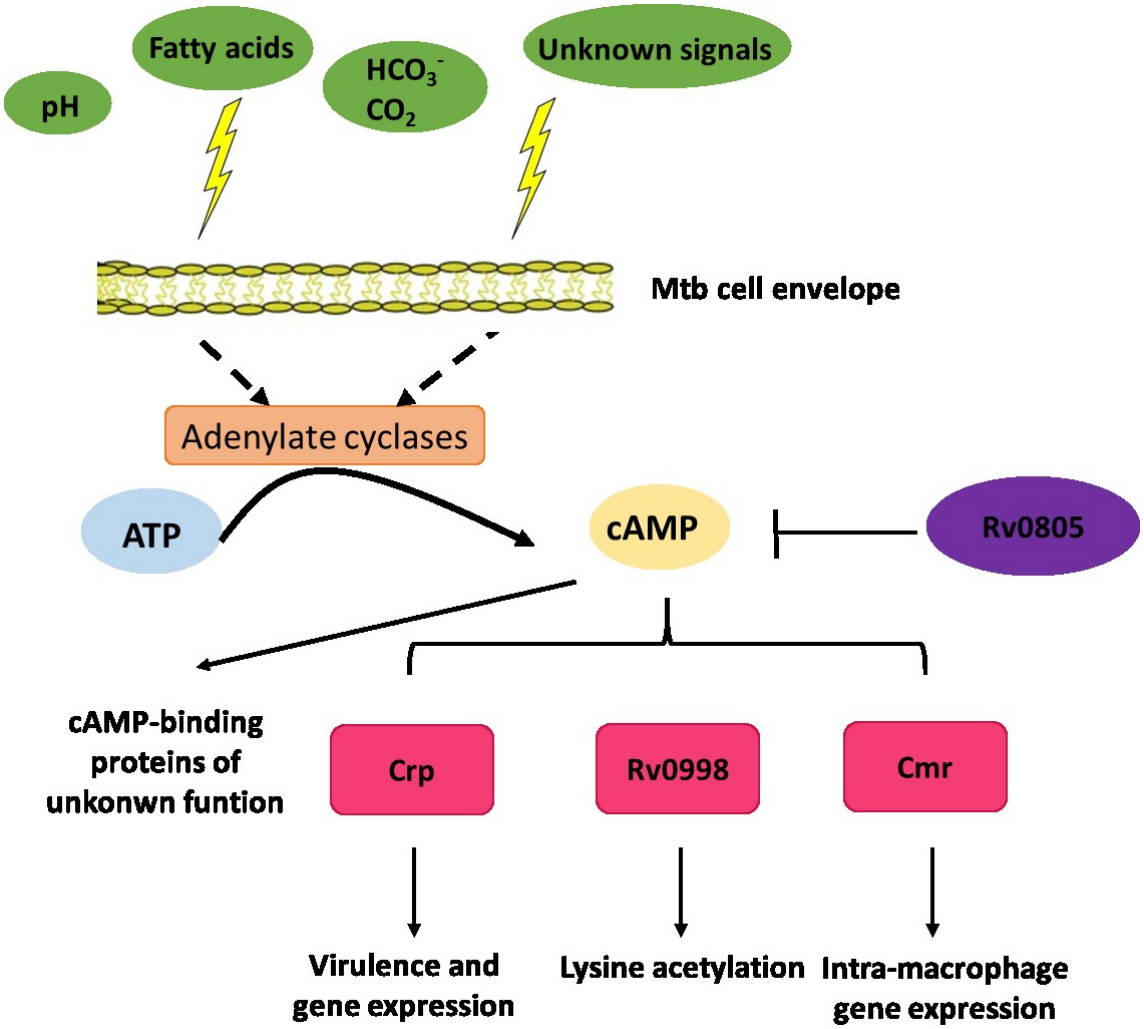


Figure 1-10. Schematic diagram of Mtb cAMP signalling pathways.
Environmental signals, which include pH, presence of fatty acids, HCO_3^-, and CO_2, among others, activate ACs which generate cAMP from ATP. cAMP can then bind to cAMP-binding proteins to regulate gene expression, virulence and protein lysine acetylation. The phosphodiesterase Rv0805 can restore basal cAMP levels by hydrolysis of the second messenger. Figure adapted from Knapp *et al.*[170]

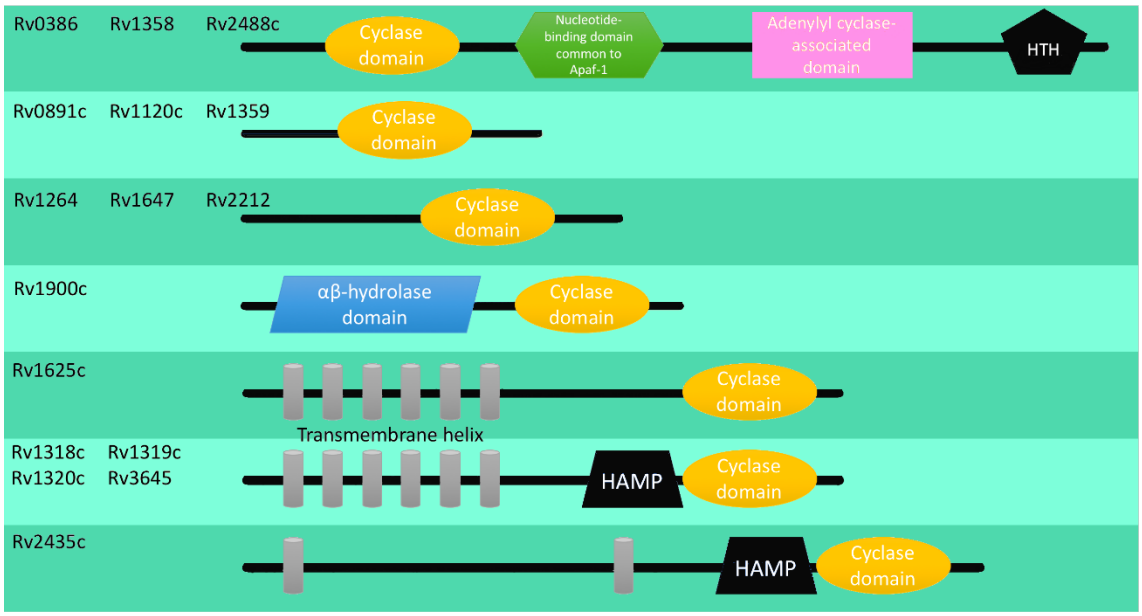


Table 1-1. Domain compositions of the 16 class III adenylyl cyclases in Mtb H37Rv.
Domain compositions were identified using the Conserved Domain Database (http://www.ncbi.nlm.nih.gov/Structure/cdd/cdd.shtml). Proteins nomenclature refers to the H37Rv genome annotation. HAMP (histidine kinases, adenylyl cyclases, methyl-accepting proteins and phosphatases), HTH (Helix-turn-helix). Table adapted from Shenoy *et al.*[168]

For instance, Rv1264 is only activated under acidic conditions since its N-terminal auto-regulatory domain is pH sensitive and inhibits AC activity above pH 6.0.[171] Closely related in domain and sequence composition to Rv1264 is Rv2212. Rv2212 is activated by unsaturated fatty acids by increasing their affinity to ATP substrate. Furthermore, the pH sensitivity of this AC is increased by fatty acids, but unlike Rv1264, its activity is not inhibited by the N-terminal domain at a pH above 6.[172] Thus, Rv2212 can integrate three signals to rule its activity *in vitro* and synthesize cAMP to control downstream effector proteins. These signals are the ATP concentration, the presence of unsaturated fatty acids and the pH and ATP concentration. Another pH sensor is Rv1647, which is found at the membrane and cell wall, and has an N-terminal domain that could interact with plasma membrane components to sense pH of the environment, responding to an alkaline pH of ~8.5.[173,174] This AC has also been shown to be activated by detergents suggesting that dimerisation is led by hydrophobic interactions.[168]

Rv3645c, Rv1318c, Rv1320c, Rv1319c and Rv1625c present hexa-helical anchors. However, the first four have an added HAMP (histidine kinases, adenylyl cyclases, methyl-accepting proteins and phosphatases) domain. They are dimeric, parallel four-helix bundles with coiled coil properties that perform as signal mediators in two-component signal transduction proteins.[175] The HAMP domains can modulate the activity of ACs and they can cause either an inhibitory

effect like in the case of Rv1319c or a stimulatory effect like in the case of Rv3645.[168] These four ACs can act as CO_2 or bicarbonate sensors.

Finally, the domain composition of Rv0386, Rv1358 and Rv2488c presents helix-turn-helix (HTH) DNA-binding domains and ATPase domains. Rv0386 is the first representative of the putative DNA-binding domain-containing cyclases family which has been biochemically characterised in mycobacteria.[176] Its non-canonical glutamine-asparagine pair of substrate specifying residues makes contact with the nucleotide and thus regulates nucleotide binding. Both Rv1358 and Rv2488c are uncharacterised enzymes and their cyclase domains might undergo structural changes if they are effectively active.[168] In contrast, Rv1900c has an N-terminal αβ-hydrolase domain, which is normally present in hydrolytic enzymes but no substrate has been found as yet[177] (Table 1-2).

Adenylyl cyclase	Location	Biochemically active	Conditions that affect gene expression	Environmental signals that affect activity
Rv0891c	Cytosol	Unknown	Nitric oxide / hypoxia	Unknown
Rv1120c		Pseudogene	Unknown	Pseudogene
Rv1264		✓	Hypoxia	Low pH (~5.5)
Rv1359		Unknown	H_2O_2 Starvation	Unknown
Rv1647		✓	Unknown	High pH (~8.5)
Rv1900c		✓	Unknown	Unknown
Rv2212		✓	Starvation	Unsaturated fatty acid
Rv1318c	Membrane-associated	✓	Starvation	Unknown
Rv1319c		✓	Starvation Hypoxia	HCO_3 / CO_2
Rv1320c		✓	Unknown	Unknown
Rv1625c		✓	Unknown	HCO_3 / CO_2
Rv2435c		Unknown	Hypoxia	Unknown
Rv3645		✓	Unknown	Unknown
Rv0386	Multidomain	✓	Unknown	Unknown
Rv1358		Unknown	Unknown	Unknown
Rv2488c		Unknown	Starvation	Unknown

Table 1-2. ACs in Mtb H37Rv
ACs with their location, their potential biochemical activity, the known conditions which affect their gene expression and the environmental signals that may affect their activity. Table adapted from Knapp *et al.*[170]

1.5.2 cAMP production

Mycobacteria produce high levels of endogenous cAMP, compared to other bacteria. The cAMP intracellular concentration has been found to be 950 picomol per milligram (pmol/mg) dry weight in Mtb H37Rv[178] compared to 370-450 pmol/mg of protein in *E. coli.*[179] Furthermore, the host environmental conditions have been shown to alter cAMP levels in mycobacteria. For instance, the levels of cAMP within macrophage-passaged Mtb and *M. bovis* BCG are approximately 50-fold higher compared to the bacterial strains just exposed to tissue culture medium.[180] This increase in cAMP levels could be because of the decrease in pH from 6.7 to 5.5 of the environment the bacteria is exposed to. This is consistent with Gazdik *et al.*'s findings

which show an enhanced cAMP production in mycobacteria exposed to pH 5.5 *in vitro.*[181] Another example of cAMP level alteration is treating *M. bovis* BCG with 0.05% sodium dodecyl sulfate (SDS) for 1.5 hours. This causes a fourteen-fold increase of cAMP intracellular levels compared to the bacterium under no stress. Furthermore, Bai *et al.* showed that an addition of 0.5% albumin to the culture medium was significantly inhibitory for cAMP production in *M. bovis* BCG. This is of importance since Mtb is exposed to different serum albumin levels depending on their location within the host.[182]

1.5.3 Secretion of cAMP into host cells and role of secreted cAMP in macrophages

Mycobacteria secrete far more cAMP compared to other bacteria[183] and have been shown to be relevant for Mtb virulence. It has been shown that the extracellular concentration of cAMP in Mtb H37Rv is 26.4 µM[178] compared to 0.03-0.5 µM *in E. coli.*[179] Nevertheless, how secretion is regulated remains unknown. Some pathogenic bacteria modulate host cell cAMP levels by secreting AC exotoxins this way elevating cAMP production within the host cell.[149]

Work from Lowrie *et al.* has shown that infection with live, but not heat-killed *M. microti* enhanced the levels of cAMP around 2.5-fold in infected macrophages, and that these increased cAMP levels matched with an impaired phagosome-lysosome fusion.[184] Elevated cAMP levels were also seen within *M. bovis* BCG infected macrophages. However, no increase in cAMP levels was seen upon infection with *M. leprae.*[185] Later on, experiments were performed on Mtb demonstrating that by delivering bacterial cAMP into the macrophage cytoplasm, host signal transduction pathways can be modulated.[186] Agarwal *et al*. demonstrated that enhanced cAMP levels within Mtb-infected macrophages are needed for production of TNF-α via the protein kinase A (PKA) and cAMP response element-binding (CREB) protein pathways (Figure 1-11). From the eight ACs investigated to understand their involvement, only Rv0386 was shown to be required[187] because macrophage infection by Mtb mutant lacking Rv0386 had a reduced CREB phosphorylation and TNF-α secretion of about 50% compared to that in macrophages infected by wild type Mtb. Mouse infection with the Mtb strain lacking Rv0386 showed a decrease in virulence and immunopathology. Therefore, activating TNF-α production via CREB is a pathogenic strategy used by Mtb to modulate the function of the host cell. The actin assembly in the phagosome allows its fusion with the lysosome and H^+-ATPase acquisition in order to be able to digest and kill the mycobacteria at an estimated pH of 5.5. Actin assembly is generally regulated by the levels of ATP, which can activate or inhibit the AC activity of the phagosomal membrane.[188] Nevertheless, enhanced levels of intramacrophage cAMP downregulate this process[188] (Figure 1-11) allowing Mtb to grow and survive within the host cell.[180] Thus, Mtb

modulates the host response in its favour due to its capability to increase the intramacrophage levels of cAMP. Other studies conducted by Bai *et al.* showed that the source of the extra cAMP within the macrophage was the infecting Mtb instead of the infected macrophages.[180] Moreover, similar to Lowrie *et al.*'s findings, inactivated Mtb did not increase cAMP levels within macrophages, demonstrating that live bacteria are crucial for cAMP secretion.[180]

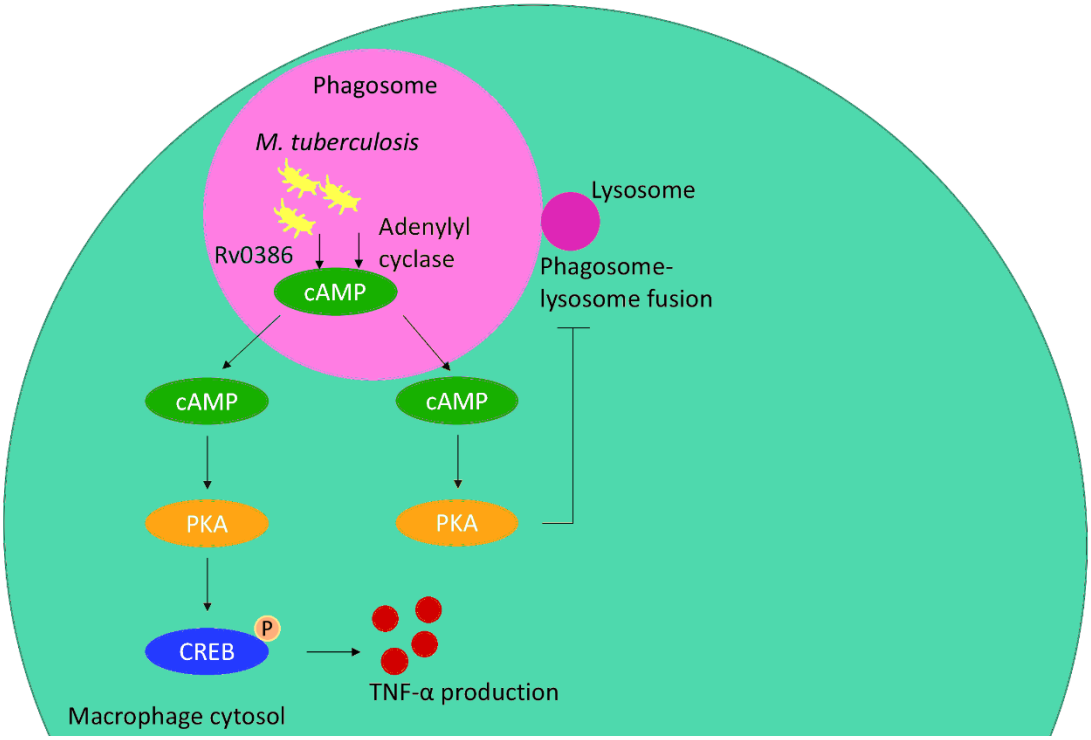


Figure 1-11. Schematic diagram with the downstream effects of cAMP upon macrophage phagocytosis.
cAMP is made by the AC Rv0386, which leads to the production of TNF-α via CREB phosphorylation by PKA promoting Mtb immunopathology and survival. Furthermore, an increase of cAMP inside the macrophage inhibits phagolysosome formation by negative regulation of phagosomal actin assembly. This also results in increased Mtb survival by preventing destruction by the host. Figure adapted from Agarwal *et al*.[187]

1.5.4 cAMP degradation

cAMP degradation also modulates levels of cAMP in mycobacteria. This degradation is conducted by Rv0805, the only PDE identified for cAMP degradation in Mtb. Rv0805 is a dimeric, Fe^{3+}-Mn^{2+} binuclear PDE and part of the class III metallophosphoesterase family of enzymes[189] homologous to CpdA, a lactose operon regulator present in *E. coli*. Rv0805 catalyses the hydrolysis of cAMP to 5'-AMP, and its orthologues are only present in slow-growing virulent mycobacteria such as *M. leprae, M. bovis* and *M. marinum.*[189] H_2O_2 activates Rv0805.[168] Purified Rv0805 hydrolyses cAMP and cGMP to AMP and GMP, respectively, *in vitro.*[189,190] However, Rv0805 has also biochemical and physiological characteristics that suggest it has functions beyond just the degradation of cAMP.[191] When Rv0805 is overexpressed, *M. smegmatis* and Mtb intracellular levels of cAMP decrease by approximately 30% and 50% respectively compared to controls.[173,187] Fe^{3+} and Mn^{2+} are active site metals involved in Rv0805 dimerisation and catalysis. Research by Shenoy *et al.* has demonstrated how crucial asparagine, aspartate and histidine residues are in co-ordinating this metal active site. Deletion of these three amino acids reduced Rv0805 catalytic activity by up to 90%.[189] Nevertheless, the 3'-5' cAMP PDE activity of Rv0805 (V_{max} = 42 nmol 3', 5'-cAMP hydrolysed/min/mg protein; K_m = 153 µM), is not as robust as CpdA, (V_{max} = 2.0 µmol/min/mg; K_m = 0.5 mM). [173,189]

Rv0805 has no strict cyclic nucleotide substrate specificity. Apart from 3'-5' cAMP they include 2',3'-cAMP and 2',3'-cGMP. Moreover, the 2',3'-cAMP PDE activity of Rv0805 *in vitro* is around 150-fold more active than its 3',5'-cAMP PDE activity. This is a result of a specific histidine residue in its active site.[192] However, the biological significance of Rv0998 is not well understood and future work is required to determine if mycobacteria encode one or more PDEs, or if there is another mechanism used to reduce the intracellular levels of cAMP.[191]

1.5.5 cAMP-binding proteins

Intracellular signalling via cAMP is involved in several physiological processes such as metabolism, virulence, and host interactions.[170] This second messenger can bind to proteins such as enzymes and transcription factors and regulate allosterically the activity of downstream molecules by inducing conformational changes. Ten cAMP-binding proteins have been found in the Mtb genome. As has already been mentioned, cAMP levels fluctuate, and during infection in macrophages these variations are exclusive to pathogenic mycobacteria.[180] Thus, changing levels of cAMP could modulate the activity of these cAMP-binding proteins through conformational changes, which would lead to a catalysis change.[193]

From the 10 cAMP binding proteins, only three have been functionally characterised. These are CRP_{Mt} (Rv3676), Cmr (Rv1675c) and lysine acetyl-transferase (Rv0998).[145] The first two are part of the fumarate and nitrate reduction family of prokaryotic transcription factors, with N-terminal cAMP-binding domains (CBD) and C-terminal HTH DNA-binding domains (Figure 1-3).[145] CRP_{Mt} and Cmr participate in the interactions between Mtb and the host by regulating gene expression. Regarding Rv0998 (MSMEG_5458 in *M. smegmatis)*, it has its N-terminal CBD associated with a C-terminal domain with similarity to the GNAT (Gcn5-related *N*-acetyltransferase) family (Table 1-3).[194] Direct binding of Cmr to cAMP has not been confirmed *in vitro*, and none of the conserved residues involved in cAMP binding in *E. coli* CRP and CRP_{Mt} are conserved in Cmr.[195] However, it is likely that it directly regulates the expressions of the cAMP induced genes *groEL2*, *mdh* and *rv1265* through specific interaction with their upstream regulatory regions. It has been shown that the DNA-binding affinity of Cmr is much lower than that of CRP_{Mt}, and is not affected by the presence of cAMP, suggesting that regulation of the proteome by Cmr is highly sensitive to environmental conditions.[195] Rv0998 and MEMSG_5458 modulate metabolism at the post-translational level via protein lysine acetylation in a cAMP dependent manner.[193]

The other seven cAMP-binding proteins are Rv2564, Rv0104, Rv2434c, Rv2565, Rv3239c, Rv0073 and Rv3728. They present CBDs bound to accessory domains with several functions such as transport activities (Table 1-4).[145] These proteins are non-essential for growth *in vitro* and no studies have been performed *in vivo* or *in cellulo*. Rv2564 and Rv0073 have been predicted to be part of an ABC transporter complex, which is involved in the active transport of glutamine across the membrane.[196] Rv2565 has a patatin-like phospholipase domain close to the C-terminus, and it has been seen to be induced during infection in humans.[197] Patatin is a storage protein and it has the enzymatic activity of phospholipase as it is able to catalyse fatty acids cleavage.[198] Furthermore, Rv2434c is likely to be a conserved transmembrane protein with a small conductance mechanosensitive ion channel.[199] Finally, Rv3278 and Rv3239c also contain a patatin domain and are involved in the efflux system involving sugar or antibiotic transport, allowing the bacteria to resist antimicrobials and to persist within the host.[197]

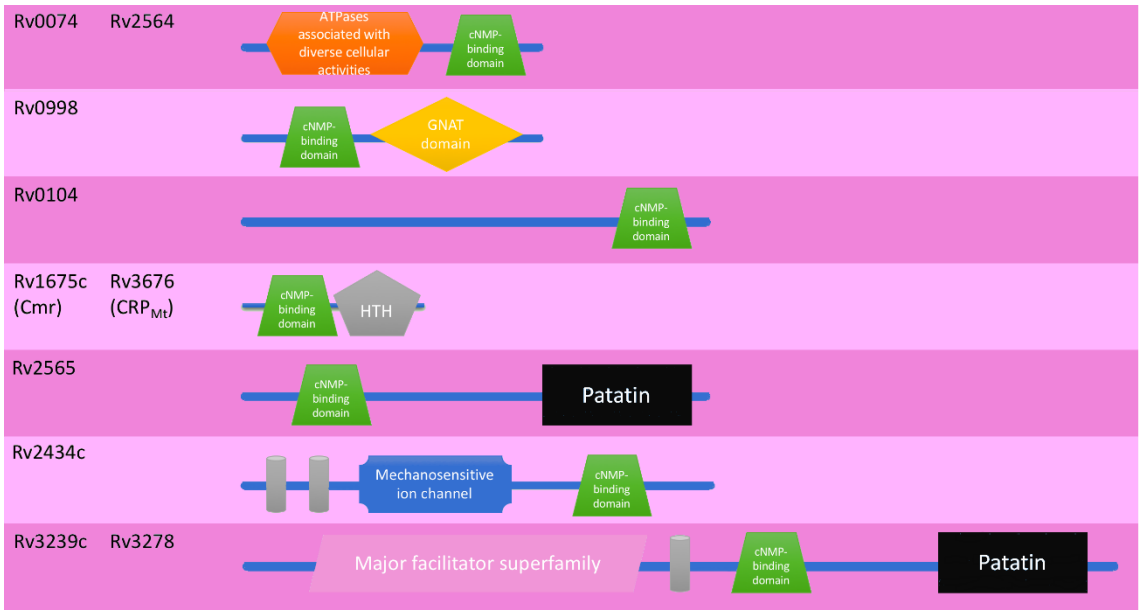


Table 1-3. Ten Mtb cAMP-binding proteins and their domain compositions.
Domain composition of putative cAMP-binding proteins in Mtb. Domain name abbreviations: HTH, helix-turn-helix DNA binding; Patatin, patatin-like phospholipase. Table adapted from Shenoy *et al.*[168]

Slow-growing mycobacteria			Fast-growing mycobacteria	Function
M. tuberculosis	***M. leprae***	***M. marinum***	***M. smegmatis***	
Rv3676 **Rv1675c**	ML2302	MMAR_1621 MMAR_5164	MSMEG_6189 MSMEG_0539	Transcription regulation
Rv0073 **Rv2564**	✕	MMAR_0216	✕	Glutamine transport
Rv0104	✕	MMAR_0285	✕	Unknown
Rv2434c	✕	MMAR_3754 MMAR_3756	MSMEG_3579	Unknown
Rv2565	✕	✕	✕	Unknown
Rv3239c **Rv3728**	✕	MMAR_1306 MMAR_0729 MMAR_2964	✕	Likely to be involved in efflux system
Rv0998	ML0187	MMAR_4496	MSMEG_5458	Acetyl-transferase

Table 1-4. Function of the 10 Mtb cAMP-binding proteins in different mycobacterial species. Distribution and function of the 10 putative Mtb cAMP binding proteins in *M. leprae*, *M. marinum* as well as *M. smegmatis*. Table adapted from Zaveri *et al.*[200]

The sequence alignment of cAMP-binding domains of Rv0998 and other uncharacterised cAMP-binding proteins in Mtb has shown that they contain several invariant residues in the 12-amino acid phosphate binding cassette (PBC) for anchoring cAMP with high affinity (Figure 1-12).[201] Most of them contain a conserved serine residue followed by an alanine at positions equivalent to Ser99 and Ala100 in Rv0998, which are often found in cAMP-binding proteins.[201,202] Ser99 interacts with exocyclic oxygen atoms of the phosphodiester bond along with Ala91 and Arg98. Other conserved residues in the PBC include Gly88 and Glu89 in Rv0998, which forms a hydrogen bond with 2'-OH of the ribose moiety. Apart from the PBC, Val67 has been postulated to position the adenine ring of cAMP through hydrophobic interactions, while Arg138 mediates hydrogen bonding with the adenine moiety. Although residues at these positions are not well-conserved, residues in the seven proteins at positions equivalent to Val67 and Arg138 in Rv0998 are capable of forming hydrophobic interactions and hydrogen bonds respectively.[201,202]

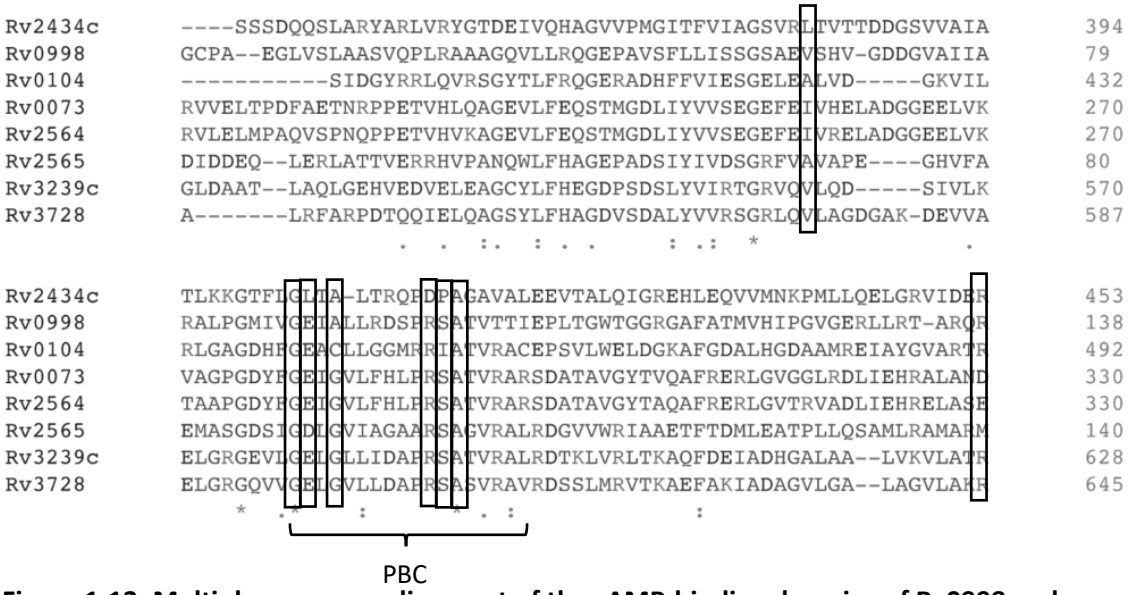


Figure 1-12. Multiple sequence alignment of the cAMP-binding domains of Rv0998 and seven uncharacterised cAMP-binding proteins in Mtb.

Residues critical for anchoring cAMP are highlighted with black boxes. The PBC indicated is essential for forming the high affinity cAMP-binding pocket. Sequence alignment performed with Clustal Omega. Courtesy of Natalie Chui.

1.6 Mass spectrometry

Mass spectrometry measures the mass-to-charge (*m/z*) ratios of molecules. Mass spectrometry is a very sensitive technique, being able to detect analytes at concentrations in the attomolar range (10^{-18}) and is widely regarded as having good selectivity, which leads to reduced noise, allowing very low levels (femtogram per millilitre (fg/mL)) to be detected. However, in many applications, it is necessary to isolate the target analyte from what could be a sample containing thousands of other different molecules.[203,204]

A mass spectrometer is an instrument which is used to define the covalent structures of substances by ionising, separating and detecting molecular and fragment ions according to their *m/z*. The three basic parts of a mass spectrometer are the ion source, the mass analyser and the detector (Figure 1-13). The ion source is used for vaporisation/ionisation of the target molecules; the mass analyser is used to separate the gas phase ions by *m/z*; and the detector is used to detect the mass separated ions and to measure their relative abundance. The detected ions are then represented in the mass spectrum where the abundance is plotted on the y-axis and the *m/z* ratio on the x-axis.[204]

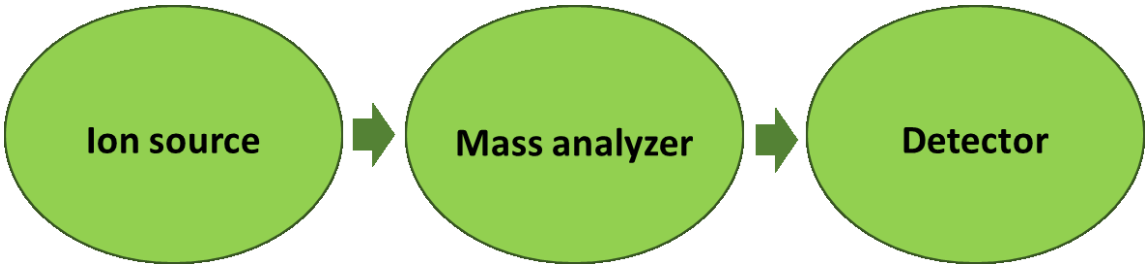


Figure 1-13. Diagram of the three basic parts of a mass spectrometer.
A mass spectrometer is composed of an ion source, a mass analyser and a detector. The first component vaporises or ionises the molecules; the second separates the gas phase ions by mass to charge ratio; and the last component detects the ions separated by mass and measures the relative abundance.

1.6.1 Ion sources

There are different ionisation methods which include Electron Impact Ionisation (EI), Fast Atom Bombardment (FAB), Electrospray Ionisation (ESI), Atmospheric Pressure Chemical ionisation (APCI) and Matrix-Assisted Laser Desorption Ionisation (MALDI). However, only two of them are the most widely used and the ones I used in my PhD. These are ESI and MALDI. The first is used for lipids, peptides, oligosaccharides and proteins greater than 500,000 Da. The latter involves short-time analysis and is used for molecules weighing up to 500,000 Da. These can be lipids,

carbohydrates or proteins.[204,205] MALDI can produce singly charged ions of molecules, which minimises spectral complexity. ESI, however, can be efficiently interfaced with separation techniques.[206]

1.6.1.1 ESI

This technique uses electrical energy to assist the transfer of ions from solution into the gaseous phase.[207] The sample is introduced into the ion source in solution through a narrow glass capillary coated with gold at the tip (Figure 1-14). A high voltage (3-4 kV) is applied to the tip and the sample emerging from the tip is then dispersed as an aerosol of highly charged droplets. The process is aided by a drying gas (nitrogen) that flows around the outside of the capillary. As the solvent evaporates the droplets become unstable due to a high surface charge and therefore 'explode' into smaller droplets containing 'naked' ions whose charge corresponds to the charge of the original molecule at the pH or other conditions of the experiment. These ions drift into the analyser because of the voltage gradient.[204]

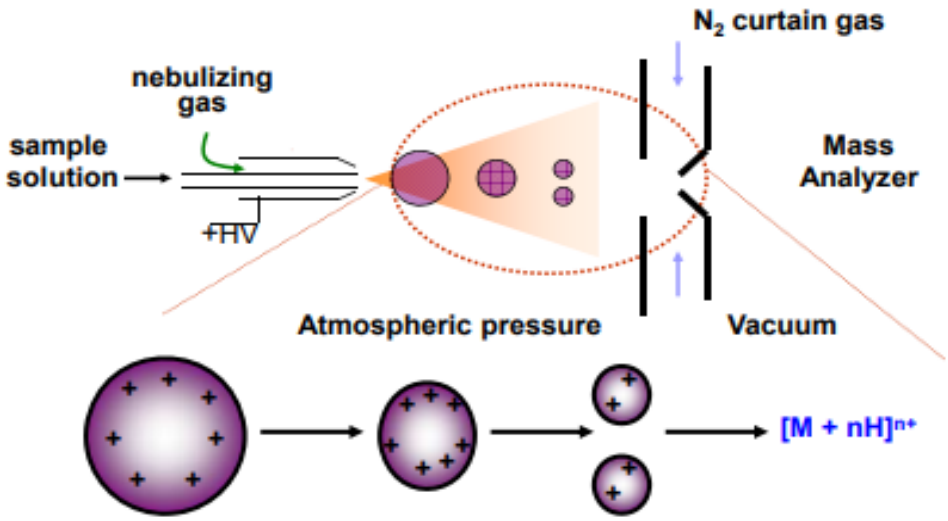


Figure 1-14. Schematic representation of sample ionisation with Electrospray Ionisation (ESI). ESI draws sample solutions to the tip of a capillary tube, where it applies a high voltage of about 3 to 4 kV. A nebuliser gas flows from outside the capillary to spray the sample. This creates a fine mist of charged droplets with the same polarity as the applied voltage. As these charged particles move, the solvent continues to evaporate, thereby increasing the electric field on the droplet surface. When the mutual repulsive force of the charges exceeds the liquid surface tension, then fission occurs. Figure adapted from Banerjee *et al.*[208]

1.6.1.2 MALDI

In MALDI, the sample is embedded in a low molecular weight ultraviolet (UV)-absorbing 'crystalline' matrix, which is chosen to have an absorption maximum near the wavelength of the pulsed laser that is used to ionise the sample. The most common matrixes are Alpha-cyano-4-hydroxycinnamin acid (αCHCA) and 2,5-dihydroxybenzoic acid (2,5-DHB). α-CHCA is more appropriate for detecting middle-weight molecules such as peptides and is mainly used in the positive ion mode. DHB detects lower-weight molecules such as carbohydrates and lipids; and is mainly used for positive-ion mode analysis.[209,210] The matrix absorbs the laser pulse and enough energy is transferred to the sample to ionise it (Figure 1-15). Two main lasers are used: the nitrogen gas UV laser and the solid-state UV laser. The first has a wavelength of 337 nm, a repetition rate of 1 to 20 Hz and a pulse energy of 120 to 200 μJ. The latter has a wavelength of 355 nm, a high repetition rate laser (from 0.1 to 5 kHz) and an Nd-YAG laser.[204,211,212]

Early MALDI experiments were characterised by poorly resolved spectra. Currently, modern MALDI instruments give well-resolved spectra and one reason for this is the so-called 'delayed extraction' (DE). This solves the problem of ions of the same mass coming from the target at different speeds due to uneven energy distribution. Ions are formed by the laser pulse in different locations in the crystal. DE keeps the ion pulse in the source for a short time after the laser pulse in order to allow time for ions formed deep in the matrix to emerge and 'catch up' with those formed near the surface. Thus DE ensures ions have the same velocity when they enter the analyser.[211,212]

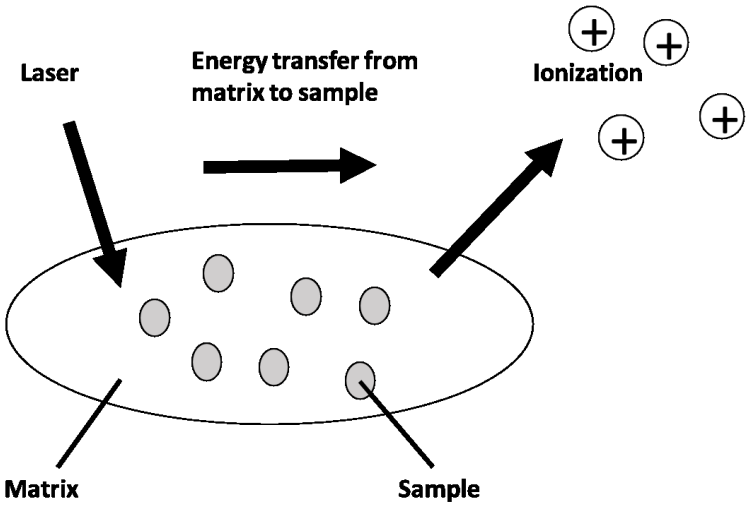


Figure 1-15. Schematic representation of sample ionisation with MALDI.
The matrix is present in vast excess of sample and, therefore, isolates individual sample molecules.[204] When the laser pulses, the sample molecules are ionised by gas phase proton transfer from the matrix. The laser pulse produces matrix neutrals (M), matrix ions, $(M+H)^+$ and $(M-H)^-$, and sample neutrals (A). The matrix ions then collide with the sample neutrals, producing sample ions, $(A+H)^+$ and $(A-H)^-$.[204] $(M+H)^+ + A \rightarrow M + (A+H)^+$, $(M-H)^- + A \rightarrow (A-H)^- + M$.

1.6.2 The analyser

There are different analysers: Quadruple (Q), Time-of-flight (TOF), Q-TOF, ion trap and ion cyclotron resonance. The key factors are the upper mass limit, ion transmission and resolution.

1.6.2.1 Quadrupole mass filter

The Q mass filter was invented in the mid-1950s. It uses a quadrupolar electrical field, which comprises radio frequency (RF) and direct current (DC) components to separate ions. It consists of four parallel rods.[203,213] Each diagonal pair of rods is connected electrically and the electrical field is obtained by the application of a voltage made up of a DC component (to one pair) and a RF potential (to the other pair). It is important to notice that up to 4,000 *m/z* ratios can be observed, and that it has relatively low resolution, which is about 3,000 per unit. Furthermore, its cost is low and the scanning is fast, with an average rate of ~20 Hz. The Q mass analyser is widely used with ESI.[203,213] The two opposite rods in the quadrupole have a potential of $+(U+V\cos(\omega t))$ (labelled '+' on the figure) and the other two $-(U+V\cos(\omega t))$ where 'U' is the fixed potential and $V\cos(\omega t)$ is the applied RF of amplitude 'V' and frequency 'ω' (Figure 1-16). The applied potentials on the opposed pairs of rods varies sinusoidally as $\cos(\omega t)$ cycles with time 't'. This results in ions being able to traverse the field-free region along the central axis of the rods but with oscillations amongst the poles themselves. These oscillations result in complex ion

trajectories dependent on the *m/z* of the ions. Specific combinations of the potentials 'U' and 'V' and frequency 'ω' will result in specific ions being in resonance, creating a stable trajectory through the quadrupole to the detector. All other *m/z* values will be non-resonant and will hit the quadrupoles and not be detected. The mass range and resolution of the instrument is determined by the length and diameter of the rods (Figure 1-16).[214]

Quadrupole mass spectrometers generally have two configurations in the modern laboratory. They are very commonly used in conjunction with either gas-chromatography (GC-MS) or liquid-chromatography (LC-MS) as a simple high throughput screening system.[214]

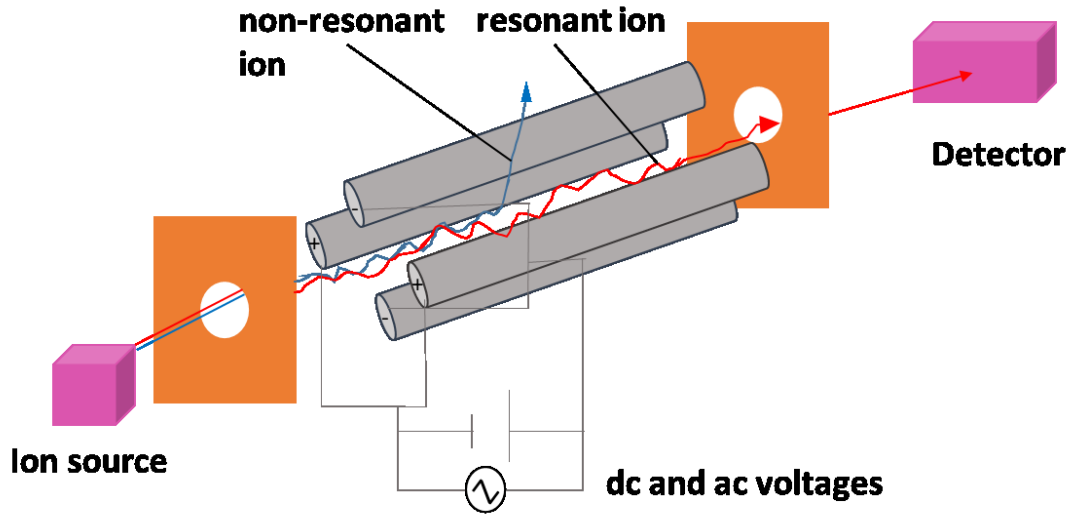


Figure 1-16. Simplified scheme of the quadrupole mass analyser.
The quadrupole mass analyser consists of four parallel rods that have fixed DC and alternating RF potentials applied to them. Ions produced in the source of the instrument are then focused and passed along the middle of the quadrupole rods. Their motion will depend on the electric fields so that only ions of a particular *m/z* will be in resonance and thus pass through to the detector. The RF is varied to bring ions of different *m/z* into focus at the detector and thus build up a mass spectrum. In blue are ions with an unstable trajectory and which are therefore not detected; in red are ions with a stable trajectory and thus detected. Figure adapted from Yost *et al*.[215,216]

1.6.2.2 TOF analyser

TOF mass spectrometry works on the principle that when ions are accelerated with the same potential from a fixed point and at a fixed initial time and are allowed to drift, the ions separate according to their *m/z.*[211] Lighter ions drift more quickly to the detector whereas heavier ions drift more slowly. The time required for ions to reach the detector at the opposite end of the flight tube (drift time) is measured. Furthermore, the number of ions reaching the detector at any given time is also measured, and is referred to as ion intensity (abundance) or signal intensity (Figure 1-17).[211]



Figure 1-17. Scheme showing the general set up of TOF analysers.
The ions are introduced either directly from the source of the instrument or from a previous analyser as a pulse. This results in all the ions receiving the same initial kinetic energy. As they then pass along the field-free drift zone, they are separated by their masses and lighter ions travel faster. This enables the instrument to record all ions as they arrive at the detector and so accounts for the technique's high sensitivity. Figure adapted from Yost *et al*. [215,216]

Early analysers had poor resolution and poor mass accuracy whereas newer analysers incorporate reflectrons at the end of the drift zone, which were first invented in 1974.[203] They correct for the effects of kinetic energy distribution of the ions and give a longer flight path. The reflectron is an ion mirror that reverses the ions' direction of travel. Ions of greater kinetic energy penetrate further and therefore have a longer flight path. Linear analysers have low resolution (< 1000) whereas reflectrons give a much higher resolution (> 3,000).[203]

ESI and MALDI sources are most commonly found on instruments with TOF analysers. MALDI-TOF is the method of choice for 'mass fingerprinting' complex mixtures of polymers, both chemical and biological.[204,211]

1.6.2.3 Tandem

Hybrid instruments consist of two or more analysers in tandem like TOF-TOF and Q-TOF and are used for MS/MS experiments. Ions produced in the source are selected by the first analyser and are collisionally activated by exposure to a collision gas as they pass through a collision chamber located between the two analysers. Fragment ions plus any non-fragmented molecular ions are separated by the second analyser and detected to give a MS/MS spectrum.[211]

TOF-TOF, or tandem TOF mass spectrometry, consists of two successive TOF accelerations. The first acceleration selects, isolates, and fragments (usually by collision with a neutral gas) a precursor ion of interest.[211] Next, the second acceleration reaccelerates the precursor ion and fragments, then measures the masses and intensities of the fragment ions. When applied to peptides, this technique is more definitive than other MS methods for protein identification and is a principal means of protein characterisation.[211]

The Q-TOF was designed and built in the mid-1990s at Imperial College London by Professor Howard Morris.[217] It is a very powerful MS/MS instrument in terms of sensitivity and resolution and has had an enormous impact on the growth of proteomics.[218] In MS mode, the quadrupole is set to allow all ions through and the TOF is the mass analyser. The pulses of ions are accelerated into the TOF by the 'pusher' and the MS spectrum is recorded. In MS/MS mode, the quadrupole is set to allow selected ions through the collision cell which contains the collision gas; the TOF is the mass analyser and pulses of fragment ions are accelerated into the TOF by the 'pusher' and the MS/MS mode is recorded.[218]

1.6.3 Liquid Chromatography MS coupling (LC-MS)

Liquid chromatography-mass spectrometry (LC-MS) is the combination of two selective techniques that allows the analyte(s) of interest in highly complex mixtures to be isolated and measured. The basic components of an LC-MS system are the liquid chromatography, the ion source, the mass analyser and the detector. Sample molecules are converted into gas phase ions in the ionisation source before being accelerated into the mass analyser via the sampling orifice and ion guide. Ions are then deflected by electrostatic fields in the quadrupoles according to their mass and their charge within the mass analyser. The detector converts the ion energy into

electrical signals, which are then transmitted to a computer for data handling, including calculations required for quantification.[203] LC differentiates compounds by their physico-chemical properties; and MS differentiates compounds by *m/z* ratio.[219] It is this dual selectivity that makes LC-MS such a powerful analytical tool. The mass spectrometer acts not only as the 'LC detector' but provides the capability to identify the species corresponding to each chromatographic peak through its unique mass spectrum.[203] Since analytes are separated by their *m/z*, the technique allows for the use of isotopically labelled internal standards, which may not separate by LC but can be separated by their mass difference. The use of stable isotopically labelled (SIL) internal standards can help control variability in a quantitative assay.[204] Since the MS will distinguish compounds based on mass, the chromatographic method does not have to separate every single component in the sample, so co-elution of non-isobaric analytes is possible. This allows fast LC analysis and reduced sample preparation, which helps with method development and high throughput sample analysis.[204]

The instrument I used during my PhD had ESI as source of ions and a Q-TOF analyser, and I used it for metabolomics experiments. Metabolomics is the identification and quantification of the complete set of metabolites in a biological system. It involves the quantitative measurement of the dynamic metabolite response of living systems to pathophysiological stimuli or genetic modifications. Furthermore, it provides important insights into physiological and disease states and facilitates in-depth understanding of underlying biochemical pathways. I performed targeted metabolomics in order to detect the levels of specific molecules that were suspected to be associated with the phenotype observed under changing conditions. Furthermore, I used untargeted metabolomics in order to investigate all possible compounds and their levels in the sample.[220] During my PhD I also used MALDI-TOF to perform lipidomics experiments to determine all lipid species in the sample. Lipids have heterogenic structures, from differences in fatty acid composition, the type of linkage between fatty acids residues and the glycerol backbone (diacyl-, alkyl-acyl, and alkenyl-acyl-) as well as differences in the headgroup structure. Therefore this technique needs sensitive and reliable methods such as MALDI-TOF[221]. Lipidomics also studies lipid metabolism and can discover the biochemical mechanisms underlying specific changes in lipid metabolism.[222]

Chapter 2: Materials and methods

2. Materials and methods

2.1 Materials

All reagents were purchased from Sigma-Aldrich, unless otherwise stated. Metabolomics reagents were purchased from Agilent Technologies (United States).

2.2 Methods

2.2.1 Bacterial strains and growth conditions

Mtb, *M. smegmatis* and *M. marinum* were cultured in Middlebrook 7H9 or 7H10 agar, at 37 °C for the first two strains and at 30 °C for the latter in shaking (1,200 rpm) or static incubators. The strains used are shown in Table 2-1.

2.2.1.1 7H9 liquid medium

Middlebrook 7H9 broth was prepared according to the manufacturer's instructions. 4.7 gram (g) 7H9 powder was added to 875 mL Milli-Q water (ddH_2O). If the osmolarity of the medium was required to be 250 millimolar (mM) sodium chloride (NaCl), 50 mL of NaCl solution 5 M in H_2O (Sigma) were added per litre of final culture medium. The pH of the solution was adjusted using the Mettler Seven Easy S20 pH meter (Sigma). Then, the solution was autoclaved at 121 °C for 20 minutes (min) and permitted to cool. 100 mL of supplement were added to the cooled 7H9 solution under sterile conditions. The 7H9 medium was stored at 4 °C.

2.2.1.2 7H10 solid medium

7H10 agar was prepared according to the manufacturer's instructions as follows: 21 g of 7H10-agar powder was dissolved in 900 mL ddH_2O and mixed well. If the osmolarity of the medium was required to be 250 mM NaCl, 50 mL of NaCl solution 5 M in H_2O (Sigma) were added per litre of final culture medium. Then, the pH of the solution was adjusted using the Mettler Seven Easy S20 pH meter (Sigma), the solution was autoclaved at 121 °C for 20 min and permitted to cool in a 55 °C incubator for 1 hour. The preparation was further cooled by stirring at 4 °C for 5 min before adding 100 mL supplement, and any other supplementation required (such as antibiotics) under sterile conditions. Approximately 20 mL were poured into 90 millimetre (mm) Petri dishes and permitted to set and dry in a laminar flow hood for 30 min, then stored at 4 °C.

2.2.1.3 Medium supplement

Medium was supplemented with the following: 0.2% of a sole carbon source (dextrose or glycerol); bovine serum albumin (0.05%), according to whether or not albumin was required in

the culture medium; NaCl (0.08%); and tyloxapol (0.05%) to final concentration. Tyloxapol stock was prepared by weighing out tyloxapol solution (Sigma) and adding an appropriate volume of ddH_2O in a conical flask to produce a 20% (v/v) stock solution. This is determined by the assumption that pure tyloxapol has a density of 1.1 g/mL. The solution was stirred for approximately 15 min, sterile filtered, and stored at room temperature.

Strain	Origin	Resistance
Mtb wt H37Rv	Laboratory	None
Mtb wt CDC1551	Prof. Sandhya Viswaswariah, Indian Institute of Science, Bangalore, India	None
Mtb CDC1551 *Δrv0998*	Prof. Sandhya Viswaswariah, Indian Institute of Science, Bangalore, India	Hygromycin 50 µg/mL
Mtb CDC1551 *Δrv0998* comp	Prof Sandhya Viswaswariah, Indian Institute of Science, Bangalore, India	Hygromycin 50 µg/mL and Kanamycin 10 µg/mL
Mtb H37Rv *Δcrp*	Dr Roger Buxton, NIMR, Mill Hill, London, UK	None
Mtb H37Rv *Δcrp* comp	Dr Roger Buxton, NIMR, Mill Hill, London, UK	None
Mtb CDC1551 *rv0516::Tn*	NIH Biodefense and Emerging Infections Research Resources Repository, NIAID, NIH	Kanamycin 10 µg/mL
***M. marinum* M wt**	Dr Brian Robertson	None
***M. smegmatis* mc^2155 wt**	Dr Brian Robertson	None

Table 2-1. Strains used in this thesis.
Mtb*, M. tuberculosis*; wt, wild type; comp, complemented strain.

2.2.2 Growth curves and Optical density (OD) monitoring

10 mL square bottles were prepared by adding 10 mL 7H9 medium supplemented with the carbon source of choice, adding the NaCl concentration of choice, and at a pH of 6.8 or 5.5 and let incubate in a static incubator to allow media to reach 37 °C or 30 °C for *M. marinum*. A pre-culture was prepared by adding 100 µL of bacteria stored at -20 °C to 10 mL of culture medium.

Once the pre-culture reached exponential phase, it was used to start the growth curve. Square bottles were inoculated with mycobacteria (from the pre-culture) with an OD_{600} of 0.01 and were then incubated at 37 °C or 30 °C in a shaking or static incubator. OD_{600} measurements were taken every two to three days for slow-growing mycobacteria and twice a day for *M. smegmatis* to produce growth curves to stationary phase.

2.2.3 Measuring Mtb viability upon stress

To investigate Mtb viability under stress, bacterial strains were grown until mid-log phase in 7H9 dextrose at a pH of 6.8 and 10 mM NaCl. Next, bacteria were exposed for a period of two doubling times to the same pH, or 5.5 and the same concentration of NaCl or 250 mM NaCl or 500 mM sucrose. I then plated for colony forming units on 7H10 agar plates. Colony forming units (CFU)/mL were determined by performing serial 10-fold dilutions in 24-well plates using culture medium Middlebrook 7H9 broth. 20 microlitres (µL) of each dilution were loaded and spread onto the Middlebrook 7H10 agar and incubated at 37 °C or 30 °C until the formation of CFU, typically four days for *M. smegmatis* and three weeks for *M. marinum* and Mtb strains.

2.2.4 Lipidomics analysis

2.2.4.1 Intact bacteria lipid profiling from solid and liquid culture

For solid culture, bacteria were grown on liquid 7H9 media until mid-log phase (OD_{600} 0.6-0.8) using dextrose as a carbon source. 10^8 bacteria/disc, which is equivalent to an OD of 1 were inoculated onto 0.22 micrometre (µm) nitrocellulose filters under vacuum filtration. Filters were put on 7H10 agar plates supplemented with dextrose and plates were incubated for five doubling times. Filters were then passed to fresh 7H10 agar plates containing dextrose at different pH levels. Bacteria were removed from filters after 1/4, one and two doubling times, by plunging the filter into ddH_2O and heat-inactivated at 98 °C for 2 hours. Next, three washes were carried out with 200 µL dH_2O by centrifuging at 17,000 x g for 5 min and bacteria were re-suspended according to the pellet size.

For liquid culture, bacteria were grown on liquid 7H9 media using dextrose as a carbon source until mid-log phase (OD_{600} 0.6-0.8). Next, cells were washed with 7H9 at different levels of pH and re-suspended in 7H9 with the desired pH level. Cultures were incubated for 0, 1/4, one and two doubling times and heat-inactivated at 98 °C for 2 hours. Next three washes were carried out with 200 µL dH_2O by centrifuging at 17,000 x g and bacteria were re-suspended according to the pellet size.

2.2.4.2 Lipid fingerprint analysis by MALDI-TOF MS

0.7 µL of bacterial pellet was loaded on the MALDI-ToF-ToF target with 0.7 µL of 2-(4-Hydroxyphenylazo)benzoic acid (HABA) matrix for total lipid extracts in ethanol: H_2O; 1:1 v/v at a final concentration of 10 µg/µL (Figure 2-1). [223] MALDI-ToF-ToF MS data on the intact bacteria were acquired in the positive ($[M+H]^+$ and $[M+Na]^+$) and the negative ion mode $[M-H]^-$ using a 4800 (Applied Biosystems) mass spectrometer in the reflector mode with delayed extraction. This analysis was performed at the Faculty of Life Sciences facility, Imperial College London.

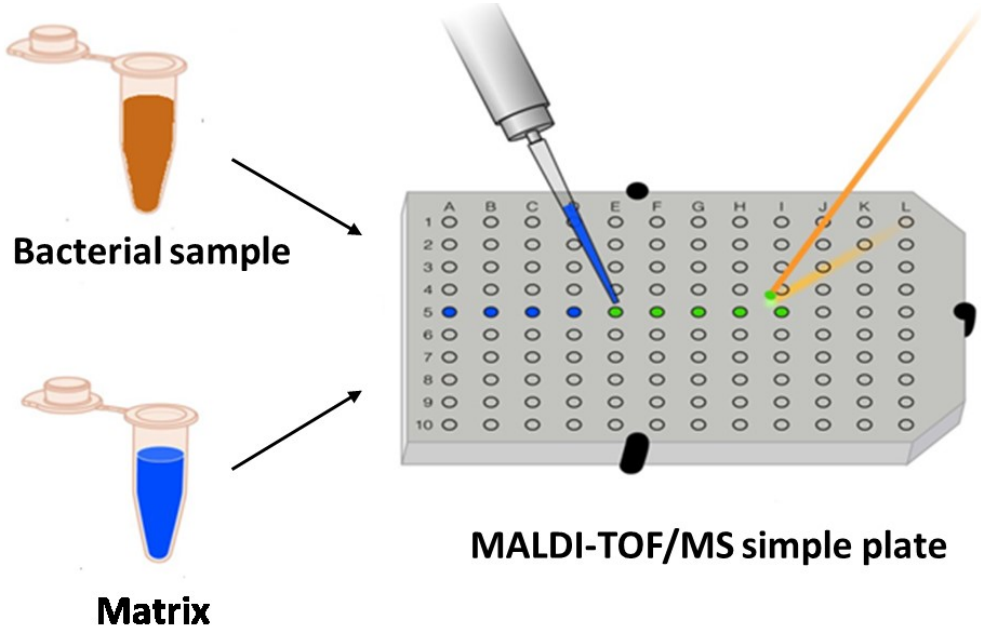


Figure 2-1. Intact cell lipidomics.
Intact cells are combined with the solubilised matrix and deposited on the MALDI plate, mixed with a micropipette and let dry gently.

2.2.4.3 Intact cell lipid profiling

Eukaryotic cells from 1.5 x 10^5 cells per mL (which is the lowest limit to perform the experiments) were seeded into 24-well tissue culture plates (Corning). Cells were allowed to adhere overnight, then scraped off and washed 3 times with 500 µL of ddH_2O by centrifuging them at 15,000 x g for 5 min and carefully discarding the supernatant. Washes were also performed using phosphate buffered saline (PBS) and the same results were observed. The final pellet was re-suspended in 100 µL of ddH_2O.

Prior to mass spectrometry analysis, the super-2,5-DHB(Sigma-Aldrich-50862) matrix was added at a final concentration of 10 mg/mL in chloroform/methanol at a ratio of 90:10 v/v. 0.4 µL of cell solution at a concentration of 1.5 x 10^5/mL to 2 x 10^6/mL, corresponding to 100 to 1,000 cells on the MALDI target plate, and 0.6 µL of the matrix solution were deposited on the MALDI target plate, mixed with a micropipette and left to dry gently. MALDI-TOF MS analysis was performed on a 4800 Proteomics Analyser (with TOF-TOF Optics, Applied Biosystems) using the reflectron mode. Samples were analysed operating at 20 kV in the negative ion mode. Mass spectrometry data were analysed using Data Explorer version 4.9 from Applied Biosystems. Assignments were based on MS/MS fragmentation profile.

2.2.5 Metabolomics analysis

2.2.5.1 Sample preparation

Bacteria were grown on liquid 7H9 media using dextrose as a carbon source until mid-log phase. 10^8 bacteria/disc, which is equivalent to an OD of 1, were inoculated onto 0.22 µm nitrocellulose filters under vacuum filtration. Filters were put on 7H10 agar plates supplemented with dextrose and plates were incubated for five doubling times. After this time period, filters were passed to fresh 7H10 agar plates containing the stress condition of choice (Figure 2-2). Metabolites were extracted at time 0, 1/4, one and two doubling times. Bacteria were metabolically quenched and removed from filters by plunging the filter into $C_2H_3N/CH_3OH/dH_2O$ (2:2:1). Metabolites were extracted by mechanical lysis via ribolysing (FastPrep-24, MP Biomedicals, United States), with 200 µL acid-washed 0.1 mm Zirconia beads per tube of bacteria-containing solution, twice for 30 seconds at 6 metre per second (m/s). Samples were then centrifuged (15,000 x g, 10 min, 4 °C) and filtered with 0.22 µm Spin-X column filters (Costar®) and the precipitate discarded. 100 µL of filtered supernatant were transferred into Eppendorf tubes containing equal volumes of 0.2% acetonitrile. Tubes were centrifuged (17,000 x g, 10 min, 4 °C) and 100 µL of supernatant from these tubes were added to V-shape LC-MS tubes containing in 0.2% acetic acid. The remaining supernatant was stored at -20 °C for further use.

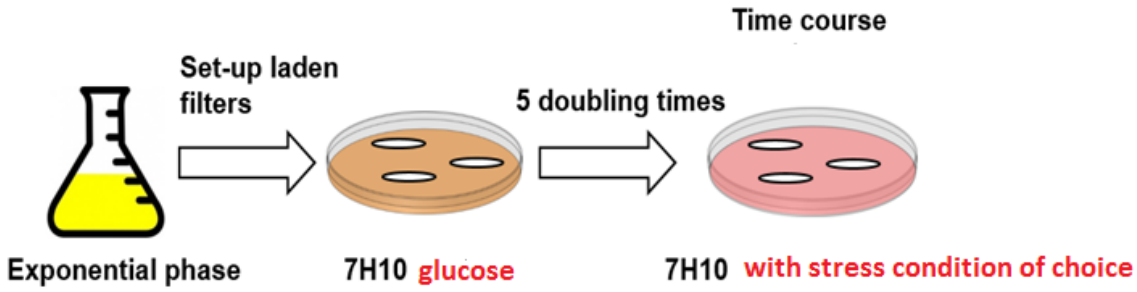


Figure 2-2. Scheme showing preparation of samples for metabolomics.

2.2.5.2 Stable isotope tracing ^{13}C metabolomics

Bacteria were grown on liquid 7H9 media using dextrose as a carbon source until mid-log phase. 10^8 bacteria/disc, which is equivalent to an OD of 1, were inoculated onto 0.22 µm nitrocellulose filters under vacuum filtration. Filters were put on 7H10 agar plates supplemented with dextrose and plates were incubated for five doubling times. After this time period, filters were passed to fresh 7H10 agar plates containing U-$^{13}C_6$ glucose at different pH ot NaCl concentrations. Metabolites were extracted at 0, 1/4, one and two doubling times. Metabolite extraction was performed as detailed previously.

2.2.5.3 LC-MS analysis

Aqueous normal phase liquid chromatography was performed using an Agilent 1290 Infinity II LC system with a binary pump, temperature-controlled auto-sampler set at 4 °C and a temperature-controlled column compartment set at 25 °C containing a Cogent Diamont Hydride Type C silica 133 column (150 mm x 2.1 mm; dead volume 315 µL). Polar metabolites were eluted using dH_2O, 0.2% acetic acid (solvent A) and acetonitrile, 0.2% acetic acid (solvent B). The following gradient was used: 0 min 85% B; 0-2 min 85% B; 3-5 min to 80% B; 6-7 min 75% B; 8-9 min 70% B; 10-11 min 50% B; 11.1-14 min 20% B; 14.1-25 min hold 20% B followed by a 5 min re-equilibration period at 85% B at a flow rate of 0.4 mL/min. Accurate mass spectrometry was carried out using an Agilent Accurate Mass 6545 QTOF apparatus. Dynamic mass axis calibration was achieved by continuous infusion, post-chromatography, of a reference mass solution using an isocratic pump connected to an ESI ionization source operated in the positive-ion mode. The nozzle voltage and fragmentor voltage were set at 2,000 V and 100 V, respectively. The nebulizer pressure was set at 50 psig, and the nitrogen drying gas flow rate was set at 5 L/min. The drying gas temperature was maintained at 300 °C. The MS acquisition rate was 1.5 spectra/sec, and *m/z* data ranging from 50-1,200 were stored. This instrument enabled accurate mass spectral measurements with an error of less than 5 parts-per-million (ppm), mass resolution ranging from

10,000-25,000 over the *m*/*z* range of 121-955 atomic mass units, and a 100,000-fold dynamic range with picomolar sensitivity. The data were collected in the centroid 4 GHz (extended dynamic range) mode. Detected *m*/*z* were deemed to be identified metabolites on the basis of unique accurate mass-retention time identifiers for masses exhibiting the expected distribution of accompanying isotopomers. Typical variation in abundance for most of the metabolites remained between 5 and 10% under these experimental conditions.

The extent of $^{13}C_6$ labelling for each metabolite was determined by dividing the added peak height ion intensities of all $^{13}C_6$-labelled species by the ion intensity of both labelled and unlabelled species using the software Agilent Profinder version B.8.0.00 service pack 3.

2.2.5.4 Bicinchoninic acid assay (BCA)

The total protein concentration of the samples analysed via LC-MS was measured using the BCA assay (ThermoFisher), carried out according to the manufacturer's instructions.

2.2.6 Detecting acetylation using Mass Spectrometry

2.2.6.1 Sample preparation

Mtb strains were grown in liquid 7H9 media until mid-log phase at pH 6.8 in the presence or absence of BSA and at pH 5.5 in the presence or absence of BSA. For preparation of the samples for auto LC-MS/MS, 1 mL of sample was taken from mid-log phase of bacterial cultures. The samples were spun down at 2000 x g for 10 min and the cell pellet was kept and stored at -80 ^{o}C. The pellet was re-suspended in 1 ml of PBS and deacetylase inhibitor was added. The samples were ribolysed (FastPrep-24, MP Biomedicals, United States) with 0.1 mm Zirconia beads per tube of bacteria-containing solution three times for 1 min at 6 m/s. Samples were then centrifuged (15,000 x g, 10 minutes, 4 °C) and filtered twice with 0.22 µm Spin-X column filters (Costar®) and the precipitate discarded. 100 µL of each sample was reduced with 10 µL of 25 mM dithiothreitol (final concentration) at 80 °C for 15 min. 10 µL of 50 mM iodoacetic acid (final concentration) was added, pipette-mixed and left in the dark for 30 min. The samples were digested for 24 hours at 37 °C by adding 20 µL of 0.10 mg/mL mass spectrometry grade trypsin (Promega, UK). 20 µL of each digested sample were injected in the LC-MS instrument.

2.2.6.2 LC-MS method used for proteomics

Liquid Chromatography with tandem mass spectrometry (LC-MS/MS) method was applied using an Agilent 1290 LC system coupled to an Agilent 6550 quadrupole –time-of-flight (Q-ToF) mass spectrometer with electrospray ionisation (Agilent, Santa Clara, CA). The LC column used was an

Agilent Zorbax Extend C-18, 2.1 x 50 mm and 1.8 µM particle size. The LC buffers were Solvent A -0.1% formic acid in water and Solvent B -0.1% formic acid in acetonitrile (v/v). A flow rate of 0.2 mL/min was used.

2.2.6.3 LC-MS/MS workflow for detection of acetylated proteins

Following trypsin digestion and generation of data using the LC-MS method for proteomics, the data of each sample were analysed in Spectrum mill software (Agilent). Figure 2-3 summarises the workflow used. The criteria chosen for spectrum mill are below:

-MS/MS search modification chosen: acetyl (k)

-Precursor mass tolerance: +/- :100 ppm

-Product mass tolerance: +/- : 100 ppm

-Minimum matched peak intensity: 50%

-Peptide score: 5

-Peptide% SPI: 50

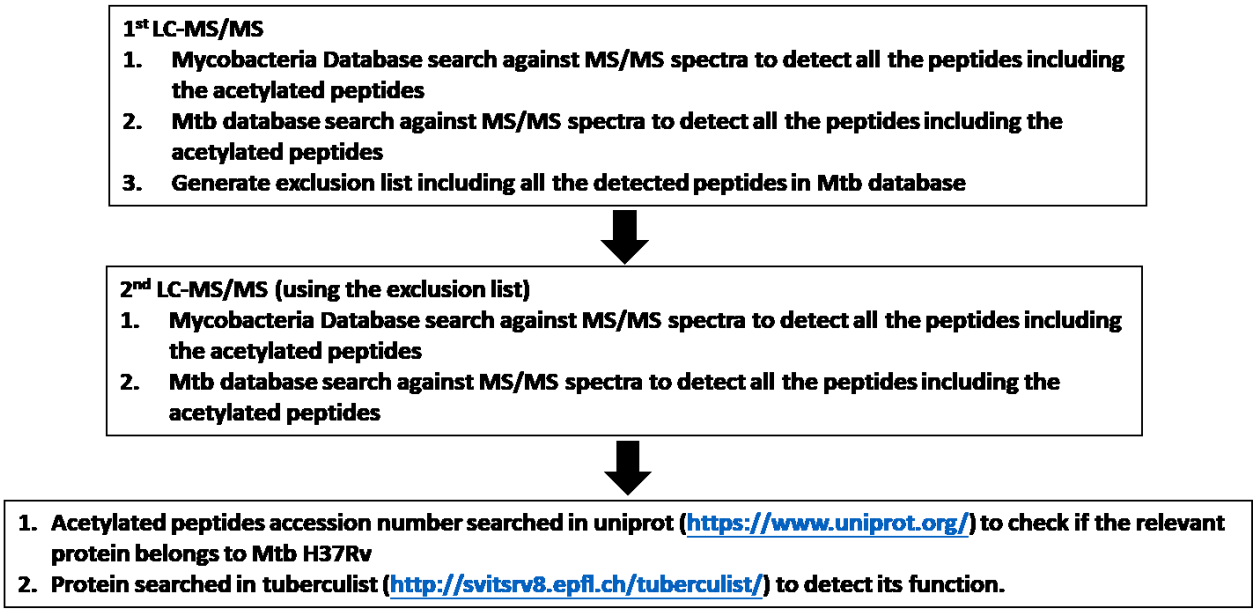


Figure 2-3. Liquid chromatography tandem mass spectrometry workflow for proteomics. Acetylated peptides were identified in the 1st LC-MS/MS. To enhance detection we proceeded to a 2nd LC-MS/MS as follows: All the peptides detected through the Mtb database were excluded in the 2nd LC-MS/MS (in order to be able to detect even more acetylated peptides).

2.2.7 Transcriptomics

Mtb H37Rv parental strain was grown in 7H9 liquid medium at 37 °C containing 10 mM NaCl as described above. Bacteria were stressed by the addition of NaCl to a concentration of 250 mM

NaCl after 1/12, 1/3 and one doubling times at mid-log phase (light transmittance at 600 nm ~0.6). Total RNA was extracted using a fast RNA pro bluekit (MP Biomedicals). RNA was treated with RNase-free DNase (Promega) and purified using RNAeasy columns (Qiagen) according to the manufacturer's instructions. Fluorescently labelled cDNA was generated from total RNA (1 µg) by direct incorporation of Cy3- or Cy5-dCTP (GE Healthcare) using Superscript III Reverse Transcriptase (Invitrogen Life Technologies) in the presence of random hexamers (3 µg), deoxyribonucleotide triphosphates (dNTPs) (185 µM deoxycytidine triphosphate (dCTP) and 463 µM each of deoxyadenosine triphosphate (dATP), deoxyguanosine triphosphate (dGTP) and thymidine triphosphate (dTTP)) and Cy3-dCTP or Cy5-dCTP (1.7 nmoles). RNA and random hexamers were initially mixed, made up to a volume of 11 µL and heated to 95 °C for 5 min. The mixture was then chilled on ice for 2 min. The remaining components of the reverse transcriptase reaction were added, and the mixture was incubated for 10 min at 25 °C, followed by 42 °C for 90 min. Samples to be compared were mixed, and the labelled cDNA was purified using MinElute PCR purification columns (Qiagen). Mtb whole-genome microarray slides (prepared at St. George's, University of London) were initially prehybridised in 3.5× saline-sodium citrate (SSC), 0.1% SDS and 10 mg/mL BSA for 20 min at 65 °C and then washed with deionised water and isopropanol. Labelled samples were heated for 2 min at 95 °C in 4xSSC and 0.3% SDS and hybridised on microarray slides under lifter slips (Thermo Scientific) for 16–20 hours at 65 °C in a dark hybridisation chamber. Hybridised slides were washed once with 1xSSC, 0.05% SDS at 65 °C and then twice with 0.06xSSC at room temperature. Washed slides were dried by centrifugation and scanned for fluorescence with a GenePix 4000B microarray scanner. Grids were fitted to the raw microarray images, and background normalisation and spot quantitation were performed using Bluefuse software (BlueGnome Ltd., Cambridge, United Kingdom); normalised readings were plotted using GeneSpring 10 software (Silicon Genetics). Data were obtained for six slides, including dye swaps, from three bacterial cultures. Data were initially filtered according to expression, and the lower 20th percentile was eliminated from the analysis. Genes that showed greater than a twofold change in absolute expression with a p-value < 0.05 (Student's t-test) were considered to be altered.

2.2.8 Tissue culture assays

2.2.8.1 Culture of RAW 264.7 macrophages

RAW 264.7 macrophages were maintained in Dulbecco's minimal essential medium (DMEM, Gibco by Life Technologies) supplemented with 10% heat-inactivated fetal bovine serum (FBS) at 37 °C. Cells were washed with supplemented DMEM at 37 °C and seeded into 24-well, 96-well (Corning) or 8-well (Agilent Technologies) plates.

2.2.8.2 Culture of HeLa cells

HeLa (ATCC CCL) cells were maintained in DMEM supplemented with 10% heat-inactivated FBS at 37 °C. Cells were washed with supplemented DMEM at 37 °C and seeded into 24-well, 96-well (Corning) or 8-well (Agilent Technologies) plates.

2.2.8.3 Isolation of mouse bone marrow-derived macrophages

Bone marrow cells from an 8 week-old female BALB/c mouse were isolated and differentiated into macrophages for 6 days in Roswell Park Memorial Institute medium (RPMI 1640) (Lonza, United Kingdom) supplemented with 1 mM sodium pyruvate (Lonza, United Kingdom), 2 mM L-glutamine (Lonza, United Kingdom), 0.05 M 2-mercaptoethanol (Invitrogen, United Kingdom), 10% heat-inactivated FBS (Biosera, United Kingdom) and 20% L-cell conditioned medium. On day 4, cells were fed with an additional 10 mL of medium. After 6 days in culture, cells were washed with supplemented RPMI at room temperature and seeded into 24-well, 96-well (Corning) or 8-well (Agilent Technologies) plates.

2.2.8.4 Antibiotics treatments of mammalian cells

Cells were treated for 24 hours at 37 °C in an incubator with 5% CO_2 with 1/5 C_{max}, C_{max} and 5*C_{max} corresponding to 0.8 µg/mL, 4 µg/mL and 20 µg/mL for ethambutol, 5 µg/mL, 25 µg/mL and 125 µg/mL for kanamycin, and 2.2 µg/mL, 11 µg/mL and 55 µg/mL for levofloxacin. After 24 hours' exposure, cells were then used for further analysis.

2.2.8.5 Seahorse XF Cell Mito Stress Test

Mouse BMDM, RAW 264.7 and Hela cells were seeded on an 8 well miniplate at a cell density of $5x10^5$, $1x10^5$ and $1.5x10^5$ cells/mL respectively and left to adhere overnight. Cells were treated or not with antibiotics and after 24 hours the oxygen consumption rate (OCR) was measured using a Seahorse XFp extracellular flux analyser (Seahorse Bioscience). The day before the assay, the sensor cartridge was hydrated by filling the utility plate with 200 µL of sterile ddH_2O and incubating overnight at 37 °C in a non-CO_2 incubator. On the day of the assay, the water was replaced with 200 µL of pre-warmed XF Calibrant (Agilent) and incubated for 1 hour at 37 °C in a non-CO_2 incubator. Also on the day of the assay, the culture medium was replaced with 180 µL of un-buffered Seahorse XF media (DMEM with phenol red supplemented with 10 mM glucose, 1 mM sodium pyruvate, 2 mM glutamine, phenol red, pH 7.4) and the cells were incubated at 37 °C in a non-CO_2 incubator for 45 min. Baseline rates were measured at 37 °C three times before sequentially injecting the following mitochondrial inhibitors: oligomycin (10

µM); carbonycyanide p-(trifluoromethoxy) phenylhydrazone (FCCP, 20 µM); and rotenone and antimycin A mixure (5 µM). After the addition of each inhibitor, three readings were also taken. OCR was automatically calculated by the Seahorse XFp software. Every point represents an average of 3 different wells.

2.2.8.6 Cell viability assay

Cell viability was assessed using Alamar Blue Cell Viability Reagent (Cat#DAL1025) (purchased from Thermo Fisher SCIENTIFIC), following the manufacturer's instructions. 9,000 cells per well were seeded on a black, clear bottom 96-well plate (Corning). Cells were treated or not with antibiotics for 24 hours. 5% dimethyl sulfoxide (DMSO) (Sigma) in media was used as a positive control. Fluorescence intensity was monitored using a HIDEX microplate reader with excitation and emission wavelengths set at 544 and 590 nm, respectively. Assay was performed in quadruplicate and repeated 3 times.

2.2.8.7 Membrane potential measurement

6,000 HeLa cells per well were seeded on a black sterile 96-well plate with a clear flat bottom. After 24 hours, cells were treated with kanaycin 25µg/mL for 24 hours and changes in membrane potential were measured by fluorescence at excitation of 475 nm and emission of 530 nm following the protocol of the JC-1-Mitochondrial Membrane potential assay kit and as recommended by the manufacturer (ab113850).

2.2.8.8 Microscopy of HeLa cells

HeLa cells were plated (1 - 5 x 10^5) on glass coverslips in 6-well plates (Thermo Scientific) and used for experiments 24 hours later. HeLa cells were treated with 25 µg/mL kanamycin for 24 hours and incubated with 0.1 µM MitoTrackerTM Red CMXRos for 30 min prior to fixation. HeLa cells were washed with 1 x phosphate-buffered saline (PBS) and fixed in 4% paraformaldehyde (PFA) for 15 min at room temperature. Following this, cells were washed with 1 x PBS, incubated for 10 min in 1 µg/mL 4',6-diamidino-2-phenylindole (DAPI) and mounted in aqua polymount mounting medium (Polyscience Inc.).

Samples were imaged on Axiovert Z1 driven by ZEN software (Carl Zeiss MicroImaging) taking Z-stack image series using a 63X oil objective. Image deconvolution was performed using ZEN software and mitochondrial morphology was analysed using the MiNA-master plugin for FIJI. At least 100 cells per experiment from 3 independent experiments were used for analysis. Image processing was performed in Icy (http://icy.bioimageanalysis.org).

2.2.8.9 Infection with Mtb of resting and IFN-γ-activated macrophages

Three strains of Mtb were used: wild type, the *Δrv0998*; and the complemented strain. BMDMs were infected with *Mtb* from mid-log phase cultures using dextrose as carbon source at a multiplicity of infection (MOI) of 1. Extracellular bacteria were killed by the use of gentamicin 50 µg/mL and removed by washings with PBS. After the washings, macrophages for days 2 and 5 were re-suspended in supplemented RPMI whereas macrophages for day 0 were lysed with sterile ddH_2O for 30 min and plated for CFU. Supernatants were removed at 2 and 5 days post-infection and filtered using 0.22 µm filters (Millipore, United Kingdom). Intracellular growth of Mtb was also determined at 2 and 5 days post-infection in the lysed cells.

2.2.8.10 TNF-α production by activated and non-activated macrophages

TNF-α production by macrophages was determined using the mouse TNF-α ELISA kit (Ready-SET-Go by Affymetrix eBioscience) according to the manufacturer's instructions. Absorbance readings were measured at 450 nm.

2.2.9 Statistical analyses

Data shown represent the average of the replicates ± standard deviation. All figures represent the average of three biological replicates except when specified. Statistical analysis was performed using Microsoft Excel Two tailed Welch's T-test. *P* values < 0.05 were considered to be statistically significant ($p < 0.05$ (*)). Were results are expressed as fold changes as described in the figures and figure legends; the standard deviation was calculated according to the error propagation in calculated ratios. [224]

Chapter 3: Intact cell lipidomics reveal changes to the ratio of cardiolipins to phosphatidylinositols in response to kanamycin

3. Intact cell lipidomics reveal changes to the ratio of cardiolipins to phosphatidylinositols in response to kanamycin

3.1 Introduction

3.1.1 Antibiotic toxicity

Antimicrobial agents were discovered for the treatment of infectious diseases in the 1930s and since then they have saved numerous lives by decreasing the mortality and morbidity caused by bacterial infections.[225] The success of penicillin for the treatment of pneumonia, tetracyclines for brucellosis, chloramphenicol for typhoid fever, and sulphonamides for meningitis and venereal diseases, was so satisfactory that the secondary effects remained practically unseen.[225] On balance, the advantages outweighed the risks of antibiotics.[225] Since the majority of patients and clinicians were completely unfamiliar with any significant toxicity, they continued to consume them, even on self-prescription, without worrying about the consequences.[225] The collective, unconscious, assumption was that antibiotics were essentially non-toxic.[225] However, they have various side effects and therefore they can be a double-edged sword. For example aminoglycosides, a group of antibiotics including streptomycin, amikacin, gentamicin, and kanamycin among others, are ototoxic and nephrotoxic in humans.[226,227] Another example is vancomycin, a glycopeptide considered to be the standard treatment for Methicillin-resistant *Staphylococcus aureus* (MRSA) and which has been linked with nephrotoxicity.[228] Additionally, fluoroquinolones, which have been widely used to treat infections caused by gram-negative organisms and more recently against gram-positive and/or anaerobic bacteria, have been associated with an increase in tendon injury incidence.[229] Even though antibiotic mechanisms of action and their targets have been extensively studied and well characterised in bacteria, the mechanistic effects of commonly prescribed antibiotics on mammalian cells remain unclear.[230]

3.1.2 Mitochondria, an antibiotic target

3.1.2.1 Mitochondrial composition

Mitochondria are cytosolic organelles which have evolved from endosymbiotic α-proteobacteria.[231] Mitochondria are maternally inherited unlike other organelles in mammalian cells. They have their own genome and a double membrane structure,[231] which is composed of an outer membrane and an inner membrane. The outer mitochondrial membrane (OMM) and inner mitochondrial membrane (IMM) contain structural PLs, which are negatively charged molecules. These include phosphatidylethanolamine (PE), phosphatidylcholine (PC), phosphatidylinositol (PI) and CL (Figure 3-1). However, PLs abundance varies between the OMM and IMM. It has been reported that in the mammalian OMM 54% of the total are PC, 29% are

PE and 14% are PI.[232] As far as the IMM is concerned, PC and PE are still the most abundant PLs. They comprise about 75% of total lipids.[233] Nevertheless, one of the largest differences between OMM and IMM lipid composition is the highest CL concentration found in the IMM.[233] CLs are found almost exclusively in the IMM making up about 15% to 20% of the total PL mass.[232]



Figure 3-1. Chemical structures of CL, PI, PC and PE.
The outer mitochondrial membrane and inner mitochondrial membrane contain structural PL, which are negatively charged molecules with the phosphate group as polar head, some of which are CL (A), PI (B), PC (C), and PE (D). [232] R1-R4 are four fatty acyl chains.

3.1.2.2 Mitochondrial function

Mitochondria contribute to a wide range of cellular events that include thermogenesis, calcium homeostasis, energy homeostasis, steroidogenesis, oxidative stress, detoxification, inflammation and cell death, among others.[234–239] Mitochondria are the main cellular energy source since they couple the oxidation of fatty acids and pyruvate to ATP production by the Electron transport chain (ETC) (Figure 3-2). In the mitochondrial matrix, the TCA cycle enzymes produce electron carriers, which include flavin adenine dinucleotide (FADH2) and nicotineamide-adeninedinucleotide (NADH).[240] These donate electrons to the ETC, which consists of protein complexes I to IV, and two soluble factors, cytochrome c and coenzyme Q. Complex I is the first and largest of the complexes comprising 45 core subunits. Complex I and II mediate a two-electron transfer from the electron carriers NADH and FADH2, respectively, to the mobile electron carrier coenzyme Q. The latter can also receive electrons from the breaking down of a number of nutrients, such as choline, oxidation of fatty acids and amino acids. Complex III is an adaptor, which receives two electrons from reduced coenzyme Q and shuttles single electrons to cytochrome c. Complex IV ends the respiratory chain by accepting electrons

from cytochrome c, to fully reduce oxygen to H_2O.[241,242] The sequential reduction/oxidation (redox) reactions in the ETC lead to conformational changes in the respiratory complexes allowing them to pump protons out from the matrix to the intermembrane space, creating an electrochemical gradient. This is known as the mitochondrial transmembrane potential (Δφm). Complex V (ATP synthase) uses the proton drive force created by the proton gradient produced by Complexes I, III and IV, to phosphorylate adenosine diphosphate (ADP) to produce ATP (Figure 3-2).[241] Apart from ATP generation, other processes, including mitochondrial protein import across the IMM, are dependent on the transmembrane potential.[231,243] A small proportion of electrons (0.15%-0.8%), which mainly leak from complexes III and V from the ETC, react with oxygen to form ROS from superoxide.[244,245] ROS are physiological signals that participate in different functions of the cell. Nevertheless, when there is too much of it, it can cause cell dysfunction and/or death. Furthermore, oxidative damage can increase the production of ROS by the mitochondria. Therefore, how mitochondria are regulated is of vital importance for the integrity of the cell.[246]

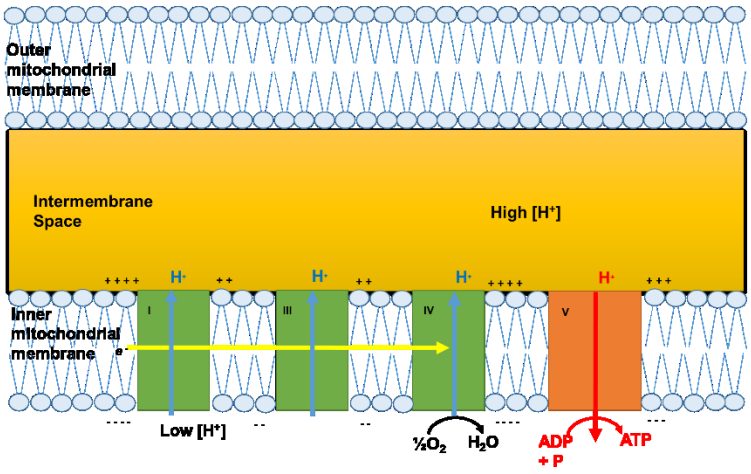


Figure 3-2. Electron transport chain.
The electron transport chain (yellow arrow) consists of transmembrane proteins located in the inner membrane of mitochondria. The electrons are shuttled between the proteins. This is used to pump protons by complexes I, II and IV (blue arrow) to the space between the inner membrane and the outer membrane, creating a gradient, which will be used for ATP production (red arrow). Figure adapted from Voet *et al.*[247]

Mitochondria are an important metabolic hub for catabolism. During glycolysis, glucose is oxidised to pyruvate in the cytosol. Pyruvate is then transported into the mitochondrial matrix where it is oxidised and it reacts with Coenzyme A, to form acetyl-CoA. Furthermore, pyruvate can also be carboxylated to directly form oxaloacetate, a component of the TCA cycle. Nevertheless, in fatty acid β-oxidation, long-chain fatty acids are catabolised in cycles where two

carbons per cycle are cleaved off in the mitochondrial matrix, to form acetyl-CoA. Additionally, glutamine forms glutamate via glutaminolysis, and the latter can be converted in the mitochondria to α-KG, a TCA cycle component.[231,248]

Mitochondria also play a role in the biosynthesis of macromolecules like lipids, nucleotides, heme and iron-sulfur clusters.[231] Mitochondria can synthesise fatty acids in an acyl carrier protein (ACP)-dependent manner (Figure 3-3). In eukaryotic cells, fatty acid synthesis (FAS) occurs in the mitochondria in addition to the 'classic' cytoplasmic FAS (FAS I).[249] Disruption of mitochondrial FAS changes the mitochondrial PL composition. Nevertheless, it is uncertain whether this is an indirect effect as a result of disturbed mitochondrial metabolism or whether it is due to a reduced channelling of mitochondrially synthesised acyl groups into PLs. Furthermore, mitochondrially synthesised long-chain fatty acids such as 3-hydroxymyristoyl-ACP, which is a component of mammalian mitochondrial complex I, can be used for protein acylation.[250] The best characterised physiological function of mitochondrial FAS is to provide the octanoyl chain for lipoic acid synthesis. Mitochondrial lipoic acid synthesis appears to be an essential process in mammals since lipoic acid synthase deletion leads to embryonic lethality in mice.[249,251]

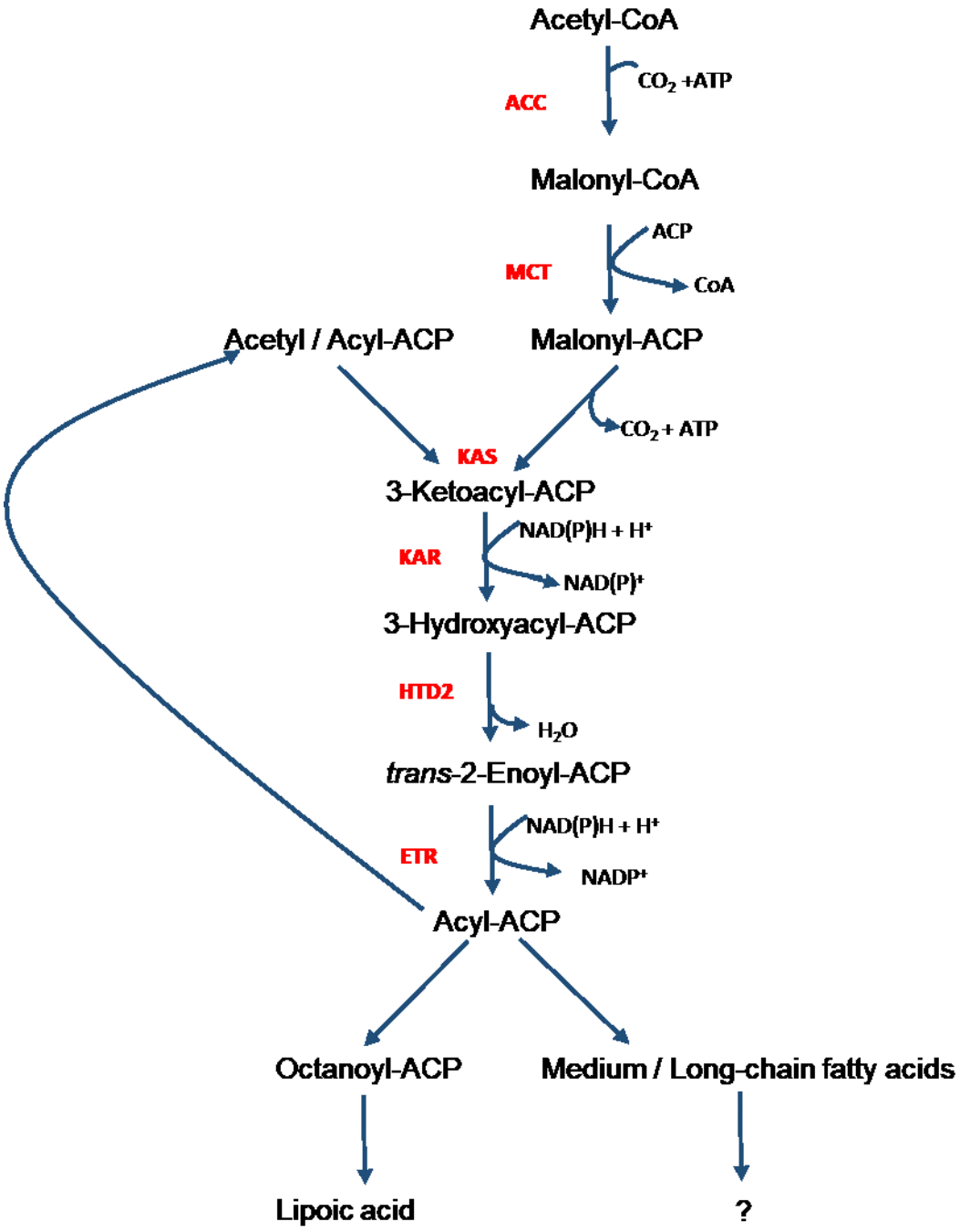


Figure 3-3. Scheme showing fatty acid synthesis in the mitochondria.
ACC, acetyl-CoA carboxylase; MCT, malonyl-CoA transferase; ACP, acyl-carrier protein; KAS, ketoacyl synthase; KAR, ketoacyl reductase; HTD2, hydroxyacyl-thioester reductase type 2; ETR, enoyl-thioester reductase. Figure adapted from Hiltunen *et al.*[249]

3.1.2.3 Mitochondrial dysfunction

Altered mitochondrial function involves pathological conditions which include neurodegeneration and cancer, cardiomyopathies, metabolic disorders, and disorders tightly associated with dysregulated cell death.[252–254] Moreover, considering that programmed cell death accompanies the impairment of metabolic functions, the impairment of mitochondrial signalling is closely related to developmental processes and tissue homeostasis.[231] Research studies have shown that clinically relevant concentrations of antibiotics induce the formation of lethal ROS and mitochondrial dysfunction in mammalian cells. This is caused by the TCA cycle and the ETC disruption.[230,255–258] CLs and PLs are associated with enzymes and oxidative phosphorylation complexes, which are involved in ATP biosynthesis and the maintenance of the ETC.[233,259] Thus, I hypothesise that mitochondrial damage caused by antibiotics could be detected at the lipid level by measuring the ratio of CL:PI.

Knowing the crucial role mitochondria play in the cell, the assessment of antibiotic toxicity is of vital importance in drug discovery. For instance, cerivastatin, a cholesterol lowering drug, and anti-inflammatory and antidiabetic drug troglitazone,[260,261] were withdrawn from the market in the early 2000s as a consequence of their impairment to mitochondrial function. It is also important to consider that between 1994 and 2006, 38 antibiotics approved by the US Food and Drug Administration (FDA) were withdrawn, which represents around 2% of commercially available drugs.[262,263] Thus, not only is it essential to develop better antibiotics but also to select antibiotics that do not generate ROS, mitochondrial damage, or other negative side effects.[258]

3.1.3 Available cell toxicity detection methods

There are commercially available assays to measure the antibiotic toxicity effect in mitochondria. They can be based on measurements of cellular ATP levels using luminescence assays, or on changes in mitochondrial membrane potential using fluorescence assays by flow cytometry by using a multi-well spectrophotometer such an ELISA reader or fluorescence microscopy.[230] Moreover, other technologies can assess antibiotic toxicity by measuring mitochondrial oxygen consumption using oxygen sensors, time-resolved fluorescence microscopy or fluorescence lifetime imaging. Nevertheless, these solutions are expensive and/or time-consuming.[264–266]

Antibiotics can affect the central carbon metabolism and thus the TCA cycle and the ETC. This then leads to a reduction in metabolic activity and to changes in metabolic pathway. One of the metabolic pathways which could be affected is fatty acid synthesis as a result of changes in the

TCA cycle activity, and an alteration of available levels of acetyl-CoA required for lipid synthesis.[258] For instance, studies conducted by Kohanski *et al.* in *E. coli* have demonstrated that bactericidal antibiotics targeting DNA replication and repair, protein synthesis or cell-wall biosynthesis, stimulate hydroxyl radical formation in bacteria by the Fenton reaction leading to cell death.[267] This reaction consists of hydroxyl radicals formation via the reduction of hydrogen peroxide by ferrous iron.[267] These events happen to be mediated by the TCA cycle and a transient depletion of NADH.[267] Studies in human cells performed by Ahler *et al.* demonstrated that treatment with doxycycline, a tetracycline, leads to a shift from TCA cycle to glycolytic pathway due to upregulation expression of the gene involved in the glycolytic pathway.[268,269]

3.1.4 Lipidomics to detect antibiotic toxicity

To access the whole of the lipidome and taking into account the heterogeneous nature of lipids, extraction procedures that enrich and pre-fractionate lipids can be vital for assessing lipidome changes.[270–273] The common separation of lipid classes is mainly accomplished by differential solvent extraction with a binary mixture of chloroform and methanol,[274] followed by silica thin-layer chromatography, gas chromatography, or liquid chromatography such as normal phase or hydrophobic interaction liquid chromatography (HILIC).[275–277] However, in the past 10 years, the capabilities of MALDI mass spectrometry in lipid analysis have been established for lipid extracts analysis coming from distinct biological materials.[278–282] Nevertheless, the most promising advantage of the MALDI-MS technique is performing lipid analysis avoiding extraction and/or separation steps. This is called intact cell lipidomics and is highly valuable for lipids that are tightly bound to membrane proteins such as CL, and may be difficult to recover completely in lipid extracts. Work by Angelini *et al.* reported the lipidomics analysis of *Saccharomyces cerevisae* and bovine heart mitochondria by first isolating mitochondria followed by direct MALDI-MS.[278] This research identified phosphatidic acid (PA), phosphatidylserine (PS), phosphatidylglycerol (PG), PE, PI, and CL, all in the negative ion mode. However, their study relied on organelle isolation such as the mitochondria and membranes. This is incompatible with high-throughput screening (HTS) to evaluate mitochondrial damage and antibiotic toxicity. Other studies performed by Jones *et al.* are suitable for HTS and used intact cell lipidomics by MALDI-Fourier transform-MS in untreated yeast which allowed them to detect PC, PI, PE, and PA in the positive ion mode.[283] This study included some steps of sample preparation before performing intact cell lipidomics. Washes with a TRIZMA (Tris; THAM; 2-Amino-2-(hydroxymethyl)-1,3-propanediol; Tromethamine; Trometamol) buffer followed by suspension of the pellet in 50% methanol were needed before intact cell lipidomics. Furthermore, the solution had to be deposited within 10 min on the target.

Caprioli *et al*. developed MALDI-based imaging mass spectrometry (IMS) for the detection of peptides and proteins in intact rat tissue slices.[284] IMS has progressed since then to include the detection of other biomolecules such as PLs. For instance, Wang *et al.* have provided direct profiling of PLs and lysophospholipids in the rat cortex after focal cerebral ischemia.[285] Previous research by Larrouy-Maumus *et al.* has reported bacterial lipidomics on intact mycobacteria and Enterobacteriacae without any isolation of membranes or subcellular compartments, and where the only sample preparation is directly loading the samples on the MALDI target followed by the addition of the matrix solubilised in organic solvents.[286,287] This method is compatible with HTS.

3.1.5 Seahorse: a tool to detect mitochondrial damage

Agilent Seahorse XF analysers, measure in real time the oxygen consumption rate (OCR) and the extracellular acidification rate (ECAR) at 5 to 8 min intervals. The OCR is a readout of mitochondrial respiration whereas ECAR is largely the result of glycolysis.[288] Measurements are done by isolation of 2 µL of medium above a monolayer of cells within the microplate.[288] The oxygen consumption of the cell and proton excretion cause fast, easily measurable changes to the concentrations of dissolved oxygen and free protons in this 'transient microchamber' which are measured every few seconds by solid state sensor probes residing 200 microns above the cell monolayer. The Seahorse measures the concentrations for 2 to 5 minutes and then calculates the OCR and ECAR, respectively. Once a measurement is completed, the probes lift, allowing the larger medium volume above to mix with the medium in the transient microchamber, restoring cell values to baseline.[288]

For my PhD research, I used the XF Cell Mito Stress Test, which measures key parameters of the mitochondrial function. This is achieved by measuring the OCR of live cells directly. Serial compound injections measure basal respiration, ATP production, proton leak, maximal respiration, spare respiratory capacity, and non-mitochondrial respiration (Figure 3-4). The kit uses modulators of cellular respiration, which target specific components of the ETC to reveal key metabolic function parameters. Oligomycin, FCCP, and a mix of rotenone and antimycin A are sequentially injected. The injection of Oligomycin (a complex V inhibitor) allows ATP production measurement, thus showing the ATP that is produced by the mitochondria which contributes to meeting the energetic needs of the cell. Injection of the ionophore uncoupler of oxidative phosphorylation FCCP [carbonyl cyanide 4-(trifluoromethoxy) phenylhydrazone] measures the maximal respiration by showing the maximum rate of respiration that the cell can achieve. Finally, the injection of rotenone (a complex I inhibitor) and antimycin A (a complex III

inhibitor) measures non-mitochondrial respiration, which is driven by processes outside the mitochondria. Proton leak and spare respiratory capacity are calculated using the three previous parameters and basal respiration, which consists of the oxygen consumption used to meet cellular ATP and which shows the cell's energy demand under baseline conditions. Proton leak is the remaining basal respiration not connected to ATP production. Furthermore, it can be a sign of mitochondrial damage. Regarding the spare respiratory capacity, it is the difference between maximal respiration and basal respiration and it is a measure of the cell capability to respond to an increased demand of energy.[289]

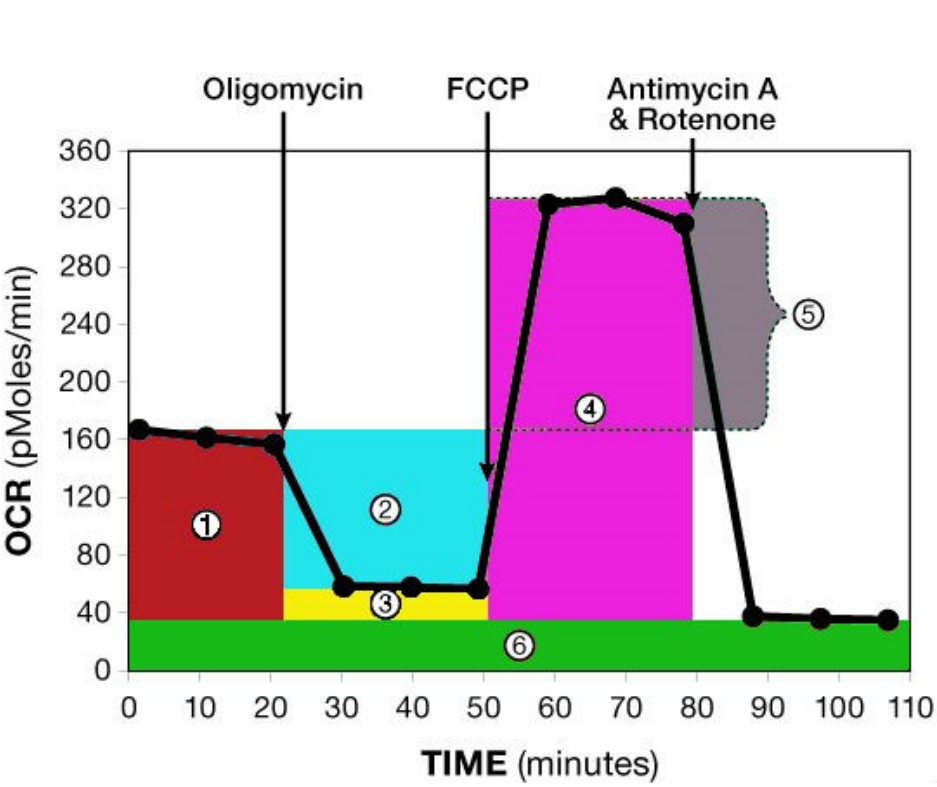


Figure 3-4. Mitochondrial respiration
The Seahorse XF Cell Mito Stress Test uses respiration modulators, which target components of the ETC revealing key parameters of the metabolic function. The serially injected compounds are oligomycin, FCCP, and a mix of rotenone and antimycin A. This allows the following measurements: (1) basal respiration; (2) ATP production; (3) proton leak; (4) maximal respiration; (5) spare respiratory capacity; (6) non-mitochondrial respiration. Figure adapted from Agilent Technologies user guide.[289]

In this chapter, I aim to investigate if treatment with antibiotics could lead to a remodelling of the cell lipidome, and if these changes can be used as potential markers of antibiotic toxicity. Therefore, the hypothesis to be tested is that lipidomics and high throughput technologies can be used as an alternative to probe changes in the relative abundance of PI and CL as a readout of mitochondrial damage resulting from antibiotic toxicity. This chapter expands and discusses my published results.[258]

3.1.6 Justification of the cell lines used

In this study three cell types were chosen; two cell lines and one primary cell. HeLa cells are a human epithelial immortal cell line and are used as a model for this study because of their widespread use in the investigation of host-pathogen interactions. HeLa cells can be invaded by a wide variety of well-studied enteropathogens, such as *Salmonella*, *Shigella*, *Listeria*, and *Yersinia.*[290–293] On the other hand, RAWs 264.7 are a murine macrophages cell line and they are able to perform phagocytosis and pinocytosis. Mouse bone marrow-derived macrophages (BMDM) are primary cells that are also widely used to study host-pathogen interactions. HeLa epithelial cells have different nutritional and metabolic requirements from those of macrophages.[294] Comparing cancer cell lines to primary cells is also of high importance. While immortalised cell lines such as HeLa cells catabolise glucose through the Embden−Meyerhof−Parnas pathway, the pentose phosphate pathway, and to a lesser extent the TCA cycle (Warburg effect), primary cells mainly employ the TCA cycle.[295–297] This can have major consequences for how the cells can respond to antibiotic stress exposure and for the CL:PI ratio.

3.1.7 Justification of antibiotic treatment and dose

The antibiotics used in this study were kanamycin, levofloxacin and ethambutol. Kanamycin is an aminoglycoside which binds to the bacterial 30S ribosomal subunit leading to t-RNA misreading; levofloxacin is a synthetic fluoroquinolone which inhibits the supercoiling activity of the DNA gyrase in bacteria, stopping DNA replication. Ethambutol inhibits the transfer of mycolic acids into the cell wall of Mtb and also inhibits mycobacterial spermidine synthesis.[298] The antibiotic concentrations used to treat mammalian cells were chosen according to the peak levels found in the serum (Cmax),[230] which were 25 µg/mL for kanamycin, 11 µg/mL for levofloxacin, and 4 µg/mL for ethambutol. To study dose-dependence effect the cells were also treated with 5-times diluted peak serum concentration (Cmax/5), and a 5-times more concentrated peak serum concentration (5*Cmax).

3.2 Results

3.2.1 Intact cell lipidomics identified different lipid classes in RAW 264.7 macrophages

The mass spectra of lipids of intact macrophages were acquired in both negative and positive ion mode using 2,5-DHB as matrix and are shown in Figures 3-5 A and B. To detect PL, a negatively charged molecule, analysis in negative ion mode was performed. In this mode, all signals in the mass spectrum are attributable to the $[M-H]^-$ molecular ions and fall into three main categories; PLs, CLs and glycosphingolipids or gangliosides. The peaks can be grouped into three main *m/z* ranges: i) m/z 700-950, attributable to major PLs; ii) *m/z* 1300-1500, attributable to CLs; and iii) m/z 1500-1650 attributable to gangliosides. In the range *m/z* 700-950, consisting of major PLs, the peaks at *m/z* 747.4 and 773.4 can be attributed to PG 34:1 and 36:2 (acyl carbons:double bonds) respectively; the peaks at *m/z* 760.4 and *m/z* 788.4 are assigned to PE 38:7 and 40:7, respectively; the peaks at *m/z* 835.4, 8611.4, 885.4 and 911.5 are assigned to PI 34:1, 36:2, 38:4 and 40:4, respectively. In this range there are also three major peaks at *m/z* 1354.7, *m/z* 1438.8 and *m/z* 1466.8, which are assigned to GalNAc-Gal-Glc-ceramides (GalNAc, *N*-Acetyl-*D*-galactosamine; Gal, *D*-galactose; and Glc, *D*-glucose) or gangliosides GM2 d18:1/16:0, GM2 d18:1/22.0, and GM2 d18:1/C24:0 respectively. In the range *m/z* 1500-1650 are found Gal-GalNAc-Gal-Glc ceramides or gangliosides GM1 at m/z 1516.8, *m/z* 1544.8, *m/z* 1572.8, *m/z* 1600.9, *m/z* 1626.9 and *m/z* 1628.9 assigned to GM1 18:1/16:0, 18:1/18:0, 18:1/20:0, 18:1/22:0, 18:1/24:1 and 18:1/24:0, respectively.

In the positive ion mode, signals in the mass spectrum can be attributed to the $[M+H]^+$ or $[M+Na]^+$ molecular ions and fall into four main categories; PLs, TAG, ganglosides and CLs. The peaks can be grouped into three main *m/z* ranges: a) *m/z* 700-1000, attributable to major PLs and TAG; b) *m/z* 1200-1300, attributable to ganglioside; and c) *m/z* 1400-1600 attributable to CLs. In the range 700-1000, the peaks at *m/z* 718.6, *m/z* 746.6, *m/z* 760.6, *m/z* 768.6, *m/z* 782.6, *m/z* 786.6, *m/z* 788.6, are assigned to PC 32:0, 34:0, 34:1, 36:3, 34:1, 36:2, 36:1 in their $[M+H]^+$ forms and the peaks at *m/z* 808.6, *m/z* 910.7, *m/z* 924.7, *m/z* 952.7 and 978.7 are still attributable to PC 36:2, 44:7, 44:0, 46:0, 48:1 in their $[M+Na]^+$ forms. The peaks at *m/z* 732.6, *m/z* 938.7 can be assigned to PE 36:0 and 48:8, respectively, in their protonated and sodiated forms. The peaks at *m/z* 885.8 and *m/z* 1005.8 are assigned to TAG 52:0 and 60:3 in their $[M+Na]^+$ forms. In the range *m/z* 1200-1300, the peaks at *m/z* 1228.8 and *m/z* 1254.8 are attributable to ganglioside GA-2 (d18:1/26:0) and GA-1 (d18:1/18:1), respectively, in their sodiated and protonated form. In the third and last range, from *m/z* 1400-1600, the peaks at *m/z* 1464.1, *m/z* 1478.1, *m/z* 1492.1, *m/z* 1506.1, *m/z* 1520.1 and *m/z* 1532.1 correspond to CLs 72:1, 74:8, 74:1, 76:8, 76:1, 78:8, respectively.

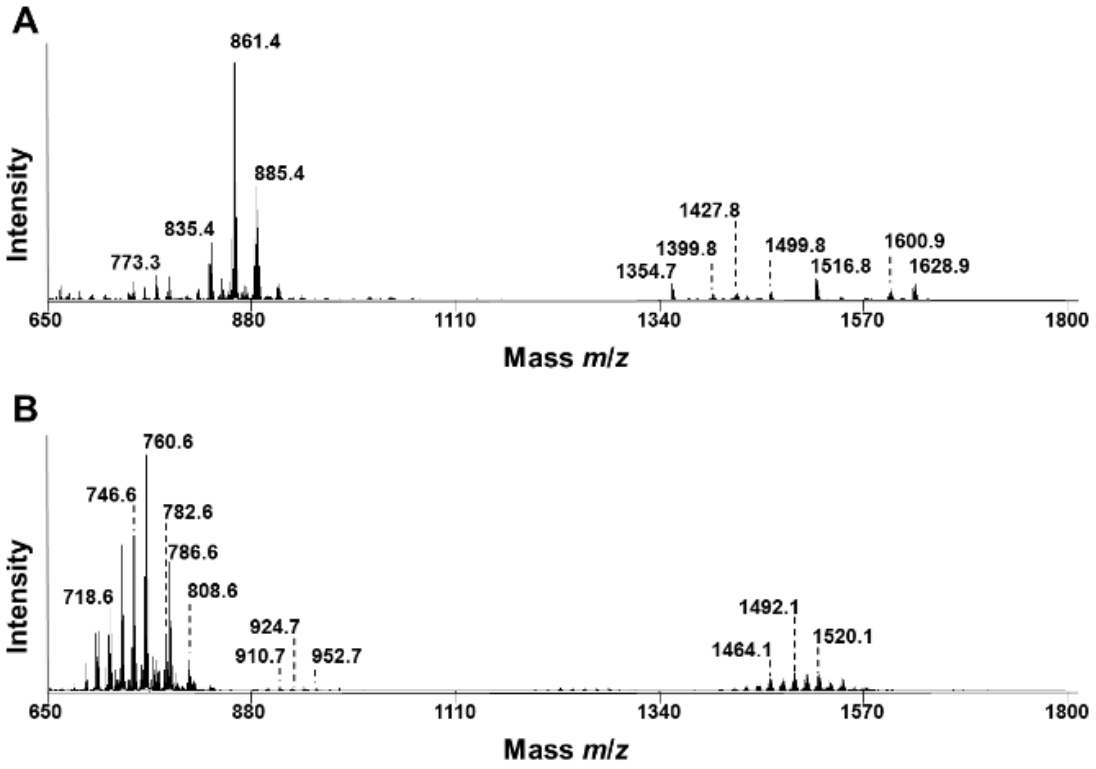


Figure 3-5. Mass spectra of lipid fingerprint on intact macrophages by MALDI MS.
Negative ion mode MALDI-TOF MS spectra of intact RAW 264.7 resting macrophages (A). The peaks can be grouped into three main *m/z* ranges: i) *m/z* 700-950, attributable to major PLs; ii) *m/z* 1300-1500, attributable to CLs and iii) *m/z* 1500-1650 attributable to gangliosides. Positive ion mode MALDI-TOF MS spectra of intact RAW 264.7 resting macrophages (B). The peaks can be grouped into three main *m/z* ranges: i) *m/z* 700-1000, attributable to major PLs and TAG; ii) *m/z* 1200-1300, attributable to gangliosides and iii) *m/z* 1400-1600 attributable to CLs. The figure shows one representative experiment from three biological replicates.

Since main lipid classes were able to be identified directly on intact macrophages I investigated this new approach in other cell types and its applicability in antibiotic toxicity screening.

3.2.2 Kanamycin treated HeLa cells suffer changes in the CL:PI ratio

HeLa cells were treated or not for 24 hours with kanamycin at the clinically relevant doses of 25 µg/mL. Clinically relevant concentrations were defined by peak levels found in the serum (Cmax).[230,299] To detect PIs and CLs by intact cell lipidomics, the mass spectra of lipids of intact HeLa cells were acquired in the negative ion mode using 2,5-DHB as the matrix (Figure 3-6 A, B). This matrix was chosen because of its versatility for the analysis of PLs.[221] In the negative ion mode all signals in the mass spectrum can be attributed to the $[M - H]^-$ molecular ions and fall into two main categories. The peaks can be grouped into two main *m/z* ranges: (i) *m/z* 800−950, attributable to major PIs; and (ii) *m/z* 1300−1500, attributable to CLs. In the range of *m/z*

800−950, consisting of major PIs, the peaks at *m/z* 835.4, 861.4, 863.4, 885.4, and 911.5 were assigned to PI 34:1, 36:2, 36:1, 38:4, and 40:4, respectively, and supported by their MS/MS profile (Figure 3-7). In the CL range, the major peaks at *m/z* 1399.8 and 1427.8 can be attributed to CL 68:4 and 70:4, where the major species are CL (16:1/C18:1)2 and CL (16:1/C18:1/ 18:1/18:1), respectively, and are supported by their MS/MS profile (Figure 3-8 and 3-9).

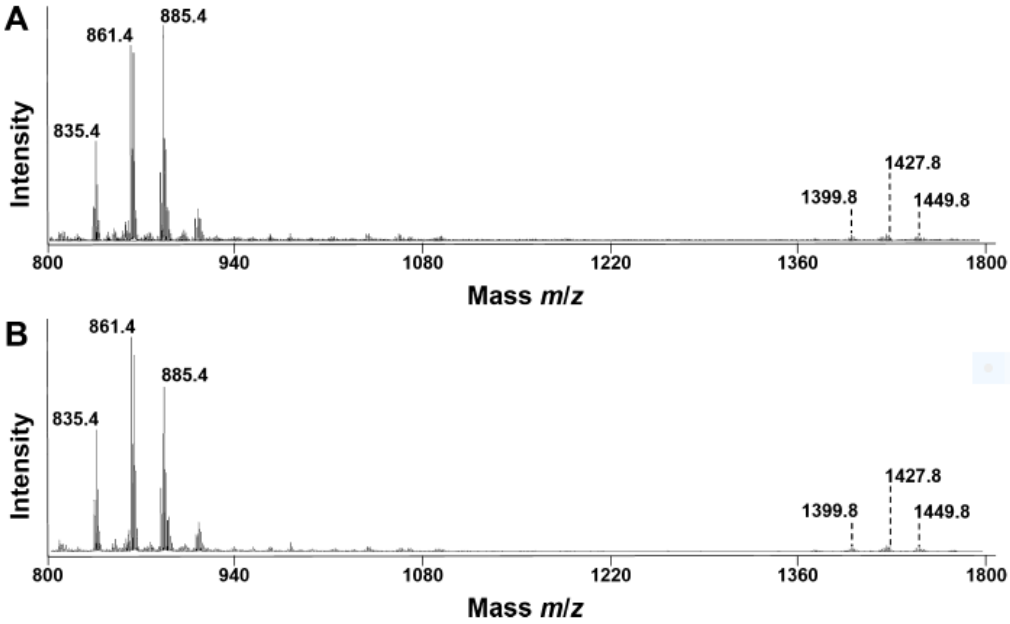


Figure 3-6. Lipid fingerprint of intact HeLa cells by MALDI-MS.
Negative ion mode MALDI-TOF MS spectra of intact untreated HeLa cells at 24 hours (A). The peaks can be grouped into two main *m/z* ranges: (i) *m/z* 800−950, attributable to major PIs, and (ii) *m/z* 1300−1500, attributable to CLs. Negative ion mode MALDI-TOF MS spectra of intact HeLa cells treated with 25 µg/mL kanamycin for 24 hours (B). Compared to untreated HeLa cells in panel A, where the major peak is at *m/z* 885.4, in kanamycin-treated cells, the major peak is at *m/z* 861.4. The figure shows one representative experiment from three biological replicates.

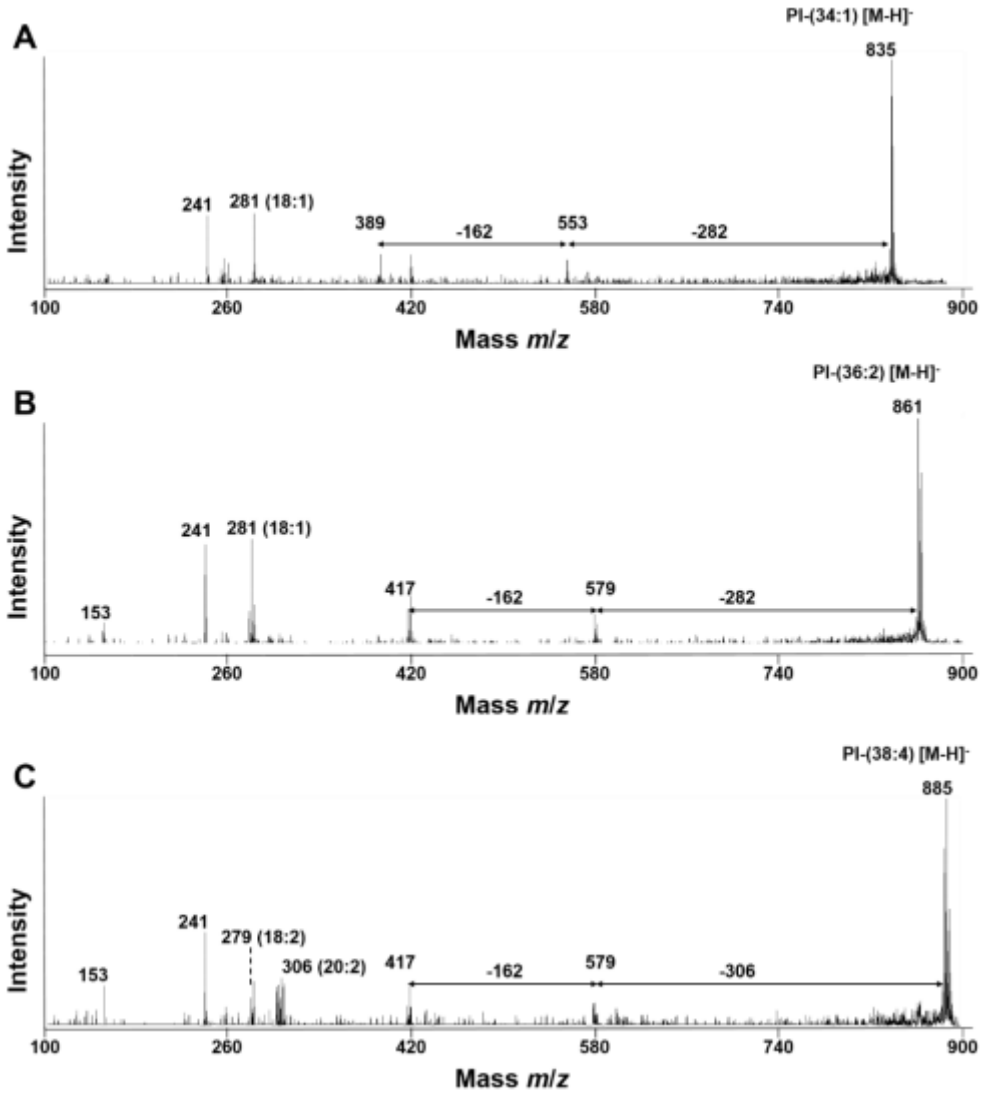


Figure 3-7. MS/MS mass spectra of peaks at *m/z* 835.4, *m/z* 861.4 and *m/z* 885.4.
MS/MS mass spectra of peaks at *m/z* 835.4, 861.4 and 885.4 are represented in A, B and C respectively. The fragment at *m/z* 241 corresponds to the polar head group fragment assigned to as inositolphosphate minus water. The fragment at *m/z* 153 corresponds to glycerophosphate minus water. The fragments at *m/z* 279 and 281 represent the fatty acid anions of linoleic and oleic acids respectively. A and B) The fragment ions at *m/z* 553 and *m/z* 579 indicate the neutral loss of 282 corresponding to an oleic acid, and the fragments ions at *m/z* 389 and *m/z* 417 show an additional neutral loss of 162 corresponding to an inositol unit minus water from the lyso-PI fragment ion at *m/z* 553 and *m/z* 579 respectively. C) The fragment ion at *m/z* 579 indicates the neutral loss of 306 corresponding to an eicosadienoic acid, and the fragment ion at *m/z* 417 shows an additional neutral loss of 162 corresponding to an inositol unit minus water from the lyso-PI fragment ion at *m/z* 579. The figure shows one representative experiment from three biological replicates.

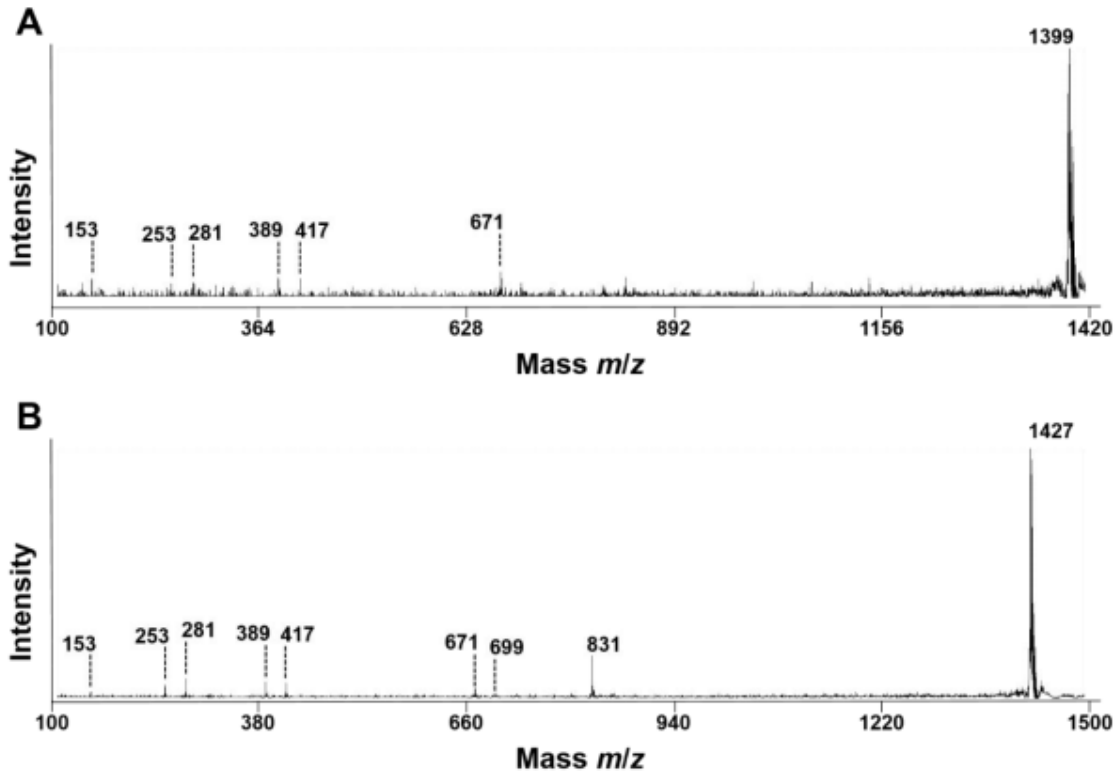


Figure 3-8. MS/MS mass spectra of CL peaks at *m/z* 1399.8 and *m/z* 1427.8.
MS/MS mass spectra of CL peaks at *m/z* 1399.8 and 1427.8 are represented in A and B respectively. The fragment at *m/z* 153 corresponds to glycerophosphate minus a molecule of water. The fragments at *m/z* 253 and 281 represent the fatty acid anions of palmitoleic (C16:1) and oleic (C18:1) acids respectively. A and B) The fragment ions at *m/z* 389 and *m/z* 417 are attributed to monoacylglycerol phosphate minus a molecule of water, C16:1GroP and C18:1GroP respectively. The peak at *m/z* 671 corresponds to diacylglycerolphosphate C16:1/C18:1GroP. B) The fragment ion at *m/z* 699 is assigned to diacylglycerolphosphate C18:1/C18:1GroP. The figure shows one representative experiment from three biological replicates.

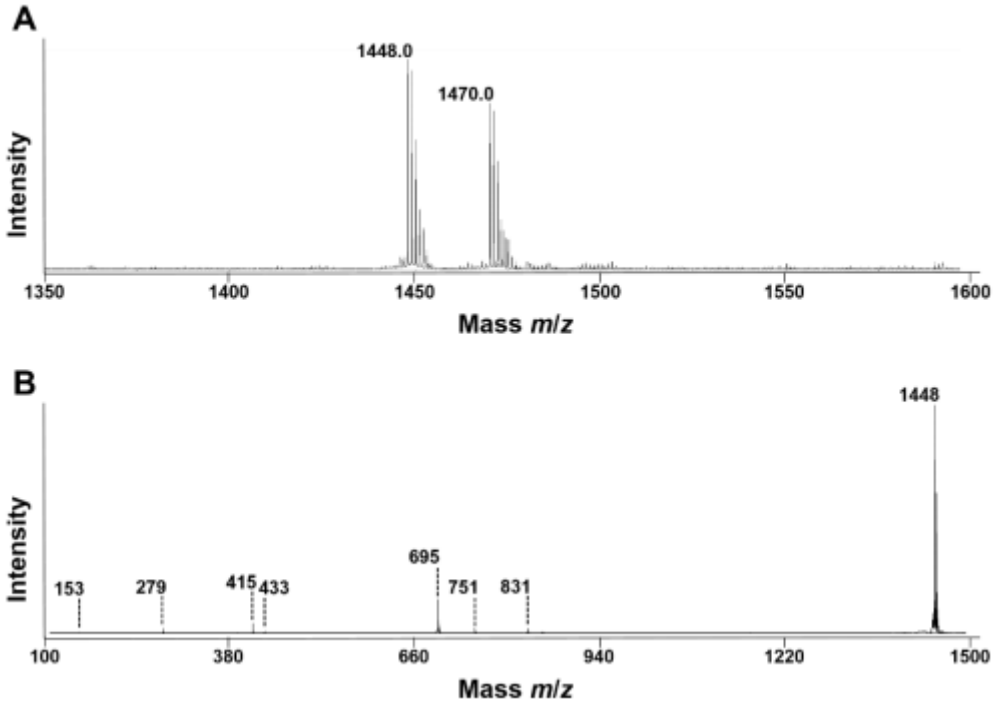


Figure 3-9. MS and MS/MS mass spectra of CL standards from mitochondria from bovine heart. MS in the negative ion mode (A) and MS/MS at *m/z* 1448.0 assigned to CL(18:2/18:2)2 (B). The fragments at *m/z* 153 corresponds to glycerophosphate minus a molecule of water. The fragment at *m/z* 279 represents the fatty acid anions of linoleic acid (C18:2). The fragment ions at *m/z* 415 and *m/z* 433 are attributed to monoacylglycerol phosphate minus and monoacylglycerol phosphate, respectively. The peak at *m/z* 695 corresponds to diacylglycerolphosphate C18:2/C18:2GroP. The figure shows one representative experiment from three biological replicates.

By comparing the mass spectra of kanamycin-treated and untreated HeLa cells (Figure 3-6 A and B), it is seen how the peak at *m/z* 885.4 decreases upon treatment with kanamycin. The ratio of long- over short-chain PI was calculated for untreated cells and kanamycin-treated cells. There was a significant change in the relative abundance of the main PI lipids, with an increase in PI lipids containing shorter fatty acid chain lengths at *m/z* 835.4, 861.4, and 863.4 compared to *m/z* 885.4, as an internal reference (Figure 3-10 A). By using the ratio of the abundance sum of PI 34:1, 36:2, and 36:1 to PI 38:4; a 25% increase in this ratio was observed in the presence of kanamycin, compared to that in untreated cells (Figure 3-10 A). Furthermore, the CL:PI ratio was calculated for kanamycin-treated and untreated cells; and a 40% decrease in CL:PI ratio was observed in kanamycin-treated cells after 24 hours compared to untreated cells (Figure 3-10 B). Taken together, these data support an alteration in PI metabolism in response to kanamycin treatment of HeLa cells for 24 hours.

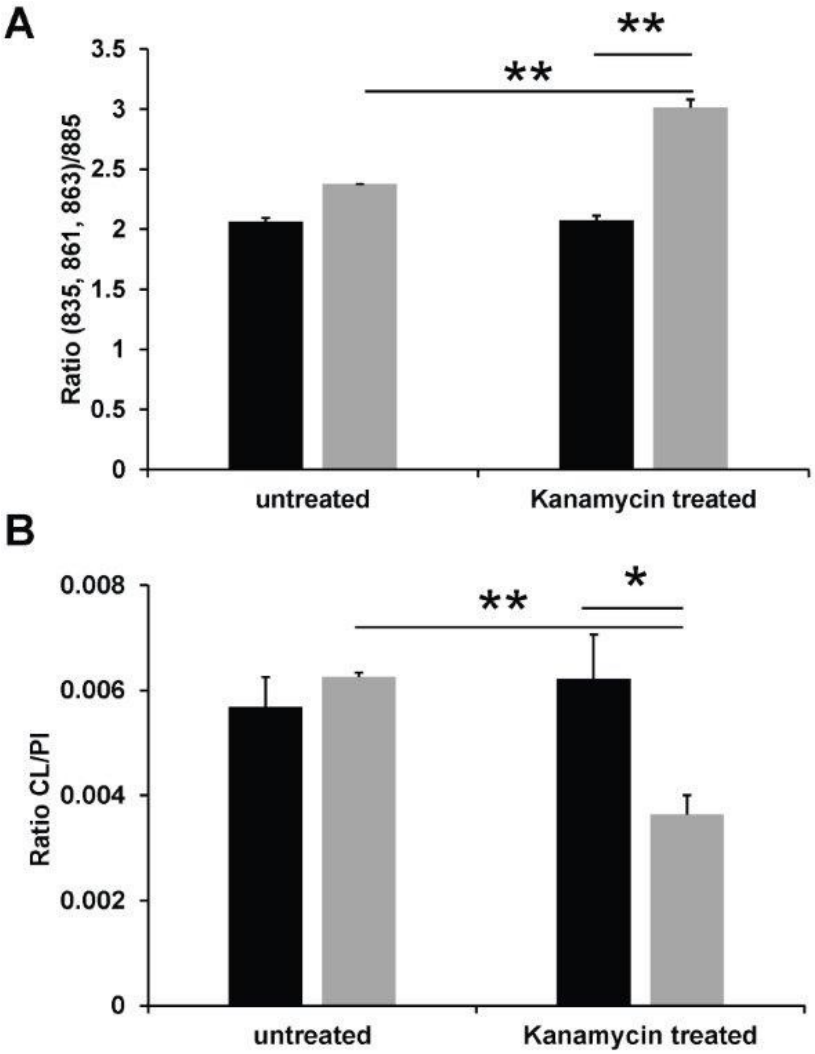


Figure 3-10. Kanamycin at 25 µg/mL for 24 hours induces changes in PLs in HeLa cells.
Ratio of the sum of the abundance of PI (34:1, 36:2, and 36:1) to PI 38:4 (A). Ratio of CL to PI lipids (B). Black bars represent time zero, and grey bars represent 24 hours. The figure shows one representative experiment out of three biological replicates. Error bars denote standard deviation. *p < 0.05 and **p < 0.005, as analysed by Student's *t*-test.

3.2.3 Kanamycin alters the membrane potential and mitochondrial morphology in HeLa cells

Membrane potential measurements provide information about the coupling of electron transfer to ATP synthesis, as well as the ability of the organelle to take up and release substrates and ions across the mitochondrial inner membrane.[300] Mitochondrial membrane potential measurements were performed on kanamycin treated and untreated HeLa cells to confirm that the observed lipid changes were due to disrupted mitochondrial bioenergetics and to mitochondrial damage instead of an indirect effect of the experimental design.[258]

HeLa cells were treated for 24 hours with 25 µg/mL kanamycin, and the mitochondrial membrane potential was measured and expressed as a ratio compared to untreated cells (Figure

3-11). In this case, a 20% decrease was observed in the membrane potential of kanamycin-treated cells compared to that of untreated cells. Furthermore, a comparison of the membrane potential of untreated cells with that of the uncoupler FCCP showed a decrease of 60% of the latter.

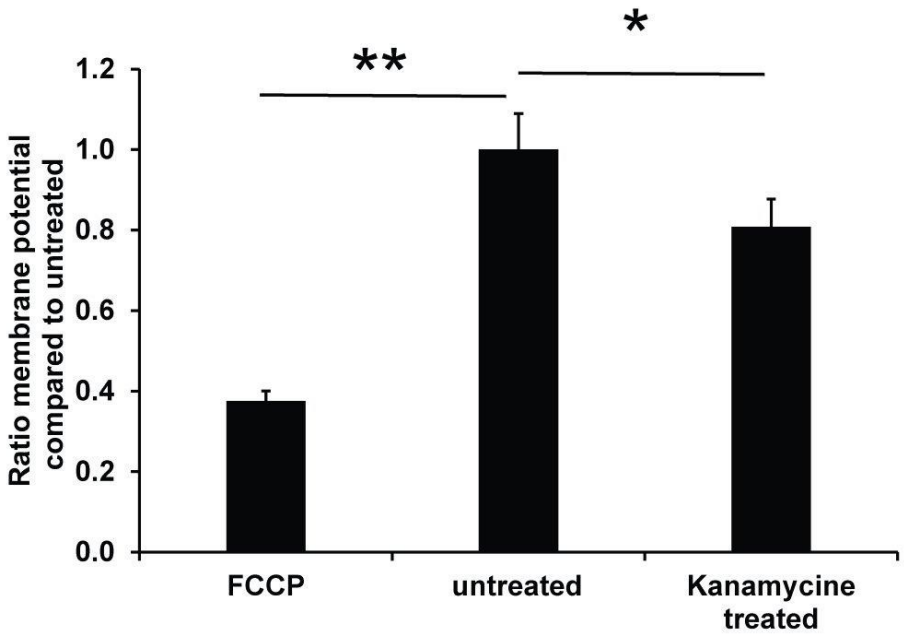


Figure 3-11. Kanamycin at 25 µg/mL for 24 hours induces a decrease in mitochondrial membrane potential.
Ratio of mitochondrial membrane potential comparing untreated cells with kanamycin-treated cells (25 µg/mL) and FCCP-treated cells as a positive control for 24 hours. The figure shows one representative experiment out of three biological replicates. Error bars denote standard deviation. *$p < 0.05$ and **$p < 0.005$, as analysed by Student's *t*-test.

To further validate intact cell lipidomics, mitochondrial morphology after kanamycin-treatment was investigated. Potential changes in mitochondrial morphology were detected using microscopy thus determining the number of mitochondrial branches and their length as a readout of changes in mitochondrial bioenergetics. To investigate this, HeLa cells were or were not treated with kanamycin (25 µg/mL for 24 hours). Untreated cells showed longer and highly branched mitochondria, whereas cells treated with kanamycin presented shorter and less branched mitochondria (Figure 3-12). In particular, mitochondrial branch lengths were significantly shorter and the number of branches was smaller in kanamycin-treated HeLa cells compared to untreated cells. Collectively, these data show that a clinically relevant concentration of kanamycin alters mitochondrial morphology and membrane potential.

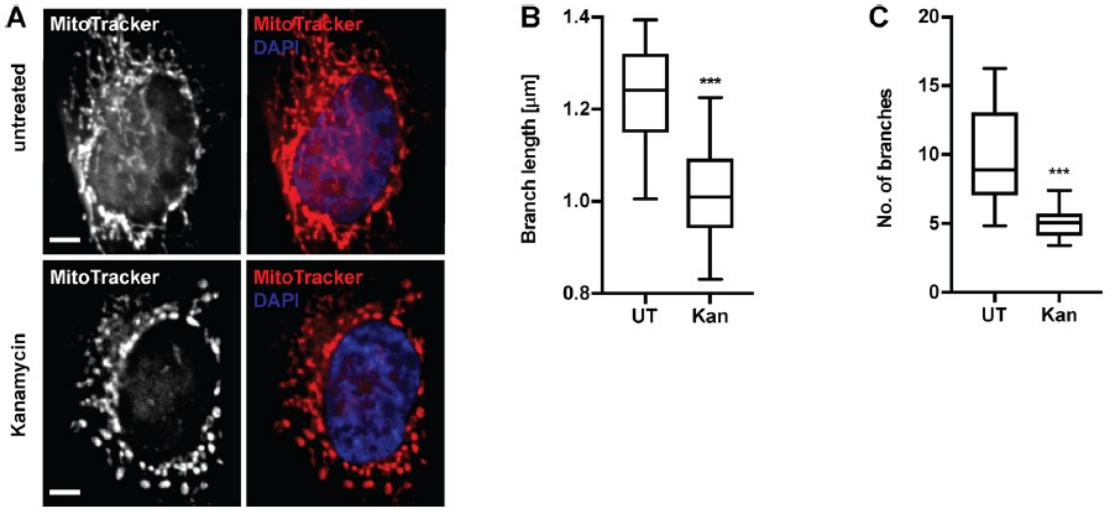


Figure 3-12. Mitochondrial morphology in untreated and kanamycin-treated HeLa cells
HeLa cells were left untreated (UT) or treated with kanamycin (Kan) for 24 hours. Mitochondrial morphology was analysed in HeLa cells using MitoTracker Red CMXros. The scale bar represents 5 µm (A). Mitochondrial branch length was measured using the MiNA-master plugin for FIJI. This graph shows median and whiskers (minimum to maximum) (B). Number of mitochondrial branches determined using the MiNA-master plugin for FIJI. This graph shows median and whiskers (minimum to maximum) three biological replicates (C). ***$p < 0.001$, as analysed by Student's *t*-test. Microscopy and data analysis performed by Sina Krokowski.

3.2.4 Kanamycin but not levofloxacin nor ethambutol induces changes in the CL:PI ratio in a dose-dependent manner in HeLa cells and BMDM but not in RAW 264.7

To investigate if the changes in the CL:PI ratio were specific to the kanamycin exposure of HeLa cells for 24 hours or to lipidome remodelling in response to antibiotic exposure, a series of intact cell lipidomics experiments were conducted by determining the CL:PI ratio of HeLa, BMDM and RAW 264.7 cells after a 24-hour exposure to levofloxacin, ethambutol, or kanamycin, each antibiotic having a different mode of action. I evaluated the CL:PI ratio after antibiotic treatment for 24 hours using HeLa, RAW 264.7 and BMDM cells to investigate if mitochondrial damage can be detected at lipid level. In both HeLa and BMDM cells, only 5*Cmax of levofloxacin (55 µg/mL) alters the CL:PI ratio with a 2.8-fold decrease in HeLa cells and 1.5-fold decrease in BMDM cells (Figure 3-13 A and D). In RAW 264.7, none of the concentrations of levofloxacin had an effect on the CL:PI ratio (Figure 3-13 G). Regarding the ethambutol treatment, none of the concentrations used induced changes on CL/PI ratio in HeLa, RAW 264.7 or BMDM cells (Figure 3-13 B, E, H). However, kanamycin treatment-induced changes in the CL:PI ratio in HeLa cells at Cmax and 5*Cmax with similar orders of magnitude with a ∼1.5-fold decrease in the CL:PI ratio (Figure 3-13 C). This effect is more pronounced in primary cells, where dose dependence is noticed. In this case, at Cmax, the CL:PI ratio decreases by 1.4-fold and by 2.5-fold at 5*Cmax (Figure 3-13 F). Nevertheless, kanamycin treatment had no effect on the CL:PI ratio in RAW 264.7 (Figure 3-13 I).

Taken together, these data suggest that kanamycin induces changes in the CL:PI ratio in a dose-dependent manner in HeLa cells and BMDM.

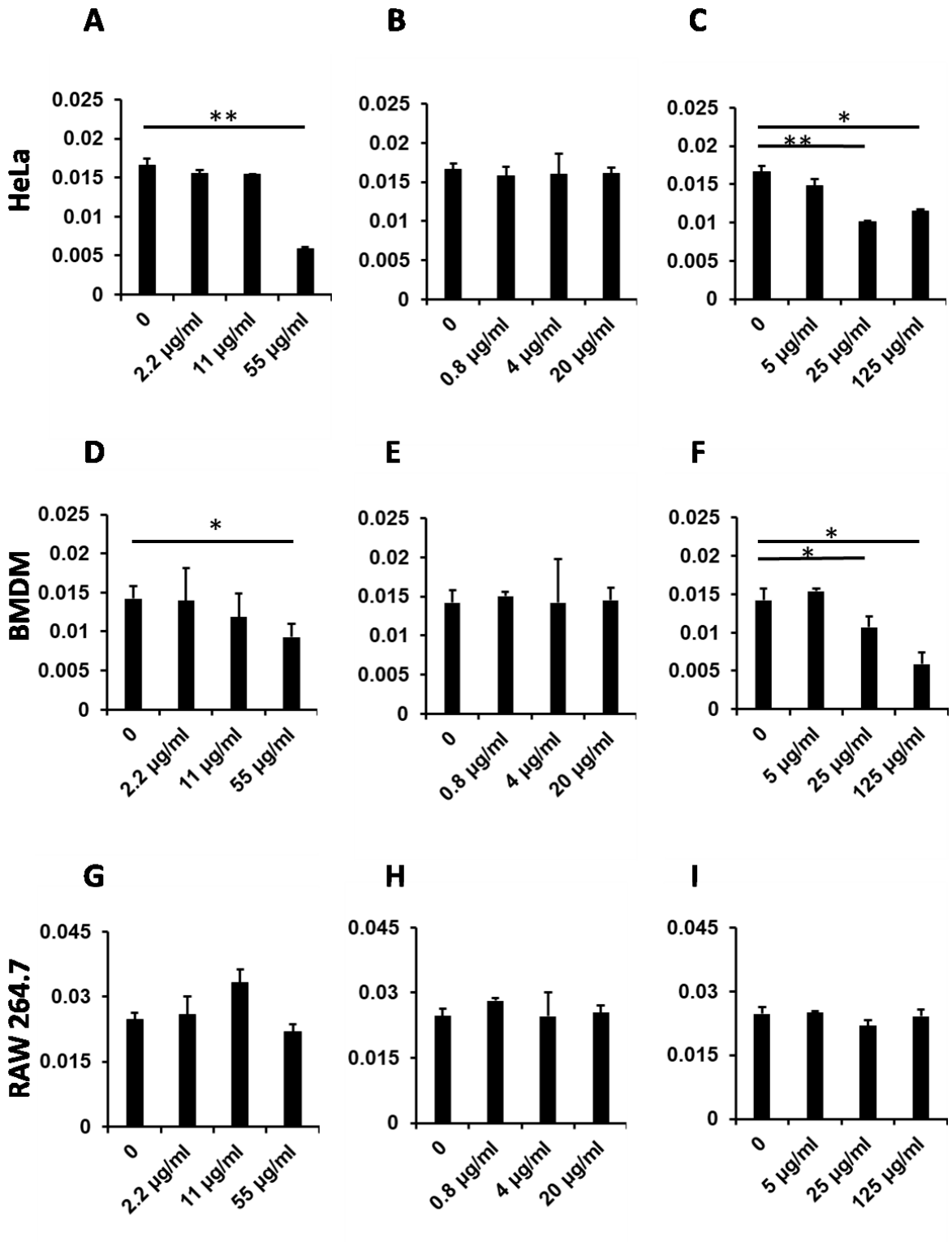


Figure 3-13. Only Levofloxacin (5*Cmax) and Kanamycin (Cmax and 5*Cmax) have an impact on CL:PI ratio in HeLa and BMDMs.

HeLa cells, BMDMs and RAW 264.7 were left untreated for 24 hours or treated with three different concentrations (1/5Cmax, Cmax, and 5*Cmax) of levofloxacin (A, D and G respectively), ethambutol (B, E and H respectively), and kanamycin (C, F and I, respectively). The figure shows one representative experiment out of three biological replicates. Error bars denote standard deviation. *$p < 0.05$ and **$p < 0.005$, as analysed by Student's *t*-test.

3.2.5 Kanamycin, levofloxacin, and ethambutol do not affect HeLa cells, RAW 264.7 or BMDM viability at Cmax or 5*Cmax

To determine if the changes in the CL:PI ratio were due to the difference in cell viability, survival after 24 hours' exposure to levofloxacin, ethambutol and kanamycin at Cmax/5, Cmax and 5*Cmax was tested. In this case, in terms of cell viability, no statistically significant differences were observed in any of the antibiotics and concentrations tested (Figure 3-14). Altogether, changes in the CL:PI ratio are due to the antibiotic exposure and not due to cell apoptosis.

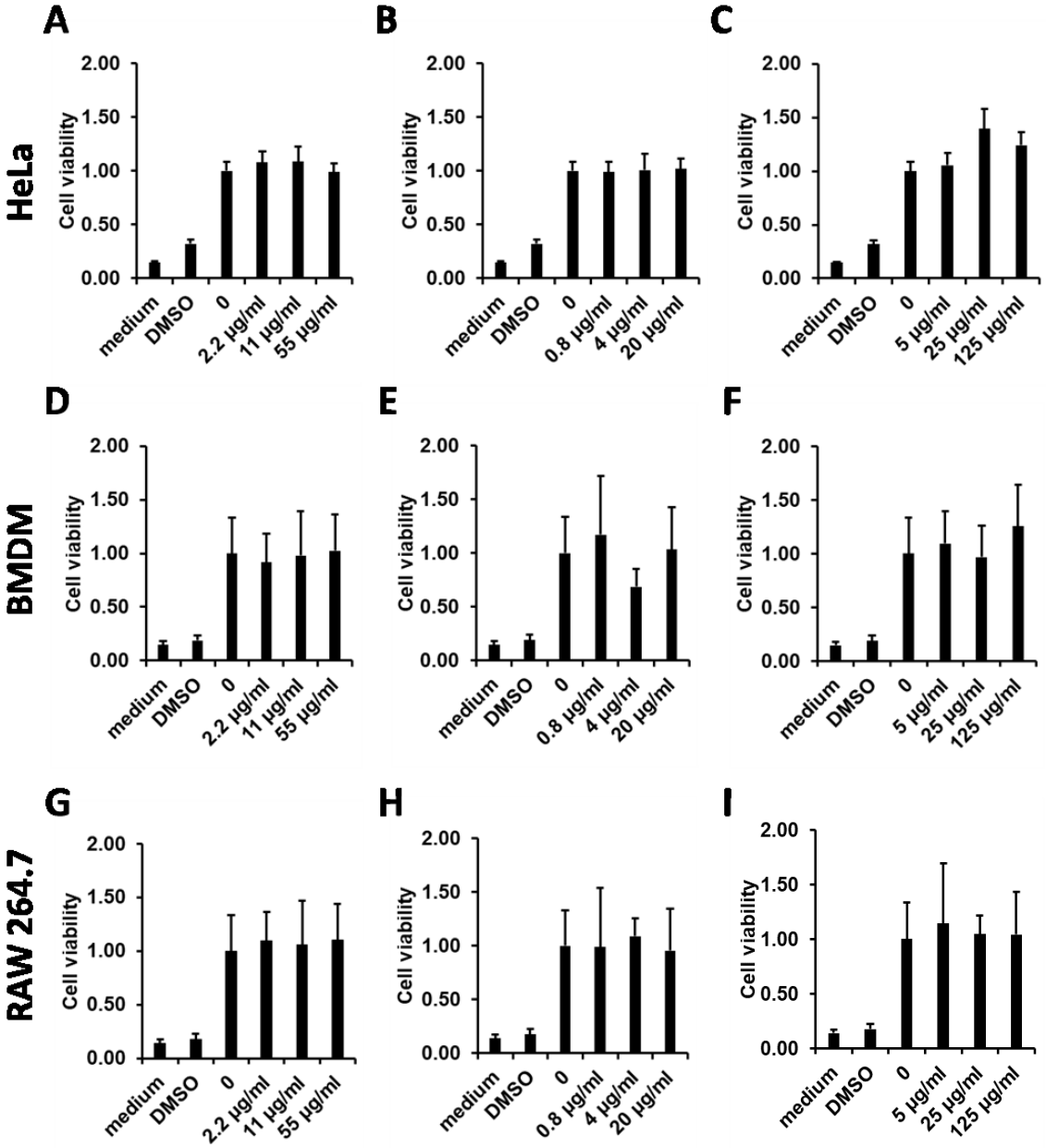


Figure 3-14. Viability does not decrease after treating HeLa, RAW 264.7 and BMDM with Levofloxacin 5*Cmax and Kanamycin Cmax and 5*Cmax.

Viability of antibiotic-treated and untreated HeLa cells, RAW 264.7 macrophages and BMDMs was tested. HeLa cells (A-C), BMDM cells (D-F) and RAW 264.7 (G-I) viability expressed as a ratio of antibiotic treated cells (1/5Cmax, Cmax and 5*Cmax) to untreated cells. Cells treated with levofloxacin (A, D and G), ethambutol (B, E and H), and kanamycin (C, F and I). The figure shows one representative experiment out of three biological replicates. Error bars denote standard deviation.

3.2.6 Kanamycin, levofloxacin, and ethambutol decrease the maximal rate of mitochondrial respiration in HeLa cells and BMDMs

To test whether changes in the CL:PI ratio can directly correlate with mitochondrial dysfunction, the maximal mitochondrial respiratory capacity was measured on HeLa cells, RAW 264.7 and BMDM cells treated with kanamycin, levofloxacin, and ethambutol at 1/5Cmax, Cmax, and 5*Cmax for HeLa cells and Cmax for RAW 264.7 and BMDMs. Changes in the OCR of intact HeLa cells, RAW 264.7 and BMDMs were monitored using the Agilent Seahorse XF Cell Mito Stress Test. The OCR was measured in picomoles per minute (pmol/min/cells) and was normalised by the number of cells in each well. For HeLa cells, kanamycin treatment at 25 μg/mL and 125 μg/mL led to a 1.2-fold decrease in maximal respiratory capacity (Figure 3-15 A). Treatment with levofloxacin at 11 μg/mL and 55 μg/mL led to a 1.4- and 1.9-fold decrease, respectively, in the maximal respiratory capacity (Figure 3-15 B). Although the treatment of HeLa cells with kanamycin did not exhibit dose dependence (Figure 3-15 A), the treatment of HeLa cells with levofloxacin did exhibit dose dependence (Figure 3-15 B). Regarding treatment with ethambutol, only 5*Cmax led to a decrease in the maximal rate of mitochondrial respiration (1.5-fold) (Figure 3-15 C). For BMDM, at Cmax, kanamycin, levofloxacin and ethambutol led to a statistically significant decrease of 1.36-, 1.19- and 1.34-fold respectively, in the maximal mitochondrial respiratory capacity (Figure 3-15 D). Nevertheless, the maximal mitochondrial respiration capacity did not change upon antibiotic treatment at Cmax in RAW 264.7 cells. Taken together, these data suggest that kanamycin, levofloxacin, and ethambutol can induce mitochondrial dysfunction in HeLa cells and BMDMs.

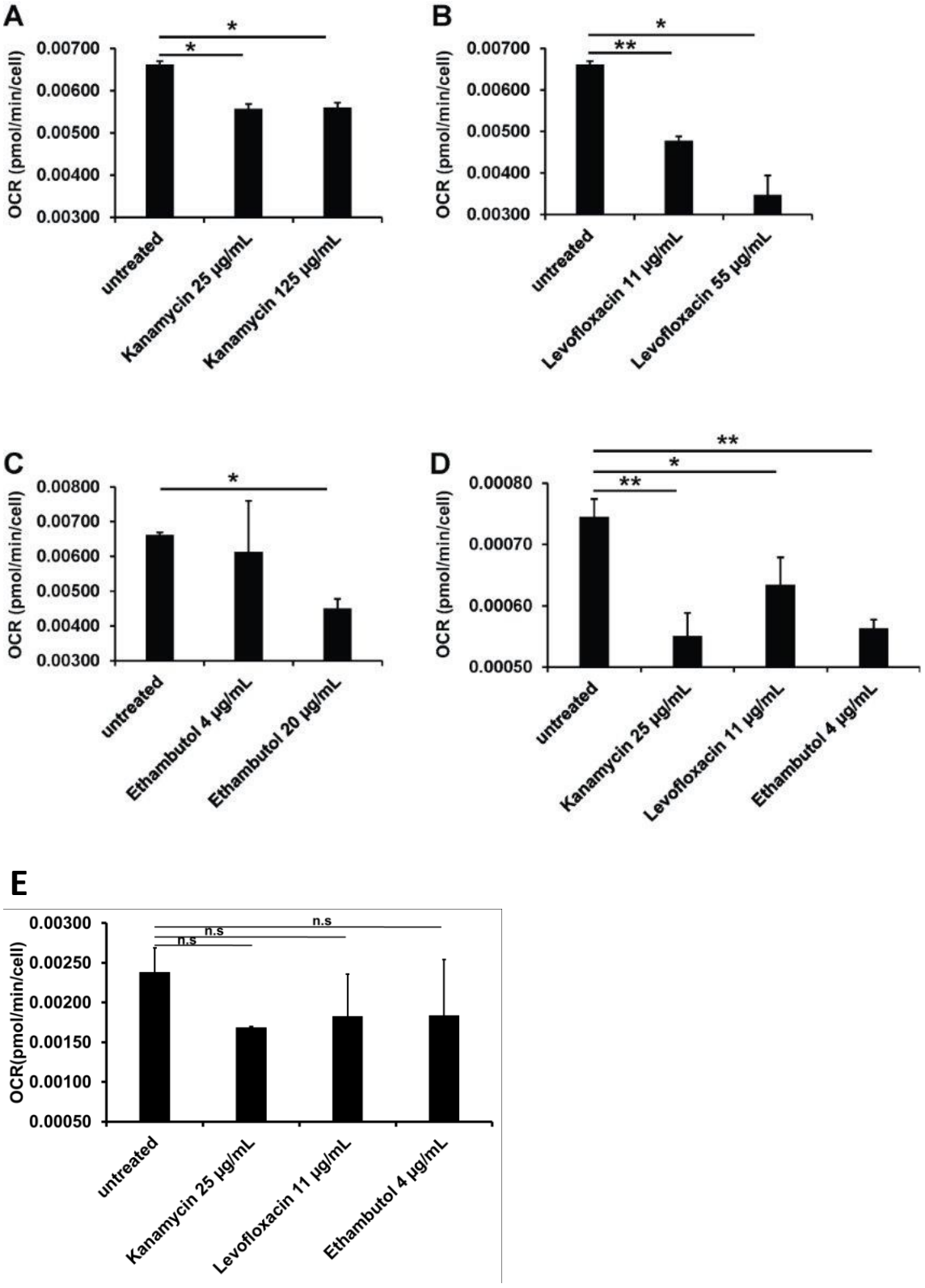


Figure 3-15. Kanamycin, levofloxacin, and ethambutol can induce mitochondrial dysfunction in HeLa cells and BMDMs.

Maximal mitochondrial oxygen consumption on HeLa cells untreated and treated with kanamycin (A), levofloxacin (B), and ethambutol (C); BMDM cells untreated and treated with kanamycin, levofloxacin, and ethambutol at Cmax (D); and RAW 264.7 cells untreated and treated with kanamycin, levofloxacin and ethambutol at Cmax (E) for 24 hours. Error bars denote standard deviation. *$p < 0.05$ and **$p < 0.005$, as analysed by Student's *t*-test.

3.3 Discussion

In this chapter my research focused on determining the impact on the targeted lipidome of cells treated with kanamycin. Kanamycin is an aminoglycoside that blocks protein synthesis by binding to the bacterial ribosomal subunit.[301] Moreover, it is broadly used to treat severe bacterial infections worldwide mainly caused by aerobic gram-negative bacteria such as *E. coli*, *Proteus* species, *Enterobacter aerogenes, Klebsiella pneumoniae, Serratia marcescens,* and *Acinetobacter* species; and some anaerobic bacilli such as *Bacteroides oralis.*[302] However, kanamycin has been associated with drastic side effects including ototoxicity and nephrotoxicity.[303]

By using MALDI-TOF/MS directly on intact cells in negative ion mode, the cell lipid profile was obtained being able to identify PLs, which are essential constituents of the plasma membrane, and CLs, which are key components of the mitochondrial membrane. This new lipidomics methodology allows the lipid analysis of intact eukaryotic cells without any extraction or purification steps, and only requires about 1 x 10^5 of cells per mL. This research used a similar approach to that of Larrouy-Maumus *et al.*, where they characterised lipid A and its modifications directly by MALDI-MS analysis of intact heat-inactivated bacteria.[304] This was done without any extraction or purification steps allowing the study of native lipid A and its modifications directly on bacteria avoiding the use of large starting volumes, chemical reagents or harsh treatments.[286]

The data obtained in this study demonstrates that kanamycin treatment of HeLa cells leads to the production of PI containing shorter fatty acids and to the alteration of CL:PI ratio. This change in PI metabolism could be due to a remodelling of the cell lipidome as a result of an alteration of available acetyl-CoA levels needed for fatty acid synthesis caused by changes in the TCA cycle activity. It is known that antibiotics can alter the central carbon metabolism and therefore the TCA cycle and the ETC resulting in a decrease in metabolic activity and changes in metabolic pathways.[305,306] Thus it was suggested that these cell lipid changes could be used as potential markers of antibiotic toxicity.

PLs (PI and CL) are associated with membranes that can generate an electrochemical gradient involved in mitochondrial bioenergetics processes. Therefore, considering that mitochondrial energy metabolism is tightly linked to organelle function, it was expected that a disruption of the ETC would lead to a decrease in mitochondrial membrane potential, ATP levels, and overall metabolic activity.[300,307] Membrane potential measurements provide information about the

coupling of electron transfer to ATP synthesis, as well as the organelle's ability to take up and release ions and substrates across the mitochondrial inner membrane. Thus, mitochondrial membrane potential measurements were performed demonstrating a 20% decrease when HeLa cells were treated with kanamycin for 24 hours compared to untreated cells. This is consistent with the literature[230] and confirms that the observed lipid changes were due to disrupted mitochondrial bioenergetics. Moreover, to further assess the lipid assay, mitochondria morphology was investigated. Effectively, more and longer branches presented by mitochondria would represent a larger surface area, suggesting a higher level of potential energy to be spent; whereas smaller mitochondria and mitochondria with simpler shapes would suggest a decrease in their energy level.[308] The results obtained showed that mitochondrial branch lengths were significantly shorter and the number of branches was smaller in kanamycin-treated HeLa cells compared to untreated cells. My work demonstrated how HeLa cells suffer a change in mitochondria morphology upon treatment for 24 hours with clinically relevant concentrations (25 µg/mL) of kanamycin presenting shorter and less branched mitochondria.

To evaluate the specificity of kanamycin's impact on the lipidome of HeLa cells, two other antibiotics with different modes of action were used. These were the fluoroquinolone levofloxacin,[309,310] which inhibits bacterial DNA gyrase and DNA topoisomerase IV,[311] and ethambutol[312] that targets the arabinosyltranferases. Ethambutol is involved in arabinogalactan biosynthesis, which is a major constituent of the mycobacterial cell wall.[313] Importantly, all antibiotics employed in this study are currently used for the treatment of bacterial infections in clinics and the concentrations tested were chosen according to the peak of antibiotic concentration found in the serum of patients treated with these antibiotics (Cmax).[230,309,310,312,314] Moreover, two other different cell types were investigated: RAW 264.7 cells and BMDMs.

Remarkably, by using intact cell lipidomics on intact HeLa, RAW 264.7 cells and BMDMs, I found that kanamycin impairs the CL:PI ratio in a dose-dependent manner in HeLa cells and BMDMs and that high levels of levofloxacin (5*Cmax) also affect the CL:PI ratio of these cell types, without affecting the viability of the cell.

However, by investigating mitochondrial respiration using the Seahorse XF mito stress test kit, I found, no direct correlation between the CL:PI ratio and mitochondrial damage. The data suggest that kanamycin, levofloxacin, and ethambutol can induce mitochondrial dysfunction. These results are in accordance with results found in the literature.[230,315,316] At this stage, from

the use of intact cell lipidomics and determination of the CL:PI ratio, my results demonstrate that even if mitochondrial function was slightly impaired by the use of antibiotics such as ethambutol or levofloxacin at Cmax, there is no direct correlation between mitochondrial dysfunction and the CL:PI ratio. The aminoglycoside kanamycin can trigger changes in the CL:PI ratio at a physiologically relevant concentration. Effectively, the results based on the intact cell lipidomics and CL:PI ratio are in line with those found in the literature where aminoglycosides, including kanamycin, have been shown to modulate phosphoinositide (phosphorylated PI) signalling and metabolism in the cytoplasm and in the nucleus.[317–319] For instance, Marche *et al.* researched aminoglycoside influence on the metabolism of phosphoinositides in kidney proximal tubules as they accumulate there[318]. Their results suggested that the impairment of phosphoinositide metabolism induced by aminoglycosides could result in an alteration of Ca^{+2} handling by the tubular cells. This could be of importance for the development of drug toxicity since phosphoinositides are involved in Ca^{+2} mobilisation and/or transport processes; and aminoglycosides hinder the Ca^{+2} binding to membranes.[318] Further studies on the influence of kanamycin on phosphoinositide signalling were done by Jiang *et al.*[319] Their work focused on phosphoinositide signalling in mouse cochlea sensory cells (hair cells) and demonstrated that kanamycin disturbs the balance between phosphatidylinositol-4,5-bisphosphate and phosphatidylinositol-3,4,5-trisphosphate, alters histone acetylation gene transcription, and decreases the phosphatidylinositol-3-kinase/Akt survival pathway, which plays a major role in cell growth and survival in tissues such as the inner ear.[319]

I cannot rule out the possibility that a decrease in the maximal rate of mitochondrial oxygen consumption alters metabolic pathways. Nevertheless, using state-of-the-art metabolomic tools such as high-sensitivity and high-resolution LC-MS-based approaches will make this area exciting for future investigations. Although the MALDI technique does not distinguish between lipid isobaric species for instance, complex lipids with the same mass but different fatty acid composition,[211] the purpose of this study was to provide a new approach for assessing antibiotic toxicity based on the lipid profile.

Altogether, intact cell lipidomics represents a major advance and can be used as an alternative to rapidly assess the toxicity of a compound that interferes with PI metabolism prior to in-depth analysis of the entire lipidome using conventional lipidomics approaches such as the ones presented earlier. This methodology can go well beyond the scope of this study and can also be applied to more cell types and to purposes such as lipidome remodelling to probe cancer diagnostics/metabolism and host-pathogen interactions.

Chapter 4: NaCl triggers the CRP-dependent increase of cAMP in Mtb

4. NaCl triggers the CRP-dependent increase of cAMP in Mtb

4.1 Introduction

4.1.1 Osmotic stress in bacteria

Bacteria can be subjected to a wide range of environmental stresses including changes of the extracellular osmolarity. Non-ionic or non-electrolytic osmotic stress and ionic or electrolytic osmotic stress mediated by sucrose or glucose and NaCl respectively are some examples.[320] Nevertheless, how bacteria perceive and respond to changes in extracellular osmolarity is not well understood.[320] Adapting to changes in osmolarity requires osmoregulatory responses. During this process the bacterium suffers structural and physiological changes, which may alter the nucleoid organisation and the cell and surface composition.[320] Upon change in extracellular osmolarity, which can include hyperosmotic stress (increased external osmolarity) and hypo-osmotic stress (decreased external osmolarity) bacteria suffer an immediate water flux across the cell envelope. Upon hyperosmotic stress, water flows out of the cell whereas the opposite happens upon hypo-osmotic stress. The cytoplasmic membrane, as the permeable barrier of cells, has a rather high water permeability. This leads to a fast transmembrane water flux as a response to changes in osmolarity. Furthermore it also results in immediate changes in the concentration of cellular components and cell structure.[321,322] Aquaporins, which are water channels and can mediate accelerated water flux across the cytoplasmic membrane,[322] have been found in some bacteria, such as *E. coli* and *Enterococcus faecalis* among others.[323] Most aquaporin-containing bacteria possess only one aquaporin gene, except *Klebsiella pneumoniae* and *Caulobacter crescentus*, which possess two chromosomal aquaporin genes.[323] However, microorganisms cannot actively pump water into or out of the cell in response to changes in osmolarity.[322] Therefore, the first and passive consequence of osmotic stress is cell swelling and increased hydration for hypo-osmotic stress; and dehydration and shrinkage in the case of hyperosmotic. Changes in cell shape are the most evident consequences of osmotic stress. Nevertheless, also of importance is the change in water-macromolecule (protein, nucleic acids) and macromolecule-solute (ions, sugars, metabolites) interactions in response to the transmembrane water flux.[321,324] Under steady-state conditions of osmotic compensation there is a strong osmotic gradient across the plasma membrane,[325] owing to the high molar intracellular concentration of solutes (including inorganic ions often K^+ and organic molecules such as trehalose, glutamate, glycine betaine, proline, proline betaine, taurine, dimethylsulfonio-propionate, ectoine and carnitine).[325] This gradient is balanced by the turgor pressure of the cell. As a consequence, hyperosmotic stress following an increase in external osmolality does not necessarily mean that the external osmolarity under these conditions is

higher than that in the cytoplasm; it simply means that the external osmolarity is higher in comparison to the conditions where it was balanced by the cell turgor pressure. Upon the fast and passive response in macromolecular crowding and cell shape, the main objective of these mechanisms is to restore the internal osmolarity by rehydration (after an osmotic increase) or by decrease of water activity (after an osmotic decrease). Since cells are not capable of active water pumping, rehydration of the cytoplasm in response to hyperosmotic stress is accomplished by an increase of the solute concentration inside the cell.[321,326] When cells are exposed to an increase in osmolarity, the intracellular concentration of K^+ immediately increases by active transport, followed by a rapid accumulation of glutamate as the primary counter ion by *de novo* synthesis.[327,328] For example, it is known that in *E. coli* intracellular K^+ can reach concentrations as high as 1 M soon after an increase in osmolarity.[327,329] Later, further biologically compatible osmoprotecting compounds such as trehalose, glycine betaine (N,N,N-trimethylglycine) and proline replace K^+ with glutamate. Through this process *E. coli* cells control a fairly constant turgor pressure on exposure to hyperosmotic shift. Similar response mechanisms happen in many other organisms including a variety of bacteria, plants, and animals.[320,327]

Osmoregulation in *E. coli* can occur via at least two mechanisms, Pro U and Pro P, and the cAMP receptor protein (CRP). During the course of the osmotic response in *E. coli*, a set of genes such as *pro U* and *pro P* are specifically induced.[327,330,331] ProU is a high-affinity transporter for glycine betaine, proline and other osmoprotecting compounds, and is a member of the ABC superfamily of transporters. ProP is a multiple-spanning transmembrane protein that is a member of a superfamily of transporters and catalyses a broad-specificity osmoprotectant-proton symport reaction.[327,330,331] *proP* is transcribed from two main promoters, P1 and P2. The P1 promoter is strongly, but only transiently, induced by a change to high-osmolarity medium. The P2 promoter is transiently activated as cells growing in rich medium start to enter stationary phase. The combined activity of the two transcription factors, RNA polymerase sigma (RpoS) σ factor and Fis, regulates this narrow window of expression as a function of the growth phase. RpoS σ factor levels increase as cells enter stationary phase, whereas Fis levels decrease as cells enter stationary phase. The presence of ProP allows cells in stationary phase to respond fast to an osmotic shock. Different mechanisms control gene expression in enteric bacteria in response to osmotic upshifts.[327] One mechanism requires a two-component regulatory system in which the osmotic sensor EnvZ controls the phosphorylation state of the transcriptional regulator OmpR.[327] A second general mechanism of osmotic control is via RpoS. RpoS levels increase mainly by post-transcriptional mechanisms upon a change to hyperosmotic conditions. This

results in increased transcription of RpoS-dependent promoters.[332] Osmotic induction of the P2 promoter is potentially a result of increased levels of RpoS.[333] Finally, the synthesis of ProU is derepressed by an increase in osmolarity partly by releasing the abundant nucleoid-associated protein H-NS from an extended regulatory sequence found downstream from its promoter.

Another known gene expression osmoregulator mechanism in *E. coli* is via the CRP, one of the best-known global regulatory proteins in *E. coli* encoded by *crp.*[334] At the *proP* P1 promoter, CRP behaves as an osmotically sensitive repressor whereas at the lac promoter, CRP works as an osmotically sensitive activator. This activity for CRP could have broad regulatory implications, considering the large number of genes under its control.[327] Landis *et al*. established that *proP* P1 correlates with CRP-cAMP binding to DNA. Under hypo-osmotic conditions, the *crp* site at *proP* is fully occupied, and transcription from this promoter is very low. After a hyperosmotic shift, CRP is released from this site, and the P1 promoter is derepressed. Induction ratios as measured by direct RNA analysis or ProP-LacZ fusions surpass 100-fold[327] and therefore are in the same range as stated for the *proU* promoter.[335] Later work by Balsalobre *et al*. demonstrated that CRP levels change with external osmolarity variation. This osmoregulation occurs at the level of *crp* gene expression and requires the cAMP molecule. Their research discovered that the total levels of cAMP, especially the intracellular levels, were significantly increased at high osmolarity in *E. coli*. This suggested that osmolarity directly affected synthesis and/or turnover of cAMP and emphasised how important cAMP is in the regulatory network by which bacterial cells adapt to changes in osmolarity.[336] Furthermore, an inverse relationship between the levels of CRP and cAMP at low and high osmolarity was seen,[320,147,336] as shown in Figure 4-1.

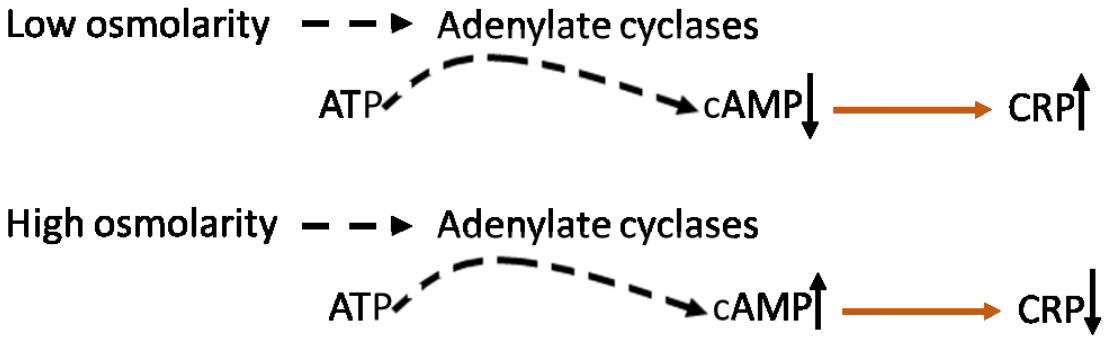


Figure 4-1. Scheme showing a simplified model of the CRP osmoregulation.
Levels of cAMP and CRP change depending on the osmolarity in the environment in *E. coli*. There is an inverse relation between the cAMP and CRP levels at high and low osmolarity. At low osmolarity in the environment the levels of cAMP are lower and the *crp* is activated. However, when the external osmolarity increases, ACs are triggered and therefore the cAMP levels increase which represses *crp.* Figure adapted from Balsalobre *et al.*[336]

4.1.2 Mycobacterial adaptation to stress via cAMP

Mtb is exposed to different environments during human infection.[337] These include acidic, hypoxic, oxidative, nutrient poor and nitrosative niches. These environments can be found extra- and intracellularly. cAMP has been seen to be crucial for Mtb host colonisation.[184] Previous studies have shown an increase in the levels of cAMP under heat stress, SDS-mediated cell envelope stress, nitosative (NO) and acidic stress.[338,339] For instance, upon heat stress (42 °C), Mtb cAMP levels increase just over 2-fold due to the induced expression of specific ACs leading to elevated intracellular levels of cAMP.[338] Nevertheless other stress factors, namely NO and pH 4.5, have a milder effect on the cAMP levels of Mtb *in vitro*, increasing its levels 1.25-fold.[338] Further studies have shown that when the non-pathogenic mycobacteria *M. smegmatis* is exposed to to 0.5% SDS for 1.5 hours, the intracellar levels of cAMP increase over 300-fold.[339] Nevertheless, no studies have shown the effect of ionic stress mediated by NaCl on the levels of cAMP in mycobacteria.

4.1.3 Osmotic stress in mycobacteria

Mycobacteria are exposed to a wide range of physiological NaCl concentrations within the host.[340–342] Even though their effects are not well understood, they could determine the outcome of infection. For instance Tan *et al.* have demonstrated how chloride is a cue used by Mtb to sense immune-mediated changes in the phagosomal environment.[343,344] During the natural infection cycle, Mtb occupies different niches which include the airway surface liquid, the plasma, cerebrospinal fluid, and macrophage.[304] All these niches have varying NaCl concentrations, from 50 mM in the airway surface liquid to 250 mM NaCl inside the macrophages (Figure 4-2). However, these concentrations are considerably higher in comparison to the ones found in conventional culture media, which are typically below 10 mM NaCl. This is important to take into account in experimental procedures.[304]

It is known that upon ionic and non-ionic osmotic stress, mycobacteria respond by increasing common solutes like trehalose and glycerol.[304] Mtb does not contain aquaporins.[323] However it is known that Mtb contains a large-conductance mechanosensitive channel (MscL) which presents 151 amino acids and a 37% sequence identity to the MscL from *E. coli*. Its function is as an ion channel which opens in response to strech forces in the membrane lipid bilayer and could participate in osmotic pressure changes regulation inside the cell.[345] Furthermore, mycobacteria have a two-step adaptation osmotic stress model.[304] This consists of a fast metabolic response and a later response which involves lipid remodelling.[304] Moreover, physiological concentrations of NaCl have been seen to impair the growth of Mtb in a reversible manner. This evidence

proposes that changes in salt concentration are also present at the cellular level during macrophage infection. This was demonstrated by examining the salinity of Mtb-mCherry-containing intracellular compartments using CoroNa Green, a sodium indicator in infected RAW 264.7 cells. Larrouy Maumus *et al.* observed that mCherry co-localised with CoroNa Green, demonstrating that there are higher levels of Na^+ in compartments, which contain Mtb.[342]

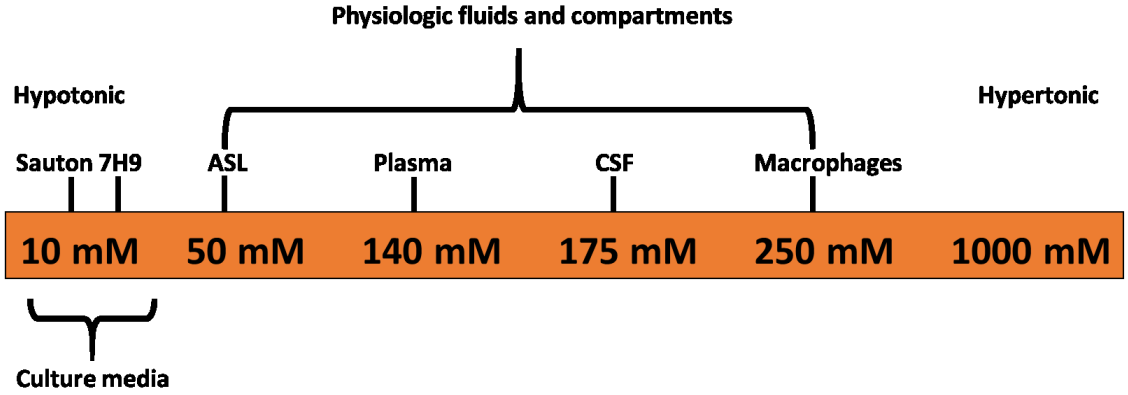


Figure 4-2. NaCl concentrations Mtb encounters in culture media and humans.
Concentration of NaCl found in culture media including Sauton and 7H9, and physiologic fluids and comparments which include; ASL as the airway surface liquid, plasma, CSF as the cerebrospinal fluid, and macrophages.[342,346,347] Figure adapted from Larrouy-Maumus *et al.*[342]

There is not much understanding about how mycobacteria adapt to the osmotic conditions they are exposed to. However, work from Hatzios *et al.* has suggested that an eukaryotic-like Serine/Threonine protein kinase (PknD), is the main protein participating in the Mtb osmosensory pathway.[340] Their proposed model indicates that osmotic stress activates PknD phosphorylation of osmosensory protein A (OprA, Rv0516c), stimulating the release of σ-factor (SigF) from an inhibitory complex and enabling the transcription of osmotically regulated genes, which include the early secretory system 1 (ESX1) substrate *espA,* which is a secreted virulence factor; and *oprA.*[340] This transcriptional response pathway leads to changes in Mtb cell wall structure and metabolism (Figure 4-3).[340] Furthermore, Hatzios *et al.* demonstrated that disruption of *oprA* decreases peptidoglycan thickness, increases resistance to osmotic stress and enhances antibiotic resistance to the peptidoglycan biosynthesis inhibitor vancomycin as the minimal inhibitory concentration of this antibiotic was 4-fold higher for the Mtb mutant (*Rv0516c::Tn*) in comparison to the wild type strain.[340]

Another potential candidate which could be involved in the osmoregulation of Mtb is CRP_{Mt}, as the *crp* gene in *E. coli* has been proven to be involved in osmoregulation with cAMP as a key regulatory component.[336]

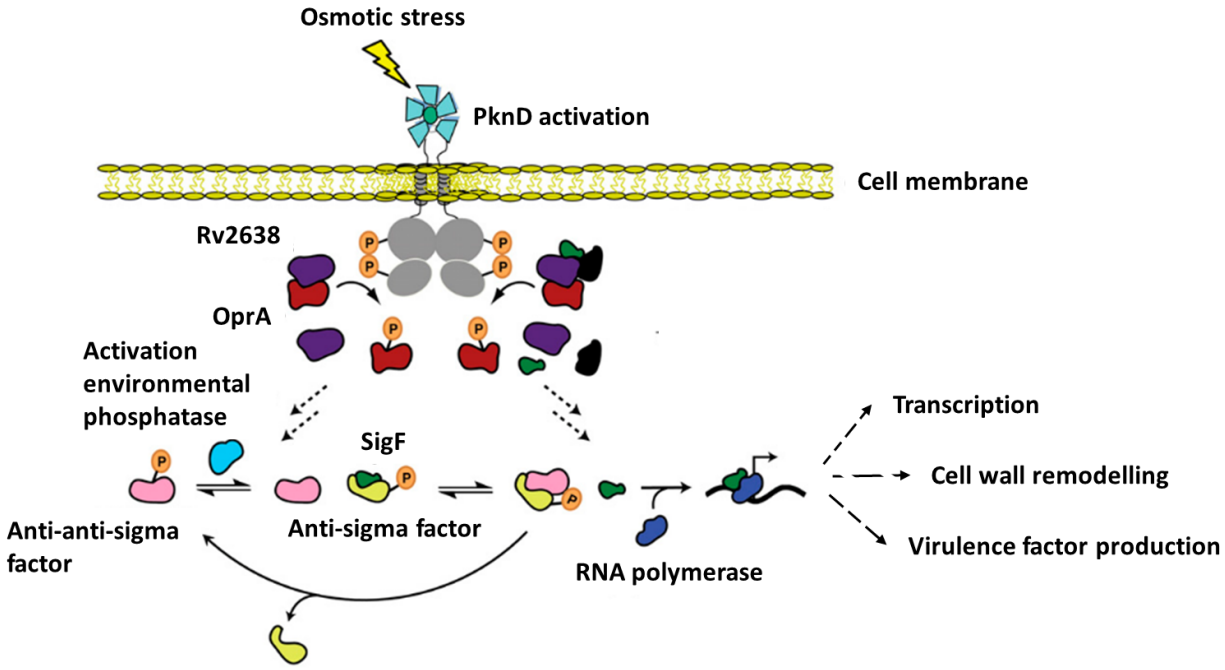


Figure 4-3. Osmosensory regulation of Mtb mediated by PknD.
PknD is activated by an increase in extracellular osmolarity and this causes the phosphorylation of OprA. This allows SigF to bind RNA polymerase promoting *oprA*, *espA* transcription as well as other genes linked to changes in the metabolism and cell wall structure of Mtb. Figure adapted from Hatzios *et al.*[340]

4.1.4 The CRP_{Mt}, a potential candidate for Mtb osmoregulation

CRP_{Mt} (Rv3676) is a transcriptional regulator which is 32% identical to CRP from *E. coli.*[348] CRP_{Mt} is a homodimer with a cAMP binding domain (CBD) per subunit.[349] The binding motifs of CRP in *E. coli* and CRP_{Mt} are very similar, which suggests that their DNA-binding domains functionally resemble each other.[348] Four out of six amino acid residues that are involved in cAMP binding in CRP from *E. coli* are conserved in CRP_{Mt}.[350] Furthermore, Arg180, Glu181 and Arg185, which are directly involved in DNA recognition in *E. coli* CRP, are well conserved in CRP_{Mt}, with only Arg185 of CRP being replaced by Lys at the corresponding position in CRP_{Mt} (Figure 4-4). Resembling CRP in *E. coli*, CRP_{Mt} experiences a conformational change induced by cAMP and bends DNA upon binding.[351] Structural research has revealed that cAMP might induce CRP_{Mt} helix-turn-helix (HTH) domain reorientation in order to increase DNA binding.[352] Nevertheless, trypsin digestion experiments have shown topological differences between the orthologues in Mtb and *E. coli*. Upon cAMP binding, CRP in *E. coli* was converted to an open structure enhancing its susceptibility to proteolytic cleavage. However, CRP_{Mt} was less vulnerable, showing how CRP_{Mt} binds to cAMP in a closed structure for protection and increases the ability to bind to DNA. In

addition, cAMP is crucial for *E. coli* CRP binding to DNA which can change its conformation to act as a transcriptional regulator. However cAMP is not crucial for CRP_{Mt} DNA binding all the time but its presence can increase the CRP_{Mt} affinity for DNA around two-fold. [348]

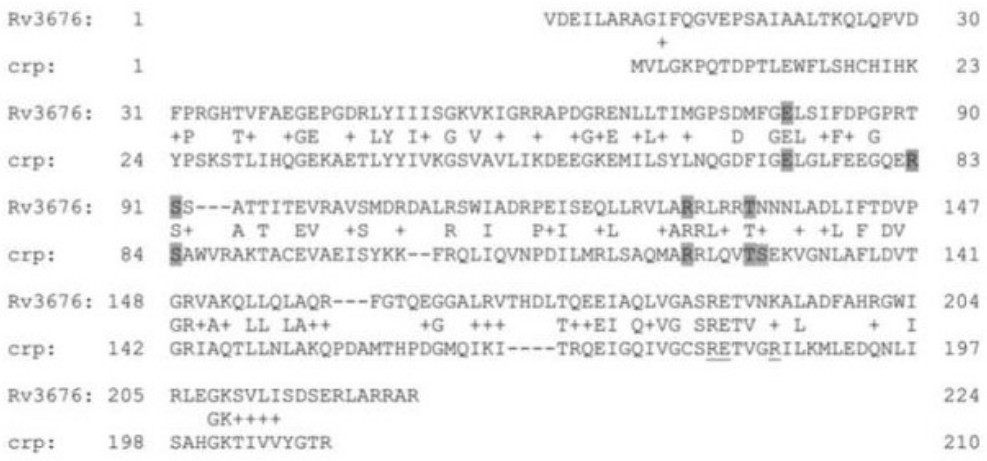


Figure 4-4. Amino acid sequence alignments of Mtb Rv3676 and CRP from *E. coli*.
Highlighted in grey are the residues involved in cyclic nucleotide binding in *E. coli* CRP and those that are conserved in Rv3676. There is no conservation between the other two cyclic nucleotide binding residues, R83 in *E. coli* (T90 in Mtb) or S129 (N135 in Mtb) or S129 (N135 in Mtb). Underlined are Arg180, Glu181 and Arg185, the amino acids of *E. coli* CRP directly involved in DNA recognition. Figure adapted from Rickman *et al.*[353]

CRP_{Mt} is a global transcriptional regulator in Mtb. It is estimated that CRP_{Mt} regulates 114 genes from 73 promoter regions.[351] CRP_{Mt} has also been shown to contribute to host persistence since the two largest groups of genes in its putative regulon are associated with starvation[354] and dormancy models, overlapping with hypoxia.[355] *crp* is upregulated in this starvation model,[355] which suggests that CRP_{Mt} could be important for starvation response regulation.[351] Further studies have predicted 19 additional putative CRP_{Mt}-binding sites and demonstrated that the regulon contains genes with critical functions (Table 4-1).[356]

The CRP_{Mt} palindromic binding motif (C/TGTGANNNNNNTCACG/A) was determined based on 58 predicted binding sites at intergenic regions of the genome of Mtb H37Rv.[351] G2 and C17 are highly conserved nucleotides in all predicted binding sites and they are of considerable importance for CRP_{Mt}-DNA interactions. Substitutions of these nucleotides have caused the complete loss of CRP_{Mt} binding to DNA. Similar to CRP regulation in *E. coli*, the increase or inhibition of RNA polymerase recruitment is determined by the distance between the CRP_{Mt}-binding site and the transcriptional start site (TSS).[349] Although binding to regions upstream of

the TSS enhances gene expression, CRP_{Mt} binding sites close to the TSS are inhibitory.[349] Thus, CRP_{Mt} can undergo different conformations to promote DNA binding when cAMP is not present. CRP_{Mt} is unable to interact with *E. coli* RNA polymerase and is limited to interacting with mycobacterial RNA polymerase.[357] This has been confirmed by the incapacity of CRP_{Mt} to substitute CRP in *E. coli* [357] and by the fact that the CRP_{Mt} lacks the conserved residues (His19 and His21) in the N-terminal region of *E. coli* CRP, which interact with the RNA polymerase.[348,351]

The impact of the lack of CRP_{Mt} has been studied. For instance, the growth of the Mtb strain lacking *crp* has been seen to be reduced in liquid culture and within macrophages,[348] and lipid metabolism genes expression was altered when lacking CRP_{Mt}.[348] Furthermore, in a mouse model, the mutant lacking *crp* was seen to have an attenuated virulence. This evidence shows how crucial CRP_{Mt} is in general metabolism and pathogenesis of Mtb.[357]

Function	Gene	Product
Cell-wall biogenesis	*rv0993*	UTP-glucose-1-phosphate uridylyltransferase
	rv3031	Glucosyltransferase
	rv3032	
	rv0643c	Methoxy mycolic acid synthase
	rv0904c	Acetyl-CoA carboxylase carboxyl transferase
Central metabolism pathways	*rv2918*	Uridylyl-transferase
	rv0992c	5-formyltetrahydrofolate cyclo-ligase
	rv0520	Methyltransferase
	rv3113	Phosphatase
	rv3114	Nucleoside deaminase
	rv3505	Acyl-CoA dehydrogenase
	rv3617	Epoxide hydrolase
Regulatory elements of cAMP signalling	*rv0104*	cAMP-binding protein
	rv0103c	Cation transporter
	rv3645	Membrane-linked adenylyl cyclase
Antibiotic resistance	*rv0906*	β-lactamase
	rv0907	
	rv0905	Enoyl-CoA hydratase
	rv0908	Methyl-accepting chemotaxis protein

Table 4-1. Functions and products of putative CRP_{Mt}-regulated genes.
Table adapted from Akhter *et al.*[356]

In this study, I aimed to investigate if mycobacteria respond to a physiological concentration of NaCl, 250 mM,[341] via modulation of their intracellular cAMP levels. This was achieved by using a combination of LC-MS based metabolite analysis, combined with stable isotope labeling, as well as genetic mutants. These analyses revealed that the pathogenic mycobacterium Mtb responds to NaCl stress via an increase in the intracellular cAMP pool size. I found that even if the increase of intracellular cAMP levels is partly mediated by PknD, it is the transcriptional regulator CRP_{Mt} that orchestrates the overall process.

4.2 Results

4.2.1 A physiological concentration of NaCl leads to an increase in intracellular cAMP levels in Mtb

To investigate if mycobacteria respond to different levels of ionic and non-ionic osmotic stress via a modulation of their intracellular cAMP levels similar to the one observed in *E. coli*,[358] three different mycobacterial species were exposed to 10 mM NaCl, 250 mM NaCl and 500 mM sucrose. *M. smegmatis* mc2155 was chosen as non-pathogenic mycobacteria, *M. marimum* M as human opportunistic mycobacteria, and Mtb H37Rv as pathogenic mycobacteria. In *M. smegmatis* one doubling time corresponds to three hours and in Mtb and *M. marinum*, to 24 hours. A concentration of 500 mM sucrose was used as a control of non-ionic osmotic stress, corresponding to ~500 mOsm/L and equivalent to the osmolarity of 250 mM NaCl, the concentration found within the macrophage phagosome .[341] In order to assess bacterial viability, growth of the three mycobacterial strains was monitored under these three conditions. As seen in Figure 4-5, compared to the control condition, where bacteria were grown at a concentration of 10 mM NaCl, the presence of 250 mM NaCl reduced but did not abolish the growth of all three mycobacterial species. However, even if the growth of *M. smegmatis* was only slightly impaired in the presence of 500 mM sucrose compared to the growth at 250 mM NaCl (Figure 4-5 A), such high concentration of sucrose drastically impaired the growth of *M. marinum* and Mtb (Figure 4-5 B and C). In order to investigate the correlation between the type of osmotic stress and the intracellular cAMP levels, mycobacteria were exposed for one doubling time to 10 mM NaCl, 250 mM NaCl and 500 mM sucrose (Figure 4-6, Table 4-3) and their intercellular cAMP levels were measured. Compared to unchallenged bacteria, the exposure to 250 mM NaCl and 500 mM sucrose of *M. smegmatis* led to a 1.65-fold and 4-fold decrease in intracellular cAMP levels. In *M. marinum*, even if the exposure to 500 mM sucrose led to a 4.5-fold decrease in intracellular cAMP levels, no changes were observed in the presence of 250 mM NaCl. In contrast, even if the exposure to 500 mM sucrose led to a 1.5-fold decrease in intracellular cAMP levels in Mtb H37Rv, a 3-fold increase in the intracellular cAMP levels was observed upon exposure to a concentration of 250 mM NaCl for one doubling time (Figure 4-6). The assignment of this molecule as the second messenger 3',5'-cAMP was confirmed using the state-of-the-art LC-MS/MS (Figure 4-7 and 4-8). Under the chromatographic conditions used, the extract ion chromatogram of the standard 2',3'-cAMP, which derives from mRNA degradation,[359] has a retention time of 2.8 min (Figure 4-7 A) and the extract ion chromatogram of the standard 3',5'-cAMP has a retention time of 3.6 minutes (Figure 4-7 B). The extract ion chromatograms for the molecule at *m/z* 330.0598 $[M+H]^+$ corresponding to cAMP in Mtb exposed to 10 mM for 24 hours and 250 mM for 24 hours are shown in Figure 4-7 C and 4-7 D, respectively. As seen in Figure 4-

7 C, both 2',3'-cAMP and 3',5'-cAMP can be detected and separated in Mtb metabolome extracts. In this extract, the second messenger, with retention time of 3.6 min, represents the majority of the total pool of cAMP. When exposed to 250 mM NaCl, only the peak at 3.6 min, assigned to 3',5'-cAMP, increased by 3-fold compared to unchallenged cells (Figure 4-7). This assignment was further confirmed using MS/MS (Figure 4-8), demonstrating that upon exposure to 250 mM NaCl, the intracellular 3',5'-cAMP levels increased in Mtb.

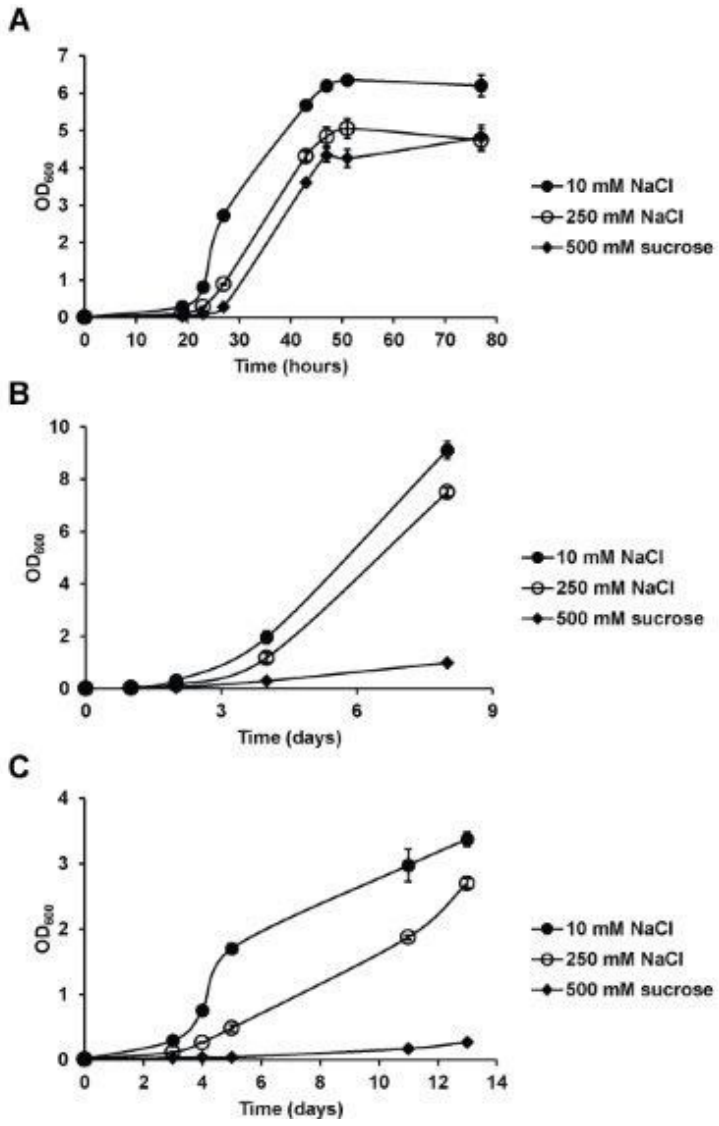


Figure 4-5. Exposure to 250mM reduced growth of *M. smegmatis*, *M. marinum* and Mtb.
Effect of ionic and non-ionic osmotic stress on the growth of *M. smegmatis* mc^2155, *M. marinum* M and Mtb H37Rv. Growth curves at 10 mM NaCl (filled circle), 250 mM NaCl (open circled) and 500 mM sucrose (filled diamond) in Middlebrook 7H9 medium, monitored at OD_{600} nm for *M. smegmatis* (A), *M. marinum* (B) and Mtb (C). The graph shows one representative experiment from three biological replicates. Error bars denote standard deviation.

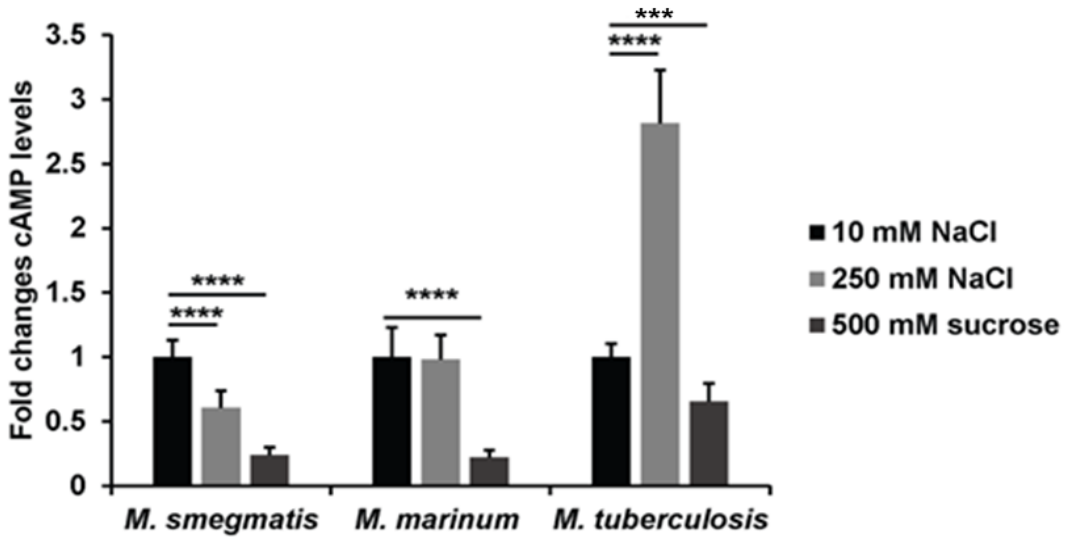


Figure 4-6. Only stress at 250 mM NaCl leads to an increase in intracellular cAMP levels in Mtb. Effect of ionic and non-ionic osmotic stress on the intracellular cAMP levels of *M. smegmatis* mc2155, *M. marinum* and Mtb H37Rv. Bar-graph showing the intracellular levels of cAMP at 10 mM NaCl (black), 250 mM NaCl (light grey) and 500 mM sucrose (dark grey) for the equivalent of one doubling time for the strains. This corresponds to 3 hours for *M. smegmatis* mc2155; and 24 hours for *M. marimum* M, and Mtb. Error bars denote standard deviation.*** $p < 0.001$, **** $p < 0.0001$ as analysed by Student's *t*-test. This figure represents the average of three biological replicates.

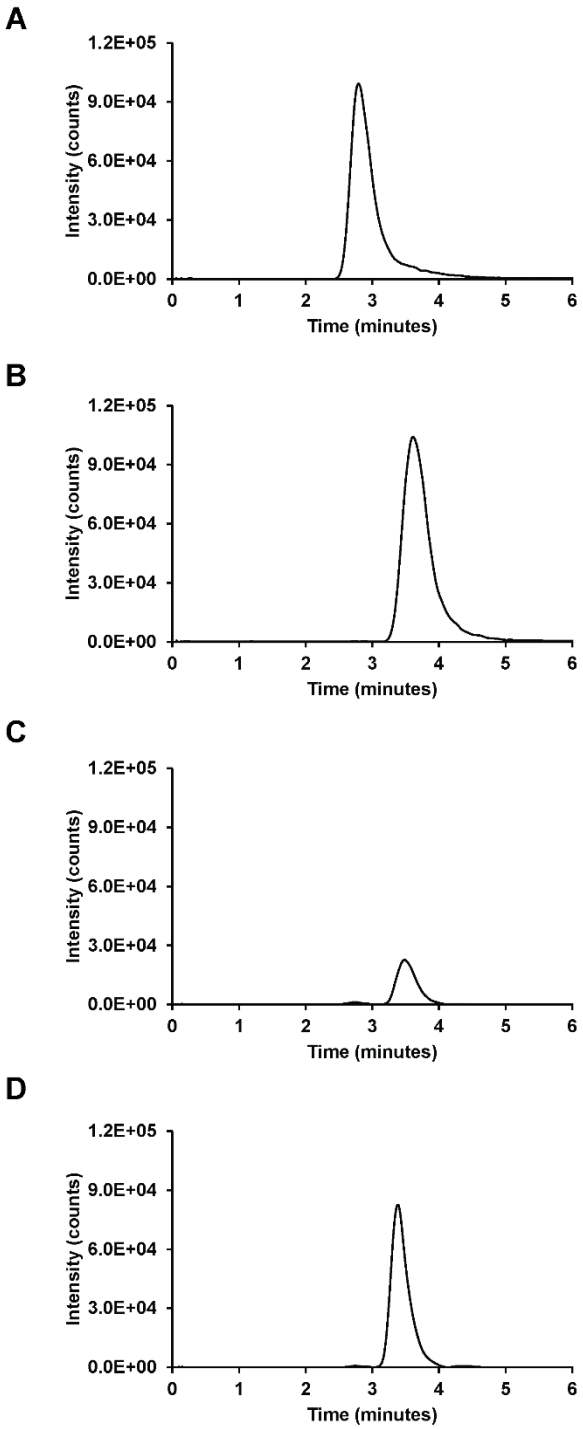


Figure 4-7. Confirmation of the assignment of the molecule of interest as 3',5'-cyclic adenosine monophosphate.

Extract ion chromatogram for the *m/z* 330.0598 in positive ion mode $[M+H]^+$ corresponding to 1 µM of the standard 2',3'-cAMP (A). Extract ion chromatogram for the *m/z* 330.0598 in positive ion mode $[M+H]^+$ corresponding to 1 µM of the standard 3',5'-cAMP (B). Extract ion chromatogram for the *m/z* 330.0598 in positive ion mode $[M+H]^+$ at time 24 hours at 10 mM NaCl in Mtb H37Rv (C). Extract ion chromatogram for the *m/z* 330.0598 in positive ion mode $[M+H]^+$ at time 24 hours at 250 mM NaCl in Mtb H37Rv (D). Both, sample run on the mass spectrometer and data analysis were performed by Dr Gerald Larrouy-Maumus.

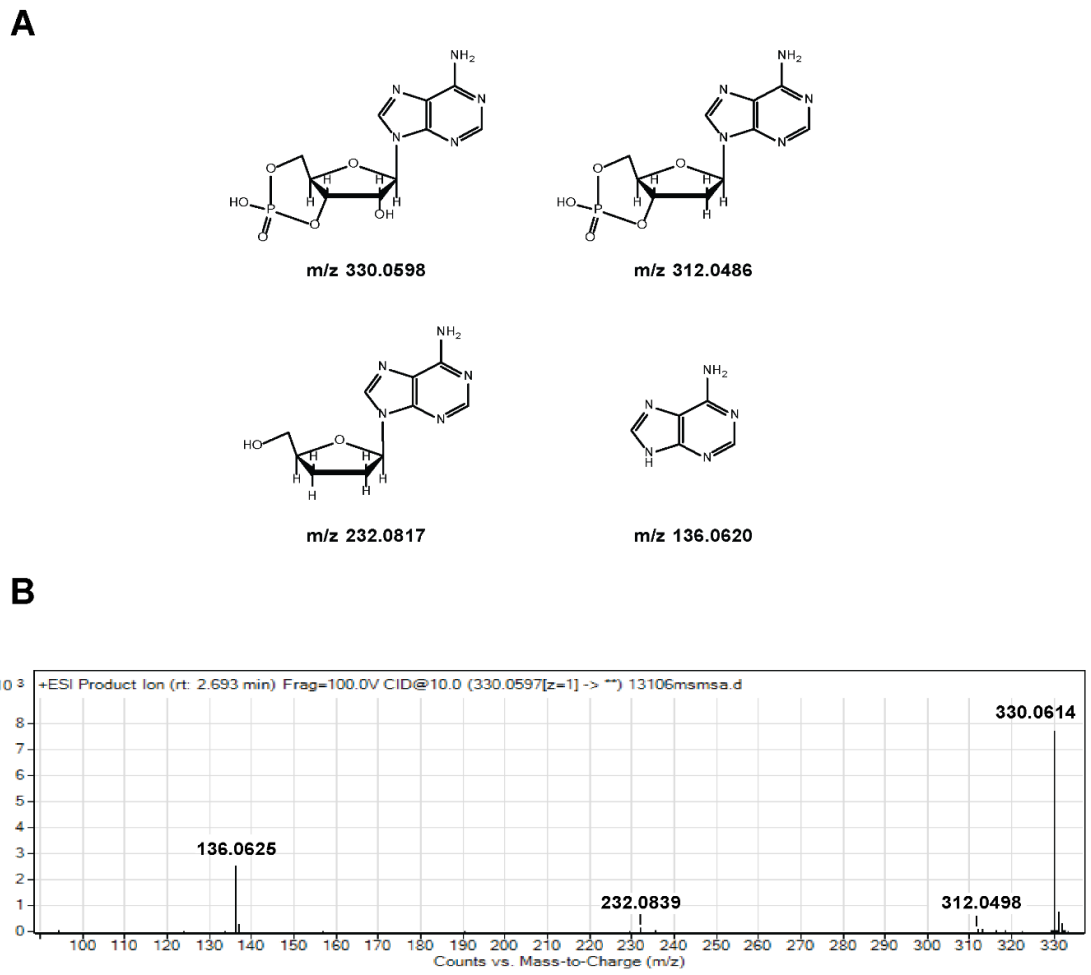


Figure 4-8. Confirmation of the assignment of the molecule as 3',5'-cyclic adenosine monophosphate by MS/MS mass spectrometry.

Predicted MS/MS fragment observed for the fragmentation of 3',5'-cyclic AMP at 10V in positive ion mode (A). Experimental MS/MS spectrum for ion at *m/z* 330.0597 in positive ion mode $[M+H]^+$ at 10V of the peak at 3.6 min retention time for present in Mtb H37Rv metabolome extract (B). Both, sample run on the mass spectrometer and data analysis were performed by Dr Gerald Larrouy-Maumus.

4.2.2 Mtb ACs are active upon exposure to 250 mM NaCl

The fact that I did not observe increases in intracellular levels of cAMP in *M. smegmatis* and *M. marinum* upon equivalent exposure to 250 mM NaCl could be due to a lack of expression of the ACs in these organisms compared to Mtb under similar conditions of growth and stress. However, according to the literature, these enzymes are expressed under conventional growth conditions, precluding a lack of expression under the conditions tested in this study.[168,360–364] Alternatively, another hypothesis could be that the ACs are expressed in those organisms but that a concentration of 250 mM NaCl is not able to alter their activity. In order to have an in-depth investigation into the synthesis and the turn-over of cAMP under the conditions used in this study, a stable isotope tracing experiment at 10 mM and 250 mM NaCl was performed in all the three mycobacterial species. Mycobacteria were stressed in a culture medium supplemented with either 10 mM or 250mM NaCl in the presence of [U-$^{13}C_3$] glycerol and [U-$^{13}C_6$] glucose. Figure 4-9 represents the percentage labelled of cAMP over time in *M. smegmatis* at 1/3, one and two doubling times (Figure 4-9 A), in *M. marinum* and Mtb at 1/4, one and two doubling times (Figure 4-9 B and C, respectively) exposed to 10 mM and 250 mM NaCl. As seen in Figure 4-9, at 10 mM NaCl, all strains used in this study exhibited an increase in the percentage labelled cAMP over time. This indicates a cAMP turn-over in all the mycobacterial species used here. After two doubling times at 10 mM NaCl, the percentage labelled reached 63% in *M. smegmatis*, 54% in *M. marinum* and 45% in Mtb. Upon exposure to 250 mM NaCl, even if the pool size of cAMP decreased in both *M. smegmatis* and remained unchanged in *M. marinum* (Figure 4-6), the percentage of molecule labelled increased, suggesting an increase in the turn-over of cAMP. Effectively, at one doubling time, a 1.3-fold increase in percentage labelled was observed in *M. smegmatis* and a 1.8-fold, 1.5-fold and 1.3-fold were observed in *M. marinum* at 1/4, one and two doubling time, respectively, compared to non-NaCl challenged mycobacteria. Similarly, in Mtb, a 1.8-fold, 1.4-fold and 1.3-fold increase of the percentage of cAMP labelled was observed upon exposure to 250 mM NaCl compared to 10 mM at 1/4, one and two doubling time, respectively (Figure 4-9 C). Nevertheless, compared to *M. smegmatis* and *M. marinum*, even if there was a slight increase in the turn-over of cAMP of those mycobacterial species, only Mtb was able to increase and maintain higher intracellular cAMP levels upon exposure to 250 mM NaCl. In summary, experiments using stable isotope labelling coupled to metabolomic analysis revealed the first evidence that mycobacteria are able to adapt intracellular cAMP levels and turn-over under NaCl stress conditions.

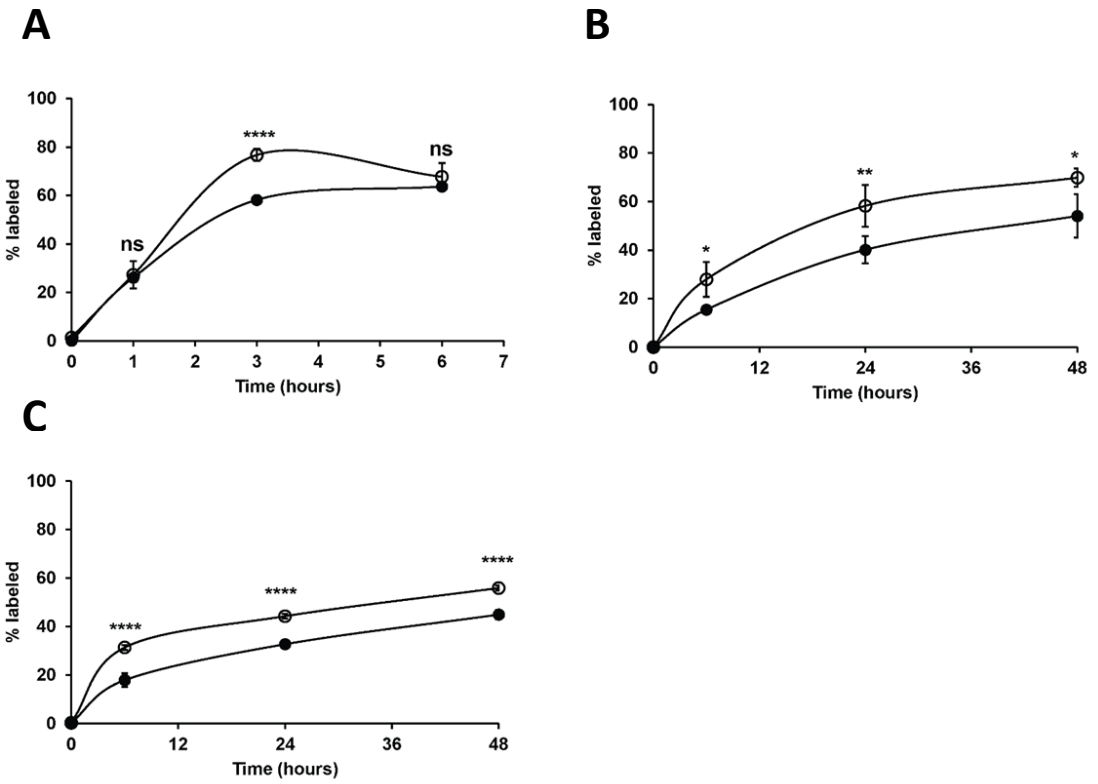


Figure 4-9. cAMP is synthesised *de novo* upon 250 mM NaCl stress.
Percentage of ^{13}C incorporation in cAMP over time at 10 mM NaCl (filled circle) and 250 mM NaCl (open circle) in *M. smegmatis* mc2155 (A), *M. marinum* M (B) and Mtb H37Rv (C). All strains used in this study exhibited an increase in the percentage labelled of cAMP over time. Error bars denote standard deviation. *p < 0.05, **p < 0.01, ***p < 0.001, ****p < 0.0001 as analysed by Student's *t*-test. This figure represents the average of three biological replicates.

4.2.3 Increase in intracellular cAMP levels is partially dependent on the PknD osmosensing signalling pathway in Mtb

At this stage, the increase in intracellular cAMP levels found in Mtb could be due to a difference in the transcriptome profile of the enzymes involved in cAMP synthesis and degradation upon exposure to 250 mM NaCl compared to 10 mM NaCl. I therefore used cDNA microarrays to test this hypothesis. cDNA microarray analysis was carried out after a shift to 250 mM NaCl-containing medium at 2, 8 and 24 hours corresponding to 1/12, 1/3 and one doubling time in Mtb. Surprisingly, at 250 mM NaCl, no significant changes in gene expression in genes involved in cAMP synthesis were observed during the measured time course (Figure 4-10, Table 4-2). This observation is consistent with data from the literature where exposure to 250 mM NaCl for 4 hours led to minor changes in transcriptome profile in Mtb CDC 1551.[341] It was then hypothesised that the increase in intracellular levels of cAMP observed in Mtb could be driven by a much faster sensing mechanism such as protein phosphorylation cascades. This fast response likely involves pre-existing signal transduction and allosteric regulation of key enzymes and transporters. Eukaryotic-like serine-threonine kinases such as PknD are candidates to orchestrate the early increase of cAMP.[340] To test the hypothesis that PknD is involved in the regulation of the intracellular cAMP levels via phosphorylation of key enzymes involved in cAMP synthesis, the parental strain and a well-characterised *pknD* transposon mutant strain were grown at 10 mM and 250 mM to assess cell viability. They were also exposed for 6 hours and 24 hours to 250 mM NaCl and their intracellular cAMP levels measured (Table 4-3). As seen in Figure 4-11 A, at 10 mM NaCl, compared to the parental strain the *pknD* transposon mutant strain exhibited a defect in growth. However, when grown in a culture medium containing 250 mM NaCl, both the parental and mutant strains exhibited a similar growth profile (Figure 4-11 B), even though a decrease in growth rate is observed compared to 10 mM NaCl. This observation is surprising since a drastic growth defect in the PknD transposon mutant compared to the parental strain was previously reported.[340] However, regarding intracellular cAMP levels in those strains (Figure 4-11 C), exposure to 250 mM NaCl for 1/4 of a doubling time led to a 3.5-fold and 2.2-fold increase of intracellular cAMP levels compared to unexposed parental and PknD::Tn strains. After 24 hours' exposure to 250 mM NaCl, a 2-fold increase in intracellular cAMP levels was observed in both strains. It is of note that a 3-fold increase in intracellular cAMP levels was observed in Mtb H37Rv and a 2-fold increase intracellular cAMP levels in Mtb CDC1551 when exposed for one doubling time at 250 mM NaCl. Taken together, at 6 hours equivalent to 1/4 doubling time, PknD may partly be involved in the process of increasing intracellular cAMP levels, but not at 24 hours where levels are similar to the ones found in the parental strain in the PknD::Tn strain.

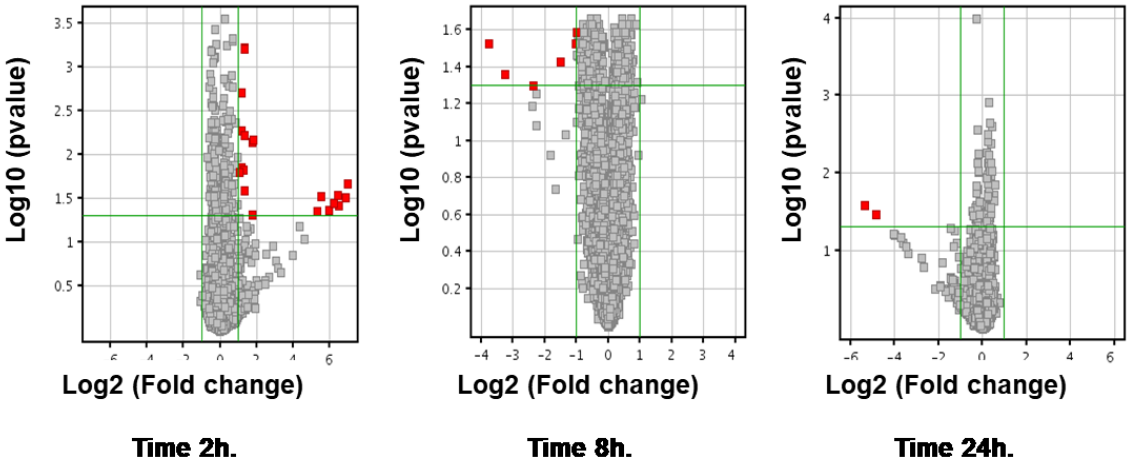


Figure 4-10. There are no changes in expression of genes involved in cAMP synthesis in Mtb. Volcano plot representing data of Mtb cDNA microarray analysis carried out at 250mM, at 2, 8 and 24 hours after shift to NaCl-containing medium corresponding to 1/12, 1/3 and one doubling time. Red dots symbolise the genes which significantly changed in comparison to 10 mM. Experiment performed by Dr Gerald Larrouy-Maumus.

Time of exposure	Log2 FC ([ha vs 0-no salt cy 5] vs [ha vs 0-no salt cy3])	Regulation ([ha vs 0-no salt cy 5] vs [ha vs 0-no salt cy3])	Description	GeneName	TargetID
2h 250mM NaCl	6.879344	up	Mycobacterium tuberculosis 16S ribosomal RNA	16S rRNA	TB-16S-rRNA
	6.9482155	up	Mycobacterium tuberculosis 16S ribosomal RNA	16S rRNA	TB-16S-rRNA
	5.9343505	up	Mycobacterium tuberculosis 16S ribosomal RNA	16S rRNA	TB-16S-rRNA
	6.511153	up	Mycobacterium tuberculosis 23S ribosomal RNA	23S rRNA	TB-23S-rRNA
	6.4087105	up	Mycobacterium tuberculosis 23S ribosomal RNA	23S rRNA	TB-23S-rRNA
	6.2245173	up	Mycobacterium tuberculosis 23S ribosomal RNA	23S rRNA	TB-23S-rRNA
	1.1473029	up	PE-PGRS FAMILY PROTEIN	PE_PGRS17	Rv0978c
	1.3366635	up	Uncharacterized PE-PGRS family protein PE_PGRS20	PE_PGRS20	Rv1068c
	1.7878151	up	PE-PGRS FAMILY PROTEIN	PE_PGRS22	Rv1091
	1.0375766	up	PE-PGRS FAMILY PROTEIN	PE_PGRS22	Rv1091
	1.2853705	up	Uncharacterized PE-PGRS family protein PE_PGRS24	PE_PGRS24	Rv1325c
	1.330654	up	PE-PGRS FAMILY PROTEIN	PE_PGRS25	Rv1396c
	1.7731402	up	Uncharacterized PE-PGRS family protein PE_PGRS34	PE_PGRS34	Rv1840c
	1.1758608	up	PE-PGRS FAMILY PROTEIN	PE_PGRS42	Rv2487c
	1.3443587	up	PE-PGRS FAMILY PROTEIN	PE_PGRS57	Rv3514
	1.3432941	up	PE-PGRS FAMILY PROTEIN	PE_PGRS6	Rv0532
	5.329161	up	Bacterial RNase P class A [Source: RFAM 9.1]	RNaseP_bact_a	EBMYCG00000003999
	5.501399	up	tmRNA [Source: RFAM 9.1]	tmRNA	EBMYCG00000004000
	1.1447992	up	hypothetical protein		TBMG_01622
	1.7376845	up	Putative ESAT-6-like protein 6		Rv3619c
8h 250mM NaCl	3.7718859	up	Mycobacterium tuberculosis 16S ribosomal RNA	TB-16S-rRNA	16S rRNA
	3.2552762	up	Mycobacterium tuberculosis 16S ribosomal RNA	TB-16S-rRNA	16S rRNA
	1.0377051	up	Polyketide synthase	Rv1664	pks9
	1.5022545	up	Uncharacterized HTH-type transcriptional regulator Rv1395/MT1440	Rv1395	
	1.0151863	up	Putative uncharacterized protein	MT1356	
24h 250mM NaCl	5.354544	up	Mycobacterium tuberculosis 16S ribosomal RNA	16S rRNA	TB-16S-rRNA
	4.8469605	up	Mycobacterium tuberculosis 16S ribosomal RNA	16S rRNA	TB-16S-rRNA

Table 4-2. cDNA microarray of Mtb H37Rv upon exposure to 250 mM NaCl.
Upregulation of genes upon Mtb exposure for 2 hours, 8 hours or 24 hours to 250 mM NaCl. The table represents data obtained via Mtb cDNA microarray. Experiments were performed by Dr Gerald Larrouy-Maumus.

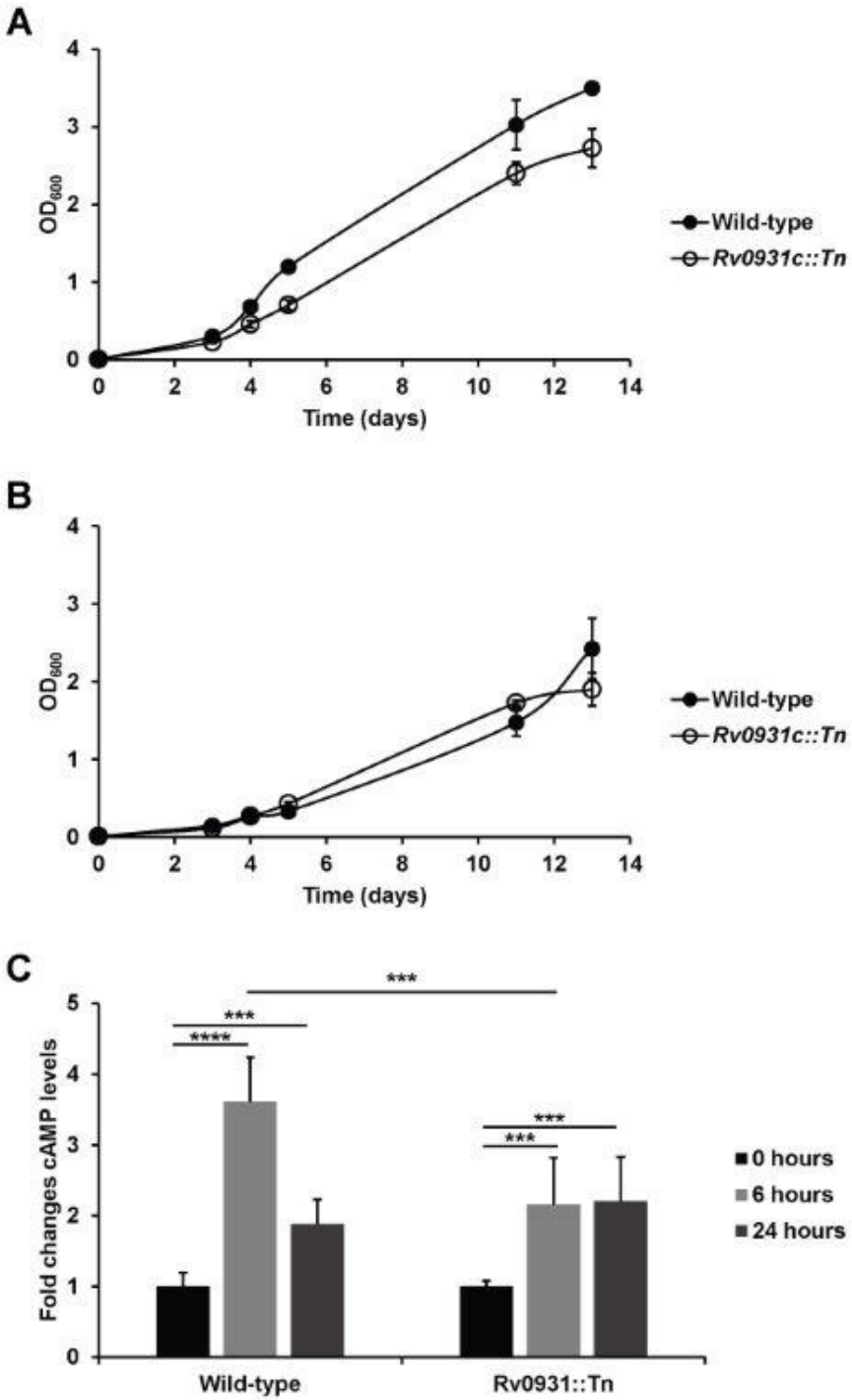


Figure 4-11. PknD is partly responsible for the cAMP increase at 250 mM NaCl in Mtb.
Effect of NaCl stress on the growth and intracellular cAMP levels of Mtb CDC1551 and PKnD::Tn deleted strains. Growth curves of parental strain (filled circle), PKnD::Tn (Rv0931::Tn) strain (open circle) at 10 mM NaCl (A) and 250 mM NaCl (B) in Middlebrook 7H9 medium, monitored at OD_{600} nm. Bar graph showing the intracellular levels of cAMP of the parental strain and PKnD::Tn strain (C). Time 0: black bar; Time 6 hours: light grey bar; Time 24 hours: dark grey bar. Error bars denote standard deviation. ***p < 0.005, ****p < 0.0005 as analysed by Student's *t*-test. This figure represents the average of three biological replicates.

4.2.4 The increase in the intracellular cAMP levels is dependent on the transcriptional regulator CRP_{Mt} in Mtb

In *E. coli*, the cAMP receptor protein CRP is involved in transcriptional regulation during NaCl stress.[327,336] In order to investigate if CRP_{Mt} plays a role in the up-regulation of cAMP under NaCl stress in Mtb, a NaCl stress assay was performed with the Mtb H37Rv strain deleted for the gene *rv3676* (*crp*) and its complemented strain. I therefore performed growth curves of Mtb wild type, Δ*crp* and complemented at 10 mM NaCl and 250 mM NaCl to investigate the impact of NaCl concentrations on growth. As expected, 250 mM NaCl did not abolish the growth of Mtb Δ*crp* but rather slowed the growth of all the strains tested (Figure 4-12 A and B). I then determined the intracellular cAMP levels in those strains when exposed for 1/4 and one doubling time to 250 mM NaCl (Figure 4-12 C, Table 4-3). As seen in Figure 4-12 C, compared to the parental strain, where the intracellular level of cAMP increased by 6-fold after 6 hours and 3-fold after 24 hours exposure to 250 mM NaCl, the Mtb strain deleted for *crp* did not exhibit an increase in the intracellular cAMP levels. This experiment clearly establishes a direct link between CRP_{Mt} and the increase and maintenance of intracellular cAMP levels in Mtb under exposure to 250 mM NaCl. In this study, the use of metabolomics and genetics provide the first evidence that only Mtb is able to increase its intracellular levels of cAMP in response to NaCl stress, and that this increase is dependent on CRP_{Mt} (Figure 4-12).

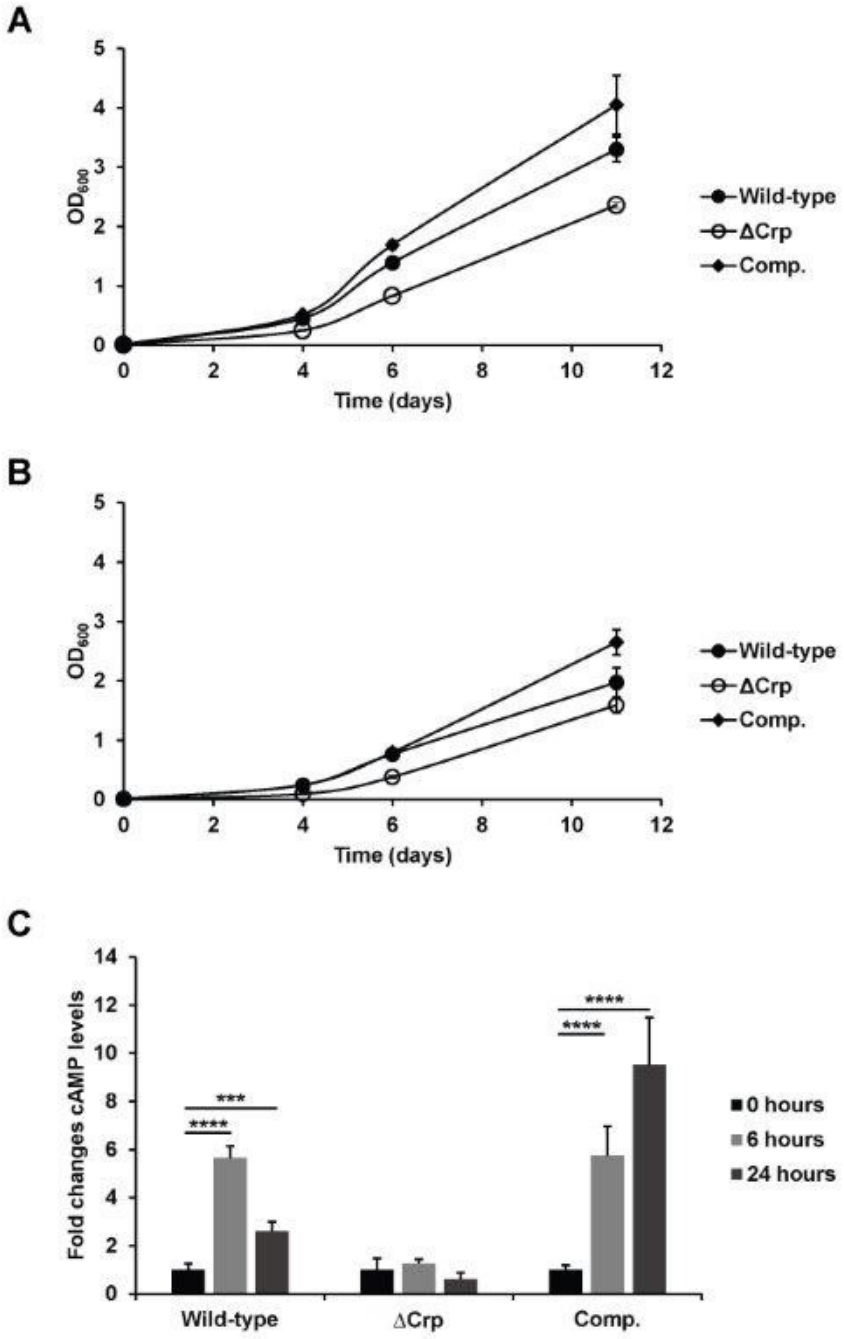


Figure 4-12. CRP_{Mt} orchestrates the cAMP increase of Mtb upon exposure to 250 mM NaCl.
Effect of NaCl stress on the growth and intracellular cAMP levels of Mtb *crp* deleted strain. Growth curves of Mtb H37Rv wild type (filled circle), MtbΔRv3676 (open circle), MtbΔRv3676::Rv3676 (filled diamond) at 10 mM NaCl (A) and 250 mM NaCl (B) in Middlebrook 7H9 medium, monitored at OD 600 nm. Bar graph showing the intracellular levels of cAMP of the parental strain Mtb H37Rv wild type, MtbΔRv3676, MtbΔRv3676::Rv3676 (complemented strain) (C). Time 0: black bar; Time 6 hours: light grey bar; Time 24 hours: dark grey bar. Error bars denote standard deviation. ***p < 0.005, ****p < 0.0005 as analysed by Student's *t*-test. This figure represents the average of three biological replicates.

Strain	Condition	Time of exposure to stress (hours)	pmol cAMP/100 µg protein
***M. smegmatis* mc^{2}155**	10 mM NaCl	3	12.4±1.1
	250 mM NaCl	3	7.5±1.5
	500 mM sucrose	3	3.0±0.7
***M. marinum* M**	10 mM NaCl	24	1.6±0.3
	250 mM NaCl	24	1.5±0.2
	500 mM sucrose	24	0.3±0.1
Mtb H37Rv	10 mM NaCl	24	11.0±-.8
	250 mM NaCl	24	31.0±4.0
	500 mM sucrose	24	7.2±1.5
Mtb CDC1551	10 mM NaCl	0	10.4±1.7
	10 mM NaC	6	17.8±2.4
	10 mM NaC	24	17.7±1.5
	250 mM NaCl	6	64.4±6.8
	250 mM NaC	24	33.5±4.3
Mtb CDC1551 PknD::Tn	10 mM NaCl	0	0.9±0.1
	10 mM NaCl	6	1.7±0.4
	10 mM NaCl	24	1.6±0.4
	250 mM NaCl	6	3.6±0.7
	250 mM NaCl	24	3.7±0.5
Mtb H37Rv	10 mM NaCl	0	1.6±0.3
	10 mM NaCl	6	5.6±0.4
	10 mM NaCl	24	7.3±0.7
	250 mM NaCl	6	31.6±1.8
	250 mM NaCl	24	17.6±2.9
Mtb Δ*rv3676*	10 mM NaCl	0	2.2±0.6
	10 mM NaCl	6	2.8±0.3
	10 mM NaCl	24	3.3±0.9
	250 mM NaCl	6	3.9±0.1
	250 mM NaCl	24	2.0±0.7
Mtb comp. *rv3676*	10 mM NaCl	0	1.8±0.3
	10 mM NaCl	6	6.5±0.3
	10 mM NaCl	24	3.1±0.6
	250 mM NaCl	6	10.3±1.6
	250 mM NaCl	24	29.5±2.5

Table 4-3. cAMP levels in mycobacteria used in this study.
cAMP in pmol per 100 µg of protein of *M. smegmatis* wild type, *M. marinum* wild type Mtb H37Rv wild type, Mtb CDC1551 wild type, Mtb CDC1551 lacking PknD, Mtb H37Rv lacking *rv3676,* and Mtb H37Rv complemented strain. cAMP levels were measured by LC-MS after exposure to 10 mM NaCl, 250 mM NaCl or 500 mM sucrose.

4.3 Discussion

cAMP contributes to signal transduction in Mtb and is important for the interaction of this pathogen with the host.[351] The Mtb H37Rv genome reveals 10 putative proteins harbouring a cAMP-binding domain.[145] Among those are two transcriptional regulators, which are crucial for virulence (CRP, Rv3676 and Cmr, Rv1675).[181,349,362] CRP_{Mt} regulates the transcription of different promoters: the serC promoter, which encodes a phosphoserine aminotransferase crucial for the production of serine;[365] the resuscitation promoting factor RpfA, involved in resuscitating of dormant Mtb;[348] the whiB1 promoter, involved in transcription regulation in response to NO produced by infected macrophages;[366,367] and the fumarate reductase-encoding gene *frdA*, which converts fumarate to succinate playing an important role in Mtb adaptation to hypoxic stress.[368] Thus, it is of vital importance to gain a better understanding of how intracellular levels of cAMP are modulated in mycobacteria.

In this study, I focused on the intracellular cAMP levels in non-pathogenic, human opportunistic and pathogenic mycobacteria grown in conventional 7H9 culture medium containing either 10 mM NaCl, considered as control or 250 mM NaCl, which is equivalent to the concentration that has been reported to be found in macrophages.[342,343] Unlike *E. coli*, *Corynebacterium glutamicum* and *Streptomyces coelicolor* that possess only one AC, mycobacteria possess several copies of these in their genome and are known to produce over 100-fold more cAMP; and secrete large amounts of cAMP during growth compared to other bacteria.[183,339] Sixteen genes are found in the Mtb H37Rv genome encoding for class III AC, 10 genes in *M. smegmatis*, 12 genes in *M. avium* and 31 genes in *M. marinum*.[168] In parallel, it is known that secretion of cAMP can subvert host cell metabolism.[186] For instance, work by Lowrie *et al.* demonstrated that infection with live, but not dead, *M. microti*, a member of the MTBC, enhanced levels of cAMP in infected macrophages and that this increase blocked phagosome maturation.[184] Furthermore, increased levels of cAMP have also been seen within *M. bovis* BCG infected macrophages.[185] It is well established that intracellular cAMP mediates its regulatory effects through allosteric interactions with cAMP-binding proteins, which undergo conformational changes, altering their activity. These modifications lead to global physiology remodelling. Due to the importance of intracellular cAMP in mycobacterial physiology, I investigated if the intracellular cAMP levels are altered upon NaCl stress in mycobacteria. NaCl concentrations vary during the natural infectious cylce of Mtb. These concentrations go from 50 mM NaCl in the airway surface liquid to 250 mM NaCl within the macrophage. Thus, gaining further understanding of the relationship between cAMP and NaCl tolerance in mycobacteria is of importance. Previous work has shown that in *M. smegmatis* and *M. bovis* BCG the intracellular cAMP levels are ~50% higher in the stationary

phase compared to the logarithmic phase.[369]. A similar trend in Mtb H37Rv, where the intracellular cAMP levels could increase slightly in stationary phase, cannot be excluded. Therefore in the experimental conditions and according to the literature, bacteria were considered to be in logarithmic phase.[112,368,370] I then investigated the growth and intracellular cAMP levels of three mycobacterial strains exposed to 10 mM NaCl, 250 mM NaCl and 500 mM sucrose (control of non-ionic osmotic stress). The three mycobacterial strains of choice were: *M. smegmatis*, as a non-pathogenic strain commonly found in soil, marine and freshwater environments; *M. marinum,* as a human opportunistic strain found in salt water and fresh water; and Mtb, as a human pathogenic strain. The data obtained suggest that *M. smegmatis* is more tolerant to non-ionic osmotic stress compared to *M. marinum* and Mtb since 500 mM sucrose only slightly impaired *M. smegmatis* growth in comparison to the drastic growth impairment seen under the same conditions in *M. marinum* and Mtb. When the intracellular levels of cAMP were measured, a decrease in cAMP levels in *M. smegmatis* after exposure to 250 mM NaCl was observed. With regard to Mtb, exposure to 250 mM NaCl led to an increase in the levels of cAMP. It cannot be excluded that higher concentrations of NaCl and sucrose such as at 1,000 mM NaCl and 2,000 mM sucrose could also have led to similar observations. However, at this stage, the biological relevance of such concentrations is questioned since, according to the available literature, it is highly unlikely that Mtb would encounter such drastic osmotic shock within the host.[342]

So far the only organisms reported to respond to NaCl stress by an increase in intracellular cAMP levels are the soil amoeba *Dictyostelium discoideum*, the cyanobacterium *Anabaena* sp. strain PCC 7120[371,372] and *E. coli.*[336] In *Dictyostelium discoideum* it has been shown that spore germination is regulated by high osmolarity.[371,373] Thus, in high osmolarity conditions the spore head would activate ACG (adenylate cylase G) in order to produce cAMP which would bind to a regulatory subunit of cAMP dependent protein kinase (PKA). This would lead to the dissociation and activation of the catalytic subunit resulting in the inhibition of the germination process.[373] Research in *Anabaena* sp. Strain PCC 7120 shows that with the addition of 200 mM NaCl, the intracellular cAMP levels increased over 4.5-fold within 3 min and then decreased, which suggested that cAMP functioned as a signalling molecule.[372] Regarding *E. coli*, Balsalobre *et al*. reported that the total cAMP levels were significantly increased at high osmolarity.[336] Specifically, the intracellular cAMP levels in *E. coli* were enhanced, which suggested that osmolarity had a direct impact on the synthesis and/or turnover of cAMP.[336]

To investigate if the increase in the intracellular levels of cAMP in Mtb after exposure to 250 mM NaCl were from *de novo* ATP synthesis or from an existing pool of ATP, I performed stable isotope tracing experiments. No changes in labelling of cAMP would have been expected if cAMP was produced from an existing ATP pool. However, if cAMP was produced following *de novo* ATP synthesis, the percentage of cAMP labelled would increase over time, in accordance with the increase in cAMP turnover. Moreover, if the ACs were not expressed under the conditions used in this study, no glucose $^{13}C_6$ incorporation in cAMP would be observed. On the other hand, if the ACs were expressed, I would expect to observe an increase in glucose $^{13}C_6$ incorporation in cAMP over time in both conditions tested, *i.e.* 10 mM and 250 mM NaCl. The data obtained from my experiments showed how there is an increase in labelling incorporation in cAMP in the three tested mycobacterial strains, which confirms how ACs are expressed on the three strains. However, only Mtb was able to increase the high levels of cAMP and maintain them under 250 mM NaCl.

In order to understand if the increase in the intracellular levels of cAMP in Mtb after exposure to 250 mM are due to changes in gene expression of genes involved in the synthesis/degradation of cAMP; cDNA microarray assays were performed. The results obtained showed no significant changes in gene expression in genes involved in cAMP synthesis after exposure for 1/12, 1/3 and one doubling time at 250 mM NaCl in comparison to 10 mM NaCl. This evidence is consistent with data from the literature, where exposure to 250 mM NaCl for 1/6 doubling time led to minor changes in the transcriptome profile in Mtb CDC 1551.[374] Therefore I hypothesised that the increase in intracellular levels of cAMP observed in Mtb have to be driven by a much faster sensing mechanism such as protein phosphorylation cascades. This fast response likely has to involve pre-existing signal transduction and allosteric regulation of key enzymes and transporters.

PknD, an eukaryotic-like-serine-threonine protein kinase is a candidate to orchestrate the early increase of cAMP.[340] Hatzios *et al.* demonstrated that Mtb uses PknD (Rv0931c) to sense and adapt to NaCl stress via phosphorylation of the anti-sigma factor (Rv0516c). Upon an increase in extracellular osmolarity the expression of a PknD substrate is induced and leads to the regulation of virulence factor production, bacterial transcription and cell wall remodelling.[340] PknD has been reported to be the sensor kinase under the concentration found in serum of 140 mM NaCl.[340] I therefore hypothesised that this kinase may also be responsible for the increase in intracellular cAMP levels observed in Mtb at 250 mM NaCl, the concentration found in macrophages according to Tan *et al*.[341] Thus, a PknD transposon mutant strain was tested. Its

growth was impaired at 10 mM NaCl compared to the wild type strain, which was consistent with the literature.[340] Furthermore, the growth of the parental and mutant strains was meaured at 250 mM NaCl and the same growth was observed even though a drastic growth impairment was seen in the parental strain in Hatzios *et al.*'s paper.[340] I then measured the intracellular levels of cAMP to ultimately reveal if PknD is modulating the changes of cAMP under osmotic stress. Thus the parental and transposon mutant strains were exposed to 250 mM NaCl for 1/4 and one doubling time. The data confirmed that PknD might be partially involved in the cAMP increase in the wild type after exposure to 250 mM NaCl for a 1/4 doubling time but not for one doubling time as the levels were similar to the ones found in the parental strain in the PknD::Tn strain. This suggests that the production of cAMP after exposure to 250 mM NaCl does not completely follow the classic osmosensory signalling mediated by PknD.

Since my results show that PknD only partially governs the intracellular cAMP increase in Mtb after exposure to 250 mM NaCl, CRP_{Mt} was investigated. In *E.coli*, the cAMP receptor protein CRP is one of the best-characterised transcription factors. It regulates 195 target promoters and is involved in transcriptional regulation during NaCl stress.[327,336] The levels of CRP are influenced by external osmolarity and an inverse relation between the levels of CRP and cAMP at low and high osmolarity has been reported.[336] Thus, the levels of cAMP are enhanced in the absence of CRP and the levels of cAMP decrease when CRP is overexpressed in *E. coli.*[375] cAMP then acts as a key regulatory component in the osmoregulation of *crp* expression.[336] Balsalobre *et al.* demonstrated that the CRP was repressed under 400 mM of NaCl, and that repression was lost in the absence of cya (AC) and restored upon addition of external cAMP. This means that cAMP is necessary to repress the CRP under 400 mM NaCl.[336]

In Mtb, CRP_{Mt} regulates 114 genes.[351] Experimental approaches are required to determine which genes belong to the CRP_{Mt} regulon and to understand which contribute to virulence in order to explore the regulation mechanisms of expression in response to metabolic and environmental signals. It is known that deletion of the *crp* gene results in an impairment of Mtb *in vitro* growth and attenuates Mtb virulence in a mouse model[348,365] (Figure 4-13). There is a clear inverse correlation between the concentration of NaCl in the culture medium and the growth kinetics of Mtb.[342] After monitoring the growth of the wild type, the *crp* mutant and the complemented strains of Mtb at 10 mM NaCl and 250 mM NaCl I confirmed that the NaCl stress applied only slowed the growth of all the strains tested and did not abolish growth. By measuring the intracellular levels of cAMP in Mtb after exposure to 250 mM NaCl for 1/4 and one doubling time, the strain deleted for *crp* did not present an increase in its cAMP levels in comparison to

the wild type and complemented strain. This clearly showed a direct relationship between CRP_{Mt} and the increase and maintenance of intracellular cAMP levels in Mtb under exposure to 250 mM NaCl. What is noticeable is that in both parental Mtb strains CDC1551, which is a clinical isolate, and in H37Rv, which is a laboratory strain,[376] I observed an increase in intracellular cAMP levels after exposure to 250 mM NaCl. This evidence rules out possible strain-specific characteristics or lab adaptation, demonstrating the robustness of my discovery.

In this study, the use of metabolomics and genetics provide the first evidence that only Mtb is able to increase its intracellular levels of cAMP in response to NaCl stress, and that CRP_{Mt} is necessary in this process. Nevertheless, the exact mechanism leading to cAMP production via CRP_{Mt} and its consequences are not fully addressed in this study and it will need to be subjected to further investigations. As a model of my hypothesis, Mtb would be pre-adapted to exposure to 250 mM NaCl. After exposure to increased osmolarity, ACs would be triggered and together with cAMP would increase cAMP levels. This increase would be orchestrated by CRP_{Mt} (Figure 4-14). Surprisingly, even though *M. marinum* possesses 31 ACs and *M. smegmatis* contains 10 ACs as well as *crp* gene,[168] these organisms are not able to increase and maintain their intracellular cAMP pool size in comparison to Mtb, in response the concentration of NaCl found in the macrophages. Based on the data obtained, this could be due to the involvement of other partners, which could be unique to Mtb and may be transcriptionally regulated by CRP_{Mt} prior to the application of stress.

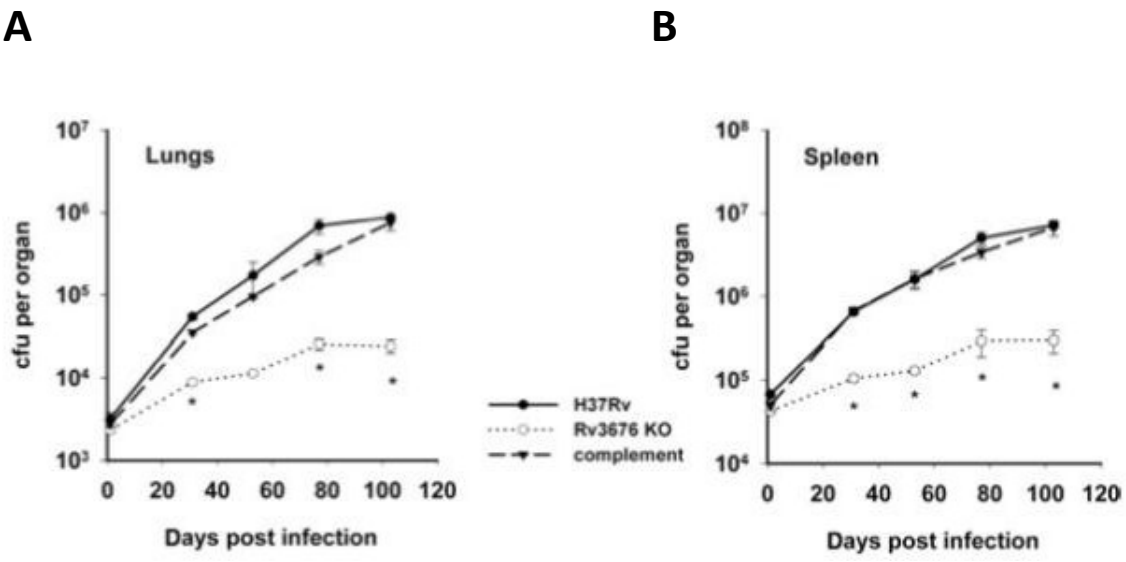


Figure 4-13. Impairment in growth of Mtb *Δcrp* in a mouse intravenous infection.
Rickman *et al*. inoculated BALB/c mice intraveously with $5x10^5$ CFU of Mtb H37Rv, *Δcrp*, and the complemented strain. Survival and multiplication of the three strains in the lungs determined by CFU counts (A). Survival and multiplication of the three strains in the spleen determined by

CFU counts (B). The mutant had an impaired bacterial growth in both the lungs and spleen from mice compared with the infection by the parental strain.[353]

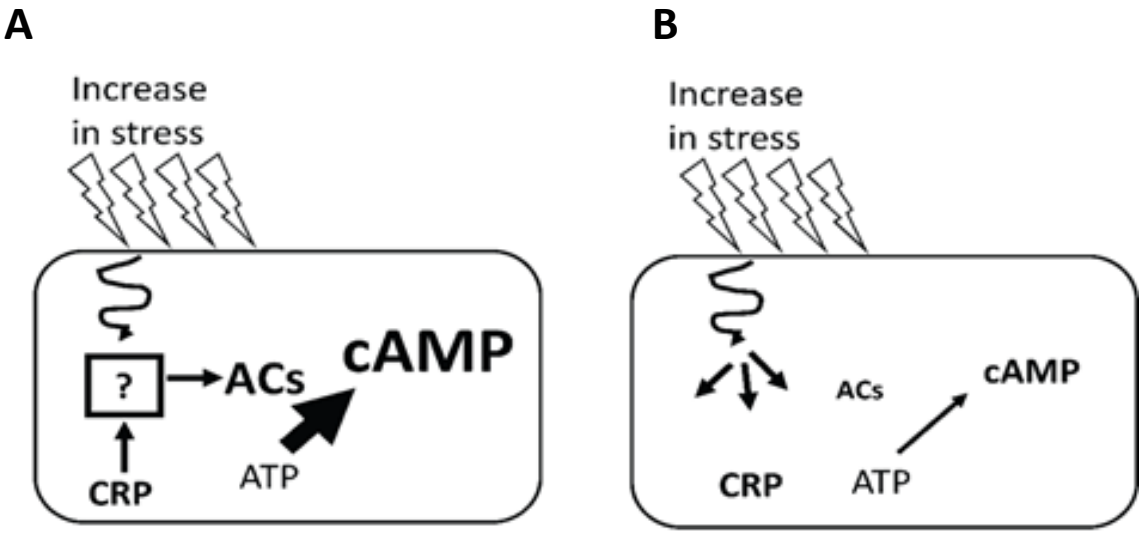


Figure 4-14. CRP_{Mt} orchestrates the increase in intracellular levels of cAMP in response to exposure to 250 mM NaCl in Mtb.
Model of the hypothesis. Mtb would be pre-adapted to osmotic stress caused by 250 mM NaCl. Upon exposure, ACs would be triggered and cAMP levels would increase. This increase would be orchestrated by CRP_{Mt} (A). In *M. smegmatis* and *M. marinum*, being a non-pathogenic and a human opportunistic strain; after exposure to 250 mM NaCl there would not be an increase in the intracellular levels of cAMP even though both mycobacterial strains present *crp* (B).

Chapter 5: Defining the role of the cAMP-dependent lysine acetyltransferase (Rv0998) in Mtb

5. Defining the role of the cAMP-dependent lysine acetyltransferase (Rv0998) in Mtb

5.1 Introduction

5.1.1 Post-translational modifications

Protein post-translational modifications (PTMs) consist of the covalent addition of a functional group to proteins.[377] This happens after or during translation of mRNA sequences to amino acid sequences, proteolytic cleavage of regulatory subunits and degradation of entire proteins.[378] By introducing new functional groups to amino acid residues, PTMs modulate protein function, charge, affinity, size, localisation, molecular weight, conformation, stability, and interactions with nucleic acids, lipids, cofactors or other proteins.[379] Thus PTMs can increase exponentially the versatility and diversity of the protein as they can take place at each of several different amino acids, as determined by the specific PTM, amino acid and position.[379] Consequently, a large number of combinations is possible.[379] Furthermore, PTMs can modulate protein function as well as responses to environmental cues.[378] Bacteria rely on PTMs for modulation of protein function and for essential biological processes and cellular pathways, some of which are involved in pathogenicity and virulence.[379] Therefore, bacteria may subvert host-cell pathways through PTMs in order to escape the host immune defence and ultimately promote bacteria replication.[380] From the different PTMs in bacteria, I chose to work on lysine acetylation as it has been seen to play an important role in Mtb pathogenesis and may regulate central metabolic pathways in Mtb.[381]

5.1.2 Lysine acetylation

Lysine acetylation is a PTM used by many organisms in order to modulate stability, protein-protein and DNA-protein interactions in biological processes, by changing protein charge or conformation.[382,383] Acetylation of lysine residues can be reversed by deacetylases (Figure 5-1).[384,385] Reactions catalysed by acetyltransferases require acetyl-CoA connecting the cell energy status to protein acetylation.[386,387] By using proteomics, 191 of 4525 proteins have been found to be lysine acetylated in *Salmonella enterica*,[388] 170 of 4124[389] in *E. coli* and over 2000[390] in humans. From these, several have been identified as stress response proteins, transcription or translation regulators and central carbon metabolism enzymes, involved in glycolysis, gluconeogenesis, the TCA cycle and fatty acid metabolism.[391]

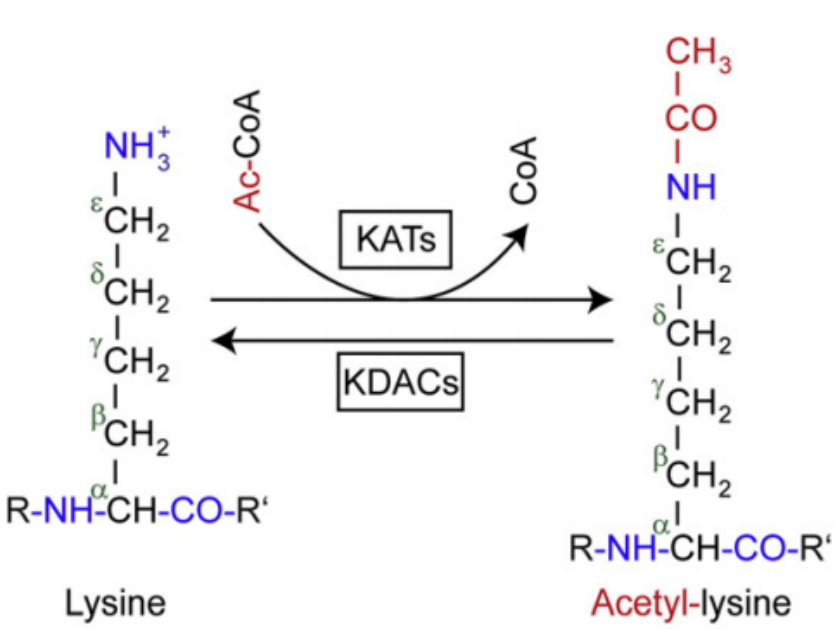


Figure 5-1. General mechanism of lysine acetylation and deacetylation.
Reversible acetylation of the ε-amino group of a lysine residue by KATs (lysine acetyltransferases). The deacetylation of the lysine residue is catalysed by KDACs (lysine deacetylases). Figure adapted from Drazic *et al.*[392]

An example to highlight the importance of lysine acetylation is YfiQ in *E. coli*. YfiQ acetylates the 3' to 5' exoribonuclease RNase R, which is in charge of degradation of structural RNAs in *E. coli.* This leads to RNase degradation. Furthermore, under stress conditions such as cold shock (10 °C for 2 hours), oxidative stress and stationary phase, RNAse R is deacetylated making it more stable, and thus increasing its levels and leading to RNA degradation.[393]

Protein acetylation is involved in energy generation and carbohydrate metabolism. In *E. coli*, around half of all acetylated proteins are involved in these processes.[388,394,395] Baeza *et al.* have developed and utilised the first unbiased and direct method for quantifying the stoichiometry of site-specific acetylation at the proteome-wide scale, without enrichment.[396] Their approach uses a stable isotope chemical labelling step that acetylates all unmodified lysines resulting in a 'heavy' and 'light' acetyl-lysine pair across the entire proteome. This pair is then analysed using high resolution, high accuracy mass spectrometry to yield proteome-wide, site specific stoichiometry. Using this approach, Baeza *et al*. interrogated the acetyl proteome of *E. coli* and investigated the functional consequences of genetically removing the sole NAD^+-dependent protein deacetylase, CobB, on both site-specific and global acetylation.[396] In prokaryotes, CobB regulates acetyl-CoA synthetase (ACS), which is required for cell growth on acetate.[397,398]

Activation of ACS by reversible acetylation is thought to be essential for 'the acetate switch'.[399] This transition occurs when bacterial cells have depleted carbon sources, such as glucose, and begin to utilise environmental acetate for growth. If flux through ACS is inhibited, for example by acetylation, then acetate can be diverted through the acetate kinase, phosphate acetyltransferase pathway to generate acetyl-CoA.[396] Baeza *et al.* observed a wide distribution of acetyl stoichiometry, ranging from less than 1% up to 98%. Among the peptides quantified, 4% of the quantified proteome exhibited a stoichiometry greater than 20% acetyl-lysine. Loss of CobB resulted in a slight increase of global acetylation at low stoichiometry sites, as well as site-specific changes at high stoichiometry sites. For instance, Lys-348, an acetyl site on ACS, displayed 32.5% acetylation in the mutant lacking CobB and 8.3% in the wild type. Proteins with the highest stoichiometry included those involved in central metabolism, transcription, and translation, such as phosphate acetyltransferase, acetyl-CoA carboxylase subunit α, biotin carboxylase, citrate synthase, and aldehyde-alcohol dehydrogenase.[396] The involvement of acetylation of lysine residues in metabolism is evolutionarily conserved, as described for *E. coli* and *S. enterica*.[379,388,394,400,401] In *E. coli* and *S. enterica,* metabolic enzyme acetylation requires carbon sources to be available. *S. enterica* has only one major bacterial protein acetyltransferase.[386,387] Work by Wang *et al*. has shown, by stable isotope labelling with amino acids in cell culture (SILAC) quantification and biochemical studies, that in *Salmonella* enzymes involved in central carbon metabolism such as glutamino synthetase, malate dehydrogenase and isocitrate lyase are acetylated in response to different carbon sources including citrate, which produces changes in cell growth and metabolic flux.[388] This indicates that acetylation can mediate adaptation to different carbon sources in *S. enterica.*[388]

In addition to stress resistance, RNA degradation and metabolism, acetylation of transcription factors is involved in the regulation of gene expression, as well as in the synthesis of flagellum and capsule in many bacteria including *E. coli* and *S. enterica.*[170,402] For instance, Thao *et al.* investigated the potential bacterial use of lysine acetylation to modulate gene expression.[402] They used proteome microarray technology to screen *E. coli* (4,256 proteins[403]) for substrates of the *S. enterica* protein acetyltransferase (Pat) enzyme, a bacterial GNAT (GCN5-related *N*-acetyltransferases) involved in the post-translational regulation of central metabolic enzymes.[388] The proteome microarray data they obtained suggested that Pat acetylated 4 different bacterial transcription factors (RpsD, McbR, RcsB and RutR).[404] Subsequent work focused on the regulator of capsule synthesis B (RcsB), the response regulator of a complex signal transduction system involved in diverse processes including cell division, and capsule and flagellum synthesis. RcsB can behave as either an activator or repressor in its regulation of target genes, and can bind DNA

either as a homodimer[405] or a heterodimer with accessory cofactor RcsA.[406,407] Research from Thao *et al.* showed how both *E. coli* and Salmonella YfiQ/Pat enzymes modify the bacterial response regulator, RcsB, by acetylation.[404] Together, RcsB/RcsA repress the expression of the flhDC genes,[408] whose products positively regulate flagellum biosynthesis genes.[404]

5.1.3 Lysine acetylation in mycobacteria

Increasing evidence shows that lysine acetylation may play an important role in the pathogenesis of Mtb and immunogenicity.[381] It is known that the Mtb heat-shock protein X (HspX) is associated with latency and known to help mycobacteria maintain long-term survival in the granuloma.[409,410] HspX is acetylated in four lysine sites (K64, K85, K114 and K132). This antigen is highly immunogenic only in its multi-acetylated state,[381] and even though both Mtb and *M. bovis* BCG express functional HspX, it is recognised by the host immune system only if individuals have been previously exposed to Mtb,[411,412] which suggests the possibility that species-specific enzymes/PTMs may play an important role in in modulating host immune responses.

By using proteomics approaches Liu *et al.* have identified acetylation sites of proteins involved in the TCA cycle, glycolysis/gluconeogenesis and fatty acid metabolism.[381] Specifically, they identified a total of 226 unique acetylated peptides from 137 Mtb acetylated proteins out of 4034 proteins of Mtb H37Ra.[381] Among the enzymes shown to be acetylated in the central carbon metabolism pathways, eight are components of the citrate cycle[390] and two enzymes, ICL-1 and malate synthase G (GlcB), are involved in the glyoxylate pathway. Apart from the enzymes in the TCA cycle and the glyoxylate pathway, 25 enzymes out of about 250 enzymes involved in Mtb fatty acid metabolism (β-oxidation of fatty acids and fatty acid biosynthesis) were shown to be acetylated.[381]

Work reported by Singhal *et al*. investigated the prevalence of lysine acetylation in mycobacteria. They applied an exhaustive approach to overexpress Mtb proteins and identify their lysine acetylation status in *M. smegmatis*. 179 protein-coding genes were chosen, with an emphasis on regulatory proteins. 71 mycobacterial proteins were successfully purified (candidate targets) in Mtb. Among the 71, 24 were acetylated proteins. Out of the 24 acetyl proteins, several were found to be unique to this study:[413] protein tyrosine phosphatase B, a secretory phosphatase which regulates host proteins phosphorylation; the transcriptional regulatory protein RegX3; L-lactate dehydrogenase LldD1, involved in respiration; TlyA, a virulence factor; Rv2611c, a probable lysine acyltransferase involved in lipid metabolism; the major secreted immunogenic protein Mpt70, a surface antigen; SpoU, involved in RNA

modification; and the early secretory antigen target EsxA, a surface antigen.[413] The two pathways that represented a majority of the Mtb acetylome were central carbon metabolism, and protein synthesis and modification. Eight acetylated proteins were shown to be involved in central carbon metabolism, with six glycolytic enzymes, one glyoxylate cycle enzyme, and one TCA cycle enzyme (Table 5-1).[414]

Gene name	Protein name	Specific pathway
Rv0467	Icl	Glyoxylate
Rv0694	LldD1	Glycolysis
Rv1240	Mdh	TCA cycle
Rv1436	Gap	Glycolysis
Rv1437	Pgk	Glycolysis
Rv1438	Tpi	Glycolysis
Rv1872c	LldD2	Glycolysis
Rv3248c	SahH	Sulphur metabolism

Table 5-1. List of eight lysine acetylated proteins involved in central carbon metabolism. Proteins involved in intermediary metabolism and respiration. Icl, isocitrate lyase; LldD1, L-lactate dehydrogenase 1; Mdh, malate dehydrogenase; glyceraldehyde 3-phosphate dehydrogenase; Pgk, phosphoglycerate kinase; Tpi, triosephosphate isomerase; LldD2, L-lactate dehydrogenase 2; SahH, S-adenosylhomocysteine hydrolase. Table adapted from Singhal *et al*.[413]

Besides central carbon metabolism, five acetylated proteins were shown to be involved in protein synthesis (Ef-Tu, Ef-Ts, and RpsF), folding, and stability (PpiA and GrpE). The virulence-associated proteins, PknG and PtpB, were also found to be acetylated, connoting an ancillary means for their regulation in addition to phosphorylation. Interestingly, secretory proteins like EsxA, Mpt70, and PpiA were also found to be acetylated.[414] Consistent with Liu *et al.* a majority of modified proteins were found to be associated with metabolism and are cytosolic.[381,414] Furthermore, inhibiting protein acetylation compromises biofilm formation, suggesting that protein acetylation may be involved in Mtb colonisation abilities.[379,381] Thus this study indicated the dynamic and widespread occurrence of lysine acetylation.[413]

5.1.4 Rv0998, a cAMP-dependent lysine acetyltransferase in Mtb

In Mtb H37Rv, *rv0998* encodes a cAMP-dependent lysine acetyltransferase.[194] Rv0998 is encoded as full-length protein in all sequenced mycobacterial species. It shares 56% protein sequence identity with its orthologue in *M. smegmatis*, MSMEG_5458,[391] and both lysine acetyltransferases have been reported to bind to cAMP (Figure 5-2). However, the cAMP affinity of Rv0998, which is 100 µM; is 1000-fold lower than the cAMP affinity of MSMEG_5458, being

100 nM.[415] Nambi *et al.* showed that by mutating Arg95 to lysine in the cAMP-binding domain (CBD) of MSMEG_5458 the cAMP binding was abolished.[194]

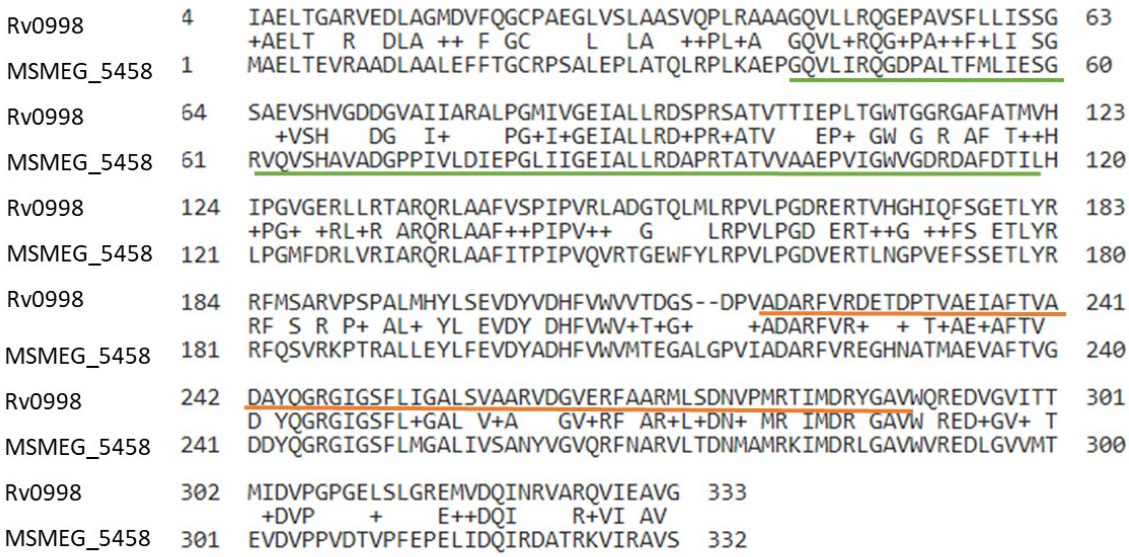


Figure 5-2. Sequence alignment of Rv0998 and its orthologue MSMEG_5458 in *M. smegmatis*. Alignment of the protein sequences of Rv0998 and MSMEG_5458 via Protein BLAST. Green, cNMP binding domain of Rv0998. Orange, acetyltransferase domain of Rv0998.

5.1.4.1 cAMP-induced activation of Rv0998

cAMP binds Rv0998 and induces conformational changes activating its function.[201] Structural and biochemical analyses confirm that there are two different functional states of Rv0998. Changes in its structure are needed for cAMP binding as well as exposure of the catalytic site. In the auto-inhibited state of Rv0998, the cAMP-binding site is blocked by the C-terminal helix from the catalytic domain. Furthermore, the lid in the catalytic domain, which mimics the substrate, buries the acetyl donor and a conserved surface that forms the protein-substrate binding site. The presence of cAMP stabilises the rotation of the regulatory domain and tertiary shifts that are incompatible with the closed lid while excluding the C-terminus.[416] These shifts release the steric double latch created by the lid and the C-terminal extension of the catalytic domain. The lid rearranges in the active state, creating a large binding surface for protein substrates (Figure 5-3).[416]

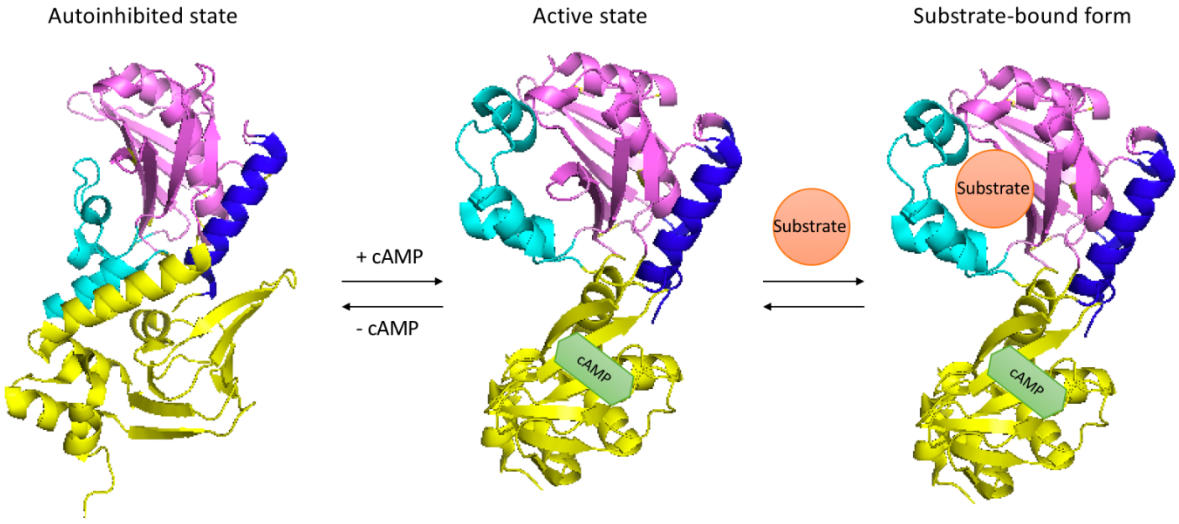


Figure 5-3. Scheme showing the autoinhibition and cAMP-induced conformational changes of Rv0998.
The N-terminal cAMP-binding domain, the GNAT catalytic domain, the lid and the C-terminal helix are shown in yellow, magenta, cyan and blue respectively. In the absence of cAMP, Rv0998 is in an auto-inhibited state. When cAMP binds, Rv0998 encounters a conformational change which allows a binding pocket to be formed. This accommodates the substrate, which will be acetylated. Figure adapted from Lee *et al.*[416]

Different substrates of Rv0998 have been identified and they will be covered in the next section. These include Acetyl-CoA synthetase, fatty acyl-CoA synthetases, FadD33 and the dormancy survival regulator DosR.[391,417,418]

5.1.4.2 Acetyl-CoA synthetase, an Rv0998 substrate

ACS has been identified as a physiologically relevant substrate for Rv0998 and MSMEG_5458 in Mtb and *M. smegmatis* respectively.[391] ACS converts acetate into acetyl-CoA, which is oxidised in the TCA cycle producing energy.[194,419,391] cAMP binding to the acetyltransferase protein is instrumental for acetylation. Acetylation of ACS at Lys167 leads to enzyme inactivation. Rv1151c is the eukaryotic sirtuin homologue (30% identity) which is a NAD^+-dependent deacetylase. During Mtb infection, environmental signals induce ACs, which increase intra-macrophage levels of cAMP. cAMP together with acetyl-CoA and NAD^+ regulate the reversible acetylation. Thus, environmental changes modify metabolic pathways and the synthesis of acetyl-CoA by ACS.[193,391]

5.1.4.3 FadDs, an Rv0998 substrate

Propionyl-CoA toxicity caused by the degradation of cholesterol and odd-chain fatty acids can be alleviated by Rv0998, which uses propionlyl-CoA to propionylate eight fatty acyl-CoA synthetases (FadDs) encoded in the mycobacterial genome, at the acetylable lysine residue.

These FadDs are involved in fatty acid and cholesterol catabolism. Moreover, they have been seen to be acetylated by Rv0998 *in vitro* in a cAMP-dependent manner which leads to the inhibition of their activity and which shows the association of cAMP signalling with mycobacterial fatty acid metabolism.[193] The eight FadDs present in Mtb are FadD31 (Rv1925), FadD22 (Rv2948c), FadD13 (Rv3089), FadD12 (Rv1427c), FadD10 (Rv0099), FadD5 (Rv0166), FadD3 (Rv3561), and FadD2 (Rv0270). Their acetylated lysine residue is the equivalent to Lys487 in the active site of FadD13.[193] In the C-terminal domain of acetylated FadDs there are conserved motifs ($GGXNX_4EXE/D$, $E/DX_7E/D$, K/AXP, and PX_4GK). However, non-acetylated FadDs presented conservation in some, but not all, of these motifs together. This suggests the influence of conserved residues set in the C-terminal domain of FadDs rather than only residues in the immediate proximity of the acetylate lysine residue, which determine substrate specificity.[193] Moreover, work from Samanta *et al*. using *M. bovis* BCG has shown that lysine acetylation in FadD22 inhibits its activity and consequently reduces PGL biosynthesis, which is known to contribute significantly to the virulence of Mtb.[46] Levels of intracellular cAMP could indeed determine the extent of FadD22 acylation in the cell, thereby determining production of PGLs via the activation of *p*-hydroxybenzoic acid *(p*-HBA).[46] Thus, a fast increase of the levels of cAMP upon macrophage phagocytosis could reduce PGL synthesis for utilisation of lipids for survival.[193]

Another FadD, which has been seen to be a substrate of Rv0998 is FadD33, a fatty acyl-AMP ligase (MbtM). FadD33, MbtK (mycobactin synthetase protein K) and MbtA (a salicyl-AMP ligase) are critical enzymes in the biosynthesis of mycobactin (MBT) (Figure 5-4). MBT and carboxymycobactin (cMBT) are two aryl-capped siderophores synthesised by Mtb which are able to chelate intracellular iron. Iron is an essential element for Mtb growth and virulence following infection.[420] Nevertheless, the host restricts the availability of free iron within the host cell by serum transferrin protein to avoid bacterial colonisation.[420] To circumvent this burden, mycobacteria can acquire and accumulate intracellular iron in conditions where the levels of iron are limited by synthesising cMBT and MBT. Mycobacterial MBT production is strongly controlled at the transcriptional level by IdeR and HupB (iron-dependent transcriptional regulators), to prevent toxicity as a result of excess iron acquisition.[420] MbtA and FadD33 both catalyse an adenylation reaction followed by thioesterification of the substrate onto an acyl carrier protein (ACP). Furthermore, they are reversibly acetylated in a cAMP-dependent manner by protein acetyltransferases leading to fast inactivation of enzyme activities.[418,420] When levels of cAMP are high, Lys511 and Lys546, in FadD33 and MbtA respectively, are acetylated resulting in decreased production of MBT.[418,420]

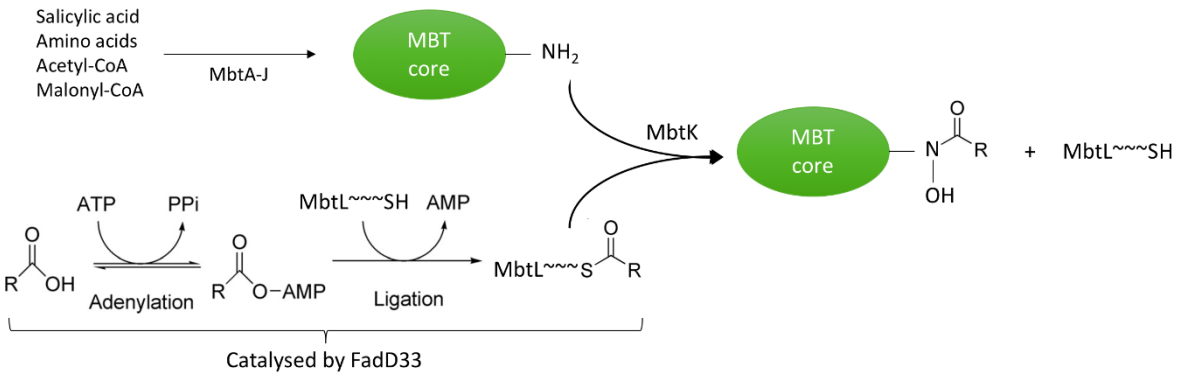


Figure 5-4. Mycobactin (MBT) synthesis.
The MBT core is first synthesised by MbtA to J which belongs to the *mbt-1* gene cluster. The fatty acyl-AMP ligase FadD33 then adenylates and loads a fatty acid chain on to a phosphopantetheinylated carrier protein to form an acylated MbtL. Finally, the lipophilic acyl chain is transferred onto the epsilon-amino group of the lysine of MBT core by MbtK. Figure adapted from Vergnolle *et al*.[418]

5.1.4.5 Transcription factor DosR, an Rv0998 substrate

The DosR regulon is a set of at least 48 coregulated genes that are induced by NO, carbon monoxide (CO) and hypoxia, three conditions that inhibit aerobic respiration.[421] The DosR regulon is controlled by a three-component regulatory system composed of two sensor histidine kinases, DosS and DosT, and a response regulator, DosR.[421] DosS and DosT both bind the respiration-impairing gases NO and CO,[422] further demonstrating that the DosR regulon responds to, and is important during, conditions that do not allow aerobic respiration.[421] DosR regulated genes can be acetylated by Rv0998 when the oxygen concentration within the macrophage is limited.[417] Yang *et al.* have shown that Rv0998 is able to acetylate Lys182 of DosR *in vitro*. Nevertheless, under hypoxic stress, there is a decrease in Lys182 acetylation.[417] This was seen by using an anti-DosR Ac-K182-specific polyclonal antibody. This increase in lysine deacetylation is critical for binding of DosR to target DNA to promote transcription of its regulon.[417] Furthermore, the strain K182R had a significant growth impairment under hypoxia even though its aerobic growth did not change. This demonstrates that lysine deacetylation directly promotes transcription of DosR regulon for fast Mtb adaption in response to hypoxia.[417] Recent work by Rittershaus *et al*., has demonstrated that the immediate response to hypoxia involves the rapid and transient induction of the DosR regulon and triglyceride synthesis. This is important for the initial growth arrest of the bacterium[423,424] and is expected to regenerate $NAD(P)^+$ through lipid anabolism. Subsequent to the transient induction of the DosR regulon, the adaptation to hypoxia relies on Rv0998.[425,426]

5.1.5 Impact of Rv0998 in mycobacterial physiology

5.1.5.1 Cholesterol acquisition

As has already been mentioned in this chapter, mycobacteria use cholesterol as a main carbon source from the host cell.[134] Cholesterol is a major component in the structure of host cell membranes and it is considered to participate in Mtb infection development.[427] The ortholog of *rv0998* in *M. bovis* BCG (BCG_1055) has been shown to be involved in propionate acquisition, the end product of cholesterol degradation.[193] This has been demonstrated by the growth impairment of a mutant strain lacking *rv0998* compared to the wild type in *M. bovis* BCG when using propionate as the sole carbon source.[193] The promiscuity of Rv0998 in utilising acetyl or propionyl groups for acylation makes it particularly suited to be enlisted in homeostatic responses to counter environmental or nutritional conditions that lead to elevated levels of propionyl-CoA. This acylation appears obligatory for the alleviation of the toxicity of propionyl-CoA metabolites by acting as a feedback loop for regulating propionyl-CoA levels in the cell, thereby accounting for the poor growth of the *M. bovis* BCG mutant strain lacking BCG_1055.[193]

5.1.5.2 Survival in acidic pH

Acidic pH is one of several environmental signals that may be sensed and responded to by Mtb inside its host.[343] It has been suggested that phagosome acidity synergises with and supports other antibacterial mechanisms of phagocytes. These include acid-dependent lysosomal hydrolases, reactive oxygen intermediates and reactive nitrogen intermediates.[428,429] The ability to sense environmental pH and other signals that likewise flux during phagosomal maturation, could play a role in determining Mtb's location in the cell. Any particle which enters a macrophage can activate specific anti-microbial responses such as remodelling the phagosome with subsequent fusion to lysosomes.[343,94,430] Phagosome acidification is a prerequisite to optimal hydrolytic enzyme function and phagosomal content degradation (Figure 5-5). This process takes place early in phagosome maturation predominantly as a direct result of the recruitment of vacuolar proton-ATPase (V-ATPase) to the phagosomal membrane.[94] The blockage in phagosome maturation depends on if the host macrophage is activated or not.[137,431,432] Activation of the cell with cytokines such as IFN-γ leads to a partial reversal of this blockage and the delivery of the bacterium into a compartment with a pH of approximately pH 4.5-5.5.[433,434] Although Mtb is capable of surviving acidic environments transiently, its growth is slowed down below pH 6.4 and undergoes growth arrest at a pH lower than 5.[435] Thus, an activated macrophage represents a hostile environment that is capable of restricting bacterial survival.[343]

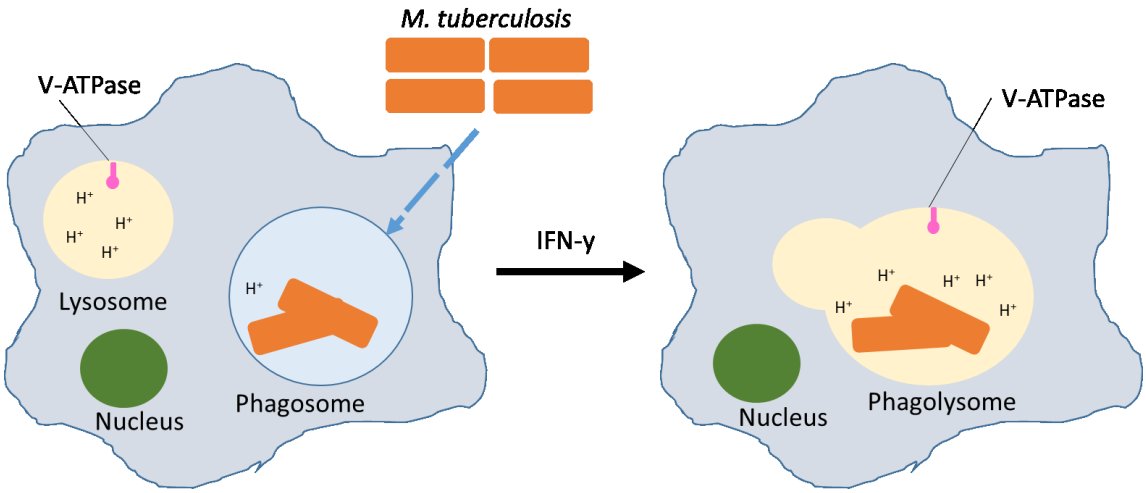


Figure 5-5. Mtb inside the macrophage.
In resting macrophages, Mtb impairs phagosome maturation and resides in a mildly acidic compartment. Activation with IFN-γ results in phagosome maturation and phagosome-lysosome fusion. This exposes the bacteria to host-derived stress including protons from the vacuolar ATPase, reactive nitrogen intermediates (RNI) and ROI, free fatty acids, ubiquitin-derived peptides, and lysosomal hydrolases. Mtb can resist acidification through different mechanisms. Figure adapted from Vandal *et al*.[429]

Studies performed by Vergnolle *et al.* used Sauton medium at pH 6 as a readout of Mtb physiology within the host. As mentioned earlier, they probed MbtA, an enzyme involved in the siderophores mycobactin biosynthesis, as a potential substrate for Rv0998 and showed that MbtA is acetylated by Rv0998 in the presence of acetyl-CoA and cAMP. To investigate the effect of *rv0998* deletion they tested the wild type, the mutant lacking *rv0998*, and the complemented strains under pH 6.[148] Low pH was chosen as it is a physiological condition at which specific ACs such as Rv1264[167,436] induce cAMP production.[420] Vergnolle *et al.* performed growth curves in Sauton medium at pH 7 (Figure 5-6 A). In contrast, when bacteria were grown in Sauton medium at pH 6, Mtb *Δrv0998* showed a gain in fitness compared with the parental and complemented strains (Figure 5-6 B). These results indicate that deletion of *rv0998* leads to an increased growth and suggests that lack of acetylation of Rv0998 substrates at pH 6 is beneficial for Mtb.[149] Moreover, their results demonstrate that deletion of *rv0998* might prevent the acetylation of FadD33 and MbtA, thus inhibiting their function, which is mycobactin production and reduction of intracellular iron.[420]

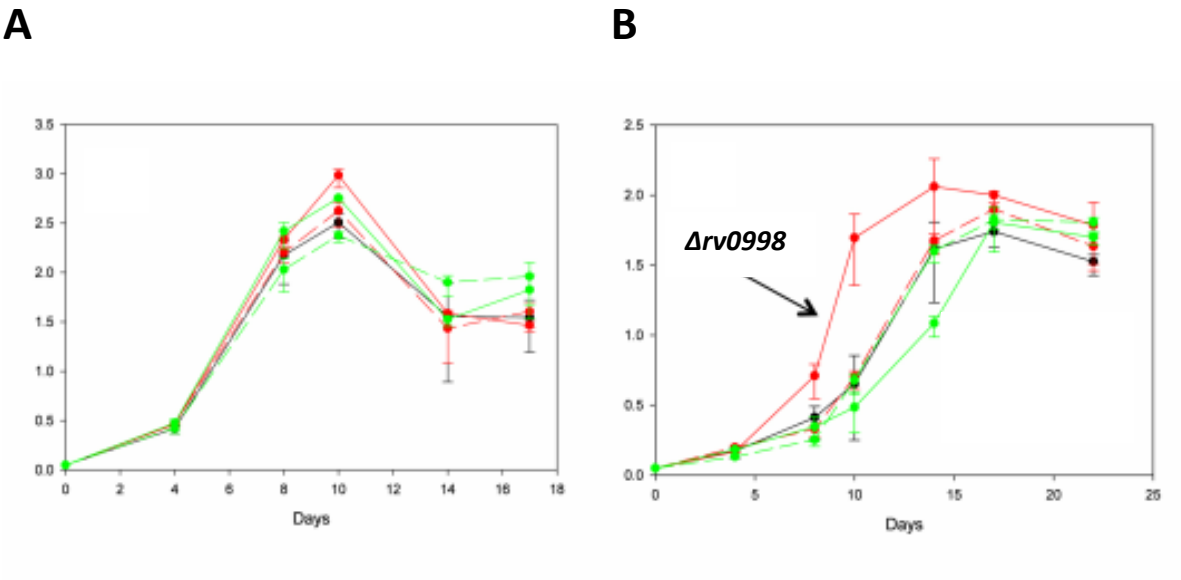


Figure 5-6. Mtb *Δrv0998* grows better than the Mtb wild type strain at low pH in Sauton medium.
Two growth conditions are presented: Sauton pH 7 medium (A); Sauton pH 6 medium (B). Black, Mtb wild type; solid red, Mtb *Δrv0998*; dotted red, Mtb ΔDAc (deacetylase); solid green, Mtb complemented *rv0998;* and dotted green, Mtb complemented DAc. Error bars represent standard deviations from the mean of results from biological duplicates. Mtb wild type corresponds to mc^{2}6206. Figure adapted from Vergnolle *et al*.[420]

The culture medium used by Vergnolle *et al.* in their experiments was Sauton.[420] This medium differs considerably from Middlebrook 7H9 broth, which is routinely used for mycobacterial growth (Table 5-2). 7H9 medium is supplemented with 0.5 g/L Fraction V bovine serum albumin, 0.05% tyloxapol, 0.2% dextrose and 10 mM NaCl. One main difference between both culture media is the carbon source as Sauton contains 6% of glycerol. Of note is that glycerol is not a carbon source either readily available or primarily used by Mtb in mouse lungs.[437] Another key difference between both culture media is the absence of albumin in Sauton medium. When culturing Mtb *in vitro*, it has been demonstrated that the addition of albumin is required for Mtb growth in medium containing Tween 80, a non-ionic detergent used to avoid bacteria clumping[438]. Lynn *et al*. have demonstrated that albumin promotes Mtb growth by binding to unesterified fatty acids otherwise toxic for the mycobacterium[439]. Albumin binds with the carboxyl group of fatty acids increasing their solubility in aqueous solutions.[438,440] Furthermore, when fatty acids are detoxified, they can be used by Mtb.[438]

Sauton	7H9
0.2% citric acid	0.5 g/L ammonium sulfate
0.05% dipotassium hydrogen	2.5 g/L disodium phosphate
0.04% L-asparagine	1 g/L monopotassium phosphate
0.2% dextrose	0.1 g/L sodium citrate
6% glycerol	0.05 g/L magnesium sulfate
0.025% tyloxapol	0.0005 g/L calcium chloride
50 µg/mL pantothenate	0.001 zinc sulfate
50 µg/mL leucine	0.001 copper sulfate
1 mg/mL zinc sulfate	0.04 g/L ferric ammonium citrate
0.5 g/L magnesium sulfate	0.5 g/L L-glutamic acid
16.2 mg/L ferric chloride	0.001 g/L pyridoxine
-	0.0005 g/L biotin
-	0.2% dextrose
-	0.5 g/L bovine serum albumin
-	0.08% sodium chloride
-	0.05% tyloxapol

Table 5-2. Components of both Middlebrook 7H9 culture medium and Sauton culture medium.

Despite being one of the most abundant proteins in human serum, no studies have investigated the role of albumin in Mtb physiology. So far the only reported study is on the effects of albumin on cAMP production and secretion. Bai *et al.* noticed that the levels of cAMP change according to the culture media used to grow bacteria.[441] Thus, they hypothesised that specific components in the medium could affect the production and/or secretion of cAMP. cAMP levels were measured in Mtb grown on different media conditions in order to determine the components that affect the production and/or secretion of cAMP by mycobacteria.[441] The culture media compared were Sauton and 7H9. Bai *et al.* showed that an addition of 0.5% albumin (the concentration found in supplemented 7H9) to Sauton medium significantly reduced the overall levels of cAMP (including secreted and bacterial cAMP) in *M bovis* BCG. Therefore the effect of albumin on cAMP production could be involved in mycobacterial physiology during infection. Mtb is exposed to different serum albumin levels depending on its location within the host.[441] There is 3.5% to 5.5% albumin in human serum.[180] Albumin levels are significantly lower in extravascular compartments, where they are affected by the nutritional status of the host and by the proximity of venules.[182] Thus, changing albumin levels could signal Mtb's transition to different host environments.[180] Bai *et al*. showed that by adding oleic acid, the levels of cAMP were restored to levels of albumin-free medium grown bacteria. However, in the presence of oleic acid, the intracellular cAMP pool did not increase since it was secreted into the medium. This evidence suggests that the regulation of cAMP production and secretion are independent

of each other.[180] As reported by Vergolle *et al.*, the lack of lysine acetylation by Mtb *Δrv0998* is proving to be beneficial for Mtb growth at low pH in the absence of albumin. Thus in this chapter I aimed to investigate the role of albumin in Mtb physiology and the impact of its presence in the role of Rv0998.

5.2 Results

5.2.1 Albumin alters Mtb physiology

5.2.1.1 Presence or absence of BSA alters Mtb growth

The wild type strain of Mtb CDC1551 was grown at pH 6.8 since it is a pH observed to be optimal for Mtb growth in enriched medium such as Midlebrook 7H9 broth.[429] Dextrose was used as the only carbon source. The culture medium contained bovine serum albumin (BSA), which is commonly added in order to grow mycobacteria as mentioned in the introduction of this chapter. Here, the growth of Mtb with BSA was compared to the growth of the same strain in culture medium without BSA. As expected, the presence of BSA increased Mtb growth in comparison to the wild type strain grown in the absence of BSA (Figure 5-7 A).

Furthermore, the wild type strain of Mtb was grown at pH of 5.5, the pH found within alveolar macrophages. Since macrophages do not present albumin, the growth of the wild type strain of Mtb was monitored at pH 5.5 in the presence and absence of BSA. In this case, the growth at acidic pH in the presence and absence of BSA proved to be slower compared to pH 6.8. Nevertheless, the absence of BSA at pH 5.5 decreased Mtb growth 5-fold compared to the growth in the presence of BSA (Figure 5-7 B).

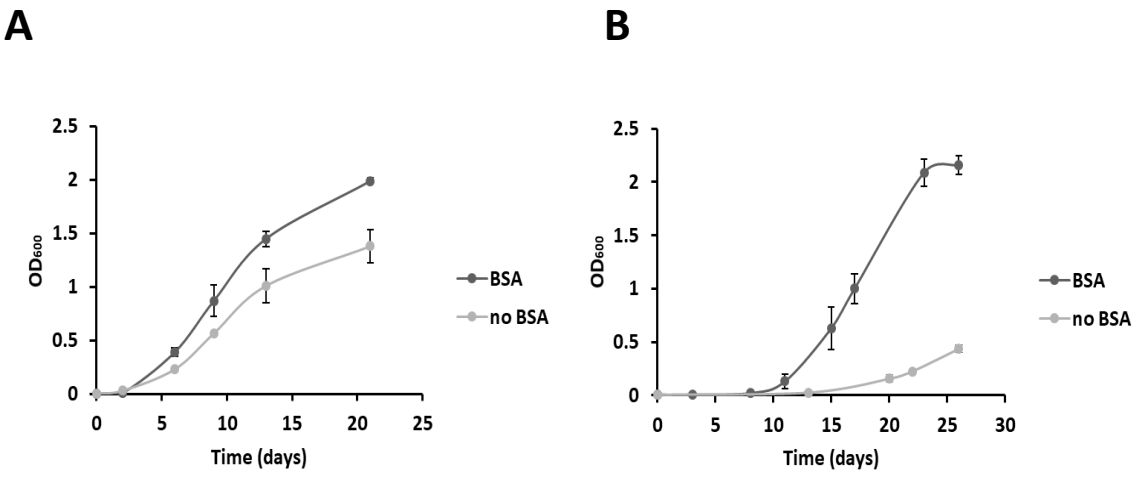


Figure 5-7. The presence of albumin alters the growth of the wild type strain of Mtb.
The wild type strain of Mtb CDC1551 was grown in 7H9 liquid medium with dextrose as sole carbon source in the presence or absence of BSA at pH 6.8 (A), and pH 5.5 (B). OD_{600} was measured regularly. Error bars denote standard deviation. This figure represents one biological replicate of three.

5.2.1.2 Presence or absence of BSA alters intracellular levels of cAMP

Previous work has shown that the presence of albumin decreases the overall amount of Mtb cAMP levels.[441] To confirm this in our experimental settings, intracellular levels of cAMP were measured by targeted metabolomics in Mtb CDC1551 strain grown in the presence and absence of BSA (0.5 g/L) in 7H9 at pH 6.8 (Figure 5-8 A). As shown on Figure 5-8 A, the intracellular levels of cAMP in Mtb grown in the absence of BSA were 4-fold higher than the intracellular cAMP levels when Mtb was grown in the presence of BSA. A similar observation is noticed at pH 5.5 where the levels of cAMP are 2.25-fold higher in the absence of BSA. This demonstrates that the presence or absence of BSA modulates the Mtb intracellular cAMP levels (Figure 5-8 B). Furthermore, cAMP levels had a 1.5-fold increase in the wild type strain exposed to pH 5.5 in comparison to pH 6.8, both in the presence of BSA.

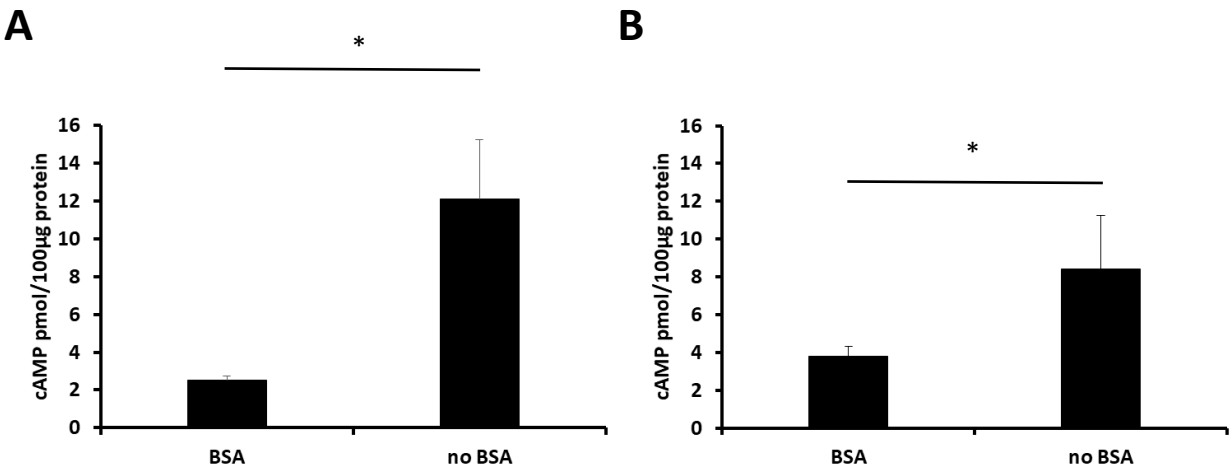


Figure 5-8. Intracellular levels of cAMP of Mtb wild type grown in culture medium with or without BSA.
Intracellular levels of cAMP were measured by targeted metabolomics after being exposed for one doubling time to pH 6.8 in the presence or absence of BSA (A), or pH 5.5 in the presence or absence of BSA (B). cAMP levels were normalised by the amount of protein using a BCA assay. Error bars denote standard deviation. This figure represents one biological replicate of two. *p < 0.05 as analysed by Student's *t*-test.

5.2.1.3 BSA leads to a global metabolome remodelling

To determine if the presence of albumin alters the metabolome of Mtb, untargeted metabolomics in the positive and negative ion mode were performed. Metabolites were extracted as mentioned earlier (in detail in Chapter 2: Materials and methods). Figure 5-9

summarises how untargeted metabolomics were analysed using Profinder B.08.00 and Mass Profiler Professional (Agilent®).

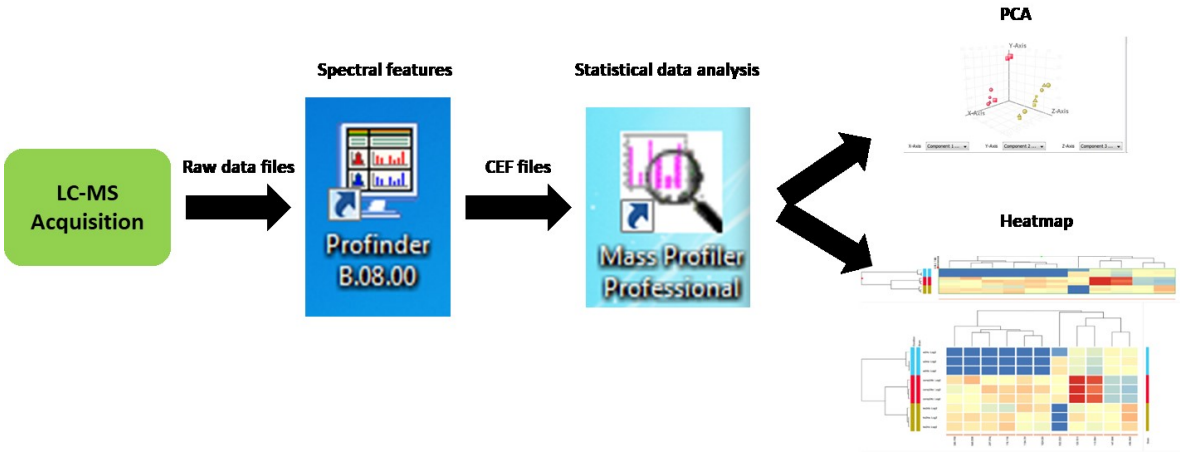


Figure 5-9. Simplified scheme showing steps and MassHunter tools used in untargeted metabolomics data analysis.
Mass Profinder was used to find features and extract these spectral features from the data files. After generating an extracted ion chromatogram (EIC) and extracting compound chromatograms (ECC) for each feature in each data file, chromatographic integration can be reviewed and the extracted features are exported to compound exchange format (CEF). CEF files are imported to MassHunter Mass Profiler Professional for statistical analysis. Mass profiler professional helps review features, compare them between two samples or sample groups, perform principal component analysis (PCA) with the samples organised into two groups or heatmaps among other options. A PCA is a statistical tool that employs a mathematical process by which the features found within the data are transformed into a new set of data in relation to variables called principal components. Each principle component is optimised to account for the maximum variability in the features among the samples in the project. Each principal component is labelled with a number corresponding to the components share of the PCA variance. The lower the number of principal components accounted for, the more variance in the sample difference.[442] Figure adapted from the MassHunter Mass Profiler Software familiarisation guide.[443]

Intracellular changing metabolites (features) between Mtb grown at pH 6.8 in the presence or absence of BSA can be seen in Table 5-3, demonstrating that Mtb intracellular metabolites change when the bacillum is grown in the presence or absence of BSA at pH 6.8 both in positive and negative ion mode. Mtb was also stressed for one doubling time at pH 5.5 in the presence or absence of BSA. Changing features in positive and negative ion mode between Mtb grown in the presence or absence of BSA stressed at pH 5.5 can be seen in Table 5-3.

To investigate if there are changing features between Mtb wild type grown at pH 6.8 or 5.5, untargeted metabolomics were performed and the results are presented in Table 5-3. The results show changes in the features in positive and negative ion mode by comparing the metabolites at pH 5.5 and 6.8 in Mtb grown in the presence of BSA (Table 5-3). Regarding

differences between pH 6.8 and 5.5 in Mtb grown in the absence of BSA, these were only seen in the positive ion mode (Table 5-3). However, no significant changes over 2-fold were found in the negative ion mode.

		Positive ion mode				Negative ion mode			
Condition		**Total features**	**FC (abs)>2**	**Up-regulated**	**Down-regulated**	**Total features**	**FC (abs)>2**	**Up-regulated**	**Down-regulated**
BSA vs no BSA	**pH 6.8**	2012	1437	1168	269	1113	1024	745	279
	pH 5.5	312	302	79	223	551	501	197	304
pH 6.8 vs pH 5.5	**BSA**	1989	1484	83	1401	384	76	26	50
	No BSA	93	4	4	0	245	0	0	0

Table 5-3. Table showing changing features greater than 2-fold between Mtb wild type strain grown at different conditions.
The features were detected using Profinder B.08.00 sp3 Batch Recursive feature extraction. The total number of changing features > 2-fold in positive and negative ion mode of Mtb wild type grown in different conditions are shown. Additionally, the number of features being up or down-regulated > 2-fold are shown. This is the representation of three technical replicates from one of two biological replicates.

Altogether, these results show that the presence of BSA causes significant changes in the metabolites in unchallenged (pH 6.8) as well as challenged bacteria at pH 5.5. This suggests changes in metabolism which could be involved in the differences in growth between Mtb grown in the presence or absence of BSA. Furthermore, these results show significant changing metabolites when Mtb is grown in the presence of BSA challenged at an acidic pH. This suggests a potential metabolome remodelling in order to adapt to the stressful conditions of acidic pH. Finally, the fact that when Mtb is grown in the absence of BSA there are only 4 changing features in positive ion mode and none in negative ion mode between bacteria challenged and unchallenged suggests that bacterial adaptations to these growth condition might not depend on metabolic changes.

5.2.2 Effect of albumin in the physiology of a cAMP dependent lysine acetyltransferase mutant.

5.2.2.1 The presence of BSA in culture medium affects growth of Mtb Δrv0998

As has been shown previously, the presence or absence of BSA in the culture medium of Mtb alters the intracellular levels of cAMP (Figure 5-8) at pH 6.8 and pH 5.5. Based on this observation and the work from Vergnolle *et al*., I hypothesised that the cAMP dependent lysine acetyltransferase Rv0998 might play a role in the changes in Mtb physiology at pH 6.8 and pH 5.5 in the presence or absence of BSA. Thus, the growth of the Mtb wild type, the mutant strain lacking *rv0998* (*Δrv0998)* and complemented strains were monitored at pH 6.8 and pH 5.5 in the presence or absence of 0.05% BSA. As can be seen in Figure 5-10, when the three strains were grown at pH of 6.8 no differences between them were seen when grown in the absence of BSA (Figure 5-10 A) and the presence of BSA (Figure 5-10 B). However, when the three strains of Mtb were grown at pH 5.5 in the absence of BSA, the mutant lacking *rv0998* had an increased growth compared to the parental strains (Figure 5-10 C). A different phenotype was seen in the presence of BSA as the mutant strain had an impairment in growth in comparison to the parental and complemented strains (Figure 5-10 D). These results confirm what Vergnolle *et al*. observed, an increased growth by the mutant strain compared to the parental strains when grown in Sauton medium at pH 6.[420] The combination of both results demonstrates that only BSA and pH affect the growth of Mtb and not the carbon source as Sauton contains 6% glycerol and 7H9 presented 0.2% dextrose as the sole carbon source.

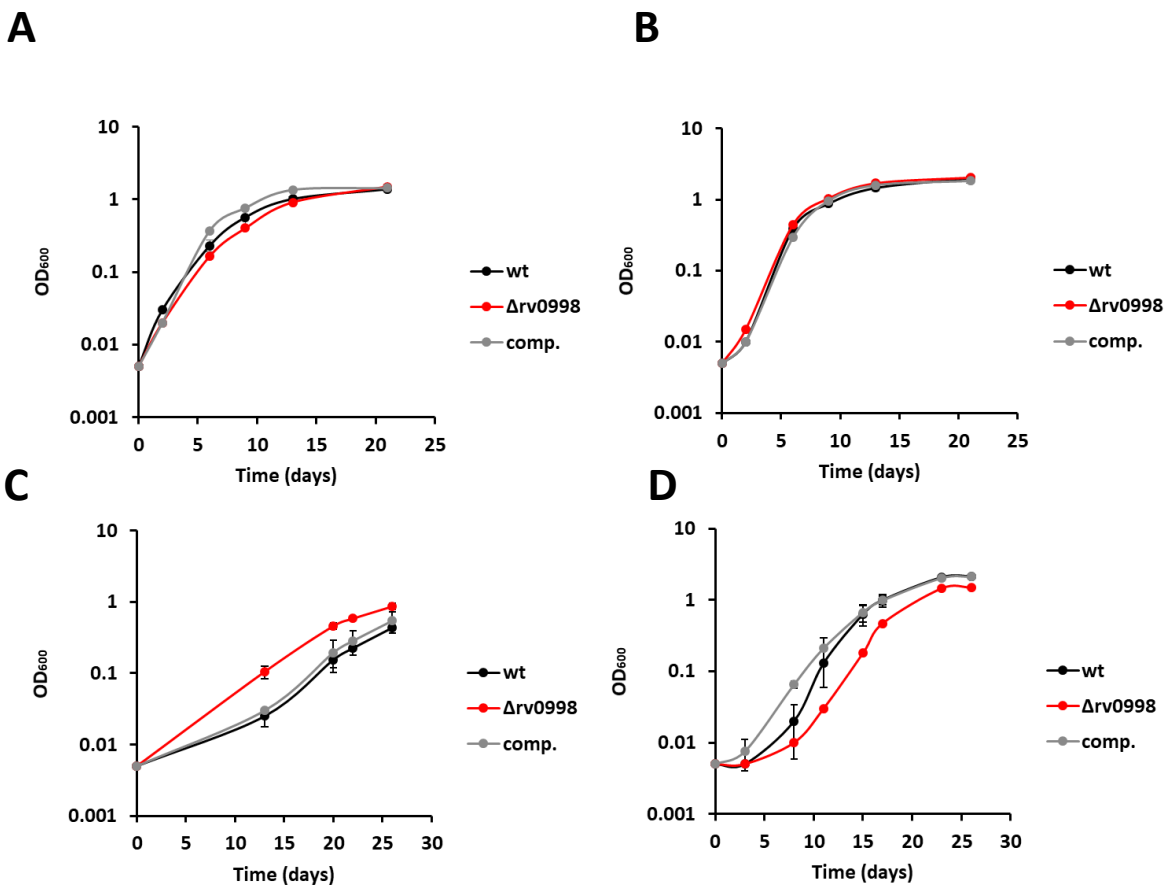


Figure 5-10. Presence or absence of albumin determines the growth at pH 5.5 of *Δrv0998*. The wild type (wt), mutant lacking *rv0998* (*Δrv0998*) and the complemented (comp.) strains of Mtb CDC 1551, were grown in 7H9 liquid medium with dextrose as the sole carbon source at pH 6.8 lacking BSA (A), at pH 6.8 with BSA (B), at pH 5.5 lacking BSA (C) and at pH 5.5 with BSA (D). OD_{600} was measured regularly. The y-axis is expressed as logarithmic scale in this figure. Error bars denote standard deviation. This figure represents one biological replicate of three.

5.2.2.2 The presence of BSA in culture medium affects cAMP intracellular levels in Mtb

Targeted metabolomics were performed to determine the intracellular levels of cAMP within the Mtb wild type, within Δ*rv0998,* and within the complemented strains, after being exposed to pH of 6.8 or 5.5 for one doubling time in the presence or absence of BSA. Intracellular levels of cAMP increased 6-, 4.5- and 2-fold in the Mtb wild type, *Δrv0998* and complemented strain respectively when grown at pH 6.8 in the absence of BSA compared to when BSA was present in the culture medium (Figure 5-11). A similar trend was seen at pH of 5.5 as intracellular cAMP levels increased 2-, 3.5-, and 1.6-fold in the Mtb wild type, *Δrv0998* and complemented strain respectively when grown in the absence of BSA in comparison to when grown in the presence of BSA (Figure 5-11). No changes in the levels of cAMP were seen between pH 6.8 and 5.5 in the

presence or absence of BSA (Figure 5-11). When grown in the presence of BSA, intracellular levels of cAMP in the wild type were 2.1-fold higher than in Mtb *Δrv0998* when exposed to pH 6.8. When exposed to pH of 5.5 the intracellular levels of cAMP of the wild type were 2-fold higher compared to Mtb *Δrv0998* (Figure 5-11 A).

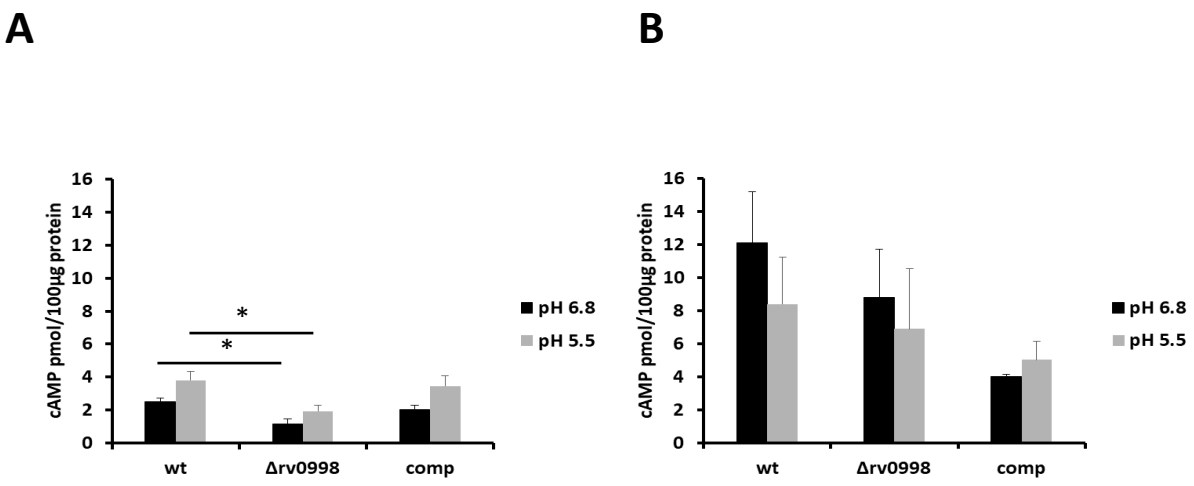


Figure 5-11. Intracellular levels of cAMP of Mtb wild type, *Δrv0998* and complemented grown in culture medium with or without BSA.
Intracellular levels of cAMP were measured by targeted metabolomics when bacteria were in the presence of BSA at pH 6.8 and 5.5 (A) and in the absence of BSA at pH 6.8 and 5.5 (B). cAMP levels were normalised by the amount of protein using a BCA assay. Error bars denote standard deviation. This figure represents one biological replicate out of two. *p < 0.05 as analysed by Student's *t*-test.

5.2.2.3 Impact of Rv0998 on Mtb viability under stress at low pH

To evaluate if Rv0998 has an impact on the viability of Mtb under stress at low pH, Mtb wild type, *Δrv0998* and complemented strains were grown until exponential phase at pH 6.8 on dextrose as a carbon source and in the presence of BSA, as preliminary experiments. Next, bacteria were exposed for a period of 48 hours (two doubling times) to the same pH, or pH 5.5, and bacterial viability was measured by monitoring colony forming units per millilitre (CFU/mL). By growing in the presence of BSA I would have expected less growth in the mutant strain lacking *rv0998* in comparison to the parental and complemented strains following what I have observed in the growth curves. However, no statistically significant differences were seen when bacteria were exposed for 48 hours at pH of 6.8 or 5.5 (Figure 5-12). A possible explanation is that the first 48-hour period is a shock for the bacteria and they do not have the chance to adapt. This experiment will need to be performed in future in the absence of BSA, where an increase in growth by the mutant strain lacking *rv0998* would be expected following 48 hours' stress at pH 5.5.

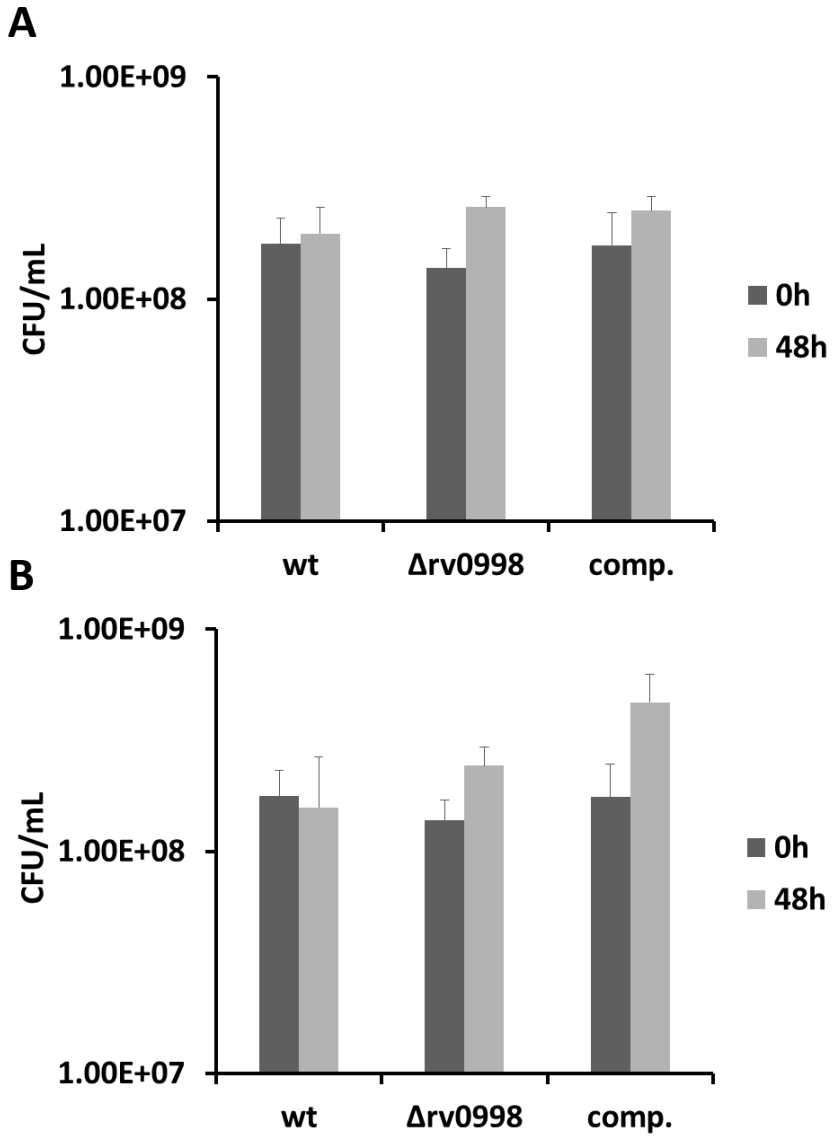


Figure 5-12. Measurement of viable Mtb wild type (wt), mutant lacking *rv0998* (*Δrv0998*) and complemented (comp.) strains after exposing them for 48 hours to pH 6.8 or 5.5.
CFU/mL of Mtb wt, *Δrv0998* and comp. strains stressed for two doubling times at pH 6.8 (A). CFU/mL of Mtb wt, *Δrv0998* and comp. strains stressed for two doubling times at pH 5.5 (B)**.** The y-axis is expressed as logarithmic scale in this figure. Error bars denote standard deviation. This figure represents one biological replicate of two.

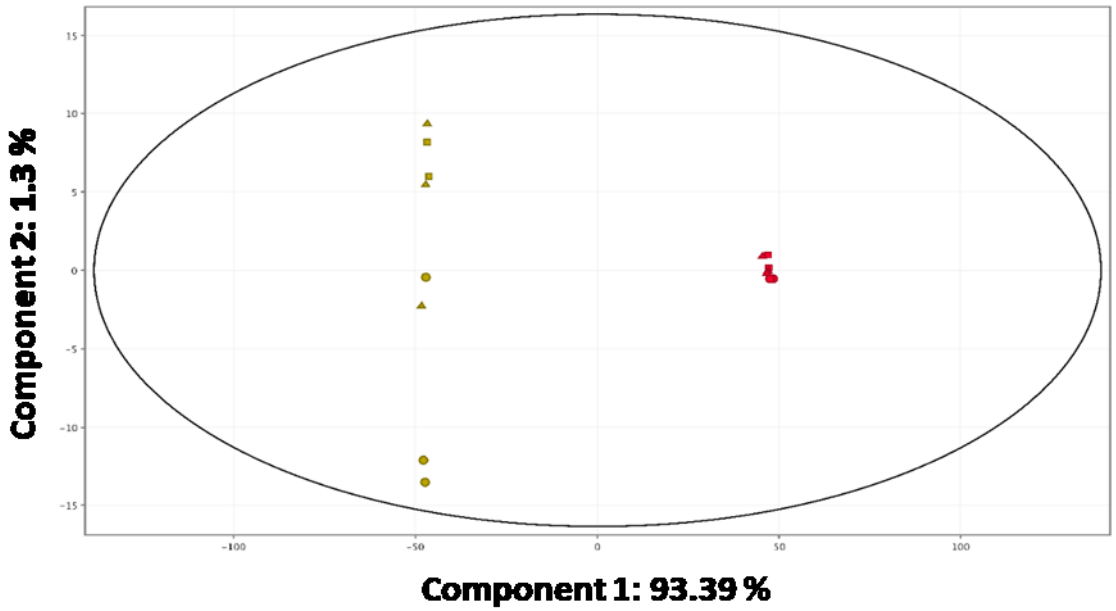
5.2.2.4 Global metabolomics profiling of Mtb wild type, Δrv0998 and complemented strains in the presence and absence of BSA

To further understand if there are any changes in other intracellular metabolites of the wild type, *Δrv0998* and complemented strain of Mtb when grown in the presence or absence of BSA; untargeted metabolomics were performed. Changing features are observed in positive and

negative ion mode when strains were grown in the presence of BSA compared to when grown in the absence of BSA (Figure 5-13). These changes in intracellular metabolites were seen in both cases, *i.e.* when Mtb was exposed to pH of 6.8 (Figure 5-13 A and B) and when it was exposed to pH 5.5 (Figure 5-13 C and D) for one doubling time. Furthermore, changing metabolites were seen by comparing Mtb exposed to pH 6.8 in comparison to being exposed to pH 5.5, both in the presence of BSA (Figure 5-14). However no changing features were observed by comparing Mtb exposed to pH 6.8 in comparison to being exposed to pH 5.5, both in the absence of BSA in positive and negative ion mode.

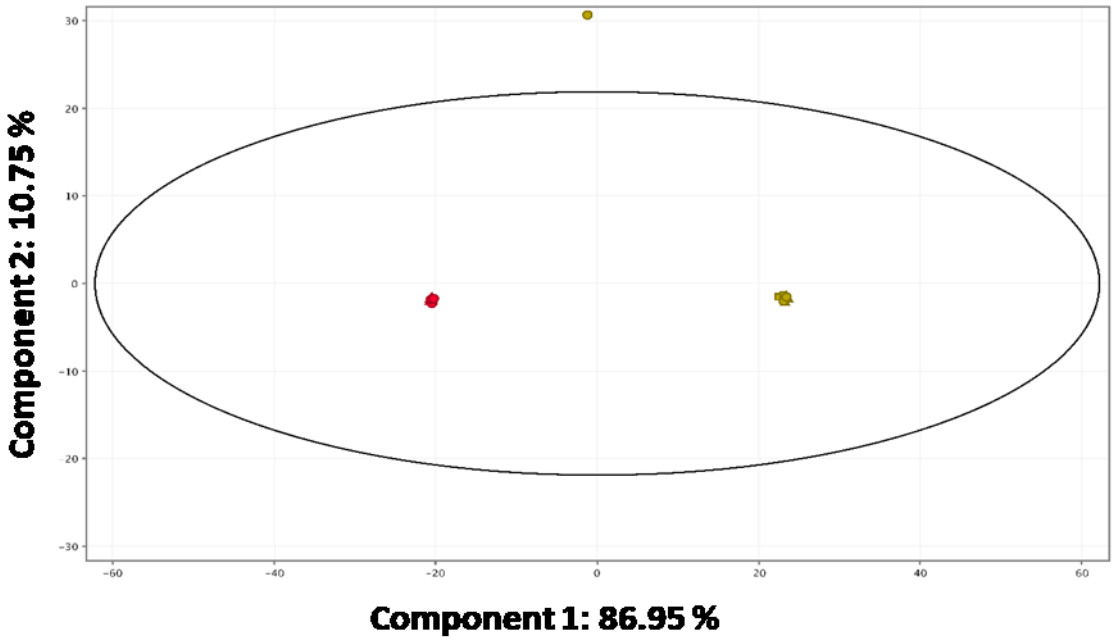
A

Positive ion mode of Mtb grown at pH 6.8



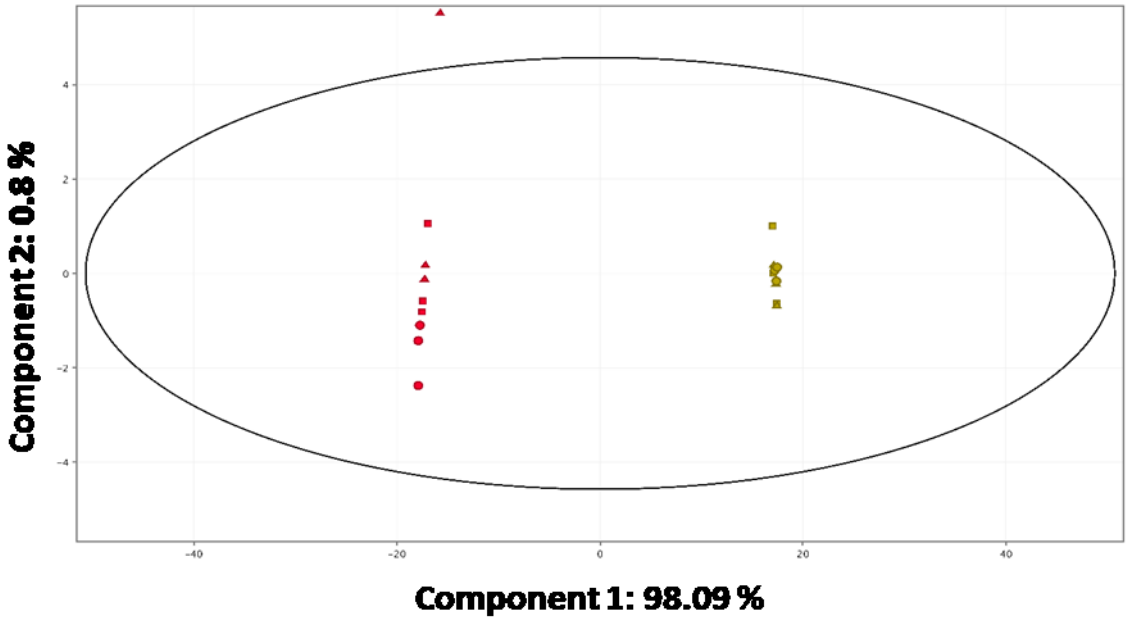
B

Negative ion mode of Mtb grown at pH 6.8



C

Positive ion mode of Mtb grown at pH 5.5



D

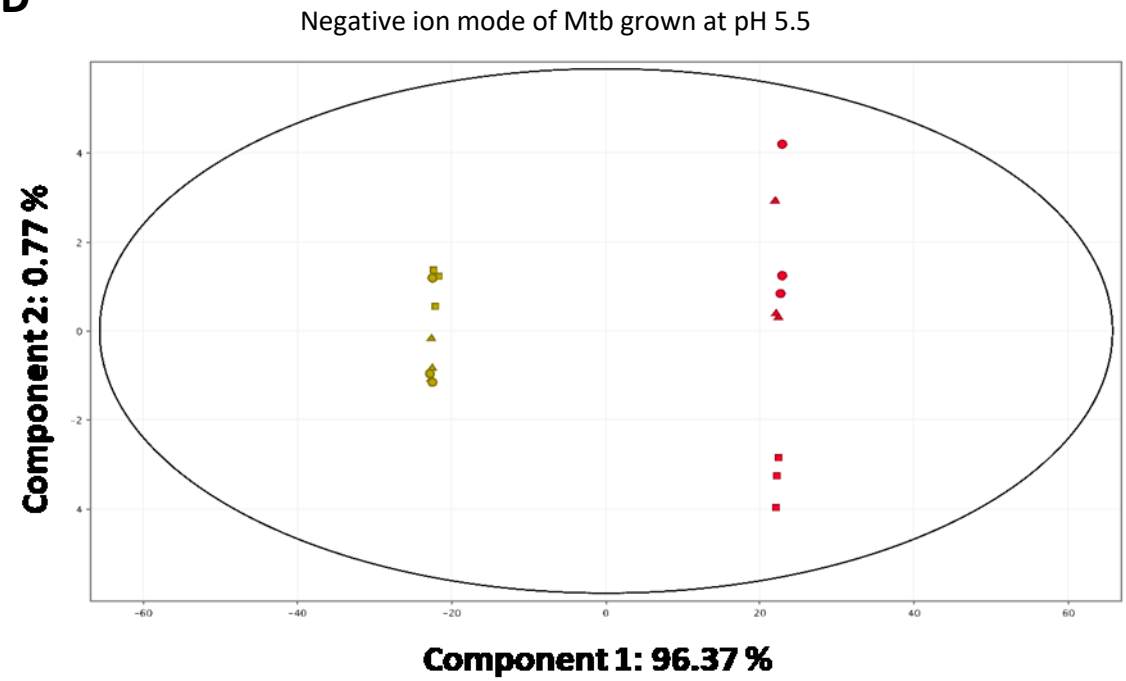
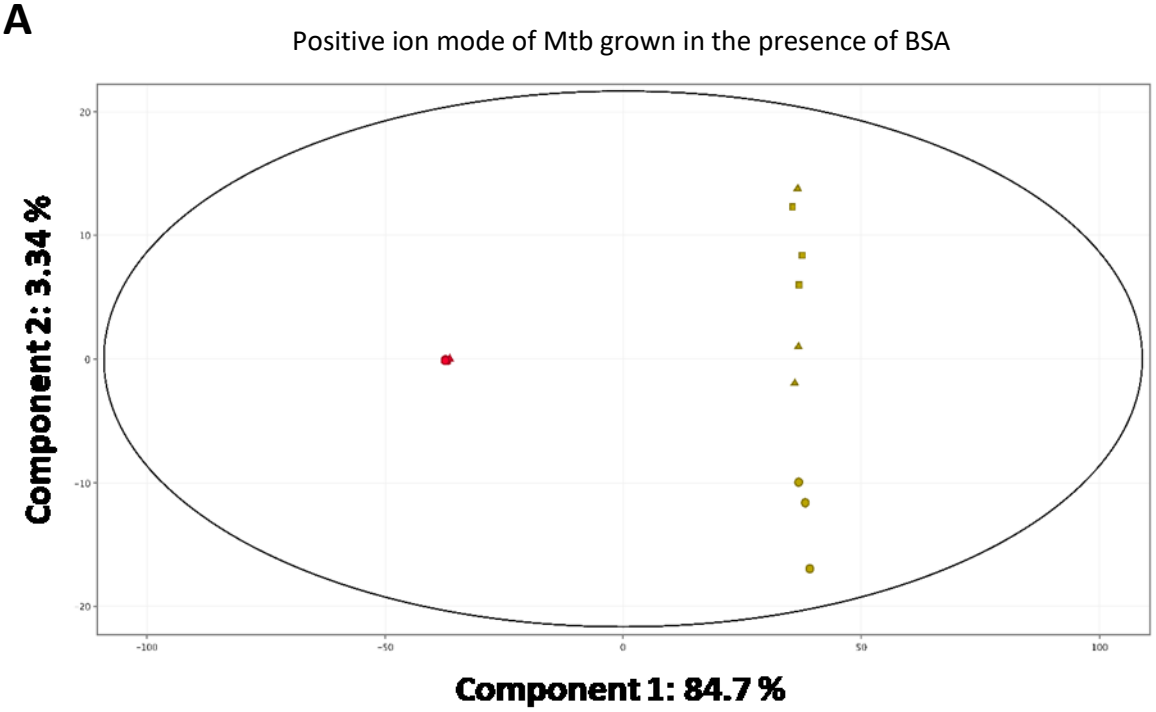


Figure 5-13. Untargeted metabolomics of Mtb wild type, *Δrv0998* and complemented strains in the presence or absence of BSA at pH 6.8 and 5.5 in positive and negative ion mode.
Principal component analysis (PCA) showing changing features > 2-fold in positive ion mode of Mtb grown at pH 6.8 (A). PCA showing changing features > 2-fold in negative ion mode of Mtb grown at pH 6.8 (B). PCA showing changing features > 2-fold in positive ion mode of Mtb grown at pH 5.5 (C). PCA showing changing features > 2-fold in negative ion mode of Mtb grown at pH 5.5 (D). Variance of 93.39% (A), 86.95% (B), 98.09% (C) and 96.37% (D) is explained by the principal component on the x-axis. Variance of 1.3% (A), 10.75% (B), 0.8% (C) and 0.77% (D) is explained by the principal component on the y-axis. Red, BSA; yellow, no BSA. Circle: wild type triangle: mutant, square: complemented. This is the representation of three technical replicates from one of two biological replicates.

A



B

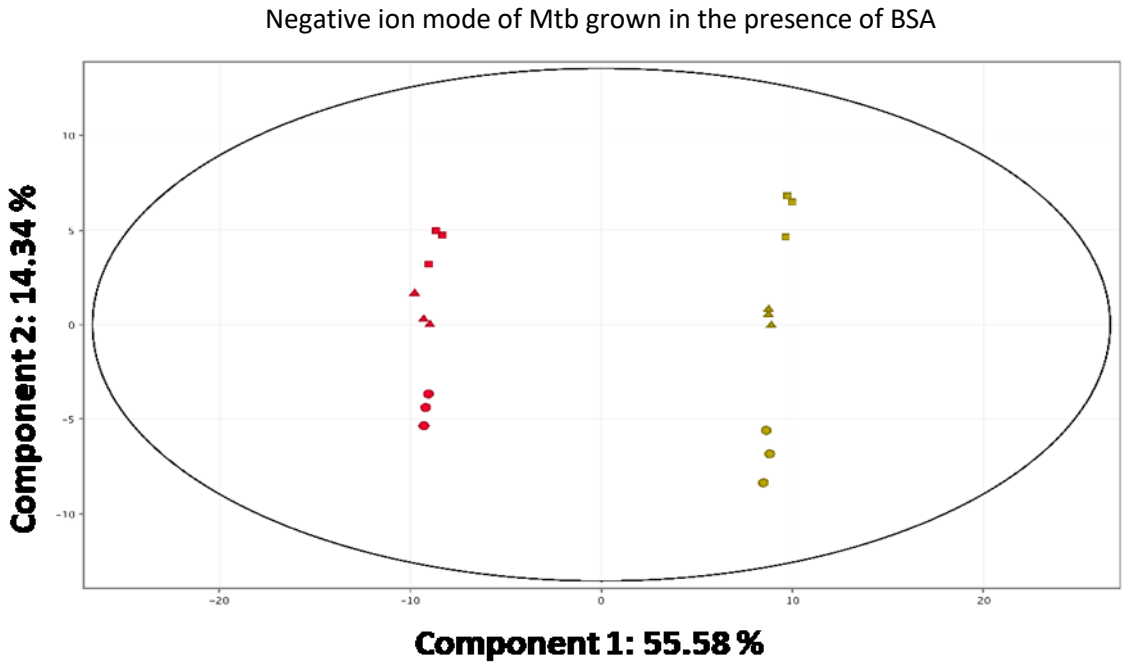
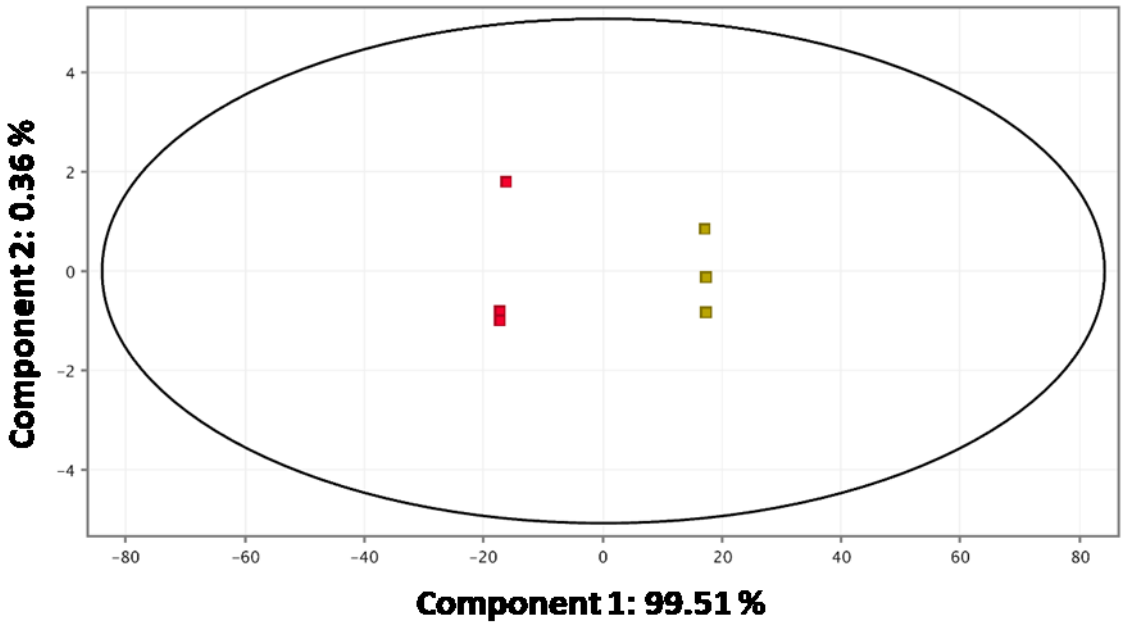


Figure 5-14. Untargeted metabolomics of Mtb wild type, *Δrv0998* and complemented strains in the presence or lack of BSA at pH 6.8 and 5.5 in positive and negative ion mode.
Principal component analysis (PCA) showing changing features > 2-fold in positive ion mode of Mtb grown in the presence of BSA (A). PCA showing changing features > 2-fold in negative ion mode of Mtb grown in the presence of BSA (B). Variance of 84.7% (A), and 55.58% (B) is explained by the principal component on the x-axis. Variance of 3.34% (A) and 14.34% (B) is explained by the principal component on the y-axis. Red, pH 5.5; yellow, pH 6.8. Square:

complemented, triangle: mutant, circle: wild type. This is the representation of three technical replicates from one of two biological replicates.

Previous results showed a difference in growth by the Mtb mutant strain lacking *rv0998* in the presence or absence of BSA (Figure 5-10). Thus, I investigated if this change in phenotype, where Mtb *Δrv0998* has an impairment in growth compared to the parental and complemented strains at pH 5.5 in the presence of BSA (Figure 5-10 B), or where Mtb *Δrv0998* grows better in comparison to the parental and complemented strains when grown at pH 5.5 in the absence of BSA (Figure 5-10 C), is caused due to changing metabolites. To do so, untargeted metabolomics were performed on the mutant strain exposed to pH 5.5, comparing the features between when grown in the presence or absence of BSA (Figure 5-15). From the results obtained changing features in positive (Figure 5-15 A) and negative ion mode (Figure 5-15 B) are observed between the strain grown in the presence or absence of BSA. These results suggest that BSA has a drastic impact on the levels of intracellular metabolites in Mtb.

A Mtb *Δrv0998* in positive ion mode



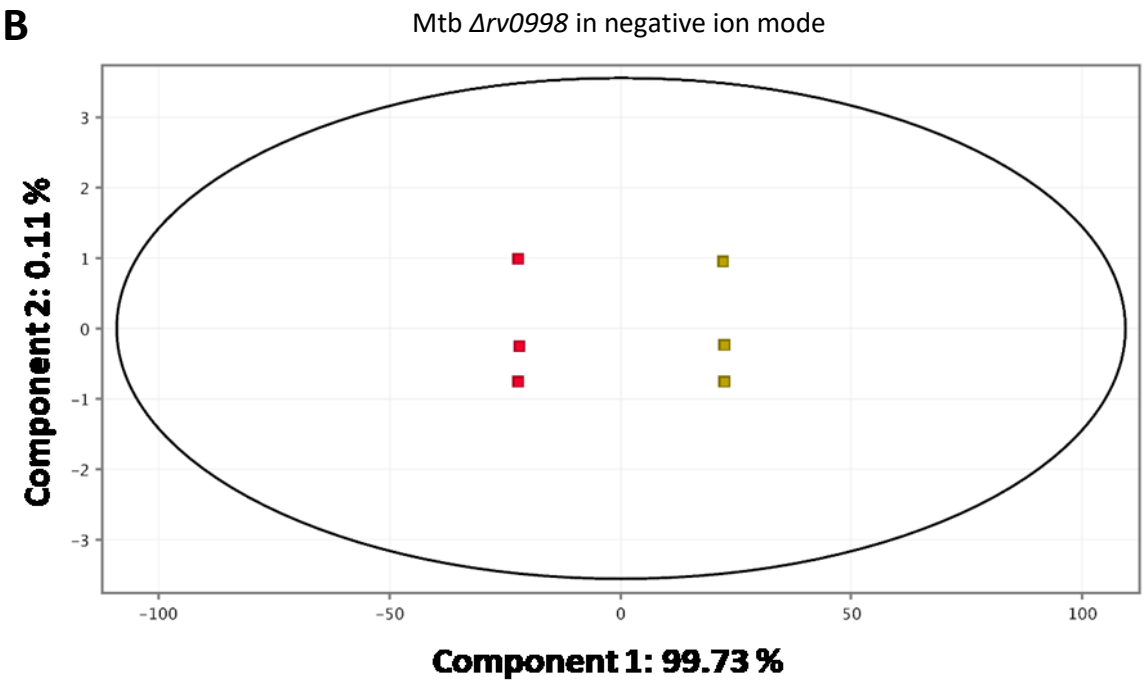


Figure 5-15. Untargeted metabolomics of Mtb *Δrv0998* in response to the presence or absence of BSA at pH 5.5.
Principal component analysis (PCA) showing changing features > 2-fold in the metabolites profile of Mtb *Δrv0998* in positive ion mode (A). PCA showing changing features > 2-fold in the metabolites profile of Mtb *Δrv0998* in negative ion (B). Variance of 99.51% (A) and 99.73% (B) is explained by the principal component on the x-axis. Variance of 0.36% (A) and 0.11% (B) is explained by the principal component on the y-axis. Red, BSA; yellow, no BSA.

The untargeted metabolomics analysis reported here shows changes in metabolites between the Mtb wild type, *Δrv0998* and complemented strains grown in the presence or absence of BSA. Furthermore, changes are seen between Mtb strains grown at pH 6.8 and 5.5, both in the presence of BSA. However, no differences between pH 6.8 and 5.5 were seen in the absence of BSA, which suggests a potential alternative to metabolism in adaptation to acidic conditions in the absence of BSA. Moreover, changes in the intracellular metabolites of Mtb *Δrv0998* stressed at pH 5.5 were seen between when grown in the presence or absence of BSA.

Rv0998 regulates acetyl-CoA formation, which feeds oxidative TCA reactions.[193] Thus, to further understand if the changing metabolites observed in the tested conditions are involved in central carbon metabolism and how are their turnover changes according to the presence or absence of BSA, and according to different pH, targeted metabolomics were performed on metabolites of the TCA cycle on the wild type, *Δrv0998* and complemented strains of Mtb.

5.2.2.5 Turnover of TCA cycle metabolites of Mtb wild type, Δrv0998 and complemented strain in the presence and absence of BSA

It is known that protein acetylation plays a role in energy generation and carbohydrate metabolism as explained in the introduction of this chapter. In *E. coli* around half of all acetylated proteins participate in these processes.[388,394,395] The involvement of acetylation of lysine residues in metabolism is evolutionarily conserved, as described for *E. coli* and *S. enterica.*[379,388,394,400,401] Furthermore, studies conducted in Mtb via proteomics approaches have identified acetylation sites of proteins involved in the TCA cycle, glycolysis/gluconeogenesis and fatty acid metabolism.[381] Hence, to further understand the changing features between Mtb grown in the presence or absence of BSA, I focused on the metabolites of the central carbon metabolism in the Mtb wild type*, Δrv0998* and complemented strains after being exposed for 24 hours, equivalent to one doubling time, at pH 5.5 or 6.8 with and without BSA. Stable isotope tracing using [U-$^{13}C_6$] glucose experiments were performed to characterise turnover of metabolites from the glycolysis and TCA cycle. Ion counts were normalised by the amount of protein present in the metabolome extract as a readout of biomass and determined by bicinchoninic acid (BCA) assay.

When the bacteria were grown at pH of 6.8 in the presence or absence of BSA, changes in the incorporation of [$^{13}C_6$-glucose] label can be observed in metabolites of the central carbon metabolism (Figure 5-16). For instance, the wild type strain exhibited a 22% increase in $^{13}C_6$-glucose incorporation in α-ketoglutarate (α-KG) and a 22% increase in 2-MethylCitrate (2-MC) when grown in the absence of BSA compared to the presence of BSA.

The effect of Rv0998 in labelling incorporation was observed in 2-MC and α-KG as Mtb *Δrv0998* exhibited an increase of 8% and 9% respectively in the label incorporation compared to the wild type strain when grown in the presence of BSA (Figure 5-16). On the other hand, Mtb *Δrv0998* had a decrease of 10% in [$^{13}C_6$-glucose] label incorporation of succinate and malate in comparison to the wild type when grown in the absence of BSA.

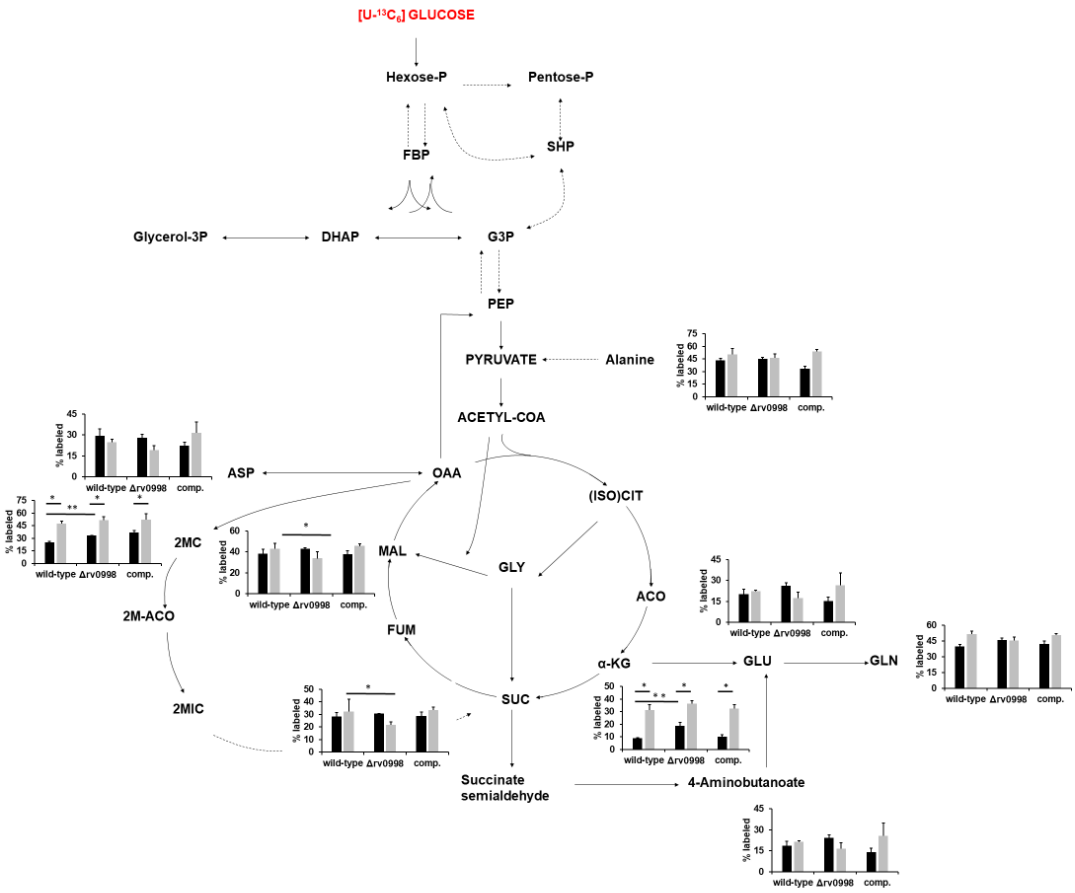


Figure 5-16. Turnover of central carbon metabolism metabolites of Mtb wild type (wt), mutant lacking *rv0998* (*Δrv0998*) and complemented (comp.) strains after exposing them for 24 hours to pH 6.8 in the presence or absence of BSA.
Percentage of label of central carbon metabolism metabolites. G-3P, glycerol 3-phosphate; DHAP, dihydroxyacetone phosphate; G3P, glyceraldehyde 3-phosphate; FBP, fructose 1,6-bisphosphate; PYR, pyruvate; ALA, alanine; ACO, aconitate; α-KG, α-ketoglutarate; SUC, succinate; MAL, malate; OAA, oxaloacetate; ASP, aspartate; GLU, glutamate; GLN, glutamine. Error bars denote standard deviation. This figure represents one biological replicate of two. Black, BSA; Grey, no BSA. *p < 0.05 as analysed by Student's *t*-test.

I also measured the incorporation of the label in targeted compounds important for Mtb. These compounds are involved in nucleotide degradation such as hypoxanthine; intermediates of peptidoglycan biosynthesis such as 2-aminoadipic acid, diaminopimelic acid and D-alanyl-D-alanine; and amino acids such as leucine, lysine, valine, threonine and ornithine. Thus, when the Mtb strains were grown at pH 6.8 in the presence or absence of BSA changes in the percentage of the label incorporated can be observed in Figure 5-17. The wild type strain exhibited 11% and

15% increases respectively in the percentage of the label in 2-aminoadipic acid and D-alanyl-D-alanine when grown in the absence of BSA compared to the presence of BSA.

To investigate if Rv0998 plays a role in the label incorporation, the [$^{13}C_6$-glucose] incorporation of Mtb *Δrv0998* was compared to the parental strains. For instance, Mtb *Δrv0998* exhibited a 15% increase in [$^{13}C_6$-glucose] label incorporation of threonine when grown in the absence of BSA compared to the wild type strain.

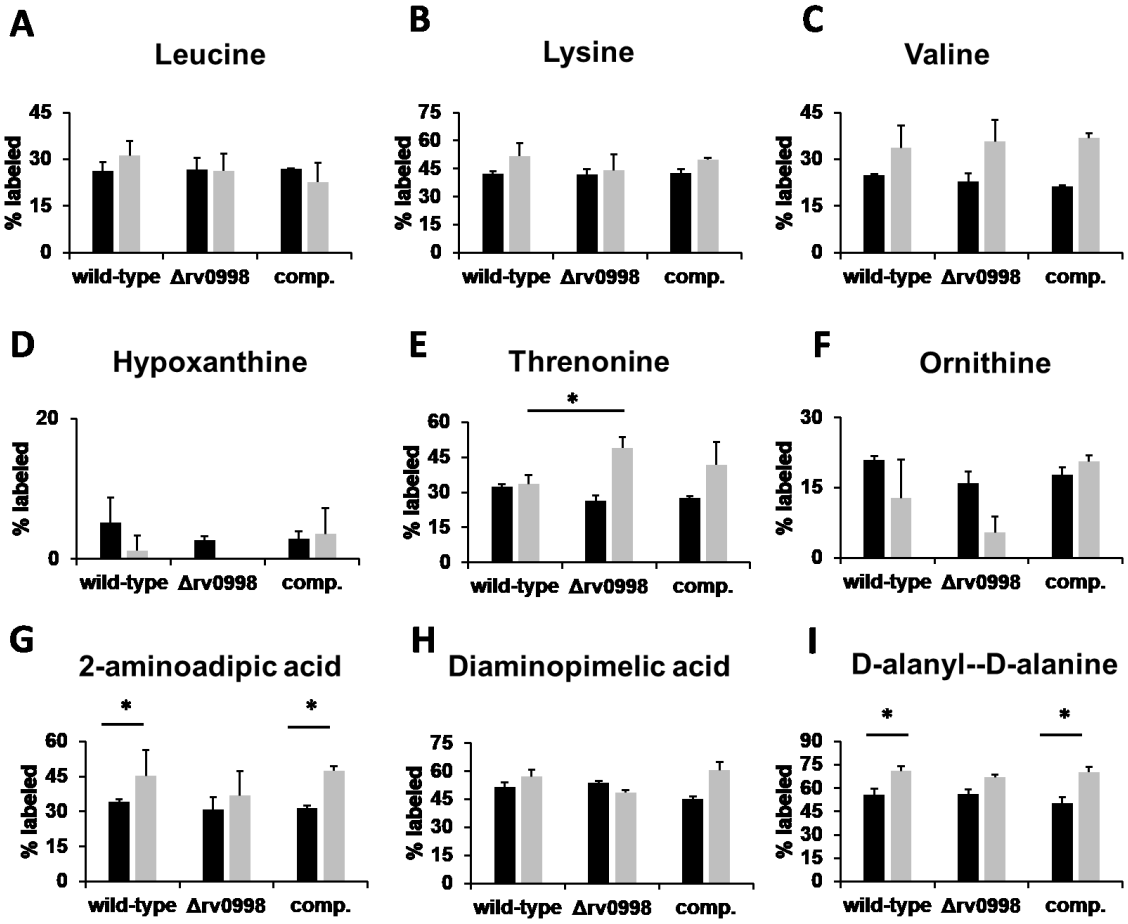


Figure 5-17. Turnover of compounds of Mtb wild type (wt), mutant lacking *rv0998* (*Δrv0998*) and complemented (comp.) strains after exposure for 24 hours to pH 6.8 in the presence or absence of BSA.
Percentage of label of Mtb compounds. Error bars denote standard deviation. This figure represents one biological replicate of two. Black, BSA; Grey, no BSA. *p < 0.05 as analysed by Student's *t*-test.

When Mtb wild type was grown at pH of 5.5 in the presence or absence of BSA, no statistically significant changes in the incorporation of [$^{13}C_6$-glucose] label were observed in metabolites of the central carbon metabolism (Figure 5-18).

To investigate if Rv0998 plays a role in the label incorporation of Mtb, the wild type strain was compared to Mtb *Δrv0998*. For instance, Mtb *Δrv0998* had a 5% increase in the percentage of the label of α-KG compared to the wild type strain when grown in the presence of BSA. When grown in the absence of BSA, Mtb *Δrv0998* exhibited a 27% increase in [$^{13}C_6$-glucose] label incorporation in 2-MC compared to the wild type strain (Figure 5-18).

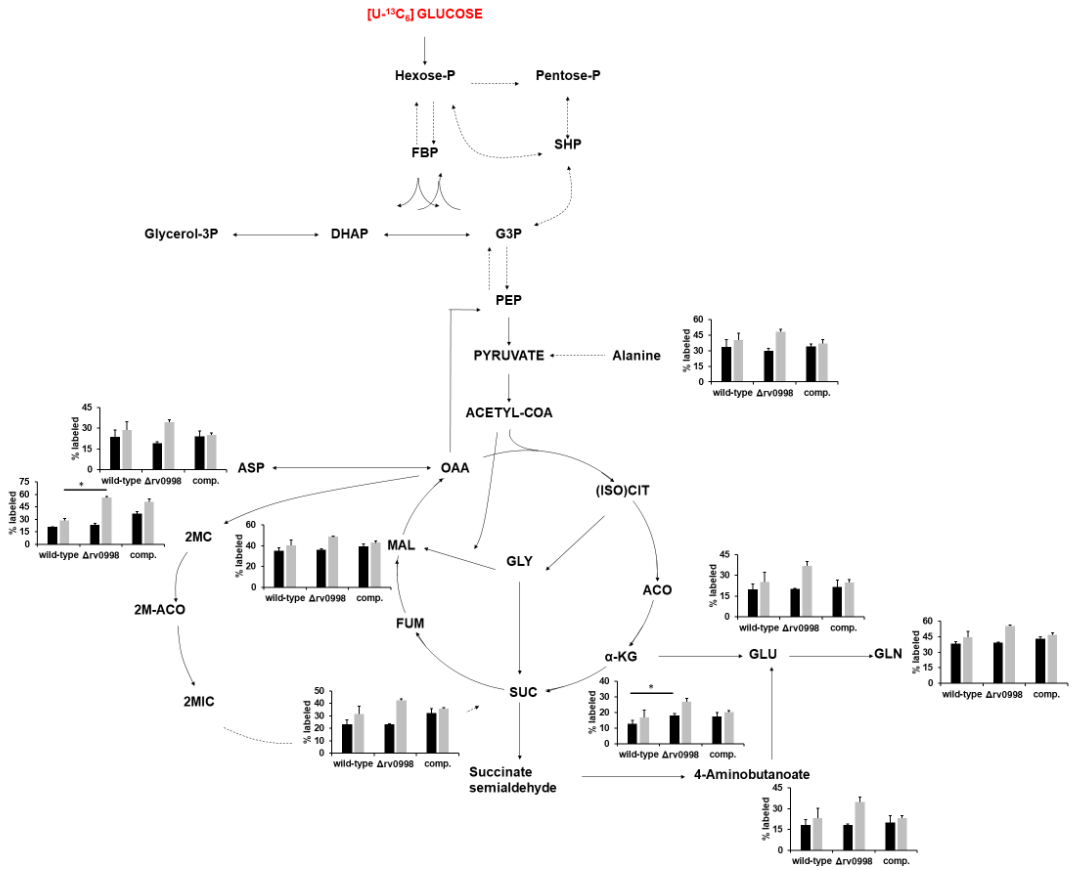


Figure 5-18.Turnover of central carbon metabolism metabolites of Mtb wild type (wt), mutant lacking *rv0998* (*Δrv0998*) and complemented (comp.) strains after exposure for 24 hours to pH 5.5 in the presence or absence of BSA.

Percentage of label of central carbon metabolism metabolites. G-3P, glycerol 3-phosphate; DHAP, dihydroxyacetone phosphate; G3P, glyceraldehyde 3-phosphate; FBP, fructose 1,6-bisphosphate; PYR, pyruvate; ALA, alanine; ACO, aconitate; α-KG, α-ketoglutarate; SUC, succinate; MAL, malate; OAA, oxaloacetate; ASP, aspartate; GLU, glutamate; GLN, glutamine. Error bars denote standard deviation. This figure represents one biological replicate of two. Black, BSA; Grey, no BSA. *p < 0.05 as analysed by Student's *t*-test.

Figure 5-19 presents the changes in the percentage of the label when the Mtb strains were exposed at pH 5.5 in the presence or absence of BSA. The wild type strain of Mtb exhibited an 8% increase in the percentage of the label of leucine, an 8% increase in valine and a 24% increase in hypoxanthine when grown in the absence of BSA compared to the presence of BSA.

To investigate if Rv0998 plays a role in Mtb adaptation to changing pH and the presence or absence of BSA; the label incorporation of the wild type strain was compared to Mtb *Δrv0998*. For instance, Mtb *Δrv0998* had a 10% increase of [$^{13}C_6$-glucose] label incorporation in threonine, compared to wild type strain, when grown in the presence of BSA. When grown at pH 5.5 in the absence of BSA, Mtb *Δrv0998* had an 8% increase in label incorporation in lysine and a 10% increase in valine compared to the wild type strain (Figure 5-19).

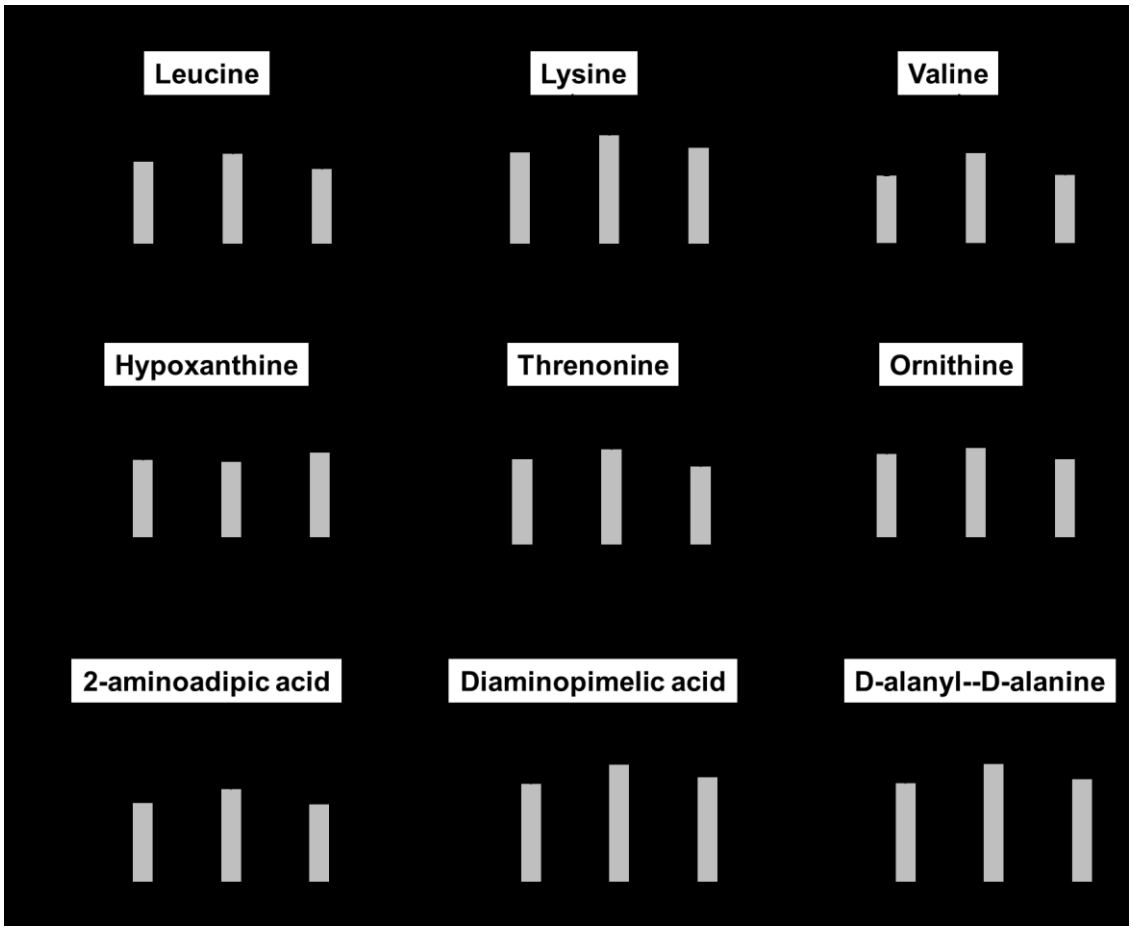


Figure 5-19. Turnover of compounds of Mtb wild type (wt), mutant lacking *rv0998* (*Δrv0998*) and complemented (comp.) strains after exposure for 24 hours to pH 5.5 in the presence or absence of BSA.
Percentage of label of Mtb compounds. Error bars denote standard deviation. This figure represents one biological replicate of two. Black, BSA; Grey, no BSA. *$p < 0.05$ as analysed by Student's *t*-test.

5.2.2.6 Investigation of Mtb cell envelope changes (PIMs) by MALDI-TOF

Rv0998 acetylates fatty acyl-CoA synthetases (FadDs) encoded in the mycobacterial genome, at the acetylable lysine residue. These FadDs are involved in fatty acid and cholesterol catabolism. Moreover, they have been seen to be acetylated by Rv0998 *in vitro* in a cAMP-dependent manner which leads to the inhibition of their activity and which shows the association of cAMP signalling with mycobacterial fatty acid metabolism.[193] In this chapter, changes in the TCA cycle haven been shown, which could lead to a change in fatty acid synthesis. As Rv0998 has been shown to be involved in propionate detoxification,[193] lipid profiling on the entire bacteria grown in the presence of BSA was performed. I hypothesised that lysine acetylation could be affecting the abundance of PIMs, which constitute 45% of the mycobacterial plasma membrane and are a readout of fatty acid synthesis.[45–47] For this reason, the percentage of Ac_4PIM_2, Ac_3PIM_2, Ac_3PIM_6 and Ac_4PIM_6 was measured in negative ion mode and the relative abundance was measured by calculating the area.

Intact bacteria lipid profiling from liquid culture was used to detect the lipids by growing the wild type, the *Δrv0998* and the complemented strains of Mtb in Middlebrook 7H9 liquid medium at pH of 6.8 and in the presence of BSA until mid-log phase. No changes in the abundance of Ac_3PIM_2 and Ac_4PIM_2 were seen between the three strains at pH 6.8 (Figure 5-20 A), or after exposing the bacteria to pH 5.5 (Figure 5-20 C) for 0, one and two doubling times. Furthermore, no changes in the abundance of Ac_3PIM_6 and Ac_4PIM_6 were seen between the three strains at pH 6.8 (Figure 5-20 B) or after exposing the bacteria to pH 5.5 (Figure 5-20 D) for 0, one and two doubling times.

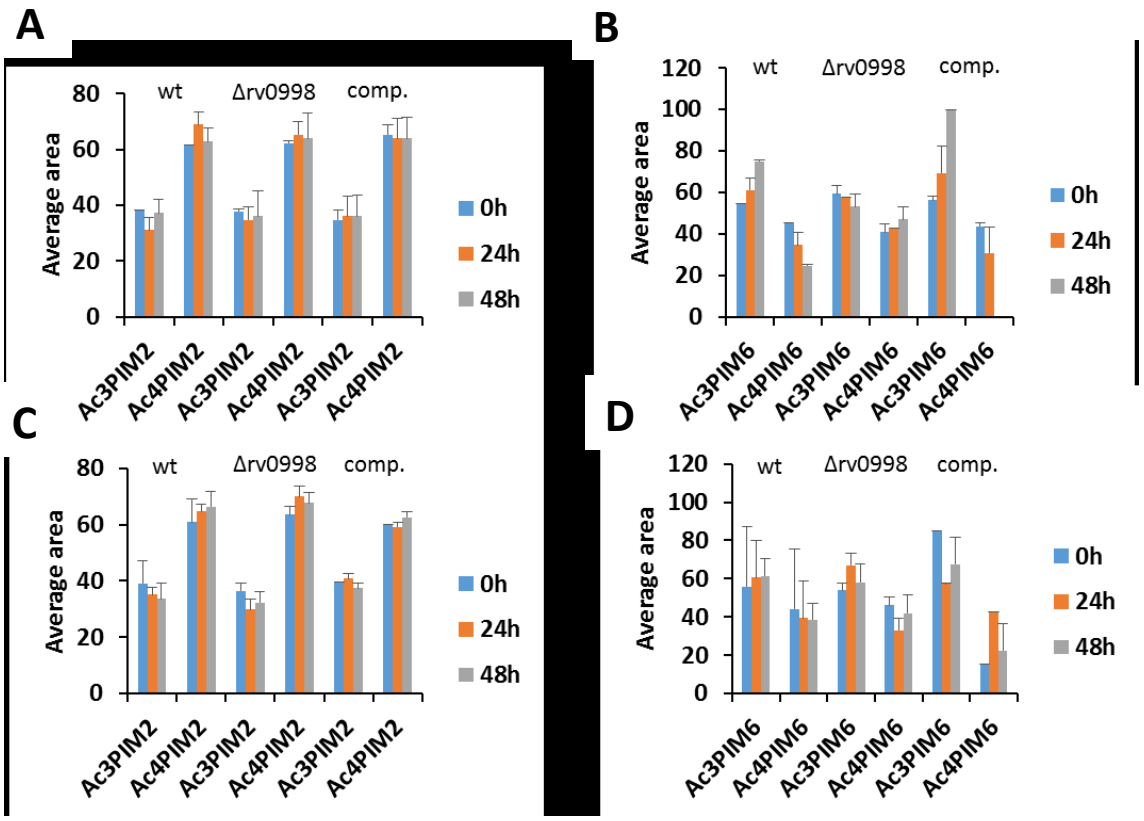


Figure 5-20. Relative abundance of Ac_3PIM_2, Ac_4PIM_2, Ac_3PIM_6 and Ac_4PIM_6 present in Mtb wild type (wt), mutant lacking *rv0998* (*Δrv0998*) and complemented (comp.) strains after exposing them for 0, 24 or 48 hours to pH 6.8 and pH 5.5.
Abundance Ac_xPIM_2 at pH 6.8 (A); Abundance Ac_xPIM_6 at pH 6.8 (B); Abundance Ac_xPIM_2 at pH 5.5 (C); Abundance Ac_xPIM_6 at pH 5.5 (D). Error bars denote standard deviation. This figure represents one biological replicate of three.

5.2.2.7 The presence of albumin in the culture medium causes changes in the Mtb acetylome

The results I have obtained so far have shown that the Mtb *Δrv0998* has an increased growth compared to the wild type and complemented strains at pH 5.5 in the absence of BSA. This observation correlates with the labelling metabolomics analysis, which shows an increase in label incorporation in Mtb *Δrv0998* compared to the parental strains at pH 5.5 when grown in the absence of BSA. Previous work reported by Singhal *et al.* and Liu *et al.* has demonstrated a majority of Mtb acetylated proteins to be associated with metabolism.[414,444] Therefore, I wanted to understand which proteins are lysine acetylated by Rv0998 under the conditions tested here; and also to examine their potential function and potential involvement in the central carbon metabolism. To investigate this, proteomics experiments were carried out by analysing the acetylome of Mtb CDC1551 wild type, *Δrv0998* and complemented strains grown at pH 6.8 or 5.5 in the presence or absence of BSA. The results obtained show the functional category of the

proteins only lysine acetylated by the wild type strain and not by Mtb *Δrv0998* at pH 6.8 and 5.5 in the presence or absence of BSA (Figure 5-21, Tables 5-4 to 5-7). This way I expected to find potential targets of Rv0998. The acetylated proteins were assigned a functional category according to Tuberculist. These functional categories were: virulence, detoxification and adaptation; lipid metabolism; information pathways; cell wall and cell processes; stable RNAs; insertion sequences and phages; PE/PPE family; intermediary metabolism and respiration; regulatory proteins; conserved hypotheticals ; and unknown.[445]

When Mtb wild type is grown at pH 6.8 with BSA, most of the acetylated proteins are involved in information pathways (Rv0706, Rv3370c, Rv2909c, Rv2594c, Rv2572c, Rv3459c, Rv0706, Rv0006, Rv2925c, Rv2737c, Rv0702, Rv3286c, and Rv2841c) and intermediary metabolism and respiration (Rv1384, Rv2607, Rv1451, Rv2334, Rv0147, Rv2427c, Rv3001c, Rv0952, and Rv1449c) (Figure 5-21 A). Rv0952 is involved in the TCA cycle as a probable succinyl-CoA synthetase; Rv1934c is a probable acyl-CoA dehydrogenase; and Rv1449c is a transketolase which together with transaldolase, provides the link between the glycolytic and the pentose-phosphate pathways.[445,446]

When Mtb wild type is grown at pH 6.8 without BSA, most of the acetylated proteins are involved in information pathways (Rv2783c, Rv3442c, Rv3297, Rv1316c, Rv0700, and Rv1329c) intermediary metabolism and respiration (Rv3324c, Rv2454c, Rv2213, Rv1248c, Rv3596c, Rv0492c, Rv0946c, Rv1832, Rv2178c, Rv3227, Rv2984, and Rv0087) and conserved hypotheticals (Rv1261c, Rv3254, Rv2307c, Rv1051c, and Rv2492) (Figure 5-21 B). Rv1248c is a multifunctional α-KG metabolic enzyme which has α-KG dehydrogenase, decarboxylase and synthase activities. Rv0946c is a probable glucose 6-phosphate isomerase (glycolysis/gluconeogenesis).[445,446] Furthermore, two of the acetylated proteins (Rv0297 and Rv0578c) in this condition are from the PE/PPE family (presenting N-terminal ProGlu and ProProGlu motifs), which promote antigenic diversity of Mtb. It is also worth noting that the lysine acetylation of Rv2384 (mbtA) replicates that observed by Vergnolle *et al*.[420]

Only when Mtb wild type was grown at pH 5.5 were proteins involved in virulence, detoxification and adaptation acetylated. These were Rv0440, Rv1908c, Rv0384c, and Rv1991c, when grown in the presence of BSA (Figure 5-21 C) and Rv1967, Rv2373c and Rv0171, when grown in the absence of BSA (Figure 5-21 D). Of note is that when Mtb wild type is grown at pH 5.5 with BSA Rv2220, a glutamine synthetase, was acetylated. When Mtb wild type is grown at pH 5.5 without BSA, Rv0157 (a probable NAD(P) transhydrogenase) was acetylated.[445,446] Nevertheless, no

proteins involved in lipid metabolism or regulation were acetylated when the wild type was grown at pH 5.5 without BSA (Figure 5-21 D). A list of acetylated proteins with their Rv number and potential function is presented in Tables 5-4 to 5-7.

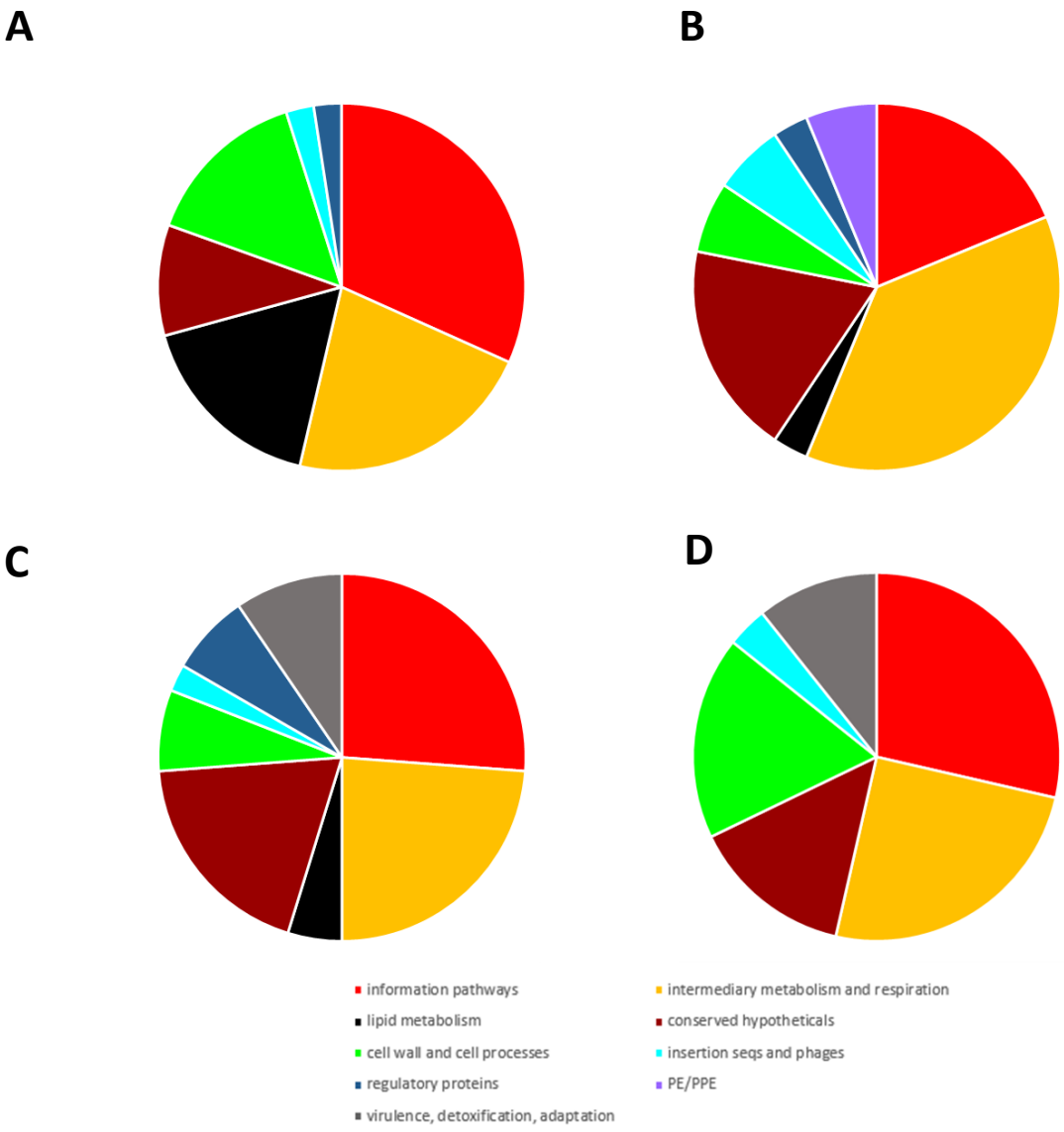


Figure 5-21. Lysine acetylated proteins exclusive to the wild type strain of Mtb.
Iterative MS experiments were used as an approach to enhance acetylation identification of Mtb peptides. Acetylated peptides were identified in LC-MS/MS. To enhance detection all the peptides detected through the Mtb database were excluded in the 2nd LC-MS/MS in order to be able to detect even more acetylated peptides. Acetylated peptides accession number was searched in uniprot (https://www.uniprot.org/) to check if the relevant protein belongs to Mtb H37Rv. Finally, the potential proteins were searched in Tuberculist (http://svitsrv8.epfl.ch/tuberculist/) to detect their function. The pie chart shows the functional categories of the proteins only acetylated by the Mtb wild type excluding those also acetylated by the mutant lacking *rv0998* (*Δrv0998*) as a way to detect Rv0998 targets. Mtb was grown at pH 6.8 with BSA (A), at pH 6.8 without BSA (B), at pH 5.5 with BSA (C), and at pH 5.5 without BSA (D). This is one representative experiment of two biological replicates. Experiment performed in collaboration with Dr. Agyro Tsipa (SyncbiCITE). Data analysis and figure made by Dr. Agyro Tsipa.

Gene name	Function	Wt	Δrv0998	Comp.
Rv0706	information pathways	+	-	-
Rv3370c	information pathways	+	-	-
Rv1384	intermediary metabolism and respiration	+	-	-
Rv0189c	intermediary metabolism and respiration	+	+	-
Rv2607	intermediary metabolism and respiration	+	-	+
Rv3130c	lipid metabolism	+	-	+
Rv2909c	information pathways	+	-	+
Rv1934c	lipid metabolism	+	-	-
Rv2594c	information pathways	+	-	-
Rv3596c	intermediary metabolism and respiration	+	+	-
Rv2572c	information pathways	+	+	-
Rv1451	intermediary metabolism and respiration	+	-	-
Rv3459c	information pathways	+	-	-
Rv2334	intermediary metabolism and respiration	+	-	-
Rv0895	lipid metabolism	+	-	-
Rv0706	information pathways	+	-	-
Rv1890c	conserved hypotheticals	+	-	-
Rv1073	conserved hypotheticals	+	-	-
Rv1183	cell wall and cell processes	+	-	-
Rv1586c	insertion seqs and phages	+	-	-
Rv0147	intermediary metabolism and respiration	+	-	-
Rv3695	cell wall and cell processes	+	-	-
Rv0006	information pathways	+	-	+
Rv2427c	intermediary metabolism and respiration	+	-	+
Rv3822	conserved hypotheticals	+	-	-
Rv3051c	information pathways	+	+	-
Rv2925c	information pathways	+	-	-
Rv0450c	cell wall and cell processes	+	-	-
Rv2737c	information pathways	+	-	+
Rv0702	information pathways	+	-	-
Rv0503c	lipid metabolism	+	-	-
Rv0682	information pathways	+	+	-
Rv2597	cell wall and cell processes	+	+	-
Rv3824c	lipid metabolism	+	-	-
Rv3286c	information pathways	+	-	-
Rv3001c	intermediary metabolism and respiration	+	-	-
Rv0952	intermediary metabolism and respiration	+	-	-
Rv2841c	information pathways	+	-	-
Rv1353c	regulatory proteins	+	-	-
Rv1449c	intermediary metabolism and respiration	+	-	-
Rv0001	information pathways	+	+	+
Rv0470c	lipid metabolism	+	-	-
Rv3234c	lipid metabolism	+	-	+
Rv0556	cell wall and cell processes	+	-	-

Rv0907	cell wall and cell processes	+	-	-
Rv1709	cell wall and cell processes	+	-	-
Rv2117	conserved hypotheticals	+	-	-

Table 5-4. Gene names and potential functions of acetylated proteins in the Mtb wild type (wt) grown at pH 6.8 in the presence of BSA.
The wt, *Δrv0998* and complemented strain of Mtb were grown in 7H9 culture medium at pH 6.8 in the presence of BSA. The table shows the genes of the acetylated proteins in the wt and if they are acetylated in the mutant strain lacking *rv0998* and/or the complemented strain of Mtb. Data were analysed by Dr. Agyro Tsipa.

Gene name	Function	Wt	Δrv0998	Comp.
Rv2783c	information pathways	+	-	-
Rv0006	information pathways	+	+	+
Rv1261c	conserved hypotheticals	+	-	-
Rv2580c	information pathways	+	+	-
Rv3442c	information pathways	+	-	-
Rv3297	information pathways	+	-	-
Rv3324c	intermediary metabolism and respiration	+	-	-
Rv1316c	information pathways	+	-	-
Rv2454c	intermediary metabolism and respiration	+	-	+
Rv2703	information pathways	+	+	-
Rv2213	intermediary metabolism and respiration	+	-	-
Rv0700	information pathways	+	-	-
Rv1183	cell wall and cell processes	+	-	-
Rv1248c	intermediary metabolism and respiration	+	-	-
Rv3596c	intermediary metabolism and respiration	+	-	-
Rv1261c	conserved hypotheticals	+	-	-
Rv3254	conserved hypotheticals	+	-	-
Rv3286c	information pathways	+	+	-
Rv0297	PE/PPE	+	-	-
Rv1329c	information pathways	+	-	-
Rv0492c	intermediary metabolism and respiration	+	-	-
Rv0946c	intermediary metabolism and respiration	+	-	-
Rv2580c	information pathways	+	+	-
Rv3849	regulatory proteins	+	-	-
Rv1128c	insertion seqs and phages	+	-	-
Rv0040c	cell wall and cell processes	+	-	-
Rv1832	intermediary metabolism and respiration	+	-	-
Rv0423c	intermediary metabolism and respiration	+	+	+
Rv2178c	intermediary metabolism and respiration	+	-	-
Rv2727c	intermediary metabolism and respiration	+	+	-
Rv2894c	insertion seqs and phages	+	-	-

Rv3227	intermediary metabolism and respiration	+	-	-
Rv2307c	conserved hypotheticals	+	-	-
Rv2984	intermediary metabolism and respiration	+	-	-
Rv1051c	conserved hypotheticals	+	-	-
Rv1516c	intermediary metabolism and respiration	+	+	-
Rv2384	lipid metabolism	+	-	-
Rv0578c	PE/PPE	+	-	-
Rv2444c	information pathways	+	+	-
Rv0087	intermediary metabolism and respiration	+	-	-
Rv2492	conserved hypotheticals	+	-	-

Table 5-5. Gene names and potential functions of acetylated proteins in the Mtb wild type (wt) grown at pH 6.8 in the absence of BSA.
The wt, *Δrv0998* and complemented strain of Mtb were grown in 7H9 culture medium at pH 6.8 in the absence of BSA. The table shows the genes of the acetylated proteins in the wt and if they are acetylated in the mutant strain lacking *rv0998* and/or the complemented strain of Mtb. Data were analysed by Dr. Agyro Tsipa.

Gene name	Function	Wt	Δrv0998	Comp.
Rv0440	virulence, detoxification, adaptation	+	+	+
Rv2845c	information pathways	+	-	-
Rv3892c	PE/PPE	+	+	-
Rv1017c	intermediary metabolism and respiration	+	-	-
Rv1161	intermediary metabolism and respiration	+	+	-
Rv2441c	information pathways	+	-	-
Rv0418	cell wall and cell processes	+	-	-
Rv3234c	lipid metabolism	+	-	-
Rv2925c	information pathways	+	-	-
Rv0001	information pathways	+	-	-
Rv0117	regulatory proteins	+	-	+
Rv3695	cell wall and cell processes	+	+	-
Rv1890c	conserved hypotheticals	+	-	-
Rv2989	regulatory proteins	+	-	-
Rv2696c	conserved hypotheticals	+	-	-
Rv0297	PE/PPE	+	+	-
Rv3735	conserved hypotheticals	+	+	-
Rv3900c	conserved hypotheticals	+	-	-
Rv3417c	virulence, detoxification, adaptation	+	+	+
Rv1908c	virulence, detoxification, adaptation	+	-	-
Rv2902c	information pathways	+	-	-
Rv1183	cell wall and cell processes	+	+	-
Rv1253	information pathways	+	-	+
Rv0384c	virulence, detoxification, adaptation	+	-	-
Rv0417	intermediary metabolism and respiration	+	-	-
Rv0706	information pathways	+	-	-

Rv1652	intermediary metabolism and respiration	+	-	-
Rv2992c	information pathways	+	-	-
Rv3849	regulatory proteins	+	-	-
Rv1274	cell wall and cell processes	+	-	-
Rv2597	cell wall and cell processes	+	-	-
Rv2448c	information pathways	+	-	-
Rv0006	information pathways	+	+	+
Rv2895c	intermediary metabolism and respiration	+	-	-
Rv2078	conserved hypotheticals	+	-	-
Rv3247c	intermediary metabolism and respiration	+	-	-
Rv2894c	insertion seqs and phages	+	-	-
Rv0682	information pathways	+	-	-
Rv2220	intermediary metabolism and respiration	+	-	-
Rv3011c	information pathways	+	-	-
Rv1300	intermediary metabolism and respiration	+	-	-
Rv1017c	intermediary metabolism and respiration	+	-	-
Rv3741c	intermediary metabolism and respiration	+	-	+
Rv1991c	virulence, detoxification, adaptation	+	-	-
Rv0384c	virulence, detoxification, adaptation	+	-	-
Rv3267	conserved hypotheticals	+	-	-
Rv3542c	conserved hypotheticals	+	-	-
Rv1925	lipid metabolism	+	-	-
Rv2734	conserved hypotheticals	+	-	-
Rv1869c	intermediary metabolism and respiration	+	-	-

Table 5-6. Gene names and potential functions of acetylated proteins in the Mtb wild type (wt) grown at pH 5.5 in the presence of BSA.
The wt, *Δrv0998* and complemented strain of Mtb were grown in 7H9 culture medium at pH 5.5 in the presence of BSA. The table shows the genes of the acetylated proteins in the wt and if they are acetylated in the mutant strain lacking *rv0998* and/or the complemented strain of Mtb. Data were analysed by Dr. Agyro Tsipa.

Gene name	Function	Wt	Δrv0998	Comp.
Rv0700	information pathways	+	-	-
Rv0006	information pathways	+	+	+
Rv2902c	information pathways	+	-	-
Rv1536	information pathways	+	-	-
Rv0566c	conserved hypotheticals	+	-	-
Rv3442c	information pathways	+	-	-
Rv1498c	intermediary metabolism and respiration	+	-	-
Rv2580c	information pathways	+	-	-
Rv2839c	information pathways	+	+	+
Rv2597	cell wall and cell processes	+	-	-
Rv1967	virulence, detoxification, adaptation	+	-	-
Rv2566	conserved hypotheticals	+	-	-

Rv0706	information pathways	+	-	-
Rv0566c	conserved hypotheticals	+	-	-
Rv0157	intermediary metabolism and respiration	+	-	+
Rv1511	intermediary metabolism and respiration	+	-	-
Rv0933	cell wall and cell processes	+	-	-
Rv2448c	information pathways	+	-	-
Rv2945c	cell wall and cell processes	+	-	-
Rv3687c	information pathways	+	-	-
Rv2373c	virulence, detoxification, adaptation	+	-	-
Rv1133c	intermediary metabolism and respiration	+	-	-
Rv0959	intermediary metabolism and respiration	+	-	-
Rv2213	intermediary metabolism and respiration	+	-	-
Rv2054	conserved hypotheticals	+	-	-
Rv0593	cell wall and cell processes	+	-	-
Rv0171	virulence, detoxification, adaptation	+	-	-
Rv0820	cell wall and cell processes	+	-	-
Rv2263	intermediary metabolism and respiration	+	-	-
Rv2812	insertion seqs and phages	+	-	-

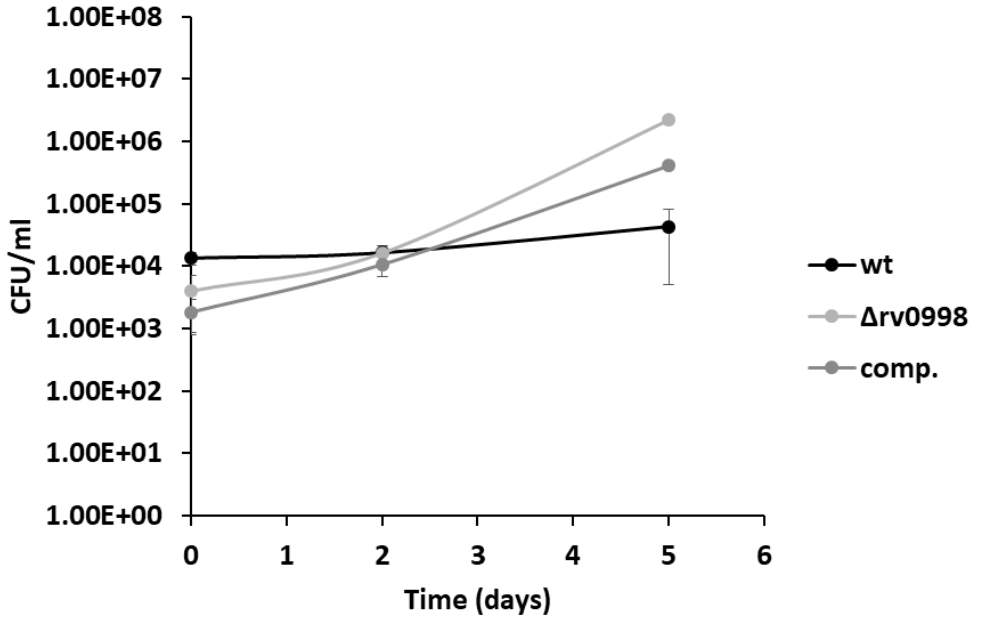
Table 5-7. Gene names and potential functions of acetylated proteins in the Mtb wild type (wt) grown at pH 5.5 in the absence of BSA.
The wt, *Δrv0998* and complemented strain of Mtb were grown in 7H9 culture medium at pH 5.5 in the absence of BSA. The table shows the genes of the acetylated proteins in the wt and if they are acetylated in the mutant strain lacking *rv0998* and/or the complemented strain of Mtb. Data were analysed by Dr. Agyro Tsipa.

5.2.2.8 Role of Rv0998 in virulence and persistence.

In this chapter, I have shown an increased growth by the Mtb mutant strain lacking *rv0998* grown at pH 5.5 in the absence of albumin in comparison to the parental strains. I have also shown a correlation of this growth with an increase in carbon incorporation in targeted metabolites in the mutant strain at pH 5.5 in the absence of BSA. The absence of albumin and the acidic conditions studied here are found within the alveolar macrophage, the Mtb host. Thus, in order to investigate the physiological impact and virulence role of Rv0998, I performed macrophage infection assays. IFN-*γ* is the main cytokine involved in the immune response against mycobacteria, and its major function is the activation of macrophages, allowing them to exert their microbicidal role.[447] Therefore, IFN-*γ*-activated and non-activated macrophages were infected at a multiplicity of infection (MOI) of 1 with Mtb grown on dextrose. A MOI of 1 was used following literature-based evidence to maintain the integrity of infected macrophage monolayers for at least 5 days.[138,448]

CFU/mL were counted at days 2 and 5 post-infection. Prior to performing the experiment, I expected that Mtb would have increased survival when infecting resting macrophages compared to IFN-γ activated macrophages as the latter would mediate the microbicidal role function of macrophages via phagocytosis, phagolysosomal fusion, oxidative burst among other mechanisms.[449] However, no changes in Mtb survival were seen between infection of resting and activated macrophages. Figure 5-22 demonstrates no Mtb growth at day 2 post-infection and no change in survival between the wild type, *Δrv0998* and complemented strains of Mtb. These results correlate with previous work by Van der Ven *et al*., who reported an initial drop in bacterial viability over the first 2 days, confirming that the transition was stressful for Mtb.[450] Nevertheless, an increased survival of the mutant lacking *rv0998* compared to the parental and complemented strains in IFN-γ-activated and resting macrophages was seen at day 5 post-infection. These results are consistent with the growth monitoring studies and with Vergnolle *et al*.'s observations, where an increased growth by Mtb *Δrv0998* in comparison to the parental strains was observed at an acidic pH in a culture medium lacking albumin.[420]

A



B

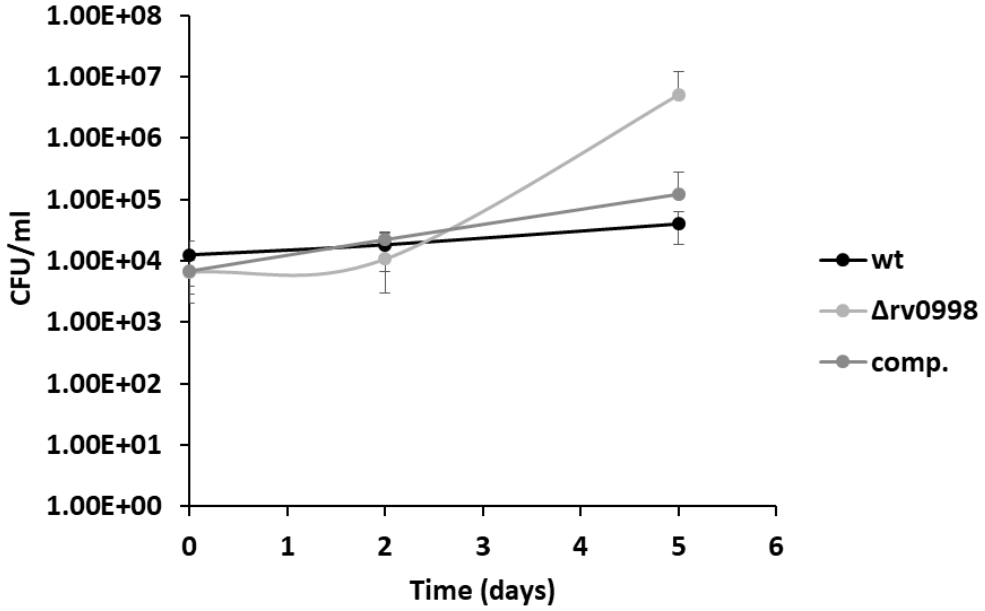


Figure 5-22. Growth of intracellular Mtb.
CFU/mL of the wild type (wt) strain, mutant strain lacking *rv0998* (*Δrv0998*) and complemented (comp.) strain of Mtb CDC1551 infecting resting bone BMDMs (A) or IFN-γ-activated BMDMs (B). The y-axis is expressed as logarithmic scale in this figure. Error bars denote standard deviation. This figure represents one biological replicate of three.

To assess further the macrophage response to Mtb I quantified the production of TNF-α by macrophages. TNF-α is a cytokine which contributes both to protection against TB and to immunopathology.[451,452] Figure 5-23 demonstrates how IFN-γ-activated macrophages infected with the Mtb wild type strain increased TNF-α production 2.5-fold after two days of infection in comparison to resting macrophages. Furthermore, resting macrophages infected with the Mtb *Δrv0998* produced 1.6-fold more TNF-α in comparison to those infected with the wild type strain at day 2 post-infection. However, at day 5 post-infection, resting macrophages infected with Mtb *Δrv0998* produced 1.9-fold less TNF-α in comparison to those infected with the wild type (Figure 5-23 A). The same trend was seen at day 5 post-infection in IFN-γ-activated macrophages, which upon infection with Mtb *Δrv0998* they produced 1.7-fold less TNF-α in comparison to the macrophages infected by the parental strain. No statistically significant differences in TNF-α production were seen in IFN-γ-activated macrophages infected with the wild type, *Δrv0998* or complemented strains of Mtb at day 2 post-infection (Figure 5-23 B).

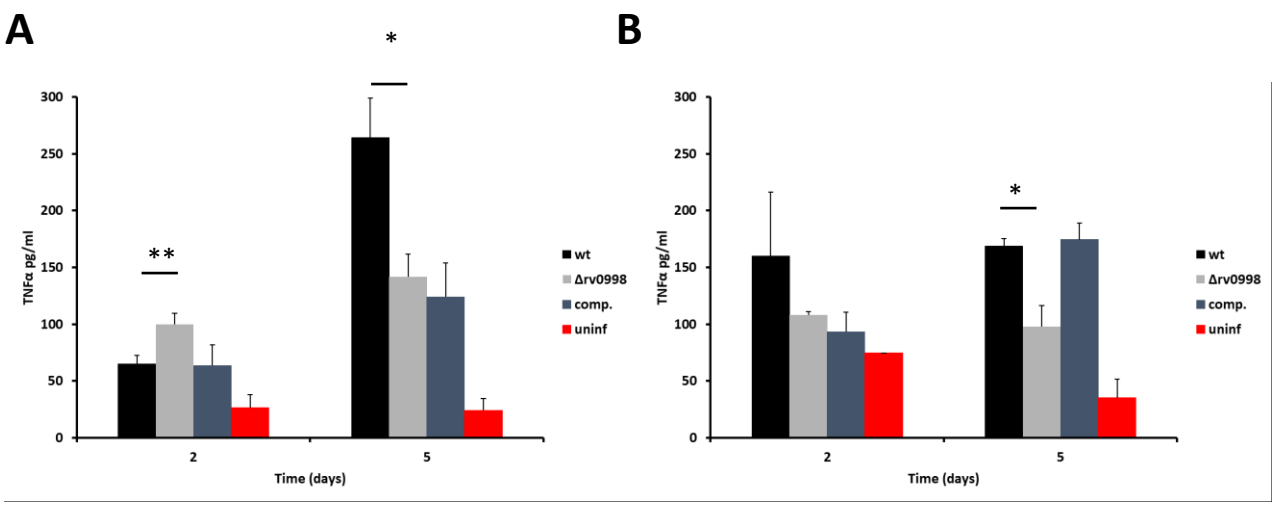


Figure 5-23. Quantification of TNF-α production by IFN-γ-activated or resting macrophages infected with wt, *Δrv0998* and the complemented strains of Mtb.
TNF-α production by resting BMDMs (A). TNF-α production by IFN-γ-activated BMDMs (B). Error bars denote standard deviation. This figure represents one biological replicate of three. *$p < 0.05$, **$p < 0.005$ as analysed by Student's *t*-test.

5.3 Discussion

Mtb is an intracellular pathogen, which infects alveolar macrophages. Once inside, it is exposed to different environmental cues such as reactive oxygen intermediates, reactive nitrogen intermediates, free fatty acids and acidic pH, which influence bacterial growth and gene expression.[137,453] The bacterium requires the regulated expression of a set of genes and metabolic pathways to maintain and persist infection in an immunocompetent host.[454] cAMP is one of the most universal second messengers and it is widely used by bacteria, fungi and eukaryotes to regulate gene expression in response to changing environmental conditions such as acidic pH.[365] The pH of the macrophage compartment, in which Mtb resides, ranges from pH 6.4 to 4.5, depending on the activation state of the macrophage.[433,434] Phagosomal acidity may provide a critical cue for adaptation of Mtb to the host niche. At the same time, to ensure survival, the bacterium must prevent excessive entry of protons into its cytosol and expel them when their concentrations threaten the pH homeostasis.[429] In macrophages that have not yet been immunologically activated, Mtb resides in an environment that is only very mildly acidic with a pH of around 6.2.[455] Lack of acidification of the mycobacterial phagosome is likely due to the absence of the vacuolar proton-ATPase. Nevertheless, after immunologic activation of the macrophage, such as by exposure to IFN-γ, the fusion block is relieved and the phagosomal compartment acidifies to pH 4.5 to 5.5.[429] Because IFN-γ drives macrophage activation and acidification of Mtb-containing phagosomes *in vitro*, it is likely that this also occurs *in vivo.*[429] To note is that the physical structure and molecular composition of bacterial cell envelopes act as an effective primary barrier against the entry of protons. If protons do enter the bacterial cytosol, an array of mechanisms regulate pH within the cell. Proton pumps, production of ammonia, amino acid decarboxylation, cell envelope modification, macromolecule protection, and cell density all contribute to the maintenance of intrabacterial pH and survival of bacteria in acid.[429] The ability to sense environmental pH, as well as other signals that likewise flux during phagosomal maturation, are suggested to play a role in determining Mtb's location in the cell.[343]

There are 10 predicted cAMP-binding proteins in Mtb with a range of potential effector functions. Nevertheless, only three of them, Cmr, CRP_{Mt} and Rv0998, have been characterised and have known functions. Of these three, Rv0998 is a cAMP-dependent lysine acetyltransferase.[365] Lysine acetylation is a post-translational modification, which is used by eukaryotes and prokaryotes in order to regulate various biological processes. Nambi *et al.* used a deletion mutant of the *rv0998* ortholog in *M. bovis* BCG (BCG_1055) and demonstrated a growth impairment of the mutant lacking BCG_1055 compared to the wild type in *M. bovis* BCG when using propionate as the sole carbon source.[193] Furthermore, studies by Rittershaus *et al*.,

have demonstrated that the immediate response of Mtb to hypoxia relies on Rv0998 and involves a fast and transient induction of the DosR regulon.[425]

Work by Vergnolle *et al*. has previously shown an increased growth by Mtb lacking *rv0998* in comparison to the parental and complemented strains at pH 6.[420] However, as it has been observed in the results section I observed a different phenotype at pH 5.5. Key drivers from these differing phenotypes could be due to the different culture media used, which was Sauton in the case of Vergnolle *et al.* and Middlebrook 7H9 in my case. Both culture media have different compositions; the main differences are the carbon source, having Sauton medium 6% glycerol in comparison to non-added in the culture medium I used, and the absence of BSA in Sauton medium. This change in composition is the reason why a different phenotype has been observed. The research I performed during my PhD has shown a change in the growth by Mtb *Δrv0998* compared to the parental strains at pH 5.5 in presence/absence of BSA.

Albumin is a 66 kDa protein constituting approximately 50% of all plasma proteins, present in blood at a concentration of 35–50 mg/mL.[456] Albumin binds fatty acids released into the blood from adipose cells. The effect of serum albumin on the growth of tubercle bacilli was investigated by Dubos *et al*. where they confirmed that purified albumin from human, equine and bovine serum facilitates the submerged growth of tubercle bacilli in synthetic liquid media.[439] BSA is commonly added in culture medium for Mtb as albumin promotes Mtb growth by binding to unesterified fatty acids otherwise toxic for the mycobacterium.[439] Albumin binds with the carboxyl group of fatty acids increasing their solubility in aqueous solutions.[438,440] Furthermore, when fatty acids are detoxified, they can be used by Mtb.[438]

The purpose of this project was firstly to determine the role of albumin in Mtb physiology. Secondly, I wanted to evaluate if the cAMP dependent lysine acetyltransferase Rv0998 played a role in the Mtb phenotype observed under the presence or absence of BSA at pH 6.8 and 5.5. Additionally, I wanted to investigate the consequences of lysine acetylation by Rv0998 for the physiology and virulence of Mtb. To investigate this, targeted and untargeted metabolomics were performed as well as proteomic and infection assays.

Optimal growth of Mtb in culture medium such as Middlebrook 7H9 medium has been observed at a slightly acid pH, between 5.8 and 6.8. However, the bacilli display almost no replication at a pH under 5.5.[429] Due to the physiological relevance of pH 5.5 in the Mtb infectious cycle and to further understand the role of BSA in Mtb physiology, I investigated the growth of Mtb at pH 5.5

in the presence or absence of BSA and at pH 6.8 (for optimal growth conditions) in the presence or absence of BSA. After growing the wild type strain of Mtb CDC1551 at pH 6.8 in the presence or absence of BSA, I demonstrated that in the presence of BSA there is an increased growth of the bacillum compared to when BSA is absent. Furthermore, when grown at pH 5.5 in the absence of BSA, the bacterium had an impaired growth compared to when BSA was present. As expected, a pH of 5.5 decreased the bacterial growth in the presence and absence of BSA. These results demonstrate that the presence of BSA in culture medium as well as the pH have an effect on Mtb growth.

To mimic one of the macrophage environmental cues in an *in vitro* setting I also studied the intracellular cAMP levels in the wild type strain of Mtb exposed to pH 5.5 in the absence of BSA. My aim was to show that intracellular levels of cAMP are modulated by the presence or absence of BSA and to investigate if these levels can also be modulated depending on the pH of the host environment. Bacteria were initially grown in the presence or absence of BSA at pH 6.8 until exponential phase and then exposed for one doubling time to pH 6.8 or pH 5.5. The results obtained demonstrate an increase in the levels of cAMP when Mtb was grown in the absence of BSA at pH 6.8 and 5.5 compared to the presence of BSA. This is consistent with Bai *et al*.'s work which reported that the addition of 0.5% albumin to Sauton, significantly inhibited cAMP secretion, and reduced the overall levels of cAMP in treated samples and thus that albumin was the cause of the reduced cAMP levels in *M. bovis* BCG.[181]

An increase in Mtb cAMP production has important implications for gene regulation and propionate acquisition while within a host.[441] It is known that the levels of cAMP levels may modulate Mtb metabolism by protein acetylation through the activity of the cAMP-dependent protein acetyltransferase Rv0998.[201,457] Therefore, I performed untargeted metabolomics on Mtb grown in the presence or absence of BSA exposed to pH 6.8 or pH 5.5 to be able to observe changing metabolites according to changes in pH or to the presence/absence of BSA. I observed 1437 and 1024 changing metabolites between Mtb grown in the absence or presence of BSA at pH 6.8 in positive and negative ion mode respectively. When exposed to pH 5.5, Mtb exhibited 302 and 501 changing metabolites when grown in the absence of BSA compared to the presence of BSA. Thus, these results suggest metabolome remodelling of Mtb in the presence or absence of BSA. Regarding the exposure of Mtb to different pH conditions, a change in metabolites was also seen except in negative ion mode when Mtb was grown without BSA. Specifically, 1484 and 76 metabolites changed between Mtb stressed at pH 5.5 or not in the presence of BSA. However, 4 metabolites changed between Mtb stressed or not at pH 5.5 in the absence of BSA. These data

suggest a potential metabolome remodelling in order to adapt to the absence of BSA, a condition found in host macrophages. Moreover, the changes in metabolites after exposure to pH 5.5 compared to 6.8 in the presence of BSA also suggest metabolome remodelling in order to adapt to the stressful conditions of acidic pH. Finally, the fact that when Mtb is grown in the absence of BSA there are only 4 changing features in positive ion mode and none in negative ion mode between bacteria challenged and unchallenged at pH 5.5 suggests that bacterial adaptations to this hostile condition might not depend on metabolic changes.

Since there is a change in cAMP levels of Mtb depending on whether it is grown in the presence or absence of BSA I decided to investigate the cAMP-dependent lysine acetyltransferase Rv0998. Rv0998 has a cAMP affinity of 100 µM[415] and a role in central carbon metabolism.[180] To understand if this protein has an impact on the changes of cAMP the wild type, *Δrv0998* and complemented strains of Mtb were grown in 7H9 medium containing dextrose as the sole carbon source at pH 6.8 and 5.5 in the presence of BSA. Surprisingly, the mutant strain lacking *rv0998* had an impaired growth compared to the parental strains at acidic pH in the presence of BSA, which differs from the phenotype Vergnolle *et al*. observed. Work by Vergnolle *et al*. reported an increased growth by Mtb *Δrv0998* compared to the parental and complemented strains at pH 6 in Sauton medium.[420] As mentioned earlier in this discussion, Sauton medium presents different components from the mycomedium (7H9) I used to perform my experiments. The main differing components are the presence of BSA in mycomedium and the different carbon source. Therefore, the wild type, *Δrv0998* and complemented strains of Mtb were grown in 7H9 medium containing dextrose as the sole carbon source at pH 6.8 and 5.5 without BSA. In this case, the same trend was observed as that seen by Vergnolle *et al*., where the mutant grew better than the parental and complemented strains.[420] This result suggested that the change in phenotype was not due to a change in carbon source but was caused by the presence or absence of BSA.

The difference in the growth of the Mtb mutant strain lacking *rv0998* when cultured in the presence or absence of BSA at pH 5.5 could be due to the release of free fatty acids from BSA. Lynn *et al*. have reported the presence of 686 µg of fatty acids per gram of albumin.[438] These are palmitic acid, stearic acid, oleic acid and linoleic acid.[438] These free fatty acids are toxic to Mtb, particularly at low pH.[429] Thus, the Mtb mutant strain lacking *rv0998* appears to be more susceptible to low pH in growth medium which contains BSA, suggesting that lysine acetylation by Rv0998 contributes to Mtb survival under pH 5.5. However, in the absence of BSA, free fatty

acids are not released and the lack of lysine acetylation by Mtb *Δrv0998* allows an increased growth from this strain in comparison to the parental and complemented strains of Mtb.

Following growth monitoring experiments, I measured the intracellular levels of cAMP in the presence and absence of BSA and in unchallenged and challenged Mtb at pH 5.5. Potential changes between the wild type, *Δrv0998* and complemented strains of Mtb were investigated. Statistically significant decreases of 2.2- and 2-fold in intracellular levels of cAMP were seen in the Mtb *Δrv0998* strain compared to the wild type strain at pH 6.8 and 5.5 respectively when grown in the presence of BSA. This suggests that a change in cAMP levels is not correlated with the impaired growth of the mutant at pH 5.5 in the presence of BSA. Moreover, untargeted metabolomics analysis was performed to be able to see a broader spectrum of the potential changes in metabolism under the presence and absence of BSA as well as between unchallenged and challenged Mtb at pH 5.5. As expected, the presence and absence of BSA caused a change in metabolites. Understanding the specifics of the changing metabolites would be valuable for this research and will need to be pursued in the future.

In a number of systems, including *E. coli* and Salmonella, lysine acetylation has been shown to regulate carbon metabolism.[388,458] In particular, analysis of the acetylome by proteomics, biochemical assays and physiological studies have implicated acetyl- and acyl-CoA ligases as targets of bacterial protein acetyltransferase mediated regulation in gram-negative bacteria.[459,460] In mycobacteria, Rv0998 has similarly been found to acetylate both the ACS and 10 different FadD paralogs that function as acyl-CoA ligases.[193] This family of enzymes activates organic acids, such as fatty acids, that are eventually catabolised to acetyl-CoA. The coordinated regulation of this class of enzymes by acetylation has led to the suggestion that Rv0998 orthologues function to regulate the formation of acetyl-CoA,[460] which feeds oxidative TCA reactions. Based on these previous observations, it was hypothesised in this study that Rv0998 may be involved in regulating TCA fluxes. To specifically quantify the effect of Rv0998 on central carbon metabolism, I used stable isotope tracing using [$^{13}C_6$-glucose].[425] The Mtb wild type, *Δrv0998* and complemented strains were exposed for one doubling time to pH 5.5 and 6.8 in the presence or absence of BSA. These assays showed the different carbon incorporation of metabolites involved in the central carbon metabolism between the wild type, *Δrv0998* and complemented strains when Mtb is exposed to the mentioned conditions for 24 hours. At pH 6.8 in the presence and absence of BSA, the wild type incorporated [$^{13}C_6$-glucose] into all measured TCA metabolites. This is consistent with the use of a canonical TCA cycle.[424] An increase of 20% and 22% in the label was seen in the wild type strain in α-KG and 2-MC

respectively when grown in the absence of BSA compared to the presence of BSA. This suggests a preferential use of oxidative reactions that convert citrate to α-KG in the absence of BSA compared to a potential preferential use of reductive reactions in the presence of BSA.[425,461,462] I also measured the incorporation of [$^{13}C_6$-glucose] label in other compounds important for the bacterium. These were: amino acids (lysine, leucine, valine, ornithine and threonine); a purine derivative involved in nucleotide degradation (hypoxanthine); and intermediates of peptidoglycan biosynthesis (2-aminoadipic acid, diaminopimelic acid and D-alanyl-D alanine).[463] The Mtb wild type, *Δrv0998* and complemented strains incorporated [$^{13}C_6$-glucose] into all targeted compounds except hypoxanthine, where [$^{13}C_6$-glucose] label was barely detectable in the parental strains when grown in the absence of BSA and non-existent in the Mtb *Δrv0998* strain. This could suggest a decrease in the deamination of adenine in the absence of BSA.[464] Furthermore, Mtb *Δrv0998* exhibited a 15% increase in label incorporation in threonine compared to the wild type when grown at pH 6.8 in the absence of BSA.

At pH 5.5 in the presence and absence of BSA, the three strains incorporated [$^{13}C_6$-glucose] into all measured TCA metabolites, which is consistent with the use of a canonical TCA cycle.[424] The wild type strain of Mtb had an increase in the percentage of the label in leucine, valine and hypoxanthine, when grown in the absence of BSA compared to the presence of BSA. This shows an increase in carbon incorporation in Mtb grown in the absence of BSA compared to the presence of BSA. Also of note is that Mtb *Δrv0998* incorporated more [$^{13}C_6$-glucose] in comparison to the wild type strain in 2-MC when grown in the absence of BSA. This demonstrates a higher turnover in this TCA cycle metabolite in the absence of BSA in Mtb *Δrv0998* when grown at pH 5.5 and correlates with my previous growth curves data, where Mtb *Δrv0998* had an increased growth at pH 5.5 in the absence of BSA. Additionally, the amino acids valine and lysine exhibited an increase in the percentage of the label in the Mtb *Δrv0998* strain compared to the wild type strain, demonstrating an increase in carbon incorporation in the absence of BSA.

Previous research by Liu *et al.* has identified acetylation sites of proteins involved in the TCA cycle, glycolysis/gluconeogenesis and fatty acid metabolism.[381] To investigate the consequences of lysine acetylation and the potential targets of Rv0998, I carried out proteomics experiments in collaboration with Dr Agyro Tsipa (SynbiCITE) by analysing the whole acetylome of Mtb wild type, *Δrv0998* and complemented strains grown at pH 6.8 and 5.5 in the presence or absence of BSA. After optimising the protocol, preliminary data were obtained with potential acetylated proteins which will require further investigation. Of note is that proteins involved in virulence,

detoxification and adaptation were only acetylated by the wild type strain and not by Mtb *Δrv0998* when grown at pH 5.5 in the presence as well as absence of BSA. In the presence of BSA; Rv0440, Rv1908c, Rv1991c and Rv0384c were lysine acetylated. Rv0440 prevents misfolding and promotes the refolding and proper assembly of unfolded polypeptides generated under stress conditions.[445] The gene which encodes this protein is essential. Rv1908c has been seen to potentially play a role in the intracellular survival of mycobacteria within macrophages; that is, protection against reactive oxygen and nitrogen intermediates produced by phagocytic cells.[445] Regarding Mtb grown at pH 5.5 in the absence of BSA, Rv1967, Rv0171 and Rv2373c appeared to be only acetylated by the wild type. The first two present unknown functions but are thought to be involved in host cell evasion which would correlate with being acetylated in the conditions found within the macrophage.

Also important to notice was that when Mtb was grown at pH 5.5 in the absence of BSA, no proteins involved in lipid metabolism were seen to be acetylated whereas Rv3234c and Rv1925 were acetylated when grown in the presence of BSA at pH 5.5. Rv1925 is a probable acyl-CoA ligase FaD31.[193] When Mtb was grown in the absence of BSA at pH 6.8, one protein involved in lipid metabolism, Rv2384 (MbtA), was lysine acetylated compared to seven when grown at the same pH in the presence of BSA. MbtA is an adenylating enzyme, which catalyses the first step of mycobactin biosynthesis as it has already been mentioned in the introduction of this chapter.[420] Vergnolle *et al*. already described MbtA as a substrate of Rv0998 and its inhibition upon lysine acetylation.[420] Furthermore, no regulatory proteins were acetylated by Mtb when grown in the absence of BSA at pH 5.5 in contrast to when grown at the same pH in the presence of BSA (Rv0117, Rv2989 and Rv3849), at pH 6.8 in the absence of BSA (Rv3849) and at pH 6.8 in the presence of BSA (Rv1353c). Rv3849 was lysine acetylated when Mtb was grown at pH 6.8 in the absence of BSA. This protein regulates transcription of genes required for ESX-1 system. Rv0117, Rv2989 and Rv3849 were lysine acetylated when Mtb was grown at pH 5.5 in the presence of BSA. Rv0117 has been seen to potentially have effect functions of OxyR during evolution whereas Rv3849 regulates the transcription of genes required for ESX-1 system. OxyR is the central regulator of the bacterial oxidative stress response, which has been inactivated during evolution of Mtb.[465] ESX-1 is a specialised secretion system that allows a 6 kDa early secretory antigenic target (ESAT-6), a pore-forming toxin, to be secreted.[466]

Proteins involved in the TCA cycle were also found to be acetylated. For instance, Rv0952, Rv1934c and Rv1449c were acetylated when Mtb was grown at pH 6.8 in the presence of BSA.

Rv0952 is a probable succinyl-CoA synthetase; Rv1934c is a probable acyl-CoA dehydrogenase; and Rv1449c is a transketolase which, together with transaldolase, provides the link between the glycolytic and the pentose-phosphate pathways.[445,446] When Mtb was grown at the same pH in the absence of BSA, Rv1248c and Rv0946c were acetylated. Rv1248c is a multifunctional α-KG metabolic enzyme having α-KG dehydrogenase, decarboxylase and synthase activities.[467] Rv0946c is a probable glucose 6-phosphate isomerase (glycolysis/gluconeogenesis).[445,446] When wild type Mtb was grown at pH 5.5 in the presence of BSA, Rv2220 was acetylated, and in the absence of BSA Rv0157 was acetylated. Rv2220 is a glutamine synthetase[468] whereas Rv0157 is a probable NAD(P) transhydrogenase.[445,446] These results confirm that Rv0998 plays a role in central carbon metabolism and that Rv0998 substrates vary according to the environmental conditions the bacterium is exposed to; in this case those conditions were pH and the presence/absence of BSA. Altogether, further analysis of the data needs to take place in order to understand in depth what roles Rv0998 plays in Mtb central carbon metabolism.

To understand if Rv0998 plays a role in Mtb virulence, infection assays were performed. Studies have shown that activation of *M. avium*-infected macrophages with IFN-γ effectively restricts mycobacterial growth[469] and also restricts the fusion of endosomes with the mycobacterial vacuole. This suggests a way of restricting access to nutrients via the endosomal pathway and raises the possibility of apoptotic macrophages limiting the access of nutrients to the infecting parasites.[140] Therefore, an increased growth of bacteria, which infected resting macrophages compared to bacteria, which infected IFN-γ activated macrophages was expected. In my study, infection of macrophages by the wild type, mutant strain lacking *rv0998* and complemented strains of Mtb were performed. No growth was seen between the three strains at day 2 post-infection. This is consistent with work by Van der Ven *et al*., which reported an initial drop in bacterial viability over the first 2 days confirming that the transition was stressful for Mtb.[450] They demonstrated that bacterial replication is rapid during early infection, which slowed considerably from days 2 to4, and then recommenced from day 4–6 onwards.[450] In the work shown in this chapter, Mtb *Δrv0998* exhibited an increased growth in both resting and activated macrophages after day 5 post-infection. This is consistent with the results shown in this chapter monitoring the growth at pH 5.5 without BSA, where an increased growth by Mtb *Δrv0998* compared to the parental and complemented strains was observed. Furthermore this is consistent with the fact that the lack of acetylation by Rv0998 increases the adaptation of Mtb to hypoxia and the transcription of DosR-targeted genes.[417]

Further cytokine quantification of TNF-α production by infected macrophages showed how IFN-γ -activated macrophages infected with the wild type strain produced 2.5-fold more TNF-α after two days of infection in comparison to resting macrophages, which was expected as one of the main TNF-α producing cells are activated macrophages.[470] TNF-α can act in synergy with IFN-γ stimulating the production of oxidative burst mediating the tuberculostatic function of macrophages[449].

Altogether, the results obtained suggest that in the presence of BSA at pH 5.5 Rv0998 contributes to Mtb growth. However, when Mtb is exposed to pH 5.5 in the absence of BSA, no free fatty acids can be released from this source; yet it cannot be discarded that other free fatty acids could be released from the own bacteria. Nevertheless, my data suggest that the absence of lysine acetylation contributes to Mtb growth at pH 5.5 in the absence of BSA. This has been confirmed with macrophage infections, where Mtb *Δrv0998* grew more than the parental and complemented strains. Additionally, the labelling analysis that was performed confirmed an increase in carbon incorporation in some metabolites by the mutant strain at pH 5.5 grown without BSA compared to the wild type.

Chapter 6: Final discussion

6. Final discussion

TB, caused by the bacillus Mtb, represents a significant healthcare burden with approximately 10 million cases of human TB and 1.6 million TB deaths per year. From those, 569,000 cases are caused by MDR and XDR TB; and 900,000 cases are from HIV-associated TB causing 300,000 deaths (World Health Organisation, 2018).[4] Mtb is transmitted through the air when fine particles containing the bacteria are coughed up by an individual with active disease. These particles travel through the respiratory tract to the lower lungs of a new host. There, bacteria infect and recruit macrophages, which can acidify after activation and are rich in cholesterol and fatty acids.[435]

It is well established that innate immunity plays an important role in the development of TB immunity under the effects of several cytokines such as IFN-γ and TNF-α. IFN-γ is crucial for the full activation of macrophage bactericidal functions (such as drop in pH, NO production and restriction of mycobacterial growth) and further enhancement of innate cytokine production;[471] TNF-α contributes both to protection against TB and to immunopathology.[451,452] The granuloma is formed by macrophages surrounded by a collar of mononuclear leukocytes, principally lymphocytes, and plasma cells. In its early stages, the granuloma expands the infection by allowing bacteria to spread to the newly arriving macrophages. However, when adaptive immunity develops, the granuloma can restrict bacterial growth. Nevertheless, under certain conditions, such as immunosuppression from the host, infected macrophages undergo necrosis, which forms a necrotic core supporting bacterial growth and transmission to the next host.[19] Within the macrophages, the bacterium is able to resist, adapt to and survive the drastic environmental cues found there.[43] These include changes in pH, osmolarity, nutrient starvation and hypoxia, among others.[472] Understanding how Mtb regulates its growth rate in response to environmental cues encountered during infection should provide insight into the physiology that makes Mtb a successful and difficult to treat pathogen.[435,473] Furthermore, understanding the mechanisms Mtb uses to adapt, and therefore persist inside the host cells, would aid the development of new drugs to fight TB. Signal transduction by secondary messengers has been seen to play a role in this process since it mediates the ability to sense and respond to changing environments.[170] Upon changes in the extracellular environment, cyclases (adenylyl and guanylyl cyclases) and PDEs synthesise or degrade the second messengers. This way the intracellular levels of second messengers are controlled. The binding between second messengers and effector molecules causes the latter to have a conformational change thus inducing a physiological output.[143,144,146] Cyclic nucleotides are second messengers and they

include 3',5' cAMP, first discovered in 1957.[143] In *E. coli,* cAMP is mainly involved in carbon catabolite repression mediated by the cAMP-CRP complex.[158,159] cAMP modulates critical signalling pathways within individual organisms[148] and exploits these pathways during their infective and disease-causing life cycles.[148,474] Mtb H37Rv encodes for 16 distinct ACs, which form cAMP from ATP in a metal-dependent manner.[145] This is an exceptionally large number compared to other bacteria such as *E. coli*, where only one AC is present in its genome. The high number and variety of ACs compared to *E. coli* suggests that cAMP signalling plays a complex and important role of in mycobacteria.[166]

The treatment for active TB is a six-month long course of antibiotics for antimicrobial sensitive TB; the course is up to four years for MDR and XDR TB.[475] In the case of sensitive TB, if the treatment is fully followed, its success is approximately 85%. However, the regimen is lengthy, hepatotoxic, and not well tolerated by a considerable proportion of patients to whom the medication has been prescribed.[22] Furthermore, in the case of MDR-TB treatment, many of the drugs used have serious side effects such as peripheral neuropathy and renal toxicity effects[25] leading to an increased rate in treatment default, further increasing resistance. Drugs to treat TB are not the only ones known to cause adverse effects on mammalian cells. For instance, vancomycin used to treat MRSA has been linked with nephrotoxicity.[228] Although antibiotic mechanisms of action and their targets have been extensively studied and well characterised in bacteria, the effects of these antibiotics on mammalian cells remains unclear.[230] There are current methods to assess antibiotic toxicity. Nevertheless, these solutions are expensive and/or time-consuming.[264–266]

Thus in Chapter 3, I developed a new and fast method to assess antibiotic toxicity. I aimed to investigate if treatment with antibiotics could lead to a remodelling of the cell lipidome, as it is known that antibiotic treatment leads to an impairment of the bioenergetics of the cell.[230] For instance, research studies have shown that clinically relevant concentrations of antibiotics induce the formation of lethal ROS and mitochondrial dysfunction in mammalian cells. This is caused by the TCA cycle and the ETC disruption.[230,255–258] Mitochondria are the main cellular energy source since they couple the oxidation of fatty acids and pyruvate to ATP production by the ETC. Mitochondria have their own genome and a double membrane structure,[231] which is composed of an outer membrane and an inner membrane. The OMM and IMM contain structural PL, which are negatively charged molecules. These include PE, PC, PI and CL. However, PL abundance varies between the OMM and IMM. It has been reported that in the mammalian OMM, 54% of the total are PC, 29% are PE and 14% are PI.[232] Regarding the IMM, PC and PE are

still the most abundant PLs. They comprise about 75% of total lipids.[233] Nevertheless, one of the largest differences between OMM and IMM lipid composition is the highest CL concentration found in the IMM.[233] CL are found almost exclusively in the IMM making up about 15% to 20% of the total PL mass.[232] Moreover, they are associated with enzymes and oxidative phosphorylation complexes involved in ATP biosynthesis and the maintenance of the ETC.[233,259] Thus, I hypothesised that mitochondrial damage caused by antibiotics could be detected at the lipid level by measuring the ratio of CL:PI and that changes in this ratio could be used as potential markers of antibiotic toxicity. This being the case, lipidomics and high throughput technologies could be used as an alternative to probe changes in the relative abundance of PI and CL as a readout of mitochondrial damage resulting from antibiotic toxicity. I assessed the toxicity of aminoglycosides such as kanamycin, in three different cell types using intact cell-targeted lipidomics. Epithelial HeLa cells, RAW 264.7 mouse macrophages and mouse BMDMs were tested. The data obtained demonstrate there is no direct correlation between the ratio of CI to PI and the maximal mitochondrial respiratory capacity (the maximum respiration rate a cell can achieve). Only the aminoglycoside kanamycin can trigger changes in the CL:PI ratio. Effectively, my results based on the intact cell lipidomics and CL:PI ratio are in line with those found in the literature where aminoglycosides, including kanamycin, have been shown to modulate phosphoinositide signalling and metabolism in the cytoplasm and in the nucleus.[318,319,476–478] I cannot rule out the possibility that a decrease in the maximal rate of mitochondrial oxygen consumption alters metabolic pathways; however, using state-of-the-art metabolomics tools such as high-sensitivity and high-resolution LC-MS-based approaches will make this area exciting for future investigations.

Altogether I have provided a new approach for assessing antibiotic toxicity based on the lipid profile. By using MALDI-MS in the negative ion mode directly on intact and unprocessed HeLa, RAW 264.7 and BMDM cells, I am able to perform targeted lipidomic profiling of PI and CL. This is achieved using as few as 100−1000 cells per MALDI well with limited sample preparation. Thus, this method represents a major advance and can be used as an alternative to rapidly assess as a screening assay, the toxicity of a compound that interferes with PI metabolism prior to in-depth analysis of the entire lipidome using conventional lipidomics approaches. I strongly believe that this methodology can go well beyond the scope of this study and can also be applied to more cell types and purposes such as lipidome remodelling to probe cancer diagnostics/metabolism, since lipids such as phosphoinositides are important signalling molecules in cancer.[479] Using this methodology could allow the profiling of changes within the lipid composition of cancer cells

and help to understand the complex connections between lipid metabolism and cell function in cancer.

In Chapter 4, I investigate how mycobacteria cope with exposure to 250 mM NaCl via cAMP. During the natural infection cycle, Mtb occupies different niches which include airway surface liquid, plasma, cerebrospinal fluid, and macrophages.[304] All these niches have varying NaCl concentrations going from 50 mM in the airway surface liquid to 250 mM NaCl inside the macrophages.[304] I investigated if mycobacteria respond to a physiological concentration of NaCl, 250 mM,[341] one of the cues found in the macrophage, via modulation of mycobacteria cAMP levels. This was achieved by using a combination of LC-MS based metabolite analysis, combined with stable isotope labelling, as well as genetic mutants. The results I obtained in this study demonstrate that only Mtb is able to increase its intracellular levels of cAMP in response to NaCl stress. PknD, an eukaryotic-like-serine-threonine protein kinase is a candidate to orchestrate the increase of cAMP.[340] Mtb uses PknD to sense and adapt to NaCl stress via phosphorylation of the anti-sigma factor. Upon an increase in extracellular osmolarity the expression of a PknD substrate is induced and leads to the regulation of virulence factor production, bacterial transcription and cell wall remodelling.[340] PknD has been reported to be the sensor kinase under the concentration found in the serum of 140 mM NaCl.[340] I therefore hypothesised that this kinase may also be responsible for the increase in intracellular cAMP levels observed in Mtb at 250 mM NaCl, which is the concentration found in macrophages.[341] Since my results show that PknD only partially governs the intracellular cAMP increase in Mtb after exposure to 250 mM NaCl, CRP_{Mt} was investigated. In *E. coli,* CRP levels change with external osmolarity variation. This osmoregulation occurs at the level of *crp* gene expression and requires the cAMP molecule. Research by Balsalobre *et al*. discovered that the total levels of cAMP, especially the intracellular levels, were significantly increased at high osmolarity in *E. coli*. This suggested that osmolarity directly affected the synthesis and/or turnover of cAMP and emphasised how important cAMP is in the regulatory network by which bacterial cells adapt to changes in osmolarity.[336] My results provide the first evidence that only Mtb is able to increase its intracellular levels of cAMP in response to NaCl stress, and that the CRP_{Mt} is necessary in this process. Nevertheless, the exact mechanism leading to cAMP production via CRP_{Mt} and its consequences are not fully addressed in this thesis and will need to be investigated further. As a model of my hypothesis, Mtb would be pre-adapted to 250 mM NaCl exposure. Upon exposure to increased osmolarity, ACs would be triggered and, together with cAMP, would increase cAMP levels. This increase would be orchestrated by CRP_{Mt}. Surprisingly, even though *M. marinum* possesses 31 ACs and *M. smegmatis* contains 10 ACs as well as *crp* gene,[168] these organisms are not able to increase and

maintain their intracellular cAMP pool size in comparison to Mtb, in response to the concentration of NaCl found in the macrophages. In the future it would be of interest to investigate the presence of common and unique ACs in Mtb compared to in *M. smegmatis*, and *M. marinum*. For instance, Rv1359 and Rv2488c are two class III ACs found only in Mtb.[168] Nevertheless they do not present significant changes in transcript levels in the Mtb *Δcrp* strain compared to the parental strain. This evidence is based on RNAseq data and excludes the potential involvement of those ACs in the increase of cAMP levels in Mtb after exposure to 250 mM NaCls.[362] Furthermore, it would be of interest to investigate the difference in expression of the ACs in Mtb wild type and Mtb *Δcrp*. As reported in the literature, compared to the parental strain, the Mtb *Δcrp* strain has a 2-fold, 2.7-fold, 1.8-fold and 1.6-fold decrease in Rv3645, Rv1320c, Rv1318c and Rv1625c and a 3-fold and 2.6-fold increase in Rv0386 and Rv0891c.[361,362]

CRP_{Mt} controlls the expression of 114 genes in Mtb, all of which are potential candidates involved in the increase of intracellular cAMP levels in Mtb. Therefore, a second route of investigation could be to determine the difference in ACs activity in the *crp* deletion mutant compared to the parental Mtb strain, *M. smegmatis* and *M. marinum*. Indeed, activation of the ACs at the post-translational level provides prominent control over cAMP production. Identification of the AC(s) that respond(s) to NaCl still needs to be investigated. However, it has been reported that CRP has the ability to bend DNA and could potentially contribute to chromatin remodelling.[351] Interestingly, Rv0386, Rv1358 and Rv2488c contain ATPase as well as HTH DNA-binding domains. Thus, it can be hypothesised that the lack of *crp* leads to chromatin remodelling, and as a consequence leads to an impairment of the ACs activity. Among the three ACs, Rv2488c is the only one that contains a HTH DNA-binding domain, found in Mtb but not in *M. smegmatis* nor *M. marinum*.[168] This makes Rv2488c an ideal candidate to investigate the hypothesis that deletion of CRP_{Mt} leads to chromatin remodelling and therefore altering the AC activity after exposure to a concentration of 250 mM NaCl.

To decipher the increase in intracellular cAMP levels observed in Mtb, a third hypothesis could be the reduction in the degradation of cAMP by a cyclic-nucleotide PDE under exposure to a concentration of 250 mM NaCl in Mtb compared to *M. smegmatis* and *M. marinum* and Mtb *Δcrp*. To date, Rv0805 is the only cAMP PDE identified and it is found only in slow-growing mycobacteria.[190,480,481] Interestingly, it is thought that the *rv0805* gene is regulated by CRP,[351,362] making Rv0805 a good candidate to explain the phenotype observed in Mtb but not in *M. smegmatis* since no homologues have been identified. To support the hypothesis that an alteration of the degradation of cAMP after exposure to a concentration of 250 mM NaCl occurs,

the presence of other cAMP PDE in mycobacteria and the modulation of their activity under NaCl stress needs to be investigated. Yet, the identification and characterisation of the cAMP PDE(s) also still needs to be explored.

Lastly, the fourth and final avenue of research which could be investigated is the secretion of cAMP as a mechanism of regulation of intracellular cAMP levels in all the strains tested in this study. Indeed, as reported in the literature, mycobacteria are known to secrete a large amount of cAMP into the culture medium.[339,482] Therefore, a concentration of 250 mM NaCl could potentially trigger the secretion of cAMP in *M. smegmatis*, *M. marimum* and Mtb Δ*crp* but not in Mtb where higher intracellular cAMP levels could be required to stimulate growth under osmotic stress at 250 mM NaCl, promoting survival of the bacilli *via* allosteric regulations of the cAMP-binding proteins.[351,483–485] Based on this reflection, in the Mtb strain lacking CRP_{Mt} an increase in cAMP secretion could be expected in comparison to the parental Mtb strains to explain such a discrepancy in intracellular cAMP levels between the two strains.

In this study, the use of metabolomics and genetics provides the first evidence that only is Mtb able to increase its intracellular levels of cAMP in response to NaCl stress, and that CRP_{Mt} is necessary in this process. However, the complete and sophisticated mechanism and role of CRP_{Mt}/cAMP in this process still needs to be elucidated. Thus understanding how CRP_{Mt} is key in Mtb adaptation could be used for the discovery of a new strategy to tackle TB.

Finally in Chapter 5 I investigate the role of Rv0998, a cAMP-dependent lysine acetyltransferase,[194,365] in Mtb adaptation and virulence. Lysine acetylation is a post-translational modification used by many organisms in order to modulate stability, protein-protein and DNA-protein interactions in biological processes, by changing protein charge or conformation.[382,383] Acetylation of lysine residues can be reversed by deacetylases.[384,385] Reactions catalysed by acetyltransferases require acetyl-CoA connecting the cell energy status to protein acetylation.[386,387] By using proteomics, 191 out of 4525,[388] 170 out of 4124[389] and over 2000[390] proteins have been found to be lysine acetylated in *S. enterica*, *E. coli* and humans respectively. From these, several have been identified as stress response proteins, transcription or translation regulators and central metabolism enzymes, involved in glycolysis, gluconeogenesis, the TCA cycle and fatty acid metabolism.[391] Increasing evidence shows that lysine acetylation may play an important role in the pathogenesis of Mtb and immunogenicity.[381] Rv0998 is encoded as full-length protein in all sequenced mycobacterial species. It shares 56% protein sequence identity with its orthologue in *M. smegmatis*,

MSMEG_5458[391] and both lysine acetyltransferases have been reported to bind to cAMP. However, the cAMP affinity of Rv0998, which is 100 µM, is 1000-fold lower than the cAMP affinity of MSMEG_5458, which is 100 nM.[415] Different substrates of Rv0998 have been identified. These include Acetyl-Coa synthetase, fatty acetyl-CoA synthetase, FadD33 and DosR.[391,417,418] Nambi *et al.* used a deletion mutant of the *rv0998* ortholog in *M. bovis* BCG (BCG_1055) and demonstrated a growth impairment of the mutant strain lacking BCG_1055 compared to the wild-type in *M. bovis* BCG when using propionate, the end product of cholesterol degradation,[193] as the sole carbon source.[193] Other experiments performed by Vergnolle *et al*. have demonstrated an increased growth of the Mtb mutant strain lacking *rv0998* in comparison to the parental and complemented strains grown in Sauton medium at pH 6.[420] By growing the same three strains in mycomedium (7H9) at pH 5.5 (pH found in the phagosome) I obtained a different phenotype, where Mtb *Δrv0998* had an impaired growth compared to the parental strains at pH of 5.5. I hypothesised that the different phenotypes could be a consequence of differing components between both culture media used; Sauton medium and 7H9. Both culture media have different compositions and the main differences are the carbon source and the presence or absence of BSA. Sauton medium contains 6% glycerol and no BSA in comparison to non-added glycerol and 0.5 g/L BSA in the culture medium I used. By monitoring the growth of the Mtb wild type, *Δrv0998* and complemented strains at pH 5.5 in 7H9 medium in the absence of BSA I suggest that the change in phenotype was not due to a change in carbon source but to the presence or absence of BSA. It is known that albumin constitutes approximately 50% of all plasma proteins, binds fatty acids released into the blood from adipose cells and is present in blood at 35–50 mg/mL.[456] Each albumin molecule can bind 10 molecules of fatty acid.[486] Moreover, albumin is commonly added in culture medium for Mtb since it promotes Mtb growth by binding to unesterified fatty acids that are otherwise toxic for the mycobacterium, causing retardation or inhibition of its growth.[438,439] Albumin binds with the carboxyl group of fatty acids, increasing their solubility in aqueous solutions.[438,440] Furthermore, when fatty acids are detoxified, they can be used by Mtb as nutrient growth factor.[438] Despite its importance, the role of albumin in Mtb physiology is not understood. Therefore I performed different experiments including growth monitoring experiments, targeted metabolomics and untargeted metabolomics, proteomics and finally macrophages infection. The results obtained demonstrate how Mtb *Δrv0998* has an increased growth at pH 5.5 in the absence of BSA at pH 5.5, and an impaired growth in the presence of BSA at pH 5.5 in comparison to the parental and complemented strains. Moreover, the data showed an increase in cAMP levels in Mtb when grown in the absence of BSA compared to when grown in the presence of BSA and a statistically significant increase in the percentage of the label in some metabolites of the central carbon

metabolism in Mtb *Δrv0998* in comparison to the parental strains when challenged at pH 5.5 in the absence of BSA. This demonstrates an increased carbon incorporation in the mutant strain compared to the parental and complemented strains, which correlates with the increase in growth by Mtb Δ*rv0998* previously observed. Moreover, the infection of BMDM with the wild type, *Δrv0998* and complemented strains of Mtb, confirmed the results, as the mutant strain had increased survival compared to the parental strains after 5 days of infection. Macrophages present no albumin and the activated phagosome has a pH of around 5.5.[429]

To better understand the phenotype observed, a whole acetylome analysis of Mtb wild type, *Δrv0998* and complemented strains grown at pH 6.8 or 5.5 in the presence or absence of BSA was performed. Previous work reported by Singhal *et al.* and Liu *et al.* has demonstrated a majority of Mtb acetylated proteins to be associated with metabolism.[414,444] Furthermore, studies by Ritterhaus *et al*., have shown that the immediate Mtb response to hypoxia relies on Rv0998 and involves a fast and transient induction of the DosR regulon, one of Rv0998 substrates.[425] Therefore, I wanted to identify what proteins are lysine-acetylated by Rv0998 at pH 5.5 in the presence and absence of BSA, and what their potential function would be. Further investigations are required to analyse the significance of the acetylation of each protein in the different conditions.

Altogether I hypothesise that the differences in growth by the Mtb mutant lacking *rv0998* at pH 5.5 in the presence or absence of BSA could be due to the release of free fatty acids by BSA in acidic pH.[429] These include palmitic acid, stearic acid, oleic acid and linoleic acid.[438] Upon growth at pH 5.5, BSA could release free fatty acids which would be detrimental to Mtb, in particular to Mtb *Δrv0998.* Thus lysine acetylation would contribute to Mtb survival in acidic pH.

Another hypothesis could be linked to the fact that BSA detoxifies free fatty acids.[438] Free fatty acids can be released by the own bacteria and by the host cell during infection. For instance, free mycolic acids can be generated during infection from trehalose-6,6´-dimycolate (TDM), a mycolic acid-containing glycolipid. TDM activates the formation of granulomas and leads to the stimulation of macrophages through receptors such as C-type lectin.[487] At this stage, the pathogen reduces its ability to cause induction of pro-inflammatory responses along with an increase in the uptake of nutrients to overcome starvation induced by the host; it also displays resistance to drugs.[487] On the other hand, fatty acids have also been seen to be liberated by the host from PL.[488] The reversible binding of fatty acids by albumin allows the fatty acids to serve as nutrient growth factors which enhance the growth of Mtb whereas in the absence of BSA the

fatty acid is bacteriostatic. Thus, BSA would buffer the fatty acid so that the concentration of free fatty acid is very low, below the bacteriostatic level.[489] As a model of my hypothesis, following Mtb exposure to acidic pH, BSA would bind to the carboxyl group of fatty acids, neutralising their bacteriostatic effect. However, when grown in the absence of BSA, the bacteriostatic effect of long-chain fatty acids would not be neutralised, and the wild type and complemented strains of Mtb would have an impaired growth compared to the mutant strain lacking *rv0998*. This could be due to the potential contribution to Mtb survival by the lack of acetylation. Thus, lysine acetylation by Rv0998 could be detrimental for Mtb growth in the absence of BSA at pH 5.5. This effect has been also seen in infected macrophages.

This research could contribute to the TB field as albumin is a highly abundant protein in the serum and could play a role in TB dissemination, defined when there are signs of TB infection in two different sites such as the lungs and the liver or the spleen.[490] It has been reported that the risk of TB increases gradually with lower serum albumin concentrations.[490] Thus it would be of interest to infect guinea pigs to understand the role of Rv0998 in a dynamic environment with changing albumin concentrations and different pH (pH 5.5 in the macrophage, pH 7.4 in the serum).

Another way to test my hypothesis could be to identify which fatty acids are released to the culture medium during the growth of the wild type, *Δrv0998* and complemented strain of Mtb. Therefore, after growing the three strains at pH 6.8 and 5.5 in the presence or absence of BSA I would extract the lipids of the culture medium and identify them by thin layer chromatography.

This thesis provides further understanding of how Mtb copes with the environmental stresses faced during its infectious cycle including osmotic and acid stress. The research shown here provides a new vision of Mtb physiology which could be used as a base for new treatments. Furthermore, I report a new methodology to assess antibiotic toxicity, which could be of use for developing new antibiotics.

Chapter 7: References

7. References

1. Comas, I. *et al.* Out-of-Africa migration and Neolithic coexpansion of Mycobacterium tuberculosis with modern humans. *Nat. Genet.* **45,** 1176–1182 (2013).
2. Wilson, L. G. Commentary: Medicine, population, and tuberculosis. *Int. J. Epidemiol.* **34,** 521–524 (2005).
3. WHO | Global tuberculosis report 2017. *WHO* (2017).
4. World Health Organization. *GLOBAL TUBERCULOSIS REPORT 2018*. (2018).
5. Demerec, M. *ORIGIN OF BACTERIAL RESISTANCE TO ANTIBIOTICS*'.
6. Barberis, I., Bragazzi, N. L., Galluzzo, L. & Martini, M. The history of tuberculosis: from the first historical records to the isolation of Koch's bacillus. *J. Prev. Med. Hyg.* **58,** E9–E12 (2017).
7. Gradmann, C. *Robert Koch and the Pressures of Scientific Research: Tuberculosis and Tuberculin*. *Medical History* **45,** (2001).
8. Singhal, R. & Myneedu, V. P. Microscopy as a diagnostic tool in pulmonary tuberculosis. *Int. J. Mycobacteriology* **4,** 1–6 (2015).
9. Rathnaiah, G. *et al.* Pathogenesis, Molecular Genetics, and Genomics of Mycobacterium avium subsp. paratuberculosis, the Etiologic Agent of Johne's Disease. *Front. Vet. Sci.* **4,** 187 (2017).
10. Liébana, E., Aranaz, a, Francis, B. & Cousins, D. Assessment of genetic markers for species differentiation within the Mycobacterium tuberculosis complex. *J. Clin. Microbiol.* **34,** 933–8 (1996).
11. Sinha, P. *et al.* Differentiation of Mycobacterium tuberculosis complex from non-tubercular mycobacteria by nested multiplex PCR targeting IS6110, MTP40 and 32kD alpha antigen encoding gene fragments. *BMC Infect. Dis.* **16,** 123 (2016).
12. Pai, M. *et al.* Tuberculosis. *Nat. Rev. Dis. Prim.* **2,** (2016).
13. Verma, R., Patil, T. B. & Lalla, R. Disseminated tuberculosis manifesting as pulmonary, meningeal and spinal tuberculosis in an immunocompetent patient. *BMJ Case Rep.* **2012,** (2012).
14. Gomes, T. *et al.* Epidemiology of extrapulmonary tuberculosis in Brazil: a hierarchical model. *BMC Infect. Dis.* **14,** 9 (2014).
15. Esmail, H., Barry, C. E., Young, D. B. & Wilkinson, R. J. The ongoing challenge of latent tuberculosis. *Philos Trans R Soc L. B Biol Sci* **369,** 20130437 (2014).
16. Barry, C. E. *et al.* The spectrum of latent tuberculosis: Rethinking the biology and intervention strategies. *Nat. Rev. Microbiol.* **7,** 845–855 (2009).

17. Wells, W. F., Ratcliffe, H. L. & Crumb, C. On the mechanics of droplet nuclei infection: II. Quantitative experimental air-borxr tuberculosis in rabbits. *Am. J. Epidemiol.* **47,** 11–28 (1948).
18. Bloom, B. R. *et al. Tuberculosis*. *Major Infectious Diseases* (2017).
19. Cambier, C. J., Falkow, S. & Ramakrishnan, L. Host Evasion and Exploitation Schemes of Mycobacterium tuberculosis. (2014). doi:10.1016/j.cell.2014.11.024
20. Pawlowski, A., Jansson, M., Sköld, M., Rottenberg, M. E. & Källenius, G. Tuberculosis and HIV co-infection. *PLoS Pathogens* (2012). doi:10.1371/journal.ppat.1002464
21. Tiemersma, E. W., van der Werf, M. J., Borgdorff, M. W., Williams, B. G. & Nagelkerke, N. J. D. Natural history of tuberculosis: Duration and fatality of untreated pulmonary tuberculosis in HIV negative patients: A systematic review. *PLoS One* **6,** (2011).
22. Tiberi, S. *et al.* Tuberculosis: progress and advances in development of new drugs, treatment regimens, and host-directed therapies. *Lancet Infect. Dis.* **18,** e183–e198 (2018).
23. WHO. *WHO treatment guidelines for drug-resistant tuberculosis OCTOBER 2016 REVISION*.
24. Caminero, J. A., Sotgiu, G., Zumla, A. & Migliori, G. B. Best drug treatment for multidrug-resistant and extensively drug-resistant tuberculosis. *Lancet Infect. Dis.* **10,** 621–629 (2010).
25. World Health Organization. *Annex 3. Potentially overlapping toxicities of antiretrovirals and anti-tuberculosis agents (including first-line anti-tuberculosis agents)*. (2011).
26. Luca, S. & Mihaescu, T. History of BCG Vaccine. *Maedica (Buchar).* **8,** 53–8 (2013).
27. Calmette, A. Preventive vaccination of the new-born against tuberculosis. *Br. Med. J.* **1,** 520 (1928).
28. Moliva, J. I., Turner, J. & Torrelles, J. B. Immune responses to bacillus Calmette-Guérin vaccination: Why do they fail to protect against mycobacterium tuberculosis? *Frontiers in Immunology* (2017). doi:10.3389/fimmu.2017.00407
29. Trunz, B. B., Fine, P. E. M., Dye, C. & Geneva, C.-. Eff ect of BCG vaccination on childhood tuberculous meningitis and miliary tuberculosis worldwide : a meta- analysis and assessment of cost-eff ectiveness. 1173–1180 (2002).
30. Feldstein, L. R. *et al.* Global Routine Vaccination Coverage, 2016. *MMWR. Morb. Mortal. Wkly. Rep.* **66,** 1252–1255 (2017).
31. Pai, M. & Sotgiu, G. Diagnostics for latent TB infection: Incremental, not transformative progress. *Eur. Respir. J.* **47,** 704–706 (2016).
32. Katial, R. K. *et al.* Cell-mediated immune response to tuberculosis antigens: comparison

of skin testing and measurement of in vitro gamma interferon production in whole-blood culture. *Clin. Diagn. Lab. Immunol.* **8,** 339–45 (2001).

33. Yang, H., Kruh-Garcia, N. A. & Dobos, K. M. Purified protein derivatives of tuberculin--past, present, and future. *FEMS Immunol. Med. Microbiol.* **66,** 273–80 (2012).
34. VILLARINO, M. E. *et al.* Comparison Testing of Current (PPD-S1) and Proposed (PPD-S2) Reference Tuberculin Standards. *Am. J. Respir. Crit. Care Med.* **161,** 1167–1171 (2000).
35. Rangel-Frausto, M. S., Ponce-de-León-Rosales, S., Martinez-Abaroa, C. & Hasløv, K. Tuberculosis and Tuberculin Quality: Best Intentions, Misleading Results. *Infect. Control Hosp. Epidemiol.* **22,** 481–484 (2001).
36. Menzies, D., Gardiner, G., Farhat, M., Greenaway, C. & Pai, M. Thinking in three dimensions: A web-based algorithm to aid the interpretation of tuberculin skin test results. *Int. J. Tuberc. Lung Dis.* **12,** 498–505 (2008).
37. Horvat, R. T. Gamma Interferon Assays Used in the Diagnosis of Tuberculosis. *Clin. Vaccine Immunol.* **22,** 845–9 (2015).
38. Herrera, V., Perry, S., Parsonnet, J. & Banaei, N. Clinical Application and Limitations of Interferon- Release Assays for the Diagnosis of Latent Tuberculosis Infection. *Clin. Infect. Dis.* **52,** 1031–1037 (2011).
39. Friedrich, S. O. *et al.* Assessment of the sensitivity and specificity of Xpert MTB/RIF assay as an early sputum biomarker of response to tuberculosis treatment. *Lancet Respir. Med.* **1,** 462–470 (2013).
40. WHO. Molecular line probe assays for rapid screening of patients at risk of multidrug-resistant tuberculosis (MDR-TB). *Policy statement* 1–9 (2008).
41. World Health Organization. WHO Guideline: The use of molecular line probe assays for the detection of resistance to isoniazid and rifampicin. 21–23 (2016).
42. World Health Organization. The use of loop-mediated isothermal amplifi cation (TB-LAMP) for the diagnosis of pulmonary tuberculosis. 52 (2016). doi:978 92 4 151118 6
43. Guirado, E., Schlesinger, L. S. & Kaplan, G. Macrophages in tuberculosis: friend or foe. *Semin. Immunopathol.* **35,** 563–83 (2013).
44. Stewart, G. R., Patel, J., Robertson, B. D., Rae, A. & Young, D. B. Mycobacterial mutants with defective control of phagosomal acidification. *PLoS Pathog.* **1,** 269–78 (2005).
45. Bansal-Mutalik, R. & Nikaido, H. Mycobacterial outer membrane is a lipid bilayer and the inner membrane is unusually rich in diacyl phosphatidylinositol dimannosides. *Proc. Natl. Acad. Sci.* **111,** 4958–4963 (2014).
46. Samanta, S., Singh, A., Biswas, P., Bhatt, A. & Visweswariah, S. S. Mycobacterial phenolic glycolipid synthesis is regulated by cAMP-dependent lysine acylation of

FadD22. *Microbiol. (United Kingdom)* **163,** 373–382 (2017).

47. Tran, V., Ahn, S. K., Ng, M., Li, M. & Liu, J. Loss of Lipid Virulence Factors Reduces the Efficacy of the BCG Vaccine. *Sci. Rep.* **6,** 29076 (2016).
48. Brennan, P. . *et al.* Structure, function, and biogenesis of the cell wall of Mycobacterium tuberculosis. *Tuberculosis* **83,** 91–97 (2003).
49. Zuber, B. *et al.* Direct visualization of the outer membrane of mycobacteria and corynebacteria in their native state. *J. Bacteriol.* **190,** 5672–80 (2008).
50. Gago, G., Diacovich, L. & Gramajo, H. Lipid metabolism and its implication in mycobacteria–host interaction. *Curr. Opin. Microbiol.* **41,** 36–42 (2018).
51. Daffé, M. & Draper, P. The Envelope Layers of Mycobacteria with Reference to their Pathogenicity. *Adv. Microb. Physiol.* **39,** 131–203 (1997).
52. Niederweis, M. Mycobacterial porins--new channel proteins in unique outer membranes. *Mol. Microbiol.* **49,** 1167–77 (2003).
53. Ortalo-Magne, A. *et al.* Molecular composition of the outermost capsular material of the tubercle bacillus. *Microbiology* **141,** 1609–1620 (1995).
54. Daffé, M. The cell envelope of tubercle bacilli. *Tuberculosis* **95,** S155–S158 (2015).
55. Karakousis, P. C., Bishai, W. R. & Dorman, S. E. Mycobacterium tuberculosis cell envelope lipids and the host immune response. *Cell. Microbiol.* **6,** 105–16 (2004).
56. van Crevel, R., Ottenhoff, T. H. M. & van der Meer, J. W. M. Innate immunity to Mycobacterium tuberculosis. *Clin. Microbiol. Rev.* **15,** 294–309 (2002).
57. Lyadova, I. V. & Panteleev, A. V. Th1 and Th17 Cells in Tuberculosis: Protection, Pathology, and Biomarkers. *Mediators Inflamm.* **2015,** 1–13 (2015).
58. Mortaz, E. *et al.* Interaction of Pattern Recognition Receptors with Mycobacterium Tuberculosis. *J. Clin. Immunol.* **35,** 1–10 (2015).
59. Mishra, A., Akhtar, S., Jagannath, C. & Khan, A. Pattern recognition receptors and coordinated cellular pathways involved in tuberculosis immunopathogenesis: Emerging concepts and perspectives. *Mol. Immunol.* **87,** 240–248 (2017).
60. Cooper, A. M. Cell-Mediated Immune Responses in Tuberculosis. *Annu. Rev. Immunol.* (2009). doi:10.1146/annurev.immunol.021908.132703
61. Akira, S., Uematsu, S. & Takeuchi, O. Pathogen recognition and innate immunity. *Cell* **124,** 783–801 (2006).
62. Takeuchi, O. & Akira, S. Pattern Recognition Receptors and Inflammation. *Cell* **140,** 805–820 (2010).
63. Gan, L. & Li, L. Regulations and roles of the interleukin-1 receptor associated kinases (IRAKs) in innate and adaptive immunity. *Immunol. Res.* **35,** 295–302 (2006).

64. Kay, E., Scotland, R. S. & Whiteford, J. R. Toll-like receptors: Role in inflammation and therapeutic potential. *BioFactors* **40,** 284–294 (2014).
65. Liu, Y., Yin, H., Zhao, M. & Lu, Q. TLR2 and TLR4 in autoimmune diseases: a comprehensive review. *Clin. Rev. Allergy Immunol.* **47,** 136–147 (2014).
66. Hossain, M. M. & Norazmi, M.-N. Pattern recognition receptors and cytokines in Mycobacterium tuberculosis infection--the double-edged sword? *Biomed Res. Int.* **2013,** 179174 (2013).
67. Ahmad, S. Pathogenesis, immunology, and diagnosis of latent mycobacterium tuberculosis infection. *Clin. Dev. Immunol.* **2011,** (2011).
68. Cui, S. *et al.* The C-Terminal Regulatory Domain Is the RNA 5'-Triphosphate Sensor of RIG-I. *Mol. Cell* **29,** 169–179 (2008).
69. Kawai, T. & Akira, S. Toll-like Receptors and Their Crosstalk with Other Innate Receptors in Infection and Immunity. *Immunity* **34,** 637–650 (2011).
70. Aderem, A. & Ulevitch, R. J. Toll-like receptors in the induction of the innate immune response. *Nature* **406,** 782–787 (2000).
71. Medzhitov, R., Preston-Hurlburt, P. & Janeway, C. A. A human homologue of the Drosophila toll protein signals activation of adaptive immunity. *Nature* **388,** 394–397 (1997).
72. Ishikawa, E., Mori, D. & Yamasaki, S. Recognition of Mycobacterial Lipids by Immune Receptors. *Trends Immunol.* **38,** 66–76 (2017).
73. Clifford V. Harding; W. Henry Boom. Regulation of antigen presentation by Mycobacterium tuberculosis: a role for Toll-like receptors. *Nat. Rev. Microbiol.* **8,** 296–307 (2011).
74. Elass, E. *et al.* Mycobacterial lipomannan induces matrix metalloproteinase-9 expression in human macrophagic cells through a Toll-like receptor 1 (TLR1)/TLR2-and CD14-dependent mechanism. *Infect. Immun.* **73,** 7064 (2005).
75. Doz, E. *et al.* Acylation determines the toll-like receptor (TLR)-dependent positive versus TLR2-, mannose receptor-, and SIGNR1-independent negative regulation of pro-inflammatory cytokines by mycobacterial lipomannan. *J. Biol. Chem.* **282,** 26014–26025 (2007).
76. Drage, M. G. *et al.* TLR2 and its co-receptros determine responses of macrophages and dendritic cells to lipoproteins of Mycobacterium tuberculosis. *Cell Immunol.* **258,** 29–37 (2010).
77. Bulut, Y. *et al.* Mycobacterium tuberculosis heat shock proteins use diverse toll-like receptor pathways to activate pro-inflammatory signals. *J. Biol. Chem.* **280,** 20961–

20967 (2005).

78. Underhill, D. M., Ozinsky, A., Smith, K. D. & Aderem, A. Toll-like receptor-2 mediates mycobacteria-induced proinflammatory signaling in macrophages. *Proc. Natl. Acad. Sci. U. S. A.* **96,** 14459–63 (1999).

79. Kleinnijenhuis, J. *et al.* Transcriptional and inflammasome-mediated pathways for the induction of IL-1?? production by Mycobacterium tuberculosis. *Eur. J. Immunol.* **39,** 1914–1922 (2009).

80. Chan, J., Xing, Y., Magliozzo, R. S. & Bloom, B. R. Killing of Virulent Mycobacterium tuberculosis by Reactive Nitrogen Intermediates Produced by Activated Murine Macrophages. **175,** (1992).

81. van Pinxteren, L. A. H., Cassidy, J. P., Smedegaard, B. H. C., Agger, E. M. & Andersen, P. Control of latentMycobacterium tuberculosis infection is dependent on CD8 T cells. *Eur. J. Immunol.* **30,** 3689–3698 (2000).

82. Ulrichs, T. & Kaufmann, S. H. E. New insights into the function of granulomas in human tuberculosis. *J. Pathol.* **208,** 261–269 (2006).

83. Torrado, E. & Cooper, A. M. IL-17 and Th17 cells in tuberculosis. *Cytokine Growth Factor Rev.* **21,** 455–62 (2010).

84. Chan, E. D., Chan, J. & Schluger, N. W. What is the role of nitric oxide in murine and human host defense against tuberculosis? Current knowledge. *Am. J. Respir. Cell Mol. Biol.* **25,** 606–612 (2001).

85. Saraav, I., Singh, S. & Sharma, S. Outcome of Mycobacterium tuberculosis and Toll-like receptor interaction: Immune response or immune evasion? *Immunol. Cell Biol.* **92,** 741–746 (2014).

86. Mootoo, A., Stylianou, E., Arias, M. A. & Reljic, R. TNF-in Tuberculosis: A Cytokine with a Split Personality. *Inflamm. Allergy -Drug Targets* (2009). doi:10.2174/187152809787582543

87. Algood, H. M. S., Lin, P. L. & Flynn, J. L. Tumor necrosis factor and chemokine interactions in the formation and maintenance of granulomas in tuberculosis. *Clin. Infect. Dis.* **41 Suppl 3,** S189–S193 (2005).

88. Roach, D. R. *et al.* TNF Regulates Chemokine Induction Essential for Cell Recruitment, Granuloma Formation, and Clearance of Mycobacterial Infection. *J. Immunol.* **168,** 4620–4627 (2002).

89. Saunders, B. M. & Britton, W. J. Life and death in the granuloma: Immunopathology of tuberculosis. *Immunol. Cell Biol.* **85,** 103–111 (2007).

90. Russell, D. G., Cardona, P. J., Kim, M. J., Allain, S. & Altare, F. Foamy macrophages and

the progression of the human tuberculosis granuloma. *Nat. Immunol.* **10,** 943–948 (2009).

91. Saunders, B. M. & Cooper, A. M. Restraining mycobacteria: Role of granulomas in mycobacterial infections. *Immunol. Cell Biol.* **78,** 334–341 (2000).
92. Puissegur, M. P. *et al.* An in vitro dual model of mycobacterial granulomas to investigate the molecular interactions between mycobacteria and human host cells. *Cell. Microbiol.* **6,** 423–433 (2004).
93. Ley, E. G. and K. Immune and Inflammatory Mechanisms of Atherosclerosis. *Annu Rev Immunol.* **1796,** 19–26 (2009).
94. Russell, D. G., VanderVen, B. C., Glennie, S., Mwandumba, H. & Heyderman, R. S. The macrophage marches on its phagosome: dynamic assays of phagosome function. *Nat. Rev. Immunol. Publ. online 10 July 2009; | doi10.1038/nri2591* **9,** 594 (2009).
95. Ramakrishnan, L. Revisiting the role of the granuloma in tuberculosis. *Nat. Rev. Immunol.* **12,** 352–366 (2012).
96. Blanc, L. *et al. Mycobacterium tuberculosis* inhibits human innate immune responses via the production of TLR2 antagonist glycolipids. *Proc. Natl. Acad. Sci.* 201707840 (2017). doi:10.1073/pnas.1707840114
97. Vergne, I., Gilleron, M. & Nigou, J. Manipulation of the endocytic pathway and phagocyte functions by Mycobacterium tuberculosis lipoarabinomannan. *Front. Cell. Infect. Microbiol.* **4,** 1–9 (2015).
98. Wagener, M., Hoving, J. C., Ndlovu, H. & Marakalala, M. J. Dectin-1-Syk-CARD9 Signaling Pathway in TB Immunity. *Front. Immunol.* **9,** 225 (2018).
99. Patin, E. C. *et al.* Trehalose dimycolate interferes with FcgammaR-mediated phagosome maturation through Mincle, SHP-1 and FcgammaRIIB signalling. *PLoS One* **12,** e0174973 (2017).
100. Axelrod, S. *et al.* Delay of phagosome maturation by a mycobacterial lipid is reversed by nitric oxide. *Cell. Microbiol.* **10,** 1530–1545 (2008).
101. Passemar, C. *et al.* Multiple deletions in the polyketide synthase gene repertoire of mycobacterium tuberculosis reveal functional overlap of cell envelope lipids in host-pathogen interactions. *Cell. Microbiol.* **16,** 195–213 (2014).
102. Cambier, C. J. *et al.* Mycobacteria manipulate macrophage recruitment through coordinated use of membrane lipids. *Nature* **505,** 218–222 (2014).
103. Mayer-Barber, K. D. *et al.* Caspase-1 independent IL-1beta production is critical for host resistance to mycobacterium tuberculosis and does not require TLR signaling in vivo. *J. Immunol.* **184,** 3326–30 (2010).

104. van der Wel, N. *et al.* M. tuberculosis and M. leprae Translocate from the Phagolysosome to the Cytosol in Myeloid Cells. *Cell* **129,** 1287–1298 (2007).
105. Simeone, R. *et al.* Phagosomal rupture by Mycobacterium tuberculosis results in toxicity and host cell death. *PLoS Pathog.* **8,** (2012).
106. Repasy, T. *et al.* Intracellular Bacillary Burden Reflects a Burst Size for Mycobacterium tuberculosis In Vivo. *PLoS Pathog.* **9,** (2013).
107. Abdallah, A. M. *et al.* Mycobacterial Secretion Systems ESX-1 and ESX-5 Play Distinct Roles in Host Cell Death and Inflammasome Activation. *J. Immunol.* **187,** 4744–4753 (2011).
108. Quigley, J. *et al.* The cell wall lipid PDIM contributes to phagosomal escape and host cell exit of Mycobacterium tuberculosis. *MBio* **8,** 1–12 (2017).
109. Simeone, R. *et al.* Cytosolic Access of Mycobacterium tuberculosis: Critical Impact of Phagosomal Acidification Control and Demonstration of Occurrence In Vivo. *PLoS Pathog.* **11,** 1–24 (2015).
110. Houben, D. *et al.* ESX-1-mediated translocation to the cytosol controls virulence of mycobacteria. *Cell. Microbiol.* **14,** 1287–1298 (2012).
111. Marrero, J., Rhee, K. Y., Schnappinger, D., Pethe, K. & Ehrt, S. Gluconeogenic carbon flow of tricarboxylic acid cycle intermediates is critical for Mycobacterium tuberculosis to establish and maintain infection. *Proc. Natl. Acad. Sci.* **107,** 9819–9824 (2010).
112. de Carvalho, L. P. S. *et al.* Metabolomics of Mycobacterium tuberculosis Reveals Compartmentalized Co-Catabolism of Carbon Substrates. *Chem. Biol.* **17,** 1122–1131 (2010).
113. Larrouy-Maumus, G. Cholesterol acquisition by Mycobacterium tuberculosis. *Virulence* **6,** 412–3 (2015).
114. Marrero, J., Trujillo, C., Rhee, K. Y. & Ehrt, S. Glucose Phosphorylation Is Required for Mycobacterium tuberculosis Persistence in Mice. *PLoS Pathog.* **9,** (2013).
115. Sassetti, C. M. & Rubin, E. J. Genetic requirements for mycobacterial survival during infection. *Proc. Natl. Acad. Sci.* **100,** 12989–12994 (2003).
116. Peyron, P. *et al.* Foamy macrophages from tuberculous patients' granulomas constitute a nutrient-rich reservoir for M. tuberculosis persistence. *PLoS Pathog.* **4,** 1–14 (2008).
117. McKinney, J. D. *et al.* Persistence of Mycobacterium tuberculosis in macrophages and mice requires the glyoxylate shunt enzyme isocitrate lyase. *Nature* **406,** 735–738 (2000).
118. Muñoz-Elías, E. J. & McKinney, J. D. Mycobacterium tuberculosis isocitrate lyases 1 and 2 are jointly required for in vivo growth and virulence. *Nat. Med.* **11,** 638–644 (2005).

119. Daniel, J., Maamar, H., Deb, C., Sirakova, T. D. & Kolattukudy, P. E. Mycobacterium tuberculosis uses host triacylglycerol to accumulate lipid droplets and acquires a dormancy-like phenotype in lipid-loaded macrophages. *PLoS Pathog.* **7,** (2011).

120. N. Rücker, S. Billing, R, Bücker, D. Jahn, C. W. and F. C. B. Acetate Dissimilation and Assimilation in Mycobacterium tuberculosis Depend on Carbon Availability. *J. Biochem.* **197,** 3182–3190 (2015).

121. Sauer, U. & Eikmanns, B. J. The PEP-pyruvate-oxaloacetate node as the switch point for carbon flux distribution in bacteria. *FEMS Microbiol. Rev.* **29,** 765–794 (2005).

122. Schnappinger, D. *et al.* Transcriptional Adaptation of *Mycobacterium tuberculosis* within Macrophages. *J. Exp. Med.* **198,** 693–704 (2003).

123. Rhee, K. Y. *et al.* Central carbon metabolism in Mycobacterium tuberculosis: an unexpected frontier. *Trends Microbiol.* **19,** 307–14 (2011).

124. Lee, W., VanderVen, B. C., Walker, S. & Russell, D. G. Novel protein acetyltransferase, Rv2170, modulates carbon and energy metabolism in Mycobacterium tuberculosis. *Sci. Rep.* **7,** 1–11 (2017).

125. Puckett, S. *et al.* Glyoxylate detoxification is an essential function of malate synthase required for carbon assimilation in *Mycobacterium tuberculosis*. *Proc. Natl. Acad. Sci.* **114,** E2225–E2232 (2017).

126. Yang, X., Nesbitt, N. M., Dubnau, E., Smith, I. & Sampson, N. S. Cholesterol metabolism increases the metabolic pool of propionate in Mycobacterium tuberculosis. *Biochemistry* **48,** 3819–3821 (2009).

127. Thomas, S. T., VanderVen, B. C., Sherman, D. R., Russell, D. G. & Sampson, N. S. Pathway profiling in Mycobacterium tuberculosis: Elucidation of cholesterol-derived catabolite and enzymes that catalyze its metabolism. *J. Biol. Chem.* **286,** 43668–43678 (2011).

128. Yang, X., Nesbitt, N. M., Dubnau, E., Smith, I. & Sampson, N. S. Cholesterol metabolism increases the metabolic pool of propionate in Mycobacterium tuberculosis. *Biochemistry* **48,** 3819–21 (2009).

129. Griffin, J. E. *et al.* Cholesterol Catabolism by Mycobacterium tuberculosis Requires Transcriptional and Metabolic Adaptations. *Chem. Biol.* **19,** 218–227 (2012).

130. Upton, A. M. & McKinney, J. D. Role of the methylcitrate cycle in propionate metabolism and detoxification in Mycobacterium smegmatis. *Microbiology* **153,** 3973–3982 (2007).

131. Savvi, S. *et al.* Functional characterization of a vitamin B12-dependent methylmalonyl pathway in Mycobacterium tuberculosis: Implications for propionate metabolism

during growth on fatty acids. *J. Bacteriol.* **190,** 3886–3895 (2008).

132. Muñoz-Elías, E. J., Upton, A. M., Cherian, J. & McKinney, J. D. Role of the methylcitrate cycle in Mycobacterium tuberculosis metabolism, intracellular growth, and virulence. *Mol. Microbiol.* **60,** 1109–1122 (2006).
133. Jain, M. *et al.* Lipidomics reveals control of Mycobacterium tuberculosis virulence lipids via metabolic coupling. *Proc. Natl. Acad. Sci.* **104,** 5133–5138 (2007).
134. Russell, D. G. *et al.* Mycobacterium tuberculosis wears what it eats. *Cell Host Microbe* **8,** 68–76 (2010).
135. Kaur, D., Guerin, M. E., Škovierová, H. & Brennan, P. J. *Biogenesis of the cell wall and other glycoconjugates of Mycobacterium tuberculosis*. *Advances in Applied Microbiology* (2009). doi:10.1016/S0065-2164(09)69002-X.Biogenesis
136. Lee, W., VanderVen, B. C., Fahey, R. J. & Russell, D. G. Intracellular Mycobacterium tuberculosis exploits host-derived fatty acids to limit metabolic stress. *J. Biol. Chem.* **288,** 6788–800 (2013).
137. Rohde, K. H., Abramovitch, R. B. & Russell, D. G. Mycobacterium tuberculosis Invasion of Macrophages: Linking Bacterial Gene Expression to Environmental Cues. *Cell Press* **2,** 352–364 (2007).
138. Pandey, A. K. & Sassetti, C. M. Mycobacterial persistence requires the utilization of host cholesterol. *PNAS* **105,** 4376–4380 (2008).
139. Nesbitt, N. M. *et al.* A Thiolase of Mycobacterium tuberculosis Is Required for Virulence and Production of Androstenedione and Androstadienedione from Cholesterol. *Infect. Immun.* **78,** 275–282 (2010).
140. Appelberg, R. Macrophage nutriprive antimicrobial mechanisms. *J. Leukoc. Biol.* **79,** 1117–1128 (2006).
141. Betts, J. C., Lukey, P. T., Robb, L. C., McAdam, R. A. & Duncan, K. Evaluation of a nutrient starvation model of Mycobacterium tuberculosis persistence by gene and protein expression profiling. *Mol. Microbiol.* **43,** 717–31 (2002).
142. Niderweis, M. Nutrient acquisition by mycobacteria. *Microbiology* **154,** 679–692 (2008).
143. Shanahan, C. A. & Strobel, S. A. The bacterial second messenger c-di-GMP: Probing interactions with protein and RNA binding partners using cyclic dinucleotide analogs. *Org. Biomol. Chem.* **10,** 9113–9129 (2012).
144. Galperin, M. Y. Bacterial signal transduction network in a genomic perspective. *Environ. Microbiol.* **6,** 552–567 (2004).
145. McCue, L. A., McDonough, K. A. & Lawrence, C. E. Functional classification of cNMP-binding proteins and nucleotide cyclases with implications for novel regulatory

pathways in Mycobacterium tuberculosis. *Genome Res.* **10,** 204–19 (2000).

146. Camilli, A. & Bassler, B. Bacterial Small-Molecule Signalling Pathways. *Science (80-.).* **311,** (2006).
147. Green, J. *et al.* Cyclic-AMP and bacterial cyclic-AMP receptor proteins revisited: Adaptation for different ecological niches. *Curr. Opin. Microbiol.* **18,** 1–7 (2014).
148. McDonough, K. A. & Rodriguez, A. The myriad roles of cyclic AMP in microbial pathogens: from signal to sword. *Nat. Rev. Microbiol.* **10,** 27–38 (2012).
149. McDonough, K. A. & Rodriguez, A. The myriad roles of cyclic AMP in microbial pathogens: From signal to sword. *Nature Reviews Microbiology* (2012). doi:10.1038/nrmicro2688
150. Marden, J. N., Dong, Q., Roychowdhury, S., Berleman, J. E. & Bauer, C. E. Cyclic GMP controls Rhodospirillum centenum cyst development. **79,** 600–615 (2011).
151. Gomelsky, M. Micro Commentary cAMP , c-di-GMP , c-di-AMP and now cGMP : bacteria use them all ! **79,** 562–565 (2011).
152. Cashel, M. & Kalbacher, B. *The Control of Ribonucleic Acid Synthesis in Escherichia coli V. Characterization of a nucleotide associated with the stringent response*. *THE JOURNAL OF BIOLOGICAL CHEMISTRY* **245,** (1970).
153. Alexander, H., Fino, C., Sørensen, M. A. & Semsey, S. Prophages and Growth Dynamics Confound Experimental Results with Antibiotic-Tolerant Persister Cells. *MBio* **8,** 1–18 (2017).
154. Lewis, K. Persister Cells. *Annu. Rev. Microbiol.* **64,** 357–372 (2010).
155. Woodward, J. J., Iavarone, A. T. & Portnoy, D. A. c-di-AMP secreted by intracellular *Listeria monocytogenes* activates a host type I interferon response. *Science* **328,** 1703–5 (2010).
156. Commichau, F. M., Gibhardt, J., Halbedel, S., Gundlach, J. & Stülke, J. A Delicate Connection: c-di-AMP Affects Cell Integrity by Controlling Osmolyte Transport. *Trends Microbiol.* **26,** 175–185 (2018).
157. Berthet, J., Rall, T. W. & Sutherland, E. W. The relationship of epinephrine and glucagon to liver phosphorylase. IV. Effect of epinephrine and glucagon on the reactivation of phosphorylase in liver homogenates. *J. Biol. Chem.* **224,** 463–75 (1957).
158. Görke, B. & Stülke, J. Carbon catabolite repression in bacteria: many ways to make the most out of nutrients. *Nat. Rev. Microbiol.* **6,** 613–24 (2008).
159. Harman, J. G. Allosteric regulation of the cAMP receptor protein. *Biochim. Biophys. Acta* **1547,** 1–17 (2001).
160. Weber, I. T. & Steitz, T. A. Structure of a complex of catabolite gene activator protein

and cyclic AMP refined at 2.5 A resolution. *J. Mol. Biol.* **198,** 311–26 (1987).

161. Kalia, D. *et al.* Nucleotide, c-di-GMP, c-di-AMP, cGMP, cAMP, (p)ppGpp signaling in bacteria and implications in pathogenesis. *Chem. Soc. Rev.* **42,** 305–341 (2013).
162. Ebright, R. H., Ebright, Y. W., Pendergrast, P. S. & Gunasekera, A. Conversion of a helix-turn-helix motif sequence-specific DNA binding protein into a site-specific DNA cleavage agent. *Proc. Natl. Acad. Sci. U. S. A.* **87,** 2882–6 (1990).
163. Engel, J. & Balachandran, P. Role of Pseudomonas aeruginosa type III effectors in disease. *Curr. Opin. Microbiol.* **12,** 61–66 (2009).
164. Hofer, A. M. Interactions between calcium and cAMP signaling. *Curr. Med. Chem.* **19,** 5768–73 (2012).
165. Fuchs, E. L. *et al.* The Pseudomonas aeruginosa Vfr regulator controls global virulence factor expression through cyclic AMP-dependent and -independent mechanisms. *J. Bacteriol.* **192,** 3553–3564 (2010).
166. Knapp, G. S. & Mcdonough, K. A. Cyclic AMP Signaling in Mycobacteria. *Microbiol Spectr.* **2,** (2014).
167. Linder, J. U. Class III adenylyl cyclases: molecular mechanisms of catalysis and regulation. *Cell. Mol. Life Sci.* **63,** 1736–1751 (2006).
168. Shenoy, A. R. & Visweswariah, S. S. Mycobacterial adenylyl cyclases: Biochemical diversity and structural plasticity. *FEBS Lett.* **580,** 3344–3352 (2006).
169. Shenoy, A. R., Srinivas, A., Mahalingam, M. & Visweswariah, S. S. An adenylyl cyclase pseudogene in Mycobacterium tuberculosis has a functional ortholog in Mycobacterium avium. *Biochimie* **87,** 557–563 (2005).
170. Knapp, G. S. & McDonough, K. A. Cyclic AMP Signaling in Mycobacteria. *Microbiol. Spectr.* **2,** (2014).
171. Tews, I. *et al.* The structure of a pH-sensing mycobacterial adenylyl cyclase holoenzyme. *Science (80-.).* **308,** 1020–3 (2005).
172. Abdel Motaal, A., Tews, I., Schultz, J. E. & Linder, J. U. Fatty acid regulation of adenylyl cyclase Rv2212 from Mycobacterium tuberculosis H37Rv. *FEBS J.* **273,** 4219–28 (2006).
173. Shenoy, A. R., Sreenath, N. P., Mahalingam, M. & Visweswariah, S. S. Characterization of phylogenetically distant members of the adenylate cyclase family from mycobacteria: Rv1647 from Mycobacterium tuberculosis and its orthologue ML1399 from M. leprae. *Biochem. J.* **387,** 541–51 (2005).
174. Linder, J. U., Schultz, A. & Schultz, J. E. Adenylyl Cyclase Rv1264 from *Mycobacterium tuberculosis* Has an Autoinhibitory N-terminal Domain. *J. Biol. Chem.* **277,** 15271–15276 (2002).

175. Mondéjar, L. G., Lupas, A., Schultz, A. & Schultz, J. E. HAMP domain-mediated signal transduction probed with a mycobacterial adenylyl cyclase as a reporter. *J. Biol. Chem.* **287,** 1022–1031 (2012).
176. Castro, L. I., Hermsen, C., Schultz, J. E. & Linder, J. U. Adenylyl cyclase Rv0386 from Mycobacterium tuberculosis H37Rv uses a novel mode for substrate selection. *FEBS J.* **272,** 3085–3092 (2005).
177. Shenroy, A. R. & Visweswariah, S. S. Class III nucleotide cyclases in bacteria and archaebacteria: lineage-specific expansion of adenylyl cyclases and a dearth of guanylyl cyclases. *FEBS Lett.* **561,** 11–21 (2004).
178. Padh, H. & Venkitasubramanian, T. A. Adenosine 3',5'-monophosphate in Mycobacterium phlei and Mycobacterium tuberculosis H37Ra. *Microbios* **16,** 183–9 (1976).
179. Botsford, J. L. Cyclic nucleotides in procaryotes. *Microbiol. Rev.* **45,** 620–42 (1981).
180. Bai, G., Schaak, D. D. & McDonough, K. A. cAMP levels within Mycobacterium tuberculosis and Mycobacterium bovis BCG increase upon infection of macrophages. *FEMS Immunol. Med. Microbiol.* **55,** 68–73 (2009).
181. Gazdik, M. A., Bai, G., Wu, Y. & McDonough, K. A. Rv1675c (cmr) regulates intramacrophage and cyclic AMP-induced gene expression in Mycobacterium tuberculosis-complex mycobacteria. *Mol. Microbiol.* **71,** 434–48 (2009).
182. Coward, W. A. & Sawyer, M. B. Whole-body albumin mass and distribution in rats fed on low-protein diets. *Br. J. Nutr.* **37,** 127–34 (1977).
183. Padh, H. & Venkitasubramanian, T. A. Cyclic adenosine 3', 5'-monophosphate in mycobacteria. *Indian J. Biochem. Biophys.* **13,** 413–4 (1976).
184. Lowrie, D. B., Jackett, P. S. & Ratcliffe, N. A. Mycobacterium microti may protect itself from intracellular destruction by releasing cyclic AMP into phagosomes. *Nature* **254,** 600–2 (1975).
185. Lowrie, D. B., Aber, V. R. & Jackett, P. S. Phagosome-lysosome fusion and cyclic adenosine 3':5'-monophosphate in macrophages infected with Mycobacterium microti, Mycobacterium bovis BCG or Mycobacterium lepraemurium. *J. Gen. Microbiol.* **110,** 431–41 (1979).
186. Agarwal, N., Lamichhane, G., Gupta, R., Nolan, S. & Bishai, W. R. Cyclic AMP intoxication of macrophages by a Mycobacterium tuberculosis adenylate cyclase. *Nature* **460,** 98–102 (2009).
187. Agarwal, N. & Bishai, W. R. cAMP signaling in Mycobacterium tuberculosis. *Indian J. Exp. Biol.* **47,** 393–400 (2009).

188. Kalamidas, S. A. *et al.* cAMP synthesis and degradation by phagosomes regulate actin assembly and fusion events: consequences for mycobacteria. *J. Cell Sci.* **119,** 3686–3694 (2006).

189. Shenoy, A. R. *et al.* Structural and Biochemical Analysis of the Rv0805 Cyclic Nucleotide Phosphodiesterase from Mycobacterium tuberculosis. *J. Mol. Biol.* **365,** 211–225 (2007).

190. Shenoy, A. R., Sreenath, N., Podobnik, M., Kovačevič, M. & Visweswariah, S. S. The Rv0805 Gene from Mycobacterium tuberculosis Encodes a 3',5'-Cyclic Nucleotide Phosphodiesterase: Biochemical and Mutational Analysis †. (2005). doi:10.1021/bi0512391

191. Johnson, R. M. & Mcdonough, K. A. Cyclic nucleotide signaling in Mycobacterium tuberculosis: an expanding repertoire. **76,** 48 (2018).

192. Keppetipola, N. & Shuman, S. A phosphate-binding histidine of binuclear metallophosphodiesterase enzymes is a determinant of 2',3'-cyclic nucleotide phosphodiesterase activity. *J. Biol. Chem.* **283,** 30942–9 (2008).

193. Nambi, S. *et al.* Cyclic AMP-dependent protein lysine acylation in mycobacteria regulates fatty acid and propionate metabolism. *J. Biol. Chem.* **288,** 14114–14124 (2013).

194. Nambi, S., Basu, N. & Visweswariah, S. S. cAMP-regulated protein lysine acetylases in mycobacteria. *J. Biol. Chem.* **285,** 24313–23 (2010).

195. Ranganathan, S. *et al.* Characterization of a cAMP responsive transcription factor, Cmr (Rv1675c), in TB complex mycobacteria reveals overlap with the DosR (DevR) dormancy regulon. *Nucleic Acids Res.* **44,** 134–51 (2016).

196. Braibant, M., Gilot, P. & Content, J. The ATP binding cassette (ABC) transport systems of Mycobacterium tuberculosis. *FEMS Microbiol. Rev.* **24,** 449–67 (2000).

197. Louw, G. E. *et al.* A Balancing Act: Efflux/Influx in Mycobacterial Drug Resistance. *Antimicrob. Agents Chemother.* **53,** 3181–3189 (2009).

198. Bánfalvi, Z., Kostyál, Z. & Barta, E. Solanum brevidens possesses a non-sucrose-inducible patatin gene. *Mol. Gen. Genet.* **245,** 517–22 (1994).

199. Kumari, S., Harjai, K. & Chhibber, S. Bacteriophage versus antimicrobial agents for the treatment of murine burn wound infection caused by Klebsiella pneumoniae B5055. *J. Med. Microbiol.* **60,** 205–210 (2011).

200. Zaveri, A. & Visweswariah, S. S. Cyclic AMP in Mycobacteria: the second messenger comes first. *Current Science* **105,** 666–675 (2013).

201. Nambi, S., Badireddy, S., Visweswariah, S. S. & Anand, G. S. Cyclic AMP-induced

conformational changes in mycobacterial protein acetyltransferases. *J. Biol. Chem.* **287,** 18115–18129 (2012).

202. Chui, Y. L. N. *Role of the second messenger cAMP during mycobacterial physiology remodelling and infection*. (2018).
203. Sargent, M. *Guide to achieving reliable quantitative LC-MS measurements*. *Analytical Methods Committee* (2013). doi:10.1017/CBO9781107415324.004
204. de Hoffmann, E. & Stroobant, V. *Mass Spectrometry Principles and Applications*. (2007).
205. Gantt, S. L., Valentine, N. B., Saenz, A. J., Kingsley, M. T. & Wahl, K. L. *Use of an Internal Control for Matrix-Assisted Laser Desorption/Ionization Time-of-Flight Mass Spectrometry Analysis of Bacteria*. (1999).
206. El-Aneed, A., Cohen, A. & Banoub, J. Mass Spectrometry, Review of the Basics: Electrospray, MALDI, and Commonly Used Mass Analyzers. *Appl. Spectrosc. Rev.* **44,** 210–230 (2009).
207. Ho, C. S. *et al.* Electrospray ionisation mass spectrometry: principles and clinical applications. *Clin. Biochem. Rev.* **24,** 3–12 (2003).
208. Banerjee, S. & Mazumdar, S. Electrospray Ionization Mass Spectrometry: A Technique to Access the Information beyond the Molecular Weight of the Analyte. *Int. J. Anal. Chem.* **2012,** 1–40 (2012).
209. Zaima, N. *et al.* Matrix-Assisted Laser Desorption/Ionization Imaging Mass Spectrometry. *Int. J. Mol. Sci.* **11,** 5040–5055 (2010).
210. Fukuyama, Y. Liquid Matrices in MALDI-MS. in *Applications of Ionic Liquids in Science and Technology* (InTech, 2011). doi:10.5772/24407
211. Gogichaeva, N. V., Williams, T. & Alterman, M. A. MALDI TOF/TOF Tandem Mass Spectrometry as a New Tool for Amino Acid Analysis. *J. Am. Soc. Mass Spectrom.* **18,** 279–284 (2007).
212. Tof, M. & Analyzer, T. O. F. Applied Biosystems / MDS SCIEX. *October* (2005).
213. Orthogonai-acceleration, N. Q. *et al.* High Sensitivity Collisionally-activated. **10,** (1996).
214. Gates, P. Mass Spectrometry Facility | Quadrupole. Available at: http://www.chm.bris.ac.uk/ms/quadrupole.xhtml. (Accessed: 28th August 2018)
215. Yost, R. A., Enke, C. G. & Lansing, E. *Iriple Quadrupole Mass Spectrometry*. **51,** (UTC, 2018).
216. Gates, P. Mass Spectrometry Facility | TOF. Available at: http://www.chm.bris.ac.uk/ms/tof.xhtml. (Accessed: 28th August 2018)
217. Morris, H. R., Paxton, T., Panico, M., Mcdowell, R. & Dell1, A. *A Novel Geometry Mass Spectrometer, the Q-TOF, for Low-Femtomole/Attomole-Range Biopolymer Sequencing*.

Journal of Protein Chemistry **16,** (1997).

218. Morris, H. R., Paxton, T., Panico, M., McDowell, R. & Dell, A. A Novel Geometry Mass Spectrometer, the Q-TOF, for Low-Femtomole/Attomole-Range Biopolymer Sequencing. *J. Protein Chem.* **16,** 469–479 (1997).
219. Taylor, P. J. Matrix effects: the Achilles heel of quantitative high-performance liquid chromatography–electrospray–tandem mass spectrometry. *Clin. Biochem.* **38,** 328–334 (2005).
220. Barnes, S. *et al.* Training in metabolomics research. I. Designing the experiment, collecting and extracting samples and generating metabolomics data. *J. Mass Spectrom.* (2016). doi:10.1002/jms.3782
221. Schiller, J. *et al.* The suitability of different DHB isomers as matrices for the MALDI-TOF MS analysis of phospholipids: which isomer for what purpose? *Eur. Biophys. J.* **36,** 517–527 (2007).
222. Yang, K. & Han, X. Lipidomics: Techniques, Applications, and Outcomes Related to Biomedical Sciences. (2016). doi:10.1016/j.tibs.2016.08.010
223. Gilleron, M., Quesniaux, V. F. J. & Puzo, G. Acylation state of the phosphatidylinositol hexamannosides from Mycobacterium bovis bacillus Calmette Guerin and mycobacterium tuberculosis H37Rv and its implication in Toll-like receptor response. *J. Biol. Chem.* **278,** 29880–9 (2003).
224. Holmes, D. T. & Buhr, K. A. Error propagation in calculated ratios. *Clin. Biochem.* **40,** 728–734 (2007).
225. Rolain, J. M. & Baquero, F. The refusal of the Society to accept antibiotic toxicity: missing opportunities for therapy of severe infections. *Clin. Microbiol. Infect.* **22,** 423–427 (2016).
226. Brummett, R. E. & Fox, K. E. Aminoglycoside-induced hearing loss in humans. *Antimicrob. Agents Chemother.* **33,** 797–800 (1989).
227. Mingeot-Leclercq, M. P. & Tulkens, P. M. Aminoglycosides: nephrotoxicity. *Antimicrob. Agents Chemother.* **43,** 1003–12 (1999).
228. Davies, S. W., Guidry, C. A., Petroze, R. T., Hranjec, T. & Sawyer, R. G. Vancomycin and nephrotoxicity. *J. Trauma Acute Care Surg.* **75,** 830–835 (2013).
229. Khaliq, Y. & Zhanel, G. G. *Fluoroquinolone-Associated Tendinopathy: A Critical Review of the Literature*.
230. Kalghatgi, S. *et al.* Bactericidal antibiotics induce mitochondrial dysfunction and oxidative damage in Mammalian cells. *Sci. Transl. Med.* **5,** 192ra85 (2013).
231. Vakifahmetoglu-Norberg, H., Ouchida, A. T. & Norberg, E. The role of mitochondria in

metabolism and cell death. *Biochem. Biophys. Res. Commun.* **482,** 426–431 (2017).

232. Daum, G. & Vance, J. E. Import of lipids into mitochondria. *Prog. Lipid Res.* **36,** 103–30 (1997).
233. Mejia, E. M. & Hatch, G. M. Mitochondrial phospholipids: role in mitochondrial function. *J. Bioenerg. Biomembr.* **48,** 99–112 (2016).
234. Duchen, M. R. Contributions of mitochondria to animal physiology: from homeostatic sensor to calcium signalling and cell death. *J. Physiol.* **516 (Pt 1),** 1–17 (1999).
235. Wallace, D. C. Mitochondrial diseases in man and mouse. *Science* **283,** 1482–8 (1999).
236. Albers, D. S. & Beal, M. F. Mitochondrial dysfunction and oxidative stress in aging and neurodegenerative disease. *J. Neural Transm. Suppl.* **59,** 133–54 (2000).
237. Enerbäck, S. *et al.* Mice lacking mitochondrial uncoupling protein are cold-sensitive but not obese. *Nature* **387,** 90–94 (1997).
238. Payne, A. H. & Hales, D. B. Overview of Steroidogenic Enzymes in the Pathway from Cholesterol to Active Steroid Hormones. *Endocr. Rev.* **25,** 947–970 (2004).
239. Wang, C. & Youle, R. J. The role of mitochondria in apoptosis*. *Annu. Rev. Genet.* **43,** 95–118 (2009).
240. Fernie, A. R., Carrari, F. & Sweetlove, L. J. Respiratory metabolism: glycolysis, the TCA cycle and mitochondrial electron transport. *Curr. Opin. Plant Biol.* **7,** 254–261 (2004).
241. Reichert, A. S. & Neupert, W. Mitochondriomics or what makes us breathe. *Trends Genet.* **20,** 555–562 (2004).
242. MITCHELL, P. Coupling of Phosphorylation to Electron and Hydrogen Transfer by a Chemi-Osmotic type of Mechanism. *Nature* **191,** 144–148 (1961).
243. Neupert, W. & Herrmann, J. M. Translocation of Proteins into Mitochondria. *Annu. Rev. Biochem.* **76,** 723–749 (2007).
244. Timmis, J. N., Ayliffe, M. A., Huang, C. Y. & Martin, W. Endosymbiotic gene transfer: organelle genomes forge eukaryotic chromosomes. *Nat. Rev. Genet.* **5,** 123–135 (2004).
245. Martin, W. *et al.* Evolutionary analysis of Arabidopsis, cyanobacterial, and chloroplast genomes reveals plastid phylogeny and thousands of cyanobacterial genes in the nucleus. *Proc. Natl. Acad. Sci. U. S. A.* **99,** 12246–51 (2002).
246. Wang, X., Ryu, D., Houtkooper, R. H. & Auwerx, J. Insights & Perspectives Antibiotic use and abuse: A threat to mitochondria and chloroplasts with impact on research, health, and environment. doi:10.1002/bies.201500071
247. Voet, D. & Voet, J. G. *Biochemistry*. (John Wiley & Sons, 2011).
248. Owen, O. E., Kalhan, S. C. & Hanson, R. W. The key role of anaplerosis and cataplerosis for citric acid cycle function. *J. Biol. Chem.* **277,** 30409–12 (2002).

249. Kalervo Hiltunen, J. *et al.* Mitochondrial fatty acid synthesis and respiration. *BBA - Bioenerg.* **1797,** 1195–1202 (2010).

250. Carroll, J., Fearnley, I. M., Shannon, R. J., Hirst, J. & Walker, J. E. Analysis of the Subunit Composition of Complex I from Bovine Heart Mitochondria. *Mol. Cell. Proteomics* **2,** 117–126 (2003).

251. Yi, X. & Maeda, N. Endogenous Production of Lipoic Acid Is Essential for Mouse Development. *Mol. Cell. Biol.* **25,** 8387–8392 (2005).

252. Fadeel, B., Orrenius, S. & Zhivotovsky, B. Apoptosis in Human Disease: A New Skin for the Old Ceremony? *Biochem. Biophys. Res. Commun.* **266,** 699–717 (1999).

253. Nunnari, J. & Suomalainen, A. Mitochondria: In Sickness and in Health. *Cell* **148,** 1145–1159 (2012).

254. Calvo, S. E. & Mootha, V. K. The Mitochondrial Proteome and Human Disease. *Annu. Rev. Genomics Hum. Genet.* **11,** 25–44 (2010).

255. Dwyer, D. J., Kohanski, M. A., Hayete, B. & Collins, J. J. Gyrase inhibitors induce an oxidative damage cellular death pathway in Escherichia coli. *Mol. Syst. Biol.* **3,** 91 (2007).

256. Shatalin, K., Shatalina, E., Mironov, A. & Nudler, E. H2S: A Universal Defense Against Antibiotics in Bacteria. *Science (80-.).* **334,** 986–990 (2011).

257. Kohanski, M. A., Tharakan, A., Lane, A. P., Ramanathan, M. & Jr. Bactericidal antibiotics promote reactive oxygen species formation and inflammation in human sinonasal epithelial cells. *Int. Forum Allergy Rhinol.* **6,** 191–200 (2016).

258. Rebollo-Ramirez, S. *et al.* Intact Cell Lipidomics Reveal Changes to the Ratio of Cardiolipins to Phosphatidylinositols in Response to Kanamycin in HeLa and Primary Cells. *Chem. Res. Toxicol.* **31,** 688–696 (2018).

259. Paradies, G., Paradies, V., De Benedictis, V., Ruggiero, F. M. & Petrosillo, G. Functional role of cardiolipin in mitochondrial bioenergetics. *Biochim. Biophys. Acta - Bioenerg.* **1837,** 408–417 (2014).

260. Westwood, F. R., Bigley, A., Randall, K., Marsden, A. M. & Scott, R. C. Statin-Induced Muscle Necrosis in the Rat: Distribution, Development, and Fibre Selectivity. *Toxicol. Pathol.* **33,** 246–257 (2005).

261. Tirmenstein, M. A. *et al.* Effects of troglitazone on HepG2 viability and mitochondrial function. *Toxicol. Sci.* **69,** 131–8 (2002).

262. Shah, R. R. Can pharmacogenetics help rescue drugs withdrawn from the market? *Pharmacogenomics* **7,** 889–908 (2006).

263. Siramshetty, V. B. *et al.* WITHDRAWN—a resource for withdrawn and discontinued

drugs. *Nucleic Acids Res.* **44,** D1080–D1086 (2016).

264. Belenky, P. *et al.* Bactericidal Antibiotics Induce Toxic Metabolic Perturbations that Lead to Cellular Damage. *Cell Rep.* **13,** 968–980 (2015).
265. Zampieri, M., Zimmermann, M., Claassen, M. & Sauer, U. Nontargeted Metabolomics Reveals the Multilevel Response to Antibiotic Perturbations. *Cell Rep.* **19,** 1214–1228 (2017).
266. Tomkova, S., Misuth, M., Lenkavska, L., Miskovsky, P. & Huntosova, V. In vitro identification of mitochondrial oxidative stress production by time-resolved fluorescence imaging of glioma cells. *Biochim. Biophys. Acta - Mol. Cell Res.* **1865,** 616–628 (2018).
267. Kohanski, M. A., Dwyer, D. J., Hayete, B., Lawrence, C. A. & Collins, J. J. A Common Mechanism of Cellular Death Induced by Bactericidal Antibiotics. *Cell* **130,** 797–810 (2007).
268. Ahler, E. *et al.* Doxycycline Alters Metabolism and Proliferation of Human Cell Lines. *PLoS One* **8,** e64561 (2013).
269. Singh, R., Sripada, L. & Singh, R. Side effects of antibiotics during bacterial infection: Mitochondria, the main target in host cell. *Mitochondrion* **16,** 50–54 (2014).
270. Layre, E. & Moody, D. B. Lipidomic profiling of model organisms and the world's major pathogens. *Biochimie* **95,** 109–115 (2013).
271. Sampaio, J. L. *et al.* Membrane lipidome of an epithelial cell line. *Proc. Natl. Acad. Sci.* **108,** 1903–1907 (2011).
272. Schuhmann, K. *et al.* Bottom-Up Shotgun Lipidomics by Higher Energy Collisional Dissociation on LTQ Orbitrap Mass Spectrometers. *Anal. Chem.* **83,** 5480–5487 (2011).
273. Pinto, G. *et al.* Fractionation of complex lipid mixtures by hydroxyapatite chromatography for lipidomic purposes. *J. Chromatogr. A* **1360,** 82–92 (2014).
274. Reis, A. *et al.* A comparison of five lipid extraction solvent systems for lipidomic studies of human LDL. *J. Lipid Res.* **54,** 1812–1824 (2013).
275. Reis, A. *et al.* A comparison of five lipid extraction solvent systems for lipidomic studies of human LDL. *J. Lipid Res.* **54,** 1812–24 (2013).
276. Dennis, E. A. *et al.* A Mouse Macrophage Lipidome. *J. Biol. Chem.* **285,** 39976–39985 (2010).
277. Lam, S. M., Tian, H. & Shui, G. Lipidomics, en route to accurate quantitation. *Biochim. Biophys. Acta - Mol. Cell Biol. Lipids* **1862,** 752–761 (2017).
278. Angelini, R. *et al.* Lipidomics of intact mitochondria by MALDI-TOF/MS. *J. Lipid Res.* **53,** 1417–1425 (2012).

279. Angelini, R., Babudri, F., Lobasso, S. & Corcelli, A. MALDI-TOF/MS analysis of archaebacterial lipids in lyophilized membranes dry-mixed with 9-aminoacridine. *J. Lipid Res.* **51,** 2818–25 (2010).

280. Tipthara, P. & Thongboonkerd, V. Differential human urinary lipid profiles using various lipid-extraction protocols: MALDI-TOF and LIFT-TOF/TOF analyses. *Sci. Rep.* **6,** 33756 (2016).

281. Alharbi, F. J., Geberhiwot, T., Hughes, D. A. & Ward, D. G. A Novel Rapid MALDI-TOF-MS-Based Method for Measuring Urinary Globotriaosylceramide in Fabry Patients. *J. Am. Soc. Mass Spectrom.* **27,** 719–725 (2016).

282. Lopalco, P. *et al.* Adjusting membrane lipids under salt stress: the case of the moderate halophilic organism *Halobacillus halophilus*. *Environ. Microbiol.* **15,** 1078–1087 (2013).

283. Jones, J. J., Stump, M. J., Fleming, R. C., Lay, J. O. & Wilkins, C. L. Strategies and data analysis techniques for lipid and phospholipid chemistry elucidation by intact cell MALDI-FTMS. *J. Am. Soc. Mass Spectrom.* **15,** 1665–1674 (2004).

284. Caprioli, R. M., Farmer, T. B. & Gile, J. Molecular imaging of biological samples: localization of peptides and proteins using MALDI-TOF MS. *Anal. Chem.* **69,** 4751–60 (1997).

285. Wang, H.-Y. J., Liu, C. Bin, Wu, H.-W. & Kuo, J. S. Direct profiling of phospholipids and lysophospholipids in rat brain sections after ischemic stroke. *Rapid Commun. Mass Spectrom.* **24,** 2057–2064 (2010).

286. Larrouy-Maumus, G., Clements, A., Filloux, A., McCarthy, R. R. & Mostowy, S. Direct detection of lipid A on intact Gram-negative bacteria by MALDI-TOF mass spectrometry. *J. Microbiol. Methods* **120,** 68–71 (2016).

287. Larrouy-Maumus, G. & Puzo, G. Mycobacterial envelope lipids fingerprint from direct MALDI-TOF MS analysis of intact bacilli. *Tuberculosis* **95,** 75–85 (2015).

288. Agilent. How Agilent Seahorse XF Analyzers Work | Agilent. Available at: https://www.agilent.com/en/products/cell-analysis/how-seahorse-xf-analyzers-work. (Accessed: 31st October 2018)

289. Agilent Technologies. *Agilent Seahorse XF Cell Mito Stress Test Kit*. (2017).

290. Giannella, R. A., Washington, O., Gemski, P. & Formal, S. B. Invasion of HeLa Cells by Salmonella typhimurium: A Model for Study of Invasiveness of Salmonella. *The Journal of Infectious Diseases* **128,** 69–75

291. Mostowy, S. *et al.* p62 and NDP52 Proteins Target Intracytosolic *Shigella* and *Listeria* to Different Autophagy Pathways. *J. Biol. Chem.* **286,** 26987–26995 (2011).

292. Stavru, F., Bouillaud, F., Sartori, A., Ricquier, D. & Cossart, P. Listeria monocytogenes

transiently alters mitochondrial dynamics during infection. *Proc. Natl. Acad. Sci. U. S. A.* **108,** 3612–7 (2011).

293. Köberle, M. *et al.* Yersinia enterocolitica Targets Cells of the Innate and Adaptive Immune System by Injection of Yops in a Mouse Infection Model. *PLoS Pathog.* **5,** e1000551 (2009).
294. Garcia-Gutierrez, E. *et al.* A Comparison of the ATP Generating Pathways Used by S. Typhimurium to Fuel Replication within Human and Murine Macrophage and Epithelial Cell Lines. *PLoS One* **11,** e0150687 (2016).
295. Liberti, M. V. & Locasale, J. W. The Warburg Effect: How Does it Benefit Cancer Cells? *Trends Biochem. Sci.* **41,** 211–218 (2016).
296. Kentner, D. *et al. Shigella* reroutes host cell central metabolism to obtain high-flux nutrient supply for vigorous intracellular growth. *Proc. Natl. Acad. Sci.* **111,** 9929–9934 (2014).
297. Eisenreich, W., Heesemann, J., Rudel, T. & Goebel, W. Metabolic host responses to infection by intracellular bacterial pathogens. *Front. Cell. Infect. Microbiol.* **3,** 24 (2013).
298. Wishart, D. S. *et al.* DrugBank 5.0: a major update to the DrugBank database for 2018. *Nucleic Acids Res.* **46,** D1074–D1082 (2018).
299. Bryskier, A. *Antimicrobial Agents: Antibacterials and Antifungals. Journal of Antimicrobial Chemotherapy* **58,** (Oxford University Press, 2005).
300. Nadanaciva, S. & Will, Y. Investigating mitochondrial dysfunction to increase drug safety in the pharmaceutical industry. *Curr. Drug Targets* **12,** 774–82 (2011).
301. Kotra, L. P., Haddad, J. & Mobashery, S. Aminoglycosides: perspectives on mechanisms of action and resistance and strategies to counter resistance. *Antimicrob. Agents Chemother.* **44,** 3249–56 (2000).
302. Finegold, S. M. & Sutter, V. L. *Susceptibility of Gram-Negative Anaerobic Bacilli to Gentamicin and Other Aminoglycosides*. *The Journal of infectious diseases* **124,** (1971).
303. Sawyers, C. L., Moore, R. D., Lerner, S. A. & Smith, C. R. A model for predicting nephrotoxicity in patients treated with aminoglycosides. *J. Infect. Dis.* **153,** 1062–8 (1986).
304. Larrouy-Maumus, G. *et al.* Cell-Envelope Remodeling as a Determinant of Phenotypic Antibacterial Tolerance in Mycobacterium tuberculosis. *ACS Infect. Dis.* **2,** 352–360 (2016).
305. Belenky, P. *et al.* Bactericidal Antibiotics Induce Toxic Metabolic Perturbations that Lead to Cellular Damage. *Cell Rep.* **13,** 968–80 (2015).
306. Zampieri, M., Zimmermann, M., Claassen, M. & Sauer Correspondence, U. Nontargeted

Metabolomics Reveals the Multilevel Response to Antibiotic Perturbations. *Cell Rep.* **19,** (2017).

307. Amacher, D. E. Drug-associated mitochondrial toxicity and its detection. *Curr. Med. Chem.* **12,** 1829–39 (2005).
308. Shin, J. W. *et al.* Changes, and the Relevance Thereof, in Mitochondrial Morphology during Differentiation into Endothelial Cells. *PLoS One* **11,** e0161015 (2016).
309. von Baum, H., Böttcher, S., Abel, R., Gerner, H. J. & Sonntag, H. G. Tissue and serum concentrations of levofloxacin in orthopaedic patients. *Int. J. Antimicrob. Agents* **18,** 335–40 (2001).
310. Swoboda, S. *et al.* Tissue and serum concentrations of levofloxacin 500 mg administered intravenously or orally for antibiotic prophylaxis in biliary surgery. *J. Antimicrob. Chemother.* **51,** 459–62 (2003).
311. Drlica, K. & Zhao, X. DNA Gyrase, Topoisomerase IV, and the 4-Quinolones. **61,** 377–392 (1997).
312. Babalık, A. *et al.* Pharmacokinetics and serum concentrations of antimycobacterial drugs in adult Turkish patients. *Int. J. Tuberc. Lung Dis.* **17,** 1442–1447 (2013).
313. Imming, P., Sinning, C. & Meyer, A. Drugs, their targets and the nature and number of drug targets. *Nat. Rev. Drug Discov.* **5,** 821–834 (2006).
314. Urso, R., Blardi, P. & Giorgi, G. A short introduction to pharmacokinetics. *Eur. Rev. Med. Pharmacol. Sci.* **6,** 33–44
315. Guillet, V. *et al.* Ethambutol-induced optic neuropathy linked to OPA1 mutation and mitochondrial toxicity. *Mitochondrion* **10,** 115–124 (2010).
316. Gu, J. *et al.* A Method for Generation Phage Cocktail with Great Therapeutic Potential. *PLoS One* **7,** e31698 (2012).
317. Marche, P., Koutouzov, S. & Girard, A. Impairment of Membrane Phosphoinositide Metabolism by Aminoglycoside Antibiotics : Streptomycin , Amikacin , Kanamycin, Dibekacin, Gentamicin and Neomycin. *J. Pharmacol. Exp. Ther.* **227,** (1983).
318. Marche, P., Olier, B., Girard, A., Fillastre, J. P. & Morin, J. P. Aminoglycoside-induced alterations of phosphoinositide metabolism. *Kidney Int.* **31,** 59–64 (1987).
319. Jiang, H., Sha, S.-H. & Schacht, J. Kanamycin alters cytoplasmic and nuclear phosphoinositide signaling in the organ of Corti *in vivo*. *J. Neurochem.* **99,** 269–276 (2006).
320. Wood, J. M. Osmosensing by bacteria: signals and membrane-based sensors. *Microbiol. Mol. Biol. Rev.* **63,** 230–262 (1999).
321. Krämer, R. Bacterial stimulus perception and signal transduction: Response to osmotic

stress. *Chem. Rec.* **10,** 217–229 (2010).

322. Wood, J. M. Bacterial responses to osmotic challenges. *J. Gen. Physiol.* **145,** 381–388 (2015).
323. Calamita, G. The Escherichia coli aquaporin-Z water channel. *Mol. Microbiol.* **37,** 254–62 (2000).
324. Zimmerman, S. B. & Minton, A. P. Macromolecular Crowding: Biochemical, Biophysical, and Physiological Consequences. *Annu. Rev. Biophys. Biomol. Struct.* **22,** 27–65 (1993).
325. Wood, J. M. *et al.* Osmotic Stress. *EcoSal Plus* **3,** (2009).
326. da Costa, M. S., Santos, H. & Galinski, E. A. An overview of the role and diversity of compatible solutes in Bacteria and Archaea. *Adv. Biochem. Eng. Biotechnol.* **61,** 117–53 (1998).
327. Landis, L., Xu, J. & Johnson, R. C. The cAMP receptor protein CRP can function as an osmoregulator of transcription in Escherichia coli. *Genes Dev.* **13,** 3081–91 (1999).
328. McLaggan, D., Naprstek, J., Buurman, E. T. & Epstein, W. Interdependence of K+ and glutamate accumulation during osmotic adaptation of Escherichia coli. *J. Biol. Chem.* **269,** 1911–7 (1994).
329. Dinnbier, U., Limpinsel, E., Schmid, R. & Bakker, E. P. Transient accumulation of potassium glutamate and its replacement by trehalose during adaptation of growing cells of Escherichia coli K-12 to elevated sodium chloride concentrations. *Arch. Microbiol.* **150,** 348–57 (1998).
330. Culham, D. E. *et al.* Isolation and Sequencing of Escherichia coli Gene proP Reveals Unusual Structural Features of the Osmoregulatory Proline/Betaine transporter, ProP. *J. Mol. Biol.* **229,** 268–276 (1993).
331. Culham,', D. E. *et al. Osmoregulatory transporter Prop influences colonization of the urinary tract by Escherichia coli*. (1998).
332. Hengge, R., Gründling, A., Jenal, U., Ryan, R. & Yildiz, F. Bacterial Signal Transduction by Cyclic Di-GMP and Other Nucleotide Second Messengers. *J. Bacteriol.* **198,** 15–26 (2016).
333. Xu, J. & Johnson, R. C. Fis activates the RpoS-dependent stationary-phase expression of proP in Escherichia coli. *J. Bacteriol.* **177,** 5222–31 (1995).
334. Jordi, B. J. *et al.* DNA binding is not sufficient for H-NS-mediated repression of proU expression. *J. Biol. Chem.* **272,** 12083–90 (1997).
335. Lucht, J. M. & Bremer, E. Adaptation of Escherichia coli to high osmolarity environments: osmoregulation of the high-affinity glycine betaine transport system proU. *FEMS Microbiol. Rev.* **14,** 3–20 (1994).

336. Balsalobre, C., Johansson, J. & Uhlin, B. E. Cyclic AMP-dependent osmoregulation of crp gene expression in Escherichia coli. *J. Bacteriol.* **188,** 5935–5944 (2006).

337. Ehrt, S. & Schnappinger, D. Mycobacterial survival strategies in the phagosome: Defense against host stresses. *Cell Microbiol.* 1170–1178 (2009).

338. Choudhary, E., Bishai, W. & Agarwal, N. Expression of a subset of heat stress induced genes of mycobacterium tuberculosis is regulated by 3',5'-cyclic AMP. *PLoS One* **9,** e89759 (2014).

339. Dass, B. K. M., Sharma, R., Shenoy, A. R., Mattoo, R. & Visweswariah, S. S. Cyclic AMP in mycobacteria: characterization and functional role of the Rv1647 ortholog in Mycobacterium smegmatis. *J. Bacteriol.* **190,** 3824–34 (2008).

340. Hatzios, S. K. *et al.* Osmosensory signaling in Mycobacterium tuberculosis mediated by a eukaryotic-like Ser/Thr protein kinase. *Proc. Natl. Acad. Sci. U. S. A.* **110,** E5069-77 (2013).

341. Tan, S. *et al.* Mycobacterium tuberculosis Responds to Chloride and pH as Synergistic Cues to the Immune Status of its Host Cell. (2013). doi:10.1371/journal.ppat.1003282

342. Gérald Larrouy-Maumus, G. *et al.* Cell-Envelope Remodeling as a Determinant of Phenotypic Antibacterial Tolerance in Mycobacterium tuberculosis. (2016). doi:10.1021/acsinfecdis.5b00148

343. Tan, S. & Russell, D. G. Trans-species communication in the Mycobacterium tuberculosis-infected macrophage. *Immunol. Rev.* **264,** 233–48 (2015).

344. Gouzy, A. *et al.* Mycobacterium tuberculosis Exploits Asparagine to Assimilate Nitrogen and Resist Acid Stress during Infection. *PLoS Pathog.* **10,** (2014).

345. Chang, G., Spencer, R. H., Lee, A. T., Barclay, M. T. & Rees, D. C. *Structure of the MscL Homolog from Mycobacterium tuberculosis: A Gated Mechanosensitive Ion Channel*. *Curr. Opin. Struct. Biol* **22,** (Freeman, 1996).

346. Bourque, C. W. Central mechanisms of osmosensation and systemic osmoregulation. *Nat. Rev. Neurosci.* **9,** 519–531 (2008).

347. Zabner, J., Smith, J. J., Karp, P. H., Widdicombe, J. H. & Welsh, M. J. Loss of CFTR chloride channels alters salt absorption by cystic fibrosis airway epithelia in vitro. *Mol. Cell* **2,** 397–403 (1998).

348. Rickman, L. *et al.* A member of the cAMP receptor protein family of transcription regulators in Mycobacterium tuberculosis is required for virulence in mice and controls transcription of the rpfA gene coding for a resuscitation promoting factor. *Mol. Microbiol.* **56,** 1274–86 (2005).

349. Stapleton, M. *et al.* Mycobacterium tuberculosis cAMP receptor protein (Rv3676)

differs from the Escherichia coli paradigm in its cAMP binding and DNA binding properties and transcription activation properties. *J. Biol. Chem.* **285,** 7016–27 (2010).

350. Rickman, L. *et al.* A member of the cAMP receptor protein family of transcription regulators in Mycobacterium tuberculosis is required for virulence in mice and controls transcription of the rpfA gene coding for a resuscitation promoting factor Europe PMC Funders Group. *Mol Microbiol* **56,** 1274–1286 (2005).
351. Bai, G., McCue, L. A. & McDonough, K. A. Characterization of Mycobacterium tuberculosis Rv3676 (CRPMt), a cyclic AMP receptor protein-like DNA binding protein. *J. Bacteriol.* **187,** 7795–804 (2005).
352. Reddy, M. C. M. *et al.* Structural Insights into the Mechanism of the Allosteric Transitions of *Mycobacterium tuberculosis* cAMP Receptor Protein. *J. Biol. Chem.* **284,** 36581–36591 (2009).
353. Rickman, L. *et al.* Erratum: A member of the cAMP receptor protein family of transcription regulators in Mycobacterium tuberculosis is required for virulence in mice and controls transcription of the rpfA gene coding for a resuscitation promoting factor Europe PMC Funders Gr. *Mol Microbiol* **56,** 1274–1286 (2005).
354. Betts, J. C., Lukey, P. T., Robb, L. C., McAdam, R. A. & Duncan, K. Evaluation of a nutrient starvation model of *Mycobacterium tuberculosis* persistence by gene and protein expression profiling. *Mol. Microbiol.* **43,** 717–731 (2002).
355. Sherman, D. R. *et al.* Regulation of the Mycobacterium tuberculosis hypoxic response gene encoding alpha -crystallin. *Proc. Natl. Acad. Sci. U. S. A.* **98,** 7534–9 (2001).
356. Akhter, Y. *et al.* Genome scale portrait of cAMP-receptor protein (CRP) regulons in mycobacteria points to their role in pathogenesis. *Gene* **407,** 148–158 (2008).
357. Spreadbury, C. L. *et al.* Point mutations in the DNA- and cNMP-binding domains of the homologue of the cAMP receptor protein (CRP) in Mycobacterium bovis BCG: implications for the inactivation of a global regulator and strain attenuation. *Microbiology* **151,** 547–556 (2005).
358. Sévin, D. C. & Sauer, U. Ubiquinone accumulation improves osmotic-stress tolerance in Escherichia coli. *Nat. Chem. Biol.* **10,** 266–272 (2014).
359. Jackson, E. K. The 2',3'-cAMP-adenosine pathway. *Am. J. Physiol. Renal Physiol.* **301,** F1160-7 (2011).
360. Shenoy, A. R., Sivakumar, K., Krupa, A., Srinivasan, N. & Visweswariah, S. S. A Survey of Nucleotide Cyclases in Actinobacteria: Unique Domain Organization and Expansion of the Class III Cyclase Family in *Mycobacterium tuberculosis*. *Comp. Funct. Genomics* **5,** 17–38 (2004).

361. Cortes, J. E. *et al.* Phase I Study of Quizartinib Administered Daily to Patients With Relapsed or Refractory Acute Myeloid Leukemia Irrespective of FMS-Like Tyrosine Kinase 3–Internal Tandem Duplication Status. *J. Clin. Oncol.* **31,** 3681–3687 (2013).

362. Kahramanoglou, C. *et al.* Genomic mapping of cAMP receptor protein (CRP Mt) in Mycobacterium tuberculosis: relation to transcriptional start sites and the role of CRPMt as a transcription factor. *Nucleic Acids Res.* **42,** 8320–9 (2014).

363. Wang, S. *et al.* Revealing of Mycobacterium marinum Transcriptome by RNA-seq. *PLoS One* **8,** e75828 (2013).

364. Li, X. *et al.* Transcriptome Landscape of Mycobacterium smegmatis. *Front. Microbiol.* **8,** 2505 (2017).

365. Bai, G., Knapp, G. S. & McDonough, K. A. Cyclic AMP signalling in mycobacteria: redirecting the conversation with a common currency. *Cell. Microbiol.* **13,** 349–58 (2011).

366. Agarwal, N., Raghunand, T. R. & Bishai, W. R. Regulation of the expression of whiB1 in Mycobacterium tuberculosis: role of cAMP receptor protein. *Microbiology* **152,** 2749–2756 (2006).

367. Smith, L. J. *et al.* Mycobacterium tuberculosis WhiB1 is an essential DNA-binding protein with a nitric oxide-sensitive iron-sulfur cluster. *Biochem. J.* **432,** 417–27 (2010).

368. Eoh, H. & Rhee, K. Y. Multifunctional essentiality of succinate metabolism in adaptation to hypoxia in Mycobacterium tuberculosis. *Proc. Natl. Acad. Sci. U. S. A.* **110,** 6554–9 (2013).

369. Banerjee, A. *et al.* A Universal Stress Protein (USP) in Mycobacteria Binds cAMP. *J. Biol. Chem.* **290,** 12731–12743 (2015).

370. Eoh, H. & Rhee, K. Y. Methylcitrate cycle defines the bactericidal essentiality of isocitrate lyase for survival of *Mycobacterium tuberculosis* on fatty acids. *Proc. Natl. Acad. Sci.* **111,** 4976–4981 (2014).

371. Ott, A., Oehme, F., Keller, H. & Schuster, S. C. Osmotic stress response in Dictyostelium is mediated by cAMP. *EMBO J.* **19,** 5782–5792 (2000).

372. Imashimizu, M., Yoshimura, H., Katoh, H., Ehira, S. & Ohmori, M. NaCl enhances cellular cAMP and upregulates genes related to heterocyst development in the cyanobacterium, *Anabaena* sp. strain PCC 7120. *FEMS Microbiol. Lett.* **252,** 97–103 (2005).

373. Saran, S. *et al.* cAMP signaling in Dictyostelium: Complexity of cAMP synthesis, degradation and detection. *J. Muscle Res. Cell Motil.* **23,** 793–802 (2002).

374. Tan, M. H. *et al.* RNA sequencing reveals a diverse and dynamic repertoire of the

Xenopus tropicalis transcriptome over development. *Genome Res.* **23,** 201–216 (2013).

375. Ishizuka, H., Hanamura, A., Kunimura, T. & Aiba, H. A lowered concentration of cAMP receptor protein caused by glucose is an important determinant for catabolite repression in *Escherichia coli*. *Mol. Microbiol.* **10,** 341–350 (1993).
376. Fleischmann, R. D. *et al.* Whole-genome comparison of Mycobacterium tuberculosis clinical and laboratory strains. *J. Bacteriol.* **184,** 5479–90 (2002).
377. Hanson, T. E., Eichler, J., Mijakovic, I., Grangeasse, C. & Stülke, J. Regulatory potential of post-translational modifications in bacteria. *Front. Microbiol. | www.frontiersin.org* **1,** 500 (2015).
378. Mowen, K. A. & David, M. Unconventional post-translational modifications in immunological signaling. *Nat. Immunol.* **15,** 512–520 (2014).
379. Bastos, P. A. D., da Costa, J. P. & Vitorino, R. A glimpse into the modulation of post-translational modifications of human-colonizing bacteria. *J. Proteomics* **152,** 254–275 (2017).
380. Ribet, D. & Cossart, P. Pathogen-mediated posttranslational modifications: A re-emerging field. *Cell* (2010).
381. Liu, F. *et al.* Acetylome Analysis Reveals Diverse Functions of Lysine Acetylation in Mycobacterium tuberculosis. *Mol. Cell. Proteomics* **13,** 3352–66 (2014).
382. Barak, R., Yan, J., Shainskaya, A. & Eisenbach, M. The Chemotaxis Response Regulator CheY Can Catalyze its Own Acetylation. *J. Mol. Biol.* **359,** 251–265 (2006).
383. Barak, R., Prasad, K., Shainskaya, A., Wolfe, A. J. & Eisenbach, M. Acetylation of the Chemotaxis Response Regulator CheY by Acetyl-CoA Synthetase Purified from Escherichia coli. *J. Mol. Biol.* **342,** 383–401 (2004).
384. Jones, J. D. & O'Connor, C. D. Protein acetylation in prokaryotes. *Proteomics* **11,** 3012–3022 (2011).
385. Ouidir, T., Kentache, T. & Hardouin, J. Protein lysine acetylation in bacteria: Current state of the art. *Proteomics* **16,** 301–309 (2016).
386. Zhao, J.-Y., Lu, N., Yan, Z. & Wang, N. SAHA and curcumin combinations co-enhance histone acetylation in human cancer cells but operate antagonistically in exerting cytotoxic effects. *J. Asian Nat. Prod. Res.* **12,** 335–48 (2010).
387. Wang, Q., Zhang, Y., Yang, C., Xiong, H. & Lin, Y. Acetylation of Metabolic Enzymes and Metabolic Flux. *Science (80-.).* **327,** 1004–1007 (2010).
388. Wang, Q. *et al.* Acetylation of Metabolic Enzymes Coordinates Carbon Source Utilization and Metabolic Flux. *Science (80-.).* **327,** 1004–1007 (2010).
389. Kuhn, M. L. *et al.* Structural, Kinetic and Proteomic Characterization of Acetyl

Phosphate-Dependent Bacterial Protein Acetylation. *PLoS One* **9,** e94816 (2014).

390. Zhao, S. *et al.* Regulation of Cellular Metabolism by Protein Lysine Acetylation. *Science (80-.).* **327,** 1000–1004 (2010).

391. Xu, H., Hegde, S. S. & Blanchard, J. S. Reversible acetylation and inactivation of Mycobacterium tuberculosis acetyl-CoA synthetase is dependent on cAMP. *Biochemistry* **50,** 5883–92 (2011).

392. Drazic, A., Myklebust, L. M., Ree, R. & Arnesen, T. The world of protein acetylation. *BBA - Proteins Proteomics* **1864,** 1372–1401 (2016).

393. Liang, W. & Deutscher, M. P. Post-translational modification of RNase R is regulated by stress-dependent reduction in the acetylating enzyme Pka (YfiQ). *RNA* **18,** 37–41 (2012).

394. Zhang, K., Zheng, S., Yang, J. S., Chen, Y. & Cheng, Z. Comprehensive Profiling of Protein Lysine Acetylation in *Escherichia coli*. *J. Proteome Res.* **12,** 844–851 (2013).

395. Kim, D. *et al.* The acetylproteome of Gram-positive model bacterium *Bacillus subtilis*. *Proteomics* **13,** 1726–1736 (2013).

396. Baeza, J. *et al.* Stoichiometry of Site-specific Lysine Acetylation in an Entire Proteome * □ S. *J. Biol. Chem.* **289,** 21326–21338 (2014).

397. Starai, V. J., Celic, I., Cole, R. N., Boeke, J. D. & Escalante-Semerena, J. C. Sir2-Dependent Activation of Acetyl-CoA Synthetase by Deacetylation of Active Lysine. *Science (80-.).* **298,** 2390–2392 (2002).

398. Starai, V. J., Takahashi, H., Boeke, J. D. & Escalante-Semerena, J. C. Short-chain fatty acid activation by acyl-coenzyme A synthetases requires SIR2 protein function in Salmonella enterica and Saccharomyces cerevisiae. *Genetics* **163,** 545–55 (2003).

399. Wolfe, A. J. The Acetate Switch. *Microbiol. Mol. Biol. Rev.* **69,** 12–50 (2005).

400. Zhang, J. *et al.* Lysine Acetylation Is a Highly Abundant and Evolutionarily Conserved Modification in Escherichia Coli* □ S. (2009).

401. Weinert, B. T. *et al.* Lysine Succinylation Is a Frequently Occurring Modification in Prokaryotes and Eukaryotes and Extensively Overlaps with Acetylation. *Cell Rep.* **4,** 842–851 (2013).

402. Thao, S., Chen, C.-S., Zhu, H. & Escalante-Semerena, J. C. Nε−Lysine Acetylation of a Bacterial Transcription Factor Inhibits Its DNA-Binding Activity. *PLoS One* **5,** e15123 (2010).

403. Chen, C.-S. *et al.* A proteome chip approach reveals new DNA damage recognition activities in Escherichia coli. *Nat. Methods* **5,** 69–74 (2008).

404. Thao, S., Chen, C.-S., Zhu, H. & Escalante-Semerena, J. C. Nε-lysine acetylation of a bacterial transcription factor inhibits Its DNA-binding activity. *PLoS One* **5,** e15123

(2010).

405. Carballès, F., Bertrand, C., Bouché, J. P. & Cam, K. Regulation of Escherichia coli cell division genes ftsA and ftsZ by the two-component system rcsC-rcsB. *Mol. Microbiol.* **34,** 442–50 (1999).

406. Wehland, M. *et al.* Identification of an RcsA/RcsB recognition motif in the promoters of exopolysaccharide biosynthetic operons from Erwinia amylovora and Pantoea stewartii subspecies stewartii. *J. Biol. Chem.* **274,** 3300–7 (1999).

407. Wehland, M. & Bernhard, F. The RcsAB box. Characterization of a new operator essential for the regulation of exopolysaccharide biosynthesis in enteric bacteria. *J. Biol. Chem.* **275,** 7013–20 (2000).

408. Francez-Charlot, A. *et al.* RcsCDB His-Asp phosphorelay system negatively regulates the flhDC operon in Escherichia coli. *Mol. Microbiol.* **49,** 823–32 (2003).

409. Yuan, Y., Crane, D. D. & Iii, C. E. B. *Stationary Phase-Associated Protein Expression in Mycobacterium tuberculosis: Function of the Mycobacterial-Crystallin Homolog*. *Journal of bacteriology* **178,** (1996).

410. Cunningham, A. F. & Spreadbury, C. L. Mycobacterial stationary phase induced by low oxygen tension: cell wall thickening and localization of the 16-kilodalton alpha-crystallin homolog. *J. Bacteriol.* **180,** 801–8 (1998).

411. Geluk, A. *et al.* T-Cell Recognition of the HspX Protein of Mycobacterium tuberculosis Correlates with Latent M. tuberculosis Infection but Not with M. bovis BCG Vaccination. *Infect. Immun.* **75,** 2914–2921 (2007).

412. Young Lin, M. *et al.* Lack of Immune Responses to Mycobacterium tuberculosis DosR Regulon Proteins following Mycobacterium bovis BCG Vaccination Downloaded from. *Infect. Immun.* **75,** 3523–3530 (2007).

413. Singhal, A. *et al.* Systematic Analysis of Mycobacterial Acylation Reveals First Example of Acylation-mediated Regulation of Enzyme Activity of a Bacterial Phosphatase. *J. Biol. Chem.* **290,** 26218–26234 (2015).

414. Singhal, A. *et al.* Systematic Analysis of Mycobacterial Acylation Reveals First Example of Acylation-mediated Regulation of Enzyme Activity of a Bacterial Phosphatase. *J. Biol. Chem.* **290,** 26218–26234 (2015).

415. Podobnik, M. *et al.* Allostery and Conformational Dynamics in cAMP-binding Acyltransferases. *J. Biol. Chem.* **289,** 16588–16600 (2014).

416. Lee, H. J., Lang, P. T., Fortune, S. M., Sassetti, C. M. & Alber, T. Cyclic AMP regulation of protein lysine acetylation in Mycobacterium tuberculosis. *Nat. Struct. Mol. Biol.* **19,** 811–8 (2012).

417. Yang, H. *et al.* Lysine acetylation of DosR regulates the hypoxia response of Mycobacterium tuberculosis. *Emerg. Microbes Infect.* **7,** 34 (2018).
418. Vergnolle, O., Xu, H. & Blanchard, J. S. Mechanism and Regulation of Mycobactin Fatty Acyl-AMP Ligase FadD33. *J. Biol. Chem.* **288,** 28116–28125 (2013).
419. Ho Jun, L., Lang, P. T., Fortune, S. M., Sassetti, C. M. & Alber, T. Cyclic-AMP regulation of protein lysine acetylation in *Mycobacterium tuberculosis*. *Nat. Struct. Biol.* **19,** 811–818 (2013).
420. Vergnolle, O. *et al.* Post-Translational Acetylation of MbtA Modulates Mycobacterial Siderophore Biosynthesis*. *J. Biol. Chem.* (2016).
421. Leistikow, R. L. *et al.* The Mycobacterium tuberculosis DosR Regulon Assists in Metabolic Homeostasis and Enables Rapid Recovery from Nonrespiring Dormancy. *J. Bacteriol.* **192,** 1662–1670 (2010).
422. Kumar, A. *et al.* Mycobacterium tuberculosis DosS is a redox sensor and DosT is a hypoxia sensor. *Proc. Natl. Acad. Sci. U. S. A.* **104,** 11568–73 (2007).
423. Baek, S.-H., Li, A. H. & Sassetti, C. M. Metabolic Regulation of Mycobacterial Growth and Antibiotic Sensitivity. *PLoS Biol* **9,** 1001065 (2011).
424. Rittershaus, E. S. C. *et al.* A Lysine Acetyltransferase Contributes to the Metabolic Adaptation to Hypoxia in Mycobacterium tuberculosis Article A Lysine Acetyltransferase Contributes to the Metabolic Adaptation to Hypoxia in Mycobacterium tuberculosis. *Cell Chem. Biol.* **25,** 1–11 (2018).
425. Rittershaus, E. S. C. *et al.* A Lysine Acetyltransferase Contributes to the Metabolic Adaptation to Hypoxia in Mycobacterium tuberculosis. *Cell Chem. Biol.* (2018).
426. Crosby, H. A., Pelletier, D. A., Hurst, G. B. & Escalante-Semerena, J. C. System-wide studies of N-lysine acetylation in Rhodopseudomonas palustris reveal substrate specificity of protein acetyltransferases. *J. Biol. Chem.* **287,** 15590–601 (2012).
427. Kim, M.-J. *et al.* Caseation of human tuberculosis granulomas correlates with elevated host lipid metabolism. *EMBO Mol. Med.* **2,** 258–274 (2010).
428. Turk, V., Turk, B. & Turk, D. Lysosomal cysteine proteases: facts and opportunities. *EMBO J.* **20,** 4629–4633 (2001).
429. Vandal, O. H., Nathan, C. F. & Ehrt, S. Acid Resistance in Mycobacterium tuberculosis. *J. Bacteriol.* **191,** 4714–4721 (2009).
430. Sturgill-Koszycki, S. *et al.* Lack of acidification in Mycobacterium phagosomes produced by exclusion of the vesicular proton-ATPase. *Science* **263,** 678–81 (1994).
431. Golby, P. *et al.* Comparative transcriptomics reveals key gene expression differences between the human and bovine pathogens of the Mycobacterium tuberculosis

complex. *Microbiology* **153,** 3323–36 (2007).

432. Walters, S. B. *et al.* The Mycobacterium tuberculosis PhoPR two-component system regulates genes essential for virulence and complex lipid biosynthesis. *Mol. Microbiol.* **60,** 312–30 (2006).
433. Schaible, U. E., Sturgill-Koszycki, S., Schlesinger, P. H. & Russell, D. G. Cytokine activation leads to acidification and increases maturation of Mycobacterium avium-containing phagosomes in murine macrophages. *J. Immunol.* **160,** 1290–6 (1998).
434. Via, L. E. *et al.* Effects of cytokines on mycobacterial phagosome maturation. *J. Cell Sci.* 897–905 (1998).
435. Baker, J. J., Johnson, B. K. & Abramovitch, R. B. Slow growth of Mycobacterium tuberculosis at acidic pH is regulated by phoPR and host-associated carbon sources. *Mol. Microbiol.* **94,** 56–69 (2014).
436. Tews, I. *et al.* The Structure of a pH-Sensing Mycobacterial Adenylyl Cyclase Holoenzyme. *Science (80-.).* **308,** 1020–1023 (2005).
437. Pethe, K. *et al.* A chemical genetic screen in Mycobacterium tuberculosis identifies carbon-source-dependent growth inhibitors devoid of in vivo efficacy. *Nat. Commun.* **1,** 57 (2010).
438. Lynn, M., Wilson, A. R. & Solotorovsky, M. *Role of bovine serum albumin in the nutrition of Mycobacterium tuberculosis*. *Applied and Environmental Microbiology* **38,** (1979).
439. Dubos, R. J. & Davis, B. D. Factors affecting the growth of tubercle bacilli in liquid media. *J. Exp. Med.* (1946).
440. Spector, A. A., John, K. & Fletcher, J. E. Binding of long-chain fatty acids to bovine serum albumin. *J. Lipid Res.* **10,** 56–67 (1969).
441. Bai, G. & Schaak, D. cAMP levels within Mycobacterium tuberculosis and Mycobacterium bovis BCG increase upon infection of macrophages. *FEMS Immunol. &* (2009).
442. Agilent Technologies. *MassHunter Mass Profiler Software Familiarization Guide*. (2015).
443. Agilent. *MassHunter Mass Profiler Software Quick Start Guide*.
444. Liu, F. *et al.* Acetylome analysis reveals diverse functions of lysine acetylation in Mycobacterium tuberculosis. *Mol. Cell. Proteomics* **13,** 3352–66 (2014).
445. TubercuList - Mycobacterium tuberculosis Database. Available at: http://svitsrv8.epfl.ch/tuberculist/. (Accessed: 29th October 2018)
446. Sassetti, C. M., Boyd, D. H. & Rubin, E. J. Genes required for mycobacterial growth defined by high density mutagenesis. *Mol. Microbiol.* **48,** 77–84 (2003).
447. Cavalcanti, Y. V. N., Brelaz, M. C. A., Neves, J. K. de A. L., Ferraz, J. C. & Pereira, V. R. A.

Role of TNF-Alpha, IFN-Gamma, and IL-10 in the Development of Pulmonary Tuberculosis. *Pulm. Med.* **2012,** 745483 (2012).

448. Nazarova, E. V & Russell, D. G. Growing and Handling of Mycobacterium tuberculosis for Macrophage Infection Assays. *Methods Mol. Biol.* **1519,** 325–331 (2017).
449. Khan, T. A. *et al.* Interferon-Gamma Improves Macrophages Function against M. tuberculosis in Multidrug-Resistant Tuberculosis Patients. *Chemother. Res. Pract.* **2016,** 7295390 (2016).
450. VanderVen, B. C., Huang, L., Rohde, K. H. & Russell, D. G. The Minimal Unit of Infection: Mycobacterium tuberculosis in the Macrophage. *Microbiol. Spectr.* **4,** (2016).
451. Sharma, S. & Bose, M. Role of cytokines in immune response to pulmonary tuberculosis. *Asian Pac. J. Allergy Immunol.* **19,** 213–9 (2001).
452. Yasui, K. Immunity against Mycobacterium tuberculosis and the risk of biologic anti-TNF-α reagents. *Pediatr. Rheumatol. Online J.* **12,** 45 (2014).
453. Pieters, J. Mycobacterium tuberculosis and the Macrophage: Maintaining a Balance. *Cell Host Microbe* **3,** 399–407 (2008).
454. Bentrup, K. H. zu & Russell, D. G. Mycobacterial persistence: adaptation to a changing environment. *Trends Microbiol.* **9,** 597–605 (2001).
455. MacMicking, J. D., Taylor, G. A. & McKinney, J. D. Immune Control of Tuberculosis by IFN- Inducible LRG-47. *Science (80-.).* **302,** 654–659 (2003).
456. Hooper, C. *et al.* Differential effects of albumin on microglia and macrophages; implications for neurodegeneration following blood-brain barrier damage. *J. Neurochem.* **109,** 694–705 (2009).
457. VanderVen, B. C. *et al.* Novel inhibitors of cholesterol degradation in Mycobacterium tuberculosis reveal how the bacterium's metabolism is constrained by the intracellular environment. *PLoS Pathog.* **11,** e1004679 (2015).
458. Castaño-Cerezo, S., Bernal, V., Blanco-Catalá, J., Iborra, J. L. & Cánovas, M. cAMP-CRP co-ordinates the expression of the protein acetylation pathway with central metabolism in Escherichia coli. *Mol. Microbiol.* **82,** 1110–1128 (2011).
459. Chan, C. H., Garrity, J., Crosby, H. A. & Escalante-Semerena, J. C. In Salmonella enterica, the sirtuin-dependent protein acylation/deacylation system (SDPADS) maintains energy homeostasis during growth on low concentrations of acetate. *Mol. Microbiol.* **80,** 168–183 (2011).
460. Crosby, H. A., Pelletier, D. A., Hurst, G. B. & Escalante-Semerena, J. C. System-wide Studies of *N* -Lysine Acetylation in *Rhodopseudomonas palustris* Reveal Substrate Specificity of Protein Acetyltransferases. *J. Biol. Chem.* **287,** 15590–15601 (2012).

461. Eoh, H. & Rhee, K. Y. Multifunctional essentiality of succinate metabolism in adaptation to hypoxia in Mycobacterium tuberculosis. *Proc. Natl. Acad. Sci.* **110,** 6554–6559 (2013).

462. Watanabe, S. *et al.* Fumarate Reductase Activity Maintains an Energized Membrane in Anaerobic Mycobacterium tuberculosis. *PLoS Pathog.* **7,** e1002287 (2011).

463. Moraes, G. L. *et al.* Structural and functional features of enzymes of Mycobacterium tuberculosis peptidoglycan biosynthesis as targets for drug development. *Tuberculosis (Edinb).* **95,** 95–111 (2015).

464. Biazus, G., Schneider, C. Z., Palma, M. S., Basso, L. A. & Santos, D. S. Hypoxanthine-guanine phosphoribosyltransferase from Mycobacterium tuberculosis H37Rv: Cloning, expression, and biochemical characterization. *Protein Expr. Purif.* **66,** 185–190 (2009).

465. Pagán-Ramos, E. *et al.* Molecular and physiological effects of mycobacterial oxyR inactivation. *J. Bacteriol.* **188,** 2674–80 (2006).

466. Conrad, W. H., Osman, M. M. & Shanahan, J. K. Mycobacterial ESX-1 secretion system mediates host cell lysis through bacterium contact-dependent gross membrane disruptions. **114,** 1371–1376 (2017).

467. de Carvalho, L. P. S. *et al.* Activity-Based Metabolomic Profiling of Enzymatic Function: Identification of Rv1248c as a Mycobacterial 2-Hydroxy-3-oxoadipate Synthase. *Chem. Biol.* **17,** 323–332 (2010).

468. Choi, S., Choi, H.-G., Lee, J., Shin, K.-W. & Kim, H.-J. Mycobacterium tuberculosis protein Rv2220 induces maturation and activation of dendritic cells. *Cell. Immunol.* **328,** 70–78 (2018).

469. Pais, T. F. & Appelberg, R. Macrophage control of mycobacterial growth induced by picolinic acid is dependent on host cell apoptosis. *J. Immunol.* **164,** 389–97 (2000).

470. Cavalcanti, Y. V. N., Brelaz, M. C. A., Neves, J. K. de A. L., Ferraz, J. C. & Pereira, V. R. A. Role of TNF-Alpha, IFN-Gamma, and IL-10 in the Development of Pulmonary Tuberculosis. *Pulm. Med.* **2012,** 745483 (2012).

471. McNab, F. W. *et al.* Type I IFN induces IL-10 production in an IL-27-independent manner and blocks responsiveness to IFN-γ for production of IL-12 and bacterial killing in Mycobacterium tuberculosis-infected macrophages. *J. Immunol.* **193,** 3600–12 (2014).

472. Korb, V. C., Chuturgoon, A. A. & Moodley, D. Mycobacterium tuberculosis: Manipulator of Protective Immunity. *Int. J. Mol. Sci.* **17,** (2016).

473. Corbett, E. L. *et al.* The growing burden of tuberculosis: global trends and interactions with the HIV epidemic. *Arch. Intern. Med.* **163,** 1009–21 (2003).

474. Weiglmeier, P. R., Rösch, P. & Berkner, H. Cure and curse: E. coli heat-stable

enterotoxin and its receptor guanylyl cyclase C. *Toxins (Basel).* **2,** 2213–29 (2010).

475. The CDC. *Tuberculosis indicators report*. (2016).

476. Marche, P., Koutouzov, S. & Girard, A. Impairment of membrane phosphoinositide metabolism by aminoglycoside antibiotics: streptomycin, amikacin, kanamycin, dibekacin, gentamicin and neomycin. *J. Pharmacol. Exp. Ther.* **227,** 415–20 (1983).

477. Arbuzova, A. *et al.* Fluorescently labeled neomycin as a probe of phosphatidylinositol-4, 5-bisphosphate in membranes. *Biochim. Biophys. Acta* **1464,** 35–48 (2000).

478. Antonietta De Matteis, M., Di Campli, A. & Godi, A. The role of the phosphoinositides at the Golgi complex. *Biochim. Biophys. Acta - Mol. Cell Res.* **1744,** 396–405 (2005).

479. Baenke, F., Peck, B., Miess, H. & Schulze, A. Hooked on fat: the role of lipid synthesis in cancer metabolism and tumour development. *Dis. Model. Mech.* **6,** 1353–63 (2013).

480. Matange, N., Hunt, D. M., Buxton, R. S. & Visweswariah, S. S. Overexpression of the Rv0805 phosphodiesterase elicits a cAMP-independent transcriptional response. *Tuberculosis (Edinb).* **93,** 492–500 (2013).

481. Matange, N. Revisiting bacterial cyclic nucleotide phosphodiesterases: cyclic AMP hydrolysis and beyond. *FEMS Microbiol. Lett.* **362,** fnv183 (2015).

482. Banerjee, A. *et al.* A universal stress protein (USP) in mycobacteria binds cAMP. *J. Biol. Chem.* **290,** 12731–43 (2015).

483. Gazdik, M. A. & McDonough, K. A. Identification of cyclic AMP-regulated genes in Mycobacterium tuberculosis complex bacteria under low-oxygen conditions. *J. Bacteriol.* **187,** 2681–92 (2005).

484. Shleeva, M. *et al.* Cyclic Amp-Dependent Resuscitation of Dormant Mycobacteria by Exogenous Free Fatty Acids. *PLoS One* **8,** e82914 (2013).

485. Shleeva, M. O. *et al.* Overexpression of Adenylyl Cyclase Encoded by the Mycobacterium tuberculosis Rv2212 Gene Confers Improved Fitness, Accelerated Recovery from Dormancy and Enhanced Virulence in Mice. *Front. Cell. Infect. Microbiol.* **7,** 370 (2017).

486. Castellano, B. & Nieto-Sampedro, M. *Glial cell function*. (Elsevier, 2003).

487. Ghazaei, C. Mycobacterium tuberculosis and lipids: Insights into molecular mechanisms from persistence to virulence. *J. Res. Med. Sci.* **23,** 63 (2018).

488. Kanai, K. & Kondo, E. *Antibacterial and cytotoxic aspects of long-chain fatty acids as cell surface events: selected topics*. *J. Med. Sci. Biol* **32,** (1979).

489. Davis, B. D. & Dubos, ~ J. The binding of fatty acids by serum albumin, a protective growth factor in bacteriological media. *J. Exp. Med.* (1947).

490. Alvarez-Uria, G. Diagnostic and Prognostic Value of Serum Albumin for Tuberculosis in

HIV Infected Patients Eligible for Antiretroviral Therapy: Data from an HIV Cohort Study in India. **3,** 123–128 (2013).